DHI

Energinet.dk

Anholt Offshore Wind Farm

Hydrography, sediment spill, water quality, geomorphology and coastal morphology.

October 2009

Energinet.dk

Anholt Offshore Wind Farm

Hydrography, sediment spill, water quality, geomorphology and coastal morphology.

October 2009

Ref   11803332-3
Version 6
Date 2009-09-24
By SLO/DMA/EKR/KLB/SLN
Controlled by RD/FLM
Approved by RD

Anholt Offshore Wind Farm

Hydrography, sediment spill, water quality, geomorphology and coastal morphology.

19-10-09

Client	Client's representative
Energinet.dk	Jan Havsager, Pernille Skyt

Project				Project No			
Anholt				11803332-3			
Authors				**Date**			
Sanne Niemann				19 October 2009			
Sabine Lohier							
Klavs Bundgaard				**Approved by**			
Damien Marigliano							
Erik Kock Rasmussen				Rolf Deigaard			
Erik Damgaard Christensen							
Flemming Møhlenberg							
Rolf Deigaard							
2	Draft Rev. 2			SLN	RD/FLM	RD	24.09.09
1	Draft Rev. 1			SLN	RD/FLM	RD	11.08.09
Revision	Description			By	Checked	Approved	Date

Key words	Classification
wind farm, Anholt, Djursland,wind turbines, impact assessment, EIA, hydrography, sediment spill, water quality, geomorphology, coastal morphology	☐ Open ☐ Internal ☒ Proprietary

Distribution	No of copies
Rambøll: Mikkel Benthien Kristensen DHI: SLN, MM, RD, FLM, JAO	Pdf Pdf

Table of contents

Appendices:

Appendix A: Details of numerical modelling of current and stratification conditions
Appendix B: Details of wave modelling
Appendix C: Details of water quality modelling
Appendix D: Details in estimating the local impact on stratification and mixing conditions

1. Summaries

1.1 Dansk resumé

<u>V</u>urderinger af <u>v</u>irkninger på <u>m</u>iljøet (VVM) i forbindelse med den planlagte opførelse af Anholt Havmøllepark ca. 20 km sydvest for Anholt i Kattegat er foretaget. VVM'en består af en vurdering af indflydelsen af havmølleparken på hydrografiske forhold (strømforhold, lagdelingsforhold og bølger), vandkvalitet, geomorfologiske forhold og kystmorfologi samt vurdering af sedimentspredning forårsaget af gravearbejder. Vurderingerne er foretaget for to udvalgte scenarier med hensyn til design af vind-mølleparken. Scenarierne i undersøgelserne er valgt som de designs, der indenfor projektbeskrivelsens rammer /1 / vil give de største påvirkninger på miljøet. Den største påvirkning forventes som følge af kombinationen af 174 2,3 MW vindmøller på gravitationsfundamenter. De to udvalgte scenarier til undersøgelserne er derfor valgt som de to forslag til opsætningerne af vindmøllerne /1 / i kombination med det nævnte antal møller på gravitationsfundamenter. I den ene opsætning placeres vindmøllerne på lige linjer, og i den anden er de placeret i buer. Resultaterne be-skrevet i det følgende er i store træk identiske for begge de undersøgte opsætninger. Konklusionerne i det følgende baserer sig i store træk på numerisk modellering.

Anholt Havmøllepark er planlagt opført mellem Anholt og Djursland i et område, hvor vanddybderne varierer mellem ca. 14,5 og 20 m. Overfladehavbundssedimenterne består af ikke-kohæsive sedimenter hovedsageligt bestående af sand, men også mo-rænerester, grus og sten. Indenfor projektområdet befinder de groveste sedimenter sig i den sydlige del (sand med perlegrus og sten), mens havbunden i den nordlige del i højere grad er dækket af et lag sand/silt.

Påvirkningerne på de hydrografiske forhold forårsaget af havmølleparken forventes at være små. Strømforholdene i området er lagdelte i størstedelen af året. Strømret-ningerne varierer både i overfladelaget og i bundlaget med tidevandet, men den fremherskende strømretning er mod nord og nordvest. Strømhastighederne er i gen-nemsnit 0,1-0,2 m/s, men kan blive omkring 1 m/s. Den ekstra strømmodstand, som havmølleparken tilføjer, resulterer i en reduktion af strømhastighederne i for-hold til de nuværende forhold i vindmølleparkens område samt i det nedstrøms om-råde, dvs. hovedsageligt nord for mølleparken. Hastighedsreduktioner på mere end 2% er begrænset til et område indenfor 5 km fra mølleparken. I gennemsnit over året er strømhastighedsændringerne dog meget små; ved overfladen er de beregnet til omkring 0,0008 m/s. Mindre stigninger forventes i området uden om mølleparken (øst og vest for parken) som kompensation for den reducerede gennemstrømning igennem mølleområdet. Lagdelingen vil blive svagt påvirket i umiddelbar nærhed af hver vindmølle, da møllefundamenterne vil medføre lettere opblanding af vandsøjlen.

Bølgerne i området er hovedsagelig vindgenererede, og bølgehøjderne begrænses af afstanden fra de nærtliggende landområder så som Djursland mod vest-sydvest, Læsø mod nord, Anholt mod øst og længere væk Skagen, Sverige, Odden og Samsø. Det årlige bølgeklima er forholdsvist mildt med bølgehøjder mindre end 2,5 m og

bølger hovedsageligt fra retninger mellem sydøst og vest. Variationer i bølgehøjden indenfor projektområdet er hovedsageligt forårsaget af læeffekten fra Djursland, som begrænser bølgehøjderne fra sydvestlige retninger. Havmølleparken medfører, at en del af bølgeenergien reflekteres og diffrakteres omkring fundamenterne. Derudover reduceres bølgeenergien i området, da vindmøllerne blokerer for vinden og reducerer vindhastighederne. Bølgedæmpningen (reduktion i bølgehøjden) på grund af refleksion/diffraktion er estimeret til at have en størrelsesorden på omkring 3% indenfor havmølleparkens område, og dæmpningen på grund af de reducerede vindhastigheder forventes at være en anelse større. De summerede ændringer i bølgefeltet er begrænsede, og kun meget små ændringer i bølgeforholdene forventes ved kysterne af Anholt og Djursland. Påvirkningerne på kysterne forventes derfor at være meget små og ikke synlige.

Mobiliteten af havbunden i projektområdet er undersøgt. De årlige sedimenttransportrater er beregnet til at være små i størrelsesordenen et par kubikmeter om året pr. meters bredde. De små transportrater skyldes de relativt små strømhastigheder, det milde bølgeklima og vanddybder på mellem 14,5 og 20 m. I umiddelbar nærhed af hvert vindmøllefundament kan havbundsniveauet dog sætte sig betragteligt. Et såkaldt scourhul med en dybde svarende til omkring diameteren af fundamentet kan udvikles, og det anbefales derfor stærkt at inkludere overvejelser omkring scour i designet af mølleparken.

Der er foretaget beregninger af aflejring og spredning af sedimentspild under gravearbejder i konstruktionsfasen. Resultaterne viser, at i graveperioden vil de dybdemidlede koncentrationer af sediment i vandfasen kun overstige 2 mg/l i korte perioder af størrelsen timer/dage. Dybdemidlede koncentrationer forventes ikke at overstige 10 mg/l. De resulterende aflejringer var beregnet til at være mindre end 1 mm i projektområdet.

1.2   Summary

An Environmental Impact Assessment (EIA) related to the erection of Anholt Offshore Wind Farm approximately 20 km south-west of Anholt in the Kattegat has been carried out. The EIA consists of assessing the impact of the wind farm on hydrographic conditions (currents, stratification and waves), water quality conditions, geomorphology and coastal morphology and assessment of sediment spreading due to dredging activities. The assessment is carried out by considering two worst case scenarios with regard to the design of the wind farm. The scenarios in the investigations are selected as the designs which within the framework of the project description /1/, are expected to cause the most significant impact on the environment. The largest impacts are expected for the combination of 174 2.3 MW wind turbines on gravity foundations. The two scenarios are hence composed of the two suggested layouts of the wind farm /1/ in combination with 174 wind turbines on gravity foundations.

Anholt Offshore Wind Farm will be located between Anholt and Djursland on a flat area characterized by a water depth varying between 14.5 m and 20 m. The surface sea bed is covered by non-cohesive sediment consisting mostly of sandy sediments

but also of exposed moraine till, gravel and stones. Within the project area sediments to be found in the south are coarser materials (sand with pebbles and stones) than in the north (sand/silt).

The expected effects of the wind farm on the hydrodynamic conditions are minor. The flow in the project area is stratified during the main part of the year. The current direction changes with the tide in the surface layer as well as in the bottom layer, but the predominantly current directions are towards the north and north-west. Current velocities are in average 0.1-0.2 m/s but can reach around 1 m/s. The additional flow resistance caused by the wind farm results in small reductions in the current speeds within and downstream the wind farm. Reductions to the current speeds larger than 2% compared with the existing conditions are limited to an area within approximately 5 km from the wind farm area. The annual mean velocity changes are, however, very small; at the surface they were found to be in the order of 0.0008 m/s. Small increases in the current speeds are expected around the wind farm (east and west) due to flow diversion. The stratification will be weakened slightly in the immediate vicinity of each wind turbine due to increased mixing of the water column caused by turbulence around the foundations.

The waves are typically wind generated waves limited by the distance to land areas such as Djursland to the west-southwest, Læsø to the north, Anholt to the east and further away to Skagen, Sweden, the spit of Odden and Samsø. The annual wave climate is relatively mild (wave height <2.5m) and waves are predominantly coming from directions between south- east and west. Spatial variation of the wave climate within the area of interest is mainly due to the lee effect caused by Djursland which limits the wave height from the south-western directions. During the operational phase, the wind farm will cause part of the wave energy to be reflected or diffracted around the foundations. Furthermore, the wave energy will be smaller due to the wind blocking effect of Anholt Offshore Wind Farm. The wave dampening due to reflection / diffraction effect is estimated to be less than 3% within the wind farm area and the wave dampening due to the wind effect is expected to be slightly higher. The overall changes to the wave field are small and only minor changes near the coast of Anholt and Djursland are expected. Consequently, the impact on the coastal morphology and shorelines of Anholt and Djursland will be very small and no noticeable effect is expected.

The annual sediment transport rates in the project area are found to be small in the order of a few cubic metres per year over a width of one metre. This is basically due to the relatively weak currents and mild wave climate combined with water depths between 15 and 20 m. The sea bed mobility is therefore small and the overall geomorphology conditions in the project area will not be affected. However, each wind mill may be subject to local scour associated with considerable bed level changes of approximately one diameter of the base at equilibrium. It is therefore strongly recommended to consider scouring in the design phase of the wind farm.

Analysis of sedimentation and spreading of the sediments due to dredging activities connected with earthworks during the construction phase has been carried out. It is found that during the construction phase depth-averaged concentrations of suspended sediment will exceed 2 mg/l only in short periods in the order of magnitude of hours or days. Depth-averaged concentrations are not expected to exceed 10 mg/l. The resulting deposition was calculated to be less than 1 mm in the project area.

Baseline water quality
Within the Kattegat the depth integrated primary production peaks along the 10-13 m depth curve in Aalborg Bugt as a result of intense mixing between surface and bottom water bringing nutrients up in the photic zone. At shallow waters, e.g. along coasts and south of Læsø pelagic primary production is low. Instead, benthic vegetation such as Eelgrass south of Læsø dominates production, but these processes are not modelled as benthic vegetation practically is absent in the wind park area.

The permanent influence on water quality in the operational phase of two different wind farm designs established between Anholt and Djursland was evaluated using a coupled hydrodynamic-water quality model. The main conclusions were:

- Changes in yearly plankton primary production occurred over a rather large area north, east and west of the wind farm but at the maximum the changes did not exceed 0.5% compared to baseline conditions. Averaged over the entire modelled area increases and decreases outbalanced each other, and the overall change was less than 0.03% compared to baseline conditions.

- Changes in yearly sedimentation of organic carbon originating from primary production and the subsequent mineralisation in sediment were most prominent north and east of the wind farm area as a result of prevailing northbound currents. Reductions in carbon sedimentation close to the wind farm area probably were a result of plankton filtration and mineralisation by mussels population on the wind mill foundations. Changes were very small and not exceeding 0.3% at any location within the modelled area compared to baseline and, the overall reductions in sedimentation and mineralisation were less than 0.06% compared to baseline conditions.

- Duration of oxygen deficiency in bottom water was hardly effected by the wind farms. At most, in areas affected by prolonged oxygen deficiency under baseline conditions the critical periods with low oxygen concentration was extended by up to 3 days, but in other areas periods with oxygen deficiency was shortened.

The two wind farm designs did show spatial differences in water quality changes but averaged over the entire model area the changes were very small and hardly significant. Hence, based on water quality predictions one farm design cannot be considered better than the other design.

The temporal influence on water quality during construction of two different wind farm designs was evaluated based on predicted sediment spread during dredging operations. Influences related to release of nutrients and reduced substances during dredging in the construction phase could not be evaluated in detail because relevant information from the sites to be dredged was not available. The main conclusion was:

- Reduction in light availability caused by shading from sediment spread was very low and confined to the wind park areas. Reduction in phytoplankton production will be very low averaging less than 0.5% inside the wind parks while no reductions are expected outside the wind parks. Benthic vegetation is very sparse in the area and accordingly shading effects are not relevant.

2. Introduction

2.1 Background

In 1998 the Ministry of Environment and Energy empowered the Danish energy companies to build offshore wind farms of a total capacity of 750 MW, as part of fulfilling the national action plan for energy, Energy 21. One aim of the action plan, which was elaborated in the wake of Denmark's commitment to the Kyoto agreement, is to increase the production of energy from wind power to 5.500 MW in the year 2030. Hereof 4.000 MW has to be produced in offshore wind farms.

In the years 2002-2003 the two first wind farms was established at Horns Rev west of Esbjerg and Rødsand south of Lolland, consisting of 80 and 72 wind turbines, respectively, producing a total of 325,6 MW. In 2004 it was furthermore decided to construct two new wind farms in proximity of the two existing parks at Horns rev and Rødsand. The two new parks, Horns rev 2 and Rødsand 2, are going to produce 215 MW each and are expected to be fully operational by the end 2010.

The 400 MW Anholt Offshore Wind Farm constitutes the next step of the fulfilment of aim of the action plan. The wind farm will be constructed in 2012, and the expected production of electricity will cover the yearly consumption of approximately 400.000 households. Energinet.dk on behalf of the Ministry of Climate and Energy is responsible for the construction of the electrical connection to the shore and for development of the wind farm site, including the organization of the impact assessment which will result in the identification of the best suitable site for constructing the wind farm. Rambøll with DHI and other sub consultants are undertaking the site development including a full-scale Environmental Impact Assessment for the wind farm.

The present report is a part of a number of technical reports forming the base for the Environmental Impact Assessment for Anholt Offshore Wind Farm.

The Environmental Impact Assessment of the Anholt Offshore Wind Farm is based on the following technical reports:

- Technical Description
- Geotechnical Investigations
- Geophysical Investigations
- Metocean data for design and operational conditions
- Hydrography including sediment spill, water quality, geomorphology and coastal morphology]
- Benthic Fauna
- Birds
- Marine mammals

- Fish
- Substrates and benthic communities
- Benthic habitat
- Maritime archaeology
- Visualization
- Commercial fishery
- Tourism and Recreational Activities
- Risk to ship traffic
- Noise calculations
- Air emissions

2.2 Content of specific memo

This report describes the baseline conditions and the impact assessment concerning the hydrographic conditions, the water quality conditions and the geomorphological conditions in the project area, as well as of relevant coastal areas at Djursland and Anholt.

The area for the environmental impact assessment for the Anholt Offshore Wind Farm has been defined as shown in Figure 2-1.

DHI has for Energinet.dk carried out the environmental impact assessment of the hydrographic conditions (currents, stratification and waves), water quality conditions, geomorphology and coastal morphology and assessment of sediment spreading due to dredging activities. This work is described in the present memo.
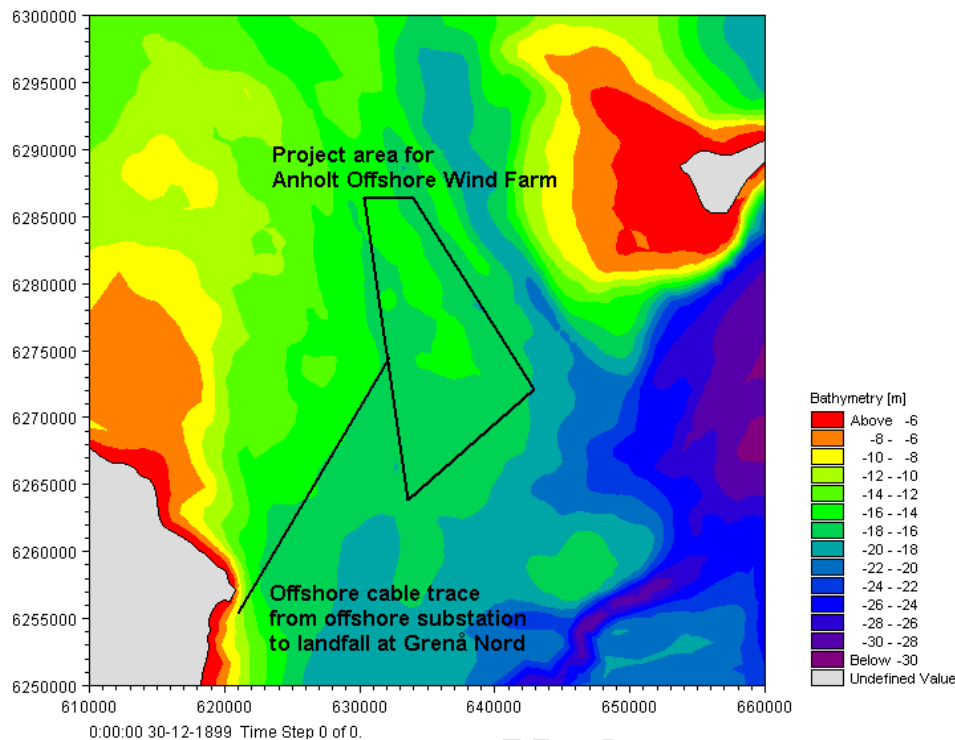
Figure 2-1:   Location of the area of environmental impact assessment in Kattegat between Anholt and Djursland.

The hydrographic conditions such as the flow conditions (currents, salinities and temperatures) and the wave field will be affected by the foundations which block the flow and waves and acts as an extra resistance to the flow. Locally around the foundations extra turbulence is generated and this causes extra mixing of the water column.

The hydrographic conditions have an influence on sediment mobility. Any impacts on the hydrographic conditions do hence affect the capacity for transporting sediment. This may cause changes to the geomorphological conditions such as the mobility of the bed. Also the coastline stability may be affected if the near shore wave conditions are influenced by wind farm. Other issues related to sediment mobility in connection with the planning of a wind farm are risk of scour around the foundations and risk of exposure of the cables.

Water quality is closely linked to the hydrographic conditions and any impacts on hydrographic conditions may affect the water quality parameters such as oxygen depletion. Water quality is also influenced by the dredging operations in the construction phase. The dredging operations will unavoidably cause sediment spill to some extent.

Sediment spill also influences benthic habitats (see /8/) and benthic fauna (see /7/). These issues are not covered by the present report.

The report is divided in two parts – the baseline study and the impact assessment.

The baseline study aims at providing a thorough description of the present conditions at the site. The analysis of the baseline conditions are to a large extent based on numerical modelling of hydrographical parameters (currents, waves, salinity, temperature) as well of water quality parameters and sediment transport rates. Analyses of available data are included.

In the impact assessment of the wind mill park the changes in the above mentioned parameters are analysed. The analysis of the impacts in the operational phase is primarily carried out as a comparative study, where the impact of the wind mills are parameterized and included in the numerical models and the impacts are evaluated by comparing the 'before' and 'after' situation.

The impacts in the construction phase such as sediment spill due to dredging operations is analysed by analysing simulations of the spill assuming likely scenarios for the dredging operations.

Impacts in the decommissioning phase are restricted to estimations of the backfilling rates of possible holes in case the foundations are removed/partly removed. These are evaluated by a desk study based on available data.

3. Offshore wind farm

This chapter describes the technical aspects of the Anholt Offshore Wind Farm. For a full project description reference is made to /1/. The following description is based on expected conditions for the technical project; however, the detailed design will not be done until a developer of the Anholt Offshore Wind Farm has been awarded.

3.1 Project description

3.1.1 Site location

The designated investigation area for the Anholt Offshore Wind Farm is located in Kattegat between the headland Djursland of Jutland and the island Anholt - see Figure 3-1. The investigation area is 144 km^2, but the planned wind turbines must not cover an area of more than 88 km^2. The distance from Djursland and Anholt to the project area is 15 and 20 km, respectively. The area is characterised by fairly uniform seabed conditions and water depths between 15 and 20 m.
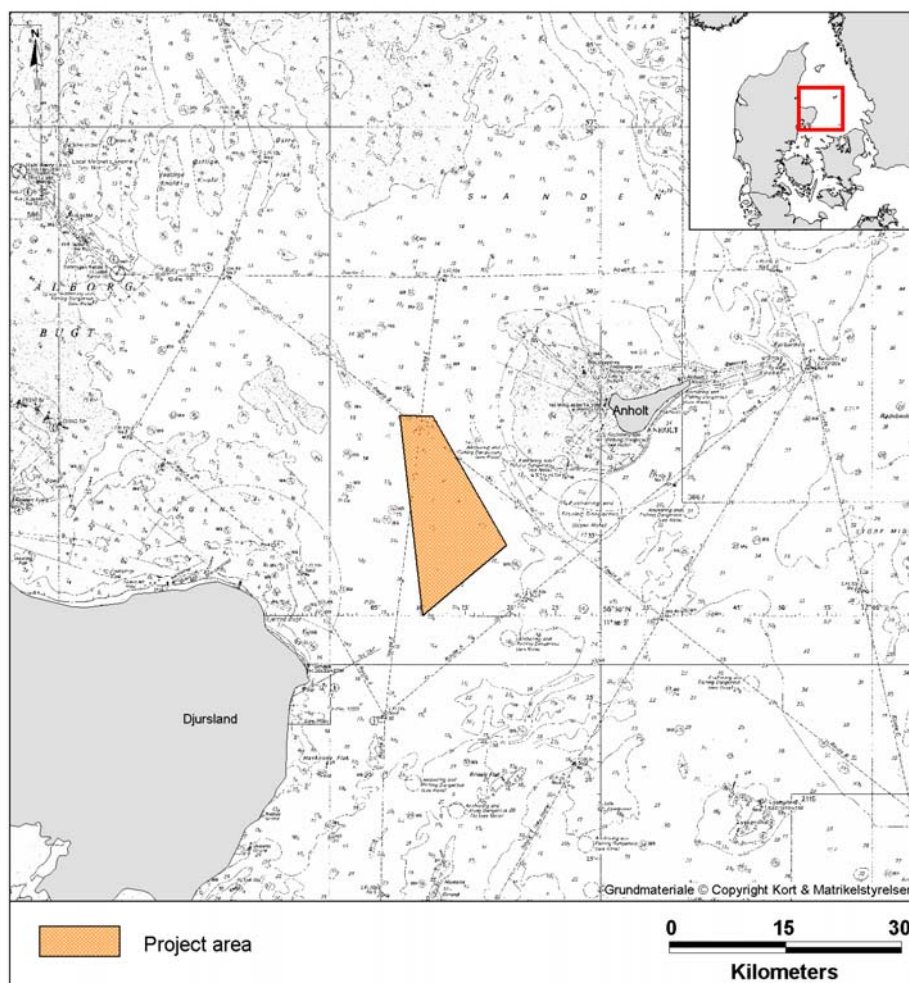
Figure 3-1   Location of the Anholt Offshore Wind Farm project area.

3.1.2   Offshore components

3.1.2.1   Foundations

The wind turbines will be supported on foundations fixed to the seabed. The foundations will be one of two types; either driven steel monopiles or concrete gravity based structures. Both concepts have successfully been used for operating offshore wind farms in Denmark /2/, /3/.

The monopile solution comprises driving a hollow steel pile into the seabed. A steel transition piece is attached to the pile head using grout to make the connection with the wind turbine tower.

The gravity based solution comprises a concrete base that stands on the seabed and thus relies on its mass including ballast to withstand the loads generated by the off-shore environment and the wind turbine.

3.1.2.2 Wind turbines

The maximum rated capacity of the wind farm is by the authorities limited to 400 MW /4/. The farm will feature from 80 to 174 turbines depending on the rated energy of the selected turbines corresponding to the range of 2.3 to 5.0 MW.

Preliminary dimensions of the turbines are not expected to exceed a maximum tip height of 160 m above mean sea level for the largest turbine size (5.0 MW) and a minimum air gap of approximately 23 m above mean sea level. An operational sound power level is expected in the order of 110 dB(A), but will depend on the selected type of turbine.

The wind turbines will exhibit distinguishing markings visible for vessels and aircrafts in accordance with recommendations by the Danish Maritime Safety Administration and the Danish Civil Aviation Administration. Safety zones will be applied for the wind farm area or parts hereof.

3.1.3 Installation

The foundations and the wind turbine components will either be stored at an adjacent port and transported to site by support barge or the installation vessel itself, or transported directly from the manufacturer to the wind farm site by barge or by the installation vessel.

The installation will be performed by jack-up barges or floating crane barges depending on the foundation design. A number of support barges, tugs, safety vessels and personnel transfer vessels will also be required.

Construction activity is expected for 24 hours per day until construction is complete. Following installation and grid connection, the wind turbines are commissioned and are available to generate electricity.

A safety zone of 500 m will be established to protect the project plant and personnel, and the safety of third parties during the construction and commissioning phases of the wind farm. The extent of the safety zone at any one time will be dependent on the locations of construction activity. However the safety zone may include the entire construction area or a rolling safety zone may be selected.

3.1.3.1 Wind turbines

The installation of the wind turbines will typically require one or more jack-up barges. These vessels stand on the seabed and create a stable lifting platform by lifting themselves out of the water. The area of seabed taken by a vessels feet is approximately 350 m^2 (in total), with leg penetrations of up to 2 to 15 m (depending on seabed properties). These holes will be left to in-fill naturally.

3.1.3.2 Foundations

The monopile concept is not expected to require any seabed preparation.

The installation of the driven monopiles will take place from either a jack-up platform or an anchored vessel. In addition, a small drilling spread may be adopted if driving difficulties are experienced. After transportation to the site the pile is transferred from the barge to the jack-up and then lifted into a vertical position. The pile is then driven until target penetration is achieved, the hammer is removed and the transition piece is installed.

For the gravity based foundations the seabed needs most often to be prepared prior to installation, i.e. the top layer of material is removed and replaced by a stone bed. The material excavated during the seabed preparation works will be loaded onto split-hopper barges for disposal. There is likely to be some discharge to water from the material excavation process. A conservative estimate is 5% material spill, i.e. up to 200 m^3 for each base, over a period of 3 days per excavation.

The installation of the concrete gravity base will likely take place using a floating crane barge, with attendant tugs and support craft. The bases will either be floated and towed to site or transported to site on a flat-top barge. The bases will then be lowered from the barge onto the prepared stone bed and filled with ballast.

After the structure is placed on the seabed, the base is filled with a suitable ballast material, usually sand. A steel 'skirt' may be installed around the base to penetrate into the seabed and to constrain the seabed underneath the base.

3.1.4 Protection systems

3.1.4.1 Corrosion

Corrosion protection on the steel structure will be achieved by a combination of a protective paint coating and installation of sacrificial anodes on the subsea structure. The anodes are standard products for offshore structures and are welded onto the steel structures.

3.1.4.2 Scour

If the seabed is erodible and the water flow is sufficient high a scour hole will form around the structure. The protection system normally adopted for scour consists of rock placement in a ring around the in-situ structure. The rock will be deployed from the host vessel either directly onto the seabed from the barge, via a bucket grab or via a telescopic tube.

For the monopile solution the total diameter of the scour protection is assumed to be 5 times the pile diameter. The total volume of cover stones will be around 850-1,000 m³ per foundation. For the gravity based solution the quantities are assessed to be 800–1100 m³ per foundation.

3.2   Baseline study

The purpose of this task is to:

- map the baseline situation with regard to:

    o hydrodynamic conditions (currents, stratification)

    o wave conditions

    o the water quality conditions

    o geomorphology in the wind farm area

    o coastal morphology of the adjacent coasts.

- provide the basis for modelling of the impacts on the same conditions.

3.2.1   Bathymetry

The bathymetry is described in this area. The bathymetry in the project area has been measured within the project by GEUS in the spring 2009. The numerical models, however, are based on older data. These are described in this part as well.

The most recent bathymetry in the project area was measured by GEUS in a multi-beam survey within this project, see Figure 3-2. The water depths in the area vary between 14.5 m and 20 m (DVR90). The bathymetry is in general quite uniform with relatively small depth variations across the area. Along the eastern part of the area and towards the south-west the deepest areas are found, while the shallowest parts are found in the central part and especially in the north-western part.
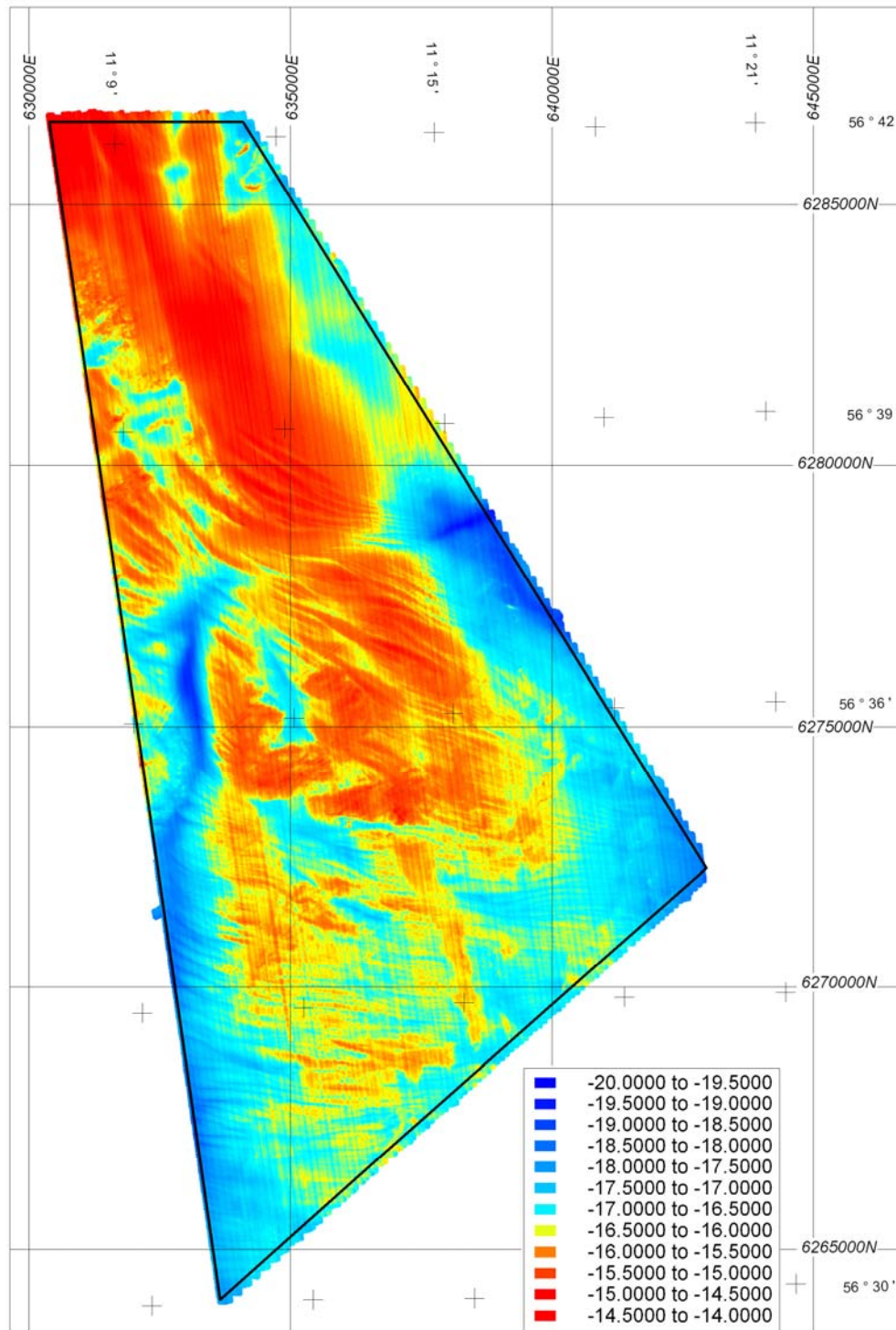
Figure 3-2   Bathymetry (m) in project area measured by GEUS 2009 /11/. Depths according to DVR90.

The new bathymetry data were not available at the time the numerical models applied in this work were setup. The bathymetries in the models are therefore based on available data from bathymetrical measurements by the Danish Naval Authorities (in Danish: 'Farvandsvæsenet') and from digitized sea maps from C-MAP.

The main part of the area of interest is covered by the data from the Danish Naval Authorities. In the area where these data are present, the resolution is 50 m. In these areas these data are used exclusively. The resolution of the data from the Danish Naval Authorities and their origin is given in Figure 3-3 and in Figure 3-4 (blue markers). In the main part the measurements are carried out before 1950. However, the sea bed is not very morphologically active in this area and thus the data are still considered applicable.

In the blank areas where no measured data were available from the Danish Naval Authorities, data from digitized seamaps (C-MAP) were used. These data are shown with orange markers in Figure 3-4.

The interpolated bathymetry applied in the numerical models is shown in Figure 3-5. The main bathymetric features found in the recently measured bathymetry in Figure 3-2 such as the area with the relatively smaller water depths in the northern part of the project area and the deeper channels in the western and eastern part, respectively, are captured in the model bathymetry.
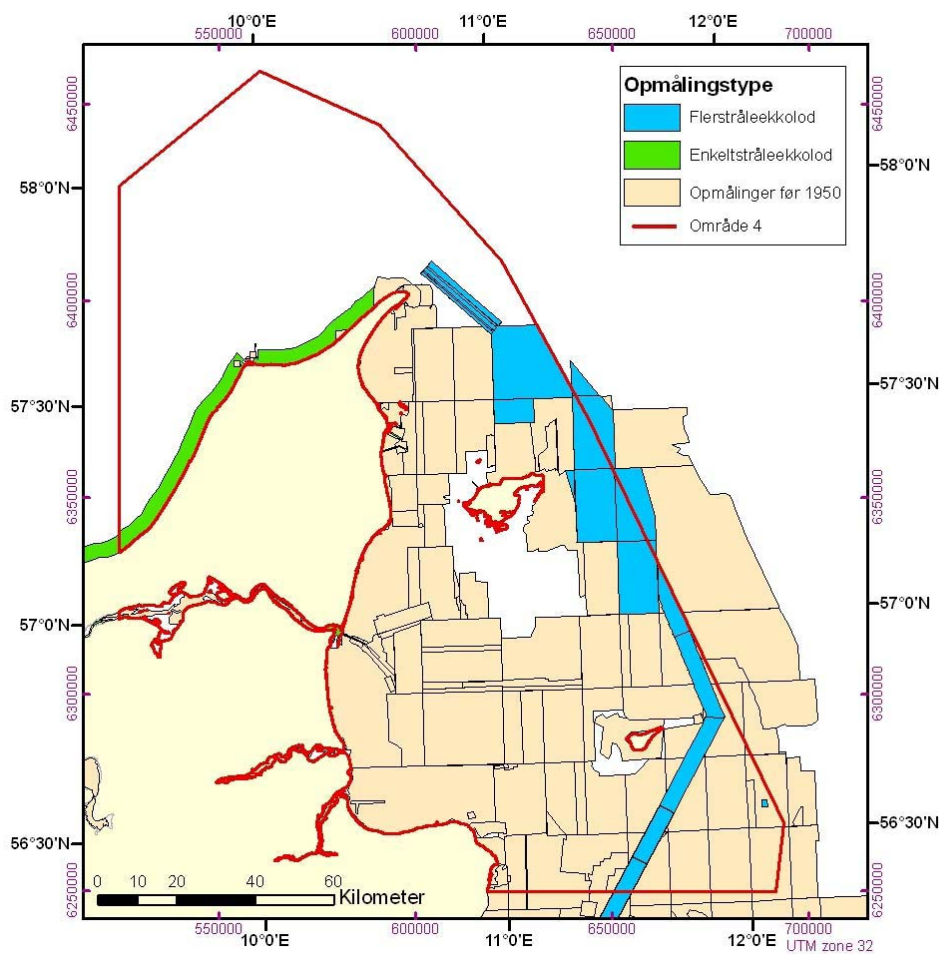
Figure 3-3   Origin of data from Danish naval authorities. Figure from www.frv.dk.
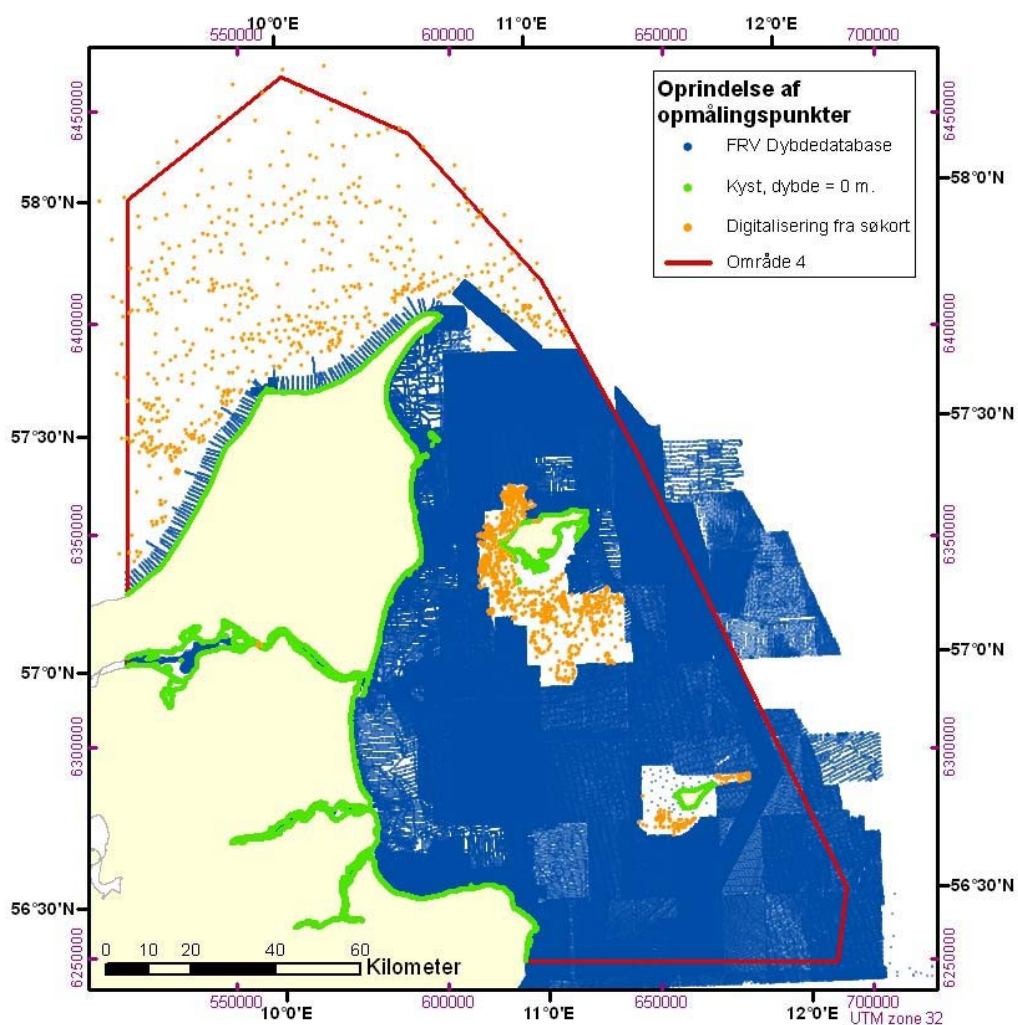
Figure 3-4   Overview over resolution of the bathymetrical data. Figure from www.frv.dk.
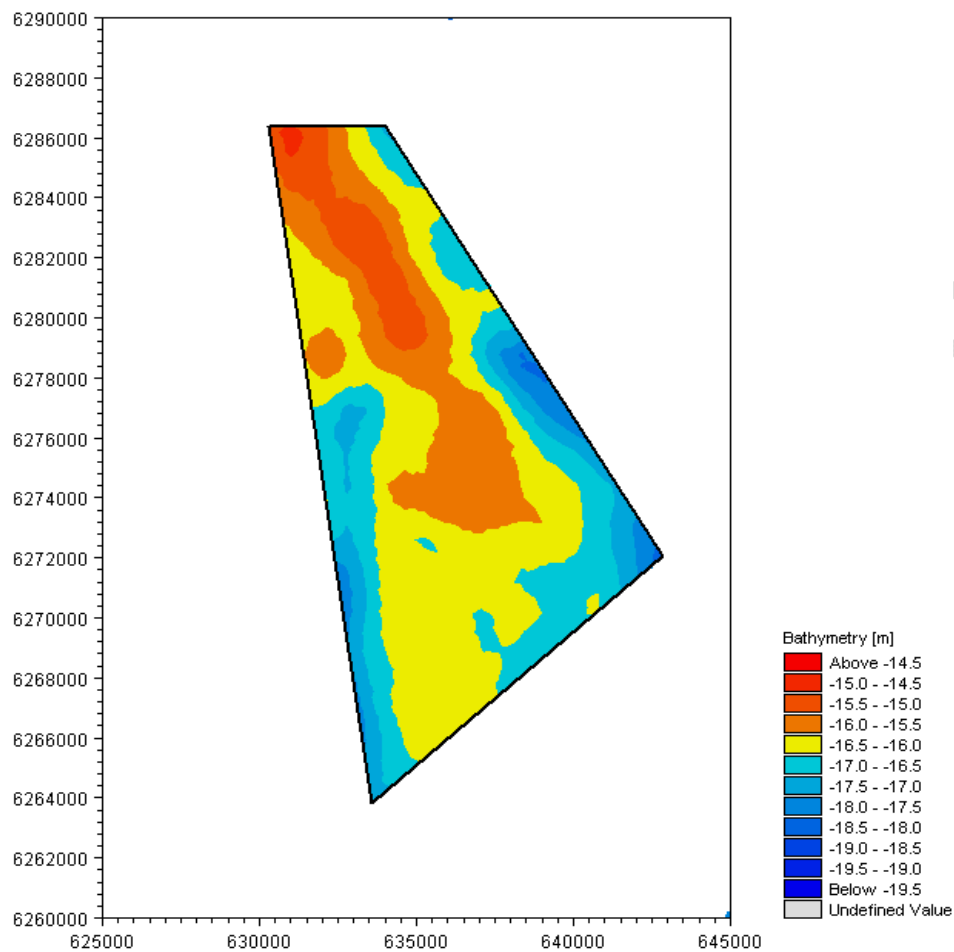
Figure 3-5   Interpolated bathymetry using data as applied in the numerical models for this project. Depths according to MSL.

3.2.2   Geology and sea bed sediments

3.2.2.1   Methods

The description of the baseline conditions is based on information from the literature and analysis of data collected during the present study on the sea bed sediments.

3.2.2.2   Data

3.2.2.2.1   Sea bed samples

Samples for analysis of benthic fauna and sediment grain sizes were collected by DHI at 80 stations in the project area between 15 and 22 of April 2009 /7/ see Figure 3-6. The samples were analysed for grain size distribution and calculation of median grain size diameter and grading of the sediment.
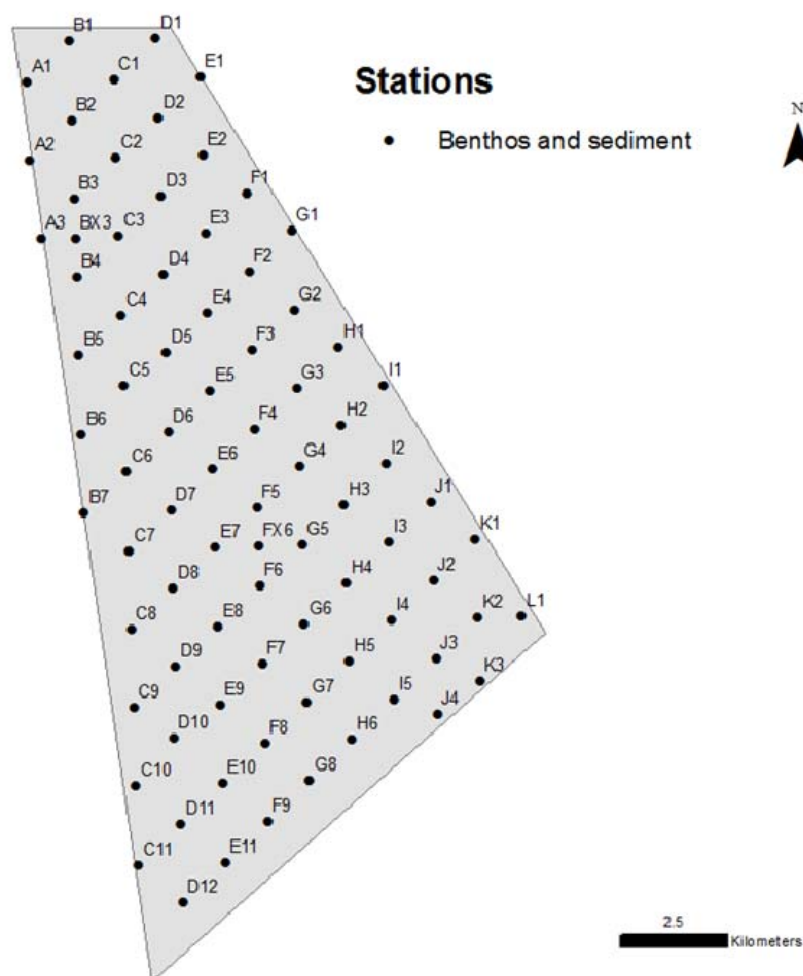
Figure 3-6   Stations where sediment samples were collected by DHI (/7/).

3.2.2.2.2 Geophysical survey

A geophysical survey was conducted by GEUS in April 2009 /11/. The project area was surveyed with side scan sonar. From this an image is obtained which can be interpreted to supply information on the geographical distribution of sea bed material which can be found in the area. Diving was used for calibration and verification of the analysis.

3.2.2.3 Description of geology and sea bed sediments

The sea bed of Kattegat in the area between Læsø, Djursland and Anholt is very flat with typical water depth between 10 and 20 m. A possible explanation for the very low relief is that melting water deposits discharged into the Yoldia Sea (approximately 15,000 yr b.p.) from the ice sheet lying to the south has covered and smoothed out the contours of the underlying glacial and pre-quaternary deposits.

The melting water is supposed to have come through the present mouth of the Randers Fjord and the Great Belt channel.

The characteristics of the surface sediments are illustrated in Figure 3-7. It describes the bed in the area of the wind mill park and the cable routes as consisting of exposed moraine till and sandy sediments with gravel or stones. Figure 3-8 shows the characteristics of the surface sediment in the wind mill area based on side scan surveys. It indicates a sandy area with a tendency for coarser material (sand with pebbles and stones) to be found in the southern part and finer material (sandy/silty) to be found in the north.
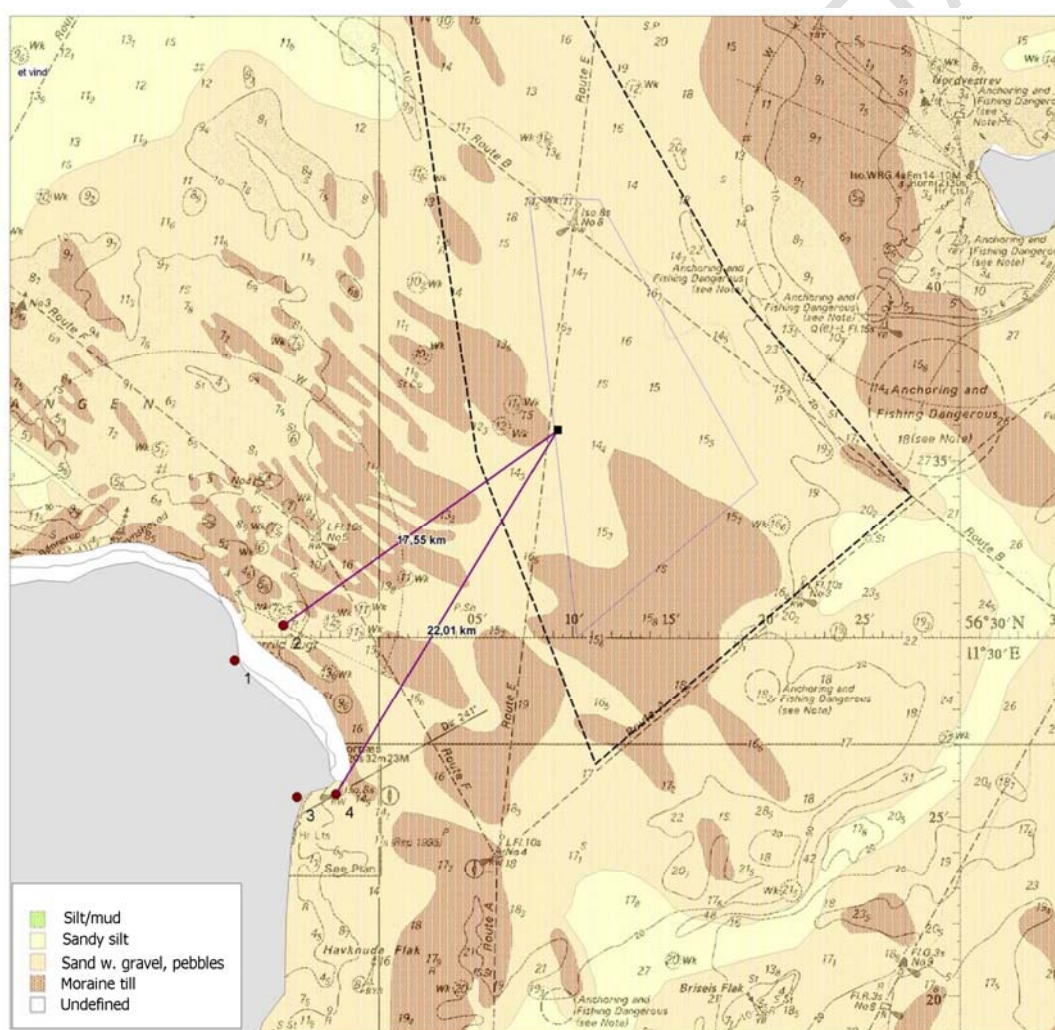
Figure 3-7   Map of sea bed sediment types. Rambøll/GEUS.
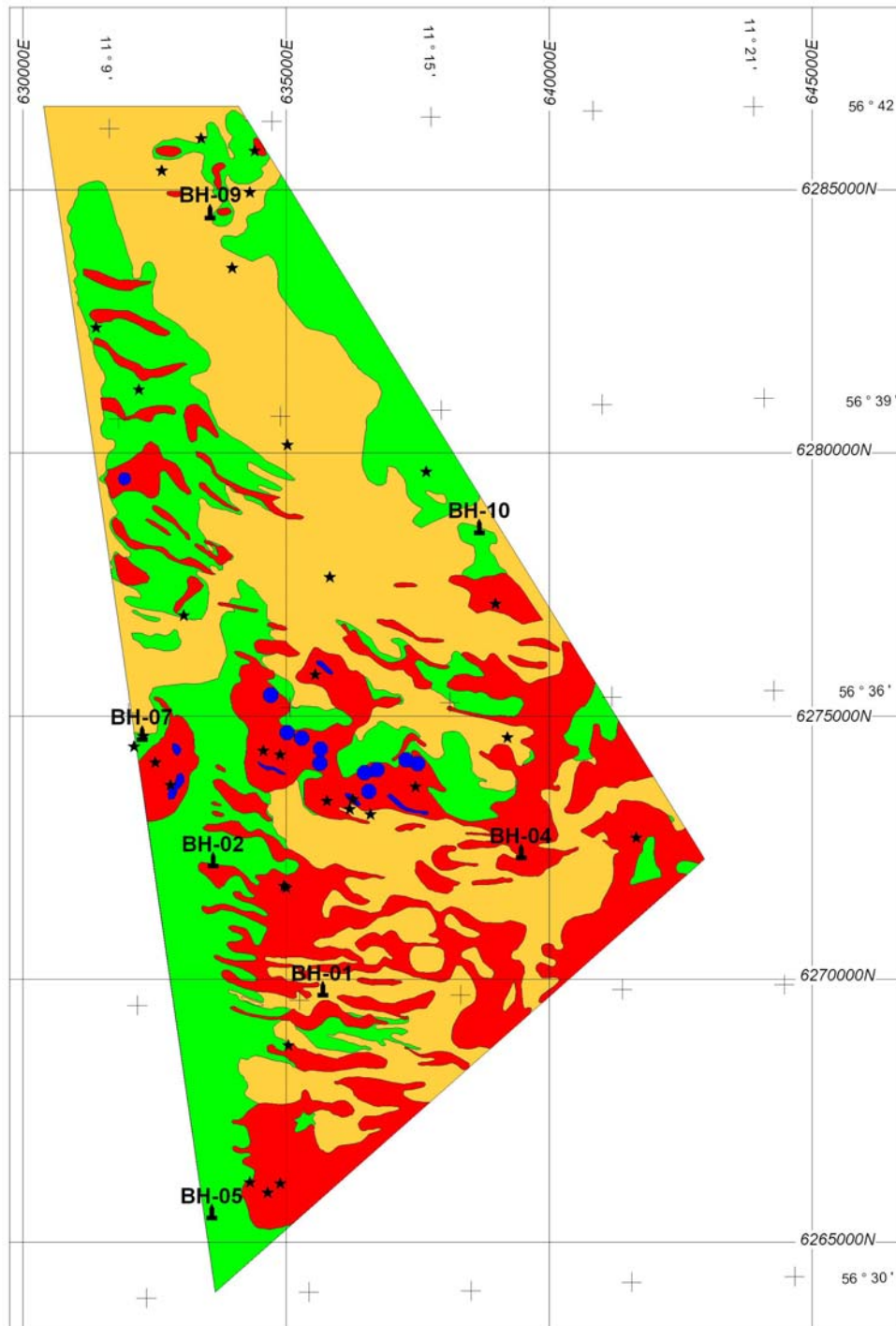
Figure 3-8 Sea bed map in the wind farm area (GEUS). Gravel/pebbles (blue), sand and pebbles with boulders with 1-25% boulders (red), mainly sand and pebbles with solitary boulders (green), sand and silt (yellow). Boreholes (BH) and dive stations (stars) are indicated on map.

Surface sea bed samples have been collected and analysed in the present project /7/. During the field trip, the samples were described and these descriptions are summarized in Figure 3-9. The samples have been analysed with respect to grain size. The fractions finer than sand (d < 63 μm) were found to be insignificant. The distribution of the median diameter is illustrated in Figure 3-10. All samples are representing sand with a median grain size from 0.2 to 0.6 mm. The tendency for finer sediment to be present in the northern part of the area is also observed here. The homogeneity of the surface sediments at each location is described by the grading coefficient, σ. The larger the grading coefficient, the larger is the variation in the grain sizes in the sample. The grading of the sea bed samples was determined by calculating the grading coefficient, $\sigma = \sqrt{d_{84}/d_{16}}$, for each sample. The distribution of the gradation is illustrated in Figure 3-11.

Based on this information it is concluded that the surface primarily is covered by non-cohesive sediments and does mainly consist of sand. The mobility and the order of magnitude of the sediment transport rate are roughly estimated by numerical model calculations in Section 3.2.8.
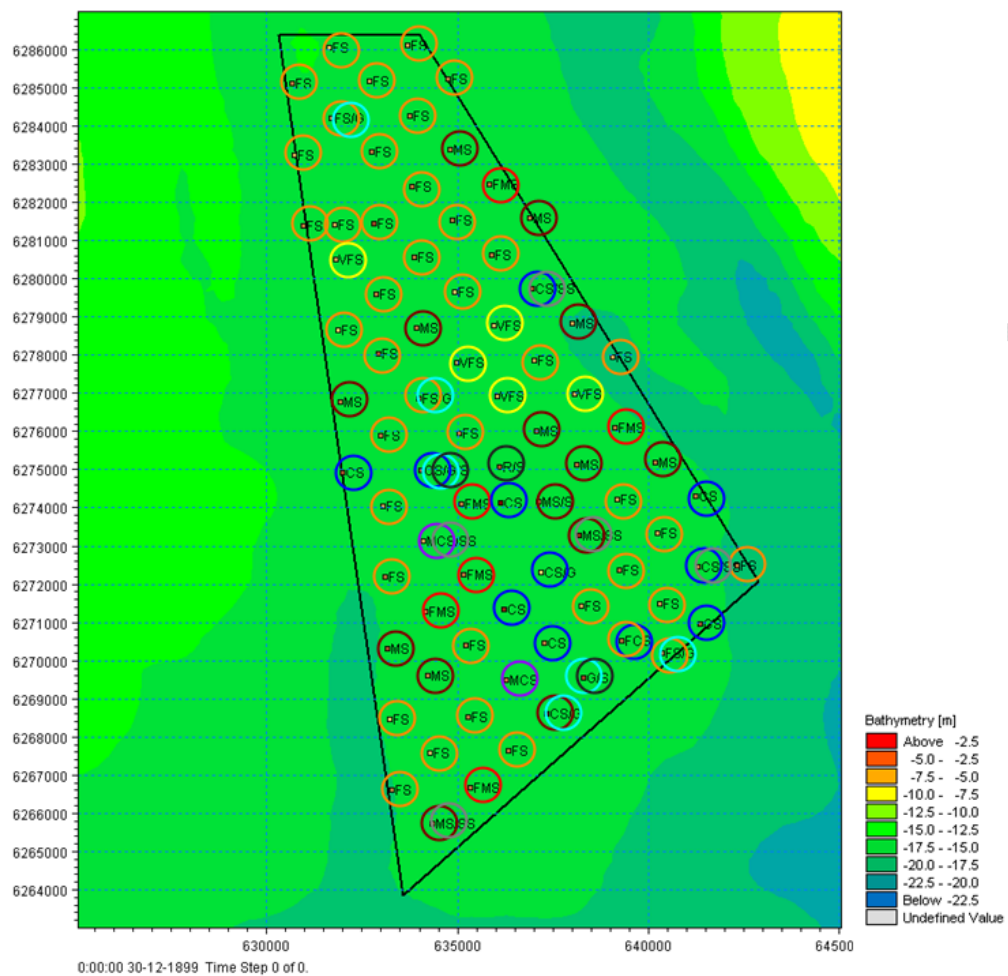
Figure 3-9   On site description of sediment samples collected in the present study in the project area by DHI /7/. VFS(yellow circle): very fine sand, FS(orange): fine sand, MS(brown): medium sand, FMS (red): fine to medium sand, CS(blue): coarse sand, MCS(purple): medium to coarse sand, SS(grey): small stones, S(black): stones, G(light blue): gravel, R: rocky bottom. The depth contours are shown by the colour coding on the right.
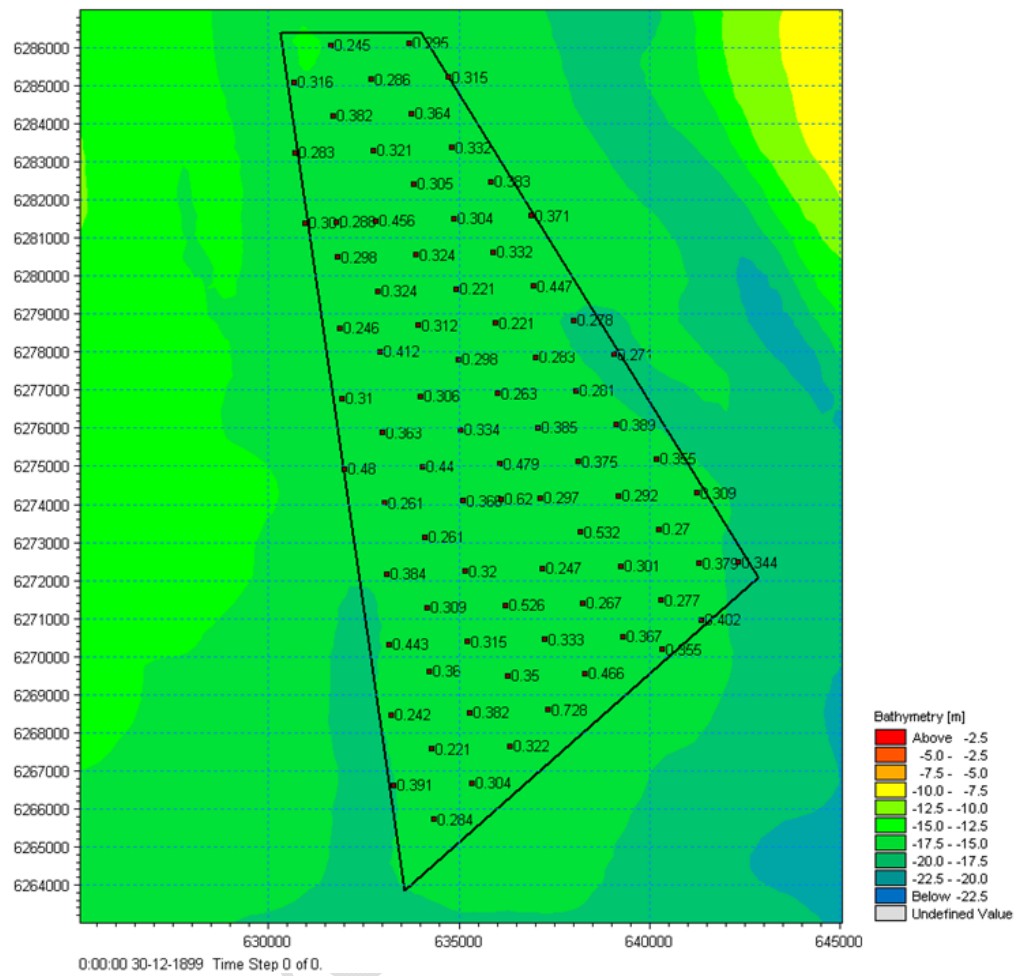
Figure 3-10   Distribution of the median grain size, d_{50}, over the wind mill area from sediment samples carried out in the present study by DHI /7/. The numbers at each location where samples are collected indicate the median grain size, d_{50}, of each sample. The depth contours are shown by the colour coding.
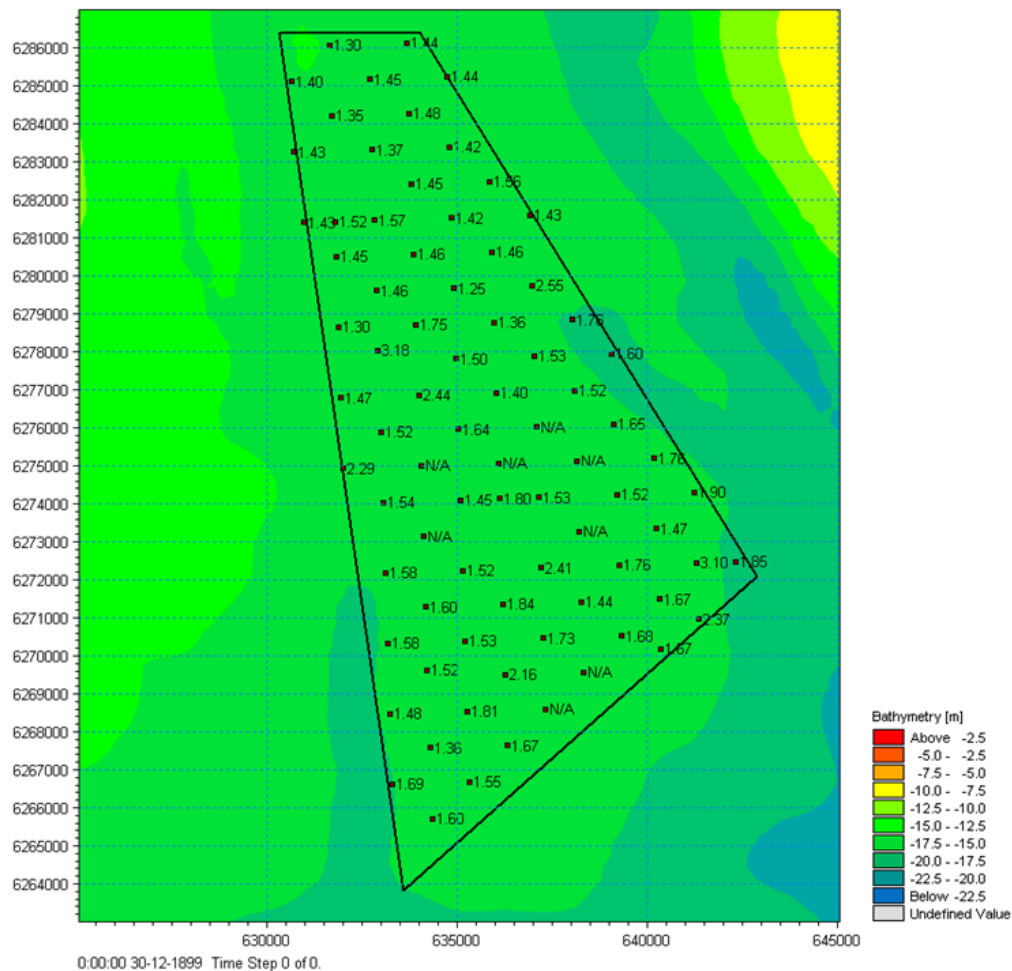
Figure 3-11   Distribution of sediment gradation, $\sigma = d_{84}/d_{16}$, in the project area as calculated by analysis of sediment samples carried out in the present study by DHI /7 /. The depth contours are shown by the colour coding.

3.2.3   General presentation of existing regional numerical models

The analyses presented in this study are to a large extent based on numerical models. This is partly due to a lack of measurements of relevant parameters within and near the project area. However, the numerical models have the advantage of being able to provide information covering the entire project area instead of pointwise, which is typically the case for measurements. Longer periods of time can also be calculated and furthermore they have the advantage that it is possible to incorporate the effects of the wind turbines in the numerical models.

The local models developed for the study of the Anholt Offshore Wind Farm can be considered as 'submodels' of large regional models existing at DHI. The local models are based on input from the large models at the edges of the local models. The qualities of the local models are hence strongly dependent on the regional models.

The regional models and the quality of these are described in the following sections. Details of the model setup are supplied in Appendix A and B along with details of the local models.

3.2.3.1 BANSAI: hydrodynamic and water quality model

DHI has several numerical 3D flow models running covering the North Sea, Kattegat and the Belt Sea and the Baltic Sea. Each of these models has individual strengths. With the purpose of water quality modelling, the best model is the so-called BANSAI model /12/. In the present study, the model provides input to the baseline study and the assessment of the impacts from the Anholt Offshore Wind Farm with regard to the flow field, water quality, geomorphology and sediment spreading caused by dredging operations. Of these issues, water quality was evaluated as the most critical.

The BANSAI model has been running operationally since 2001. The model covers the inner Danish waters including the Baltic Sea, and the North Sea.

The numerical model system consists of two parts:

- A hydrodynamic module for calculating the evolution in water levels, currents, salinity, and water temperature.

- An ecological module that calculates the spreading of nutrients, the primary production, the biomass, and other ecological parameters.

The main objective of this integrated model system is to calculate the environmental status in the area. This includes source apportioning, transport, dispersion, transformation and removal in the coastal and open sea marine waters of nutrients inputs to the North and Baltic Seas. Originally the BANSAI model /12/ was created in a co-operation between the Swedish Meteorological and Hydrological Institute (SMHI, Sweden), Finnish Institute of Marine Research (FIMR) and Danish Hydraulic Institute (DHI) supported by the Nordic Council of Ministers' Sea and Air Group.

The model is using DHI's 3-dimensional model system MIKE3 Classic. In the waters nearest Denmark (the eastern part of the North Sea, Skagerrak, Kattegat, the Belts and the western Baltic) a 3 nautical miles grid is used while a 9 nautical miles grid is used in the North Sea and in the eastern Baltic Sea. The model represents the water column with a 2m resolution. The model extension is shown in Figure 3-12.
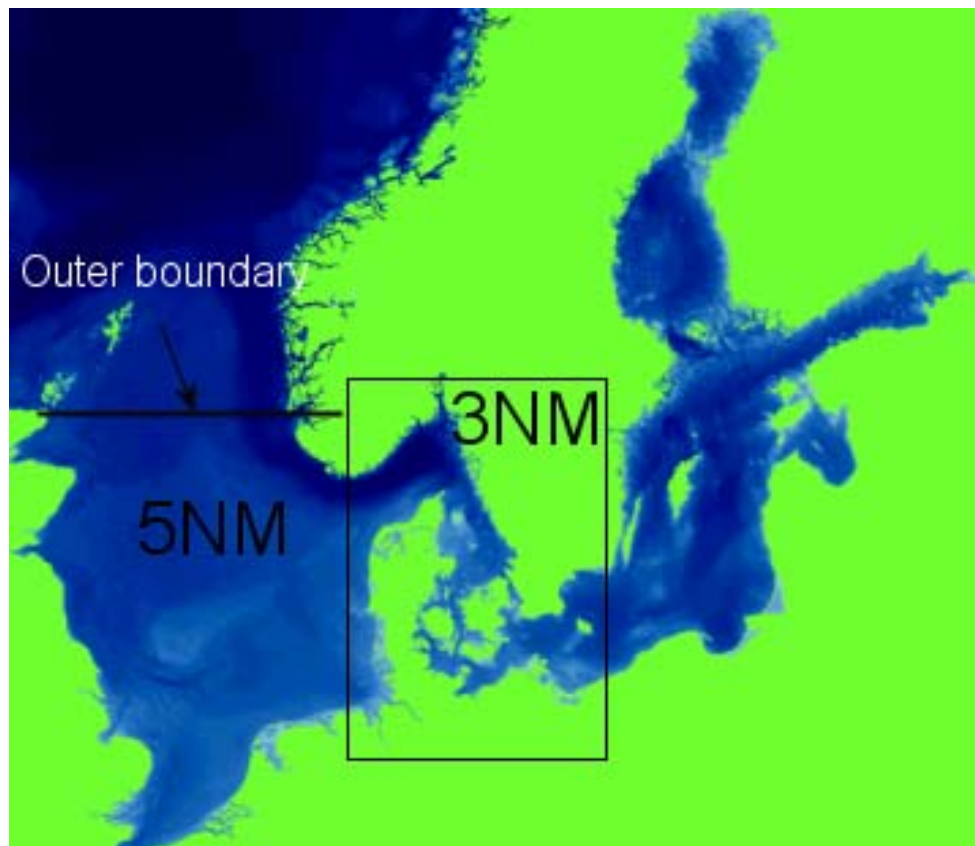
Figure 3-12   Overview of the BANSAI model extension

The model is operational and based on:

• Meteorology (model data from VEJR2 (2201-2007), Storm (2008-present))

• Tide, salinity-, temperature and nutrients on the edge of the Atlantic (tide from tidal constituents, salinity and temperature from monthly climatology from ICES, nutrients from climatology supplied with monitoring data from NERI and BSH)

• Runoff and nutrient loadings from land (runoff from monthly climatology from HELCOM, OSPAR, monitoring data from NERI, BSH and SMHI. nutrient loadings from climatology supplied with monitoring data from NERI and BSH).

The model was first calibrated based on measurements from the year 2000 and has been continuously improved since then.

The main calibration parameters and stations were the fluxes of salinity and heat (temperature) through the Belts since these control the flux of saline water in and out of the Kattegat. The representation of salinity in the Belts is extremely important

for ecological modelling in the area and is the key to obtain correct salinities, temperatures and nutrient loadings on both sides of the Belts.

Comparisons of measured and modelled salinities and temperatures from 2004 for stations in the Belts are shown in Figure 3-13 - Figure 3-15. In Figure 3-16 the salinity and temperature are given for a station near Bornholm. In Figure 3-17 measured and modelled data are shown for a location in Aalborg Bugt, which is the nearest measurement station to the project area. The location of the Aalborg Bugt Station is shown in Figure 3-17.

Results from the BANSAI model have been published in yearly status reports (see /9/) for the Nordic council of ministers among other places.
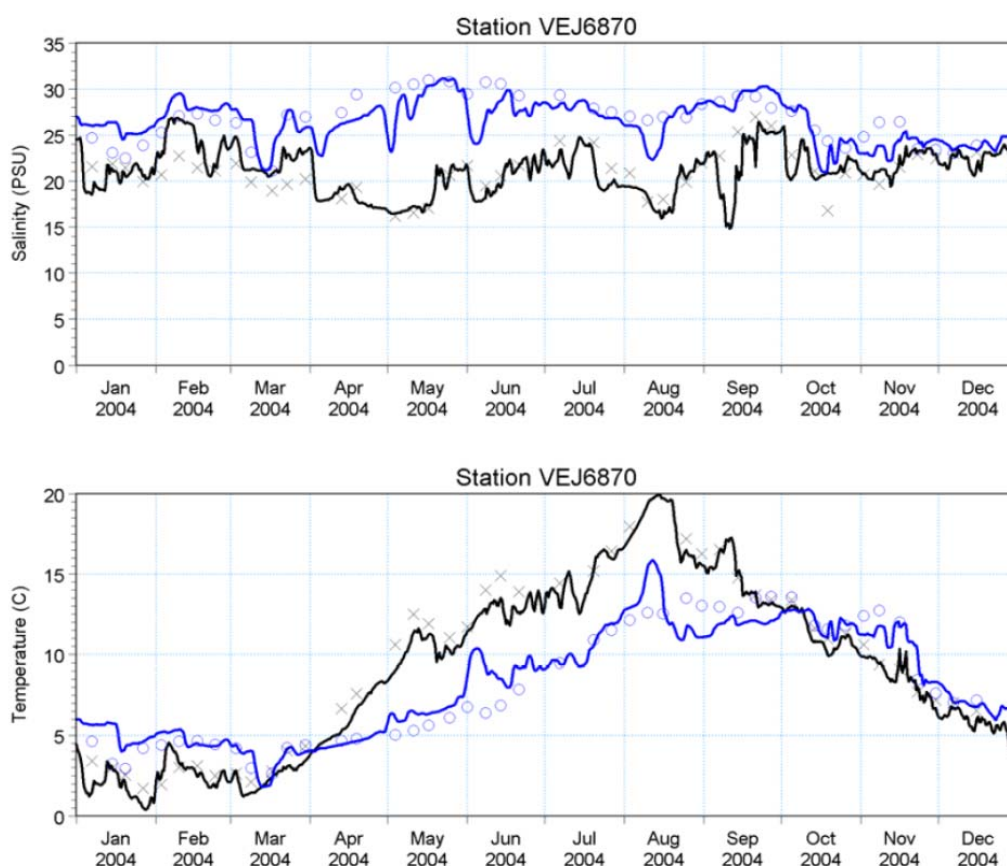
Figure 3-13   Comparison of measured and modelled salinities and temperatures in Little Belt, applying the BANSAI model. Surface (0 to -6 m, black), bottom (-21 m, blue). Monitoring data (symbols) and model data (curves).
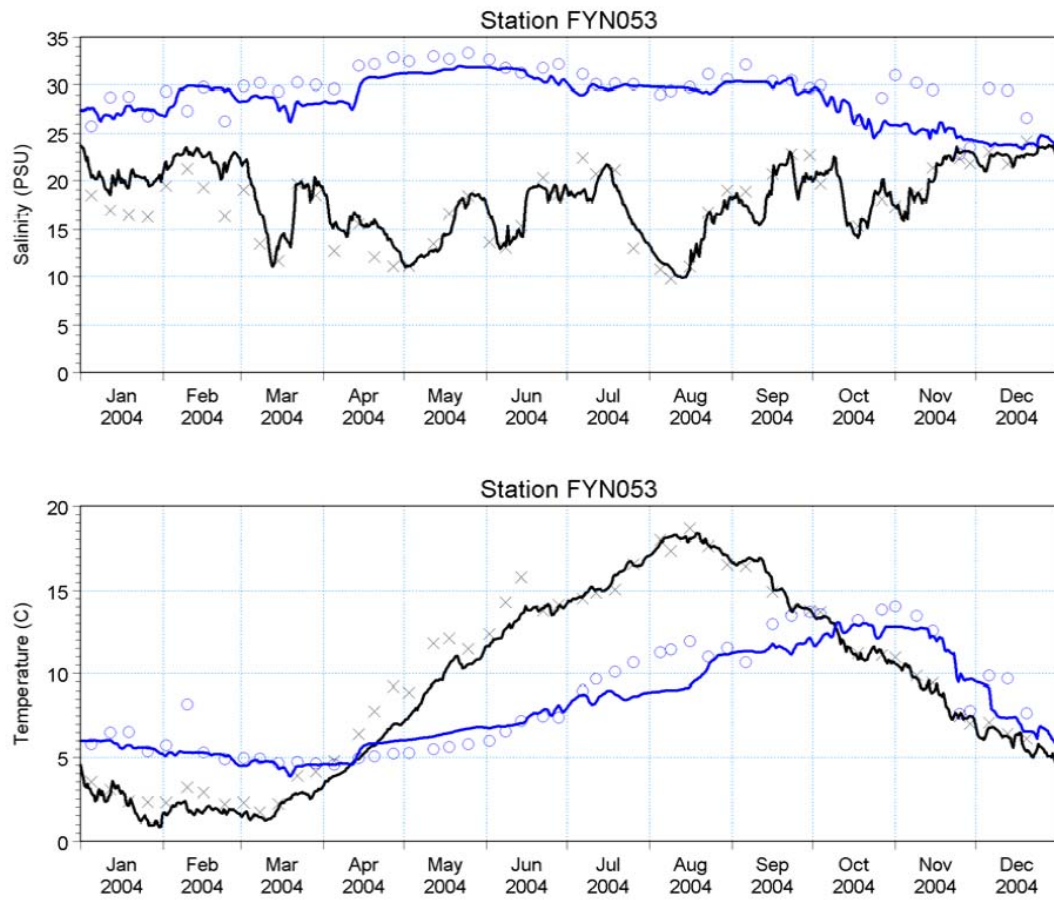
Figure 3-14   Comparison of measured and modelled salinities and temperatures in the Great
Belt, applying the BANSAI model.
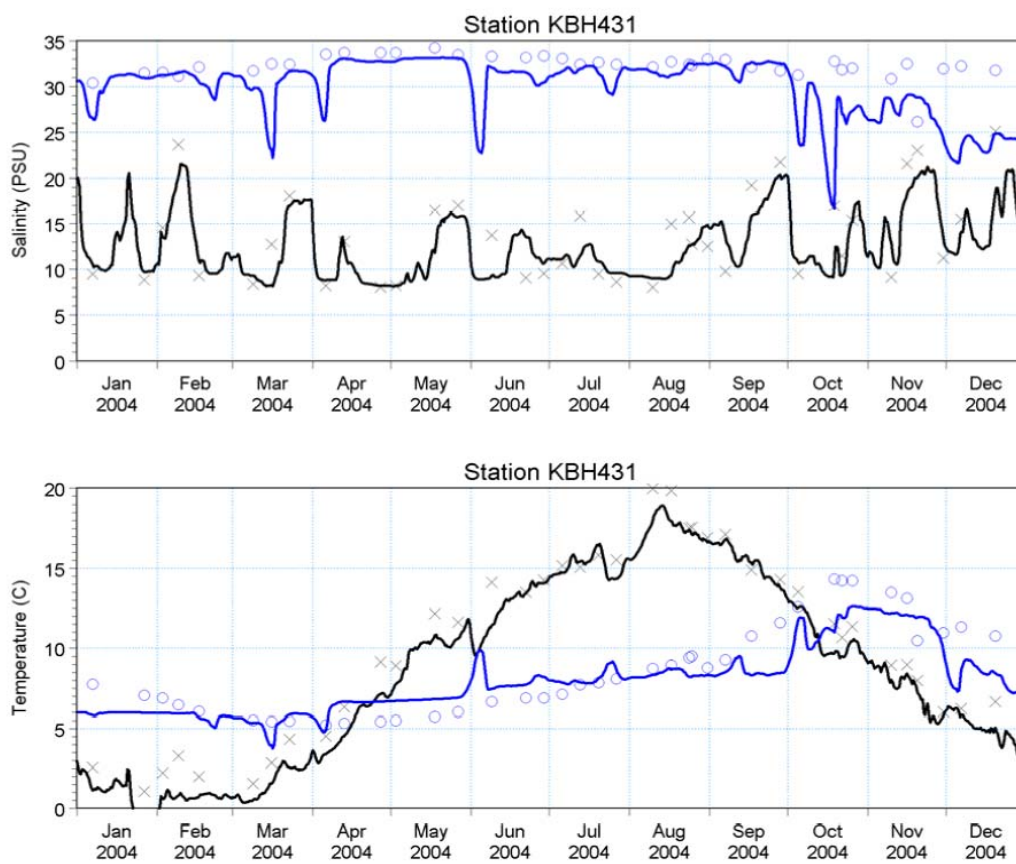
Figure 3-15   Comparison of measured and modelled salinities and temperatures in the Ore
sound, applying the BANSAI model.
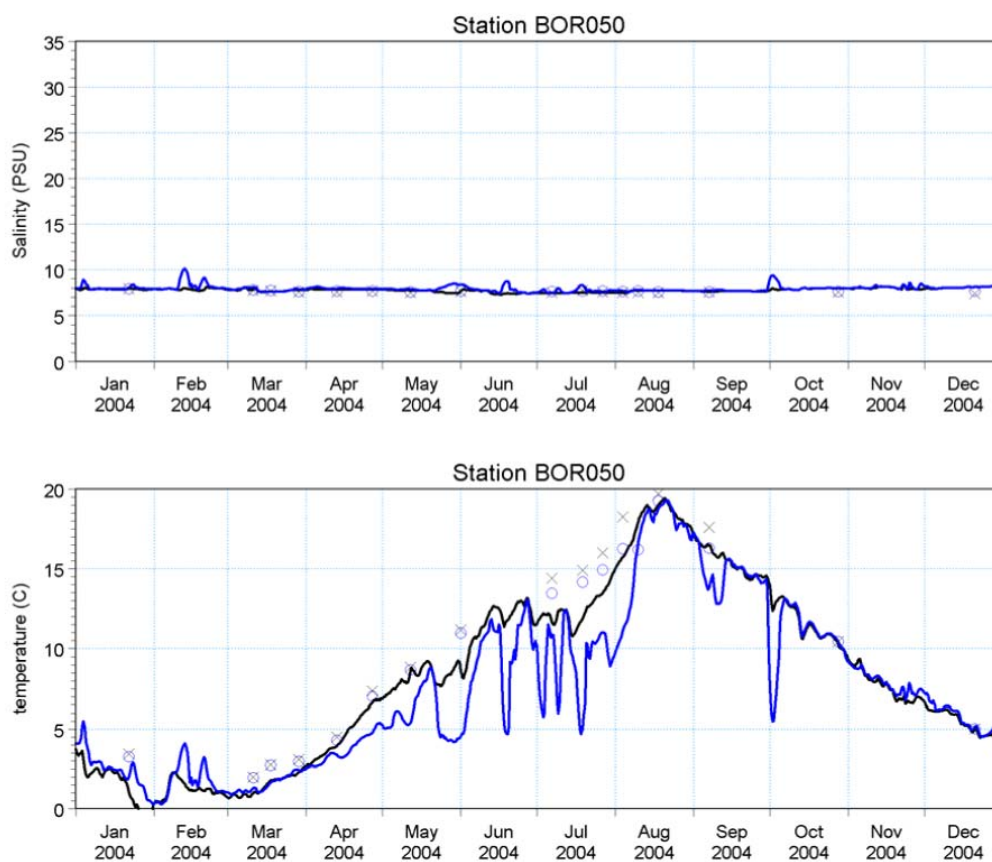
Figure 3-16   Comparison of measured and modelled salinities and temperatures near Born-
holm, applying the BANSAI model.
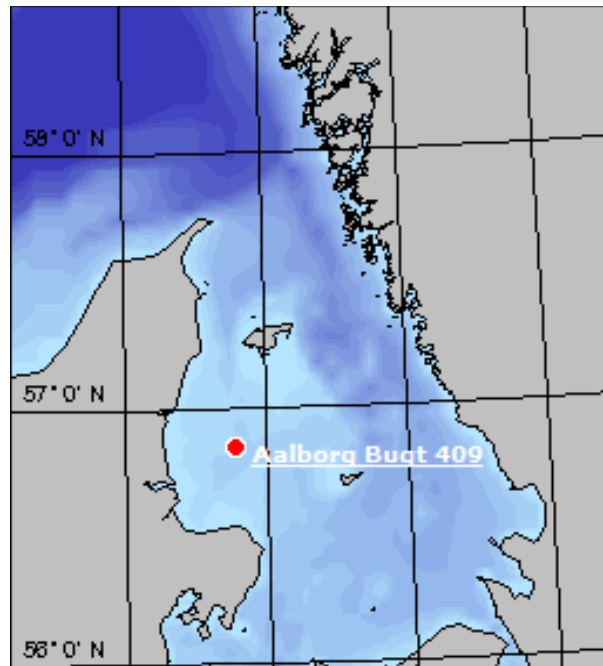
Figure 3-17   Location of Aalborg bugt station.
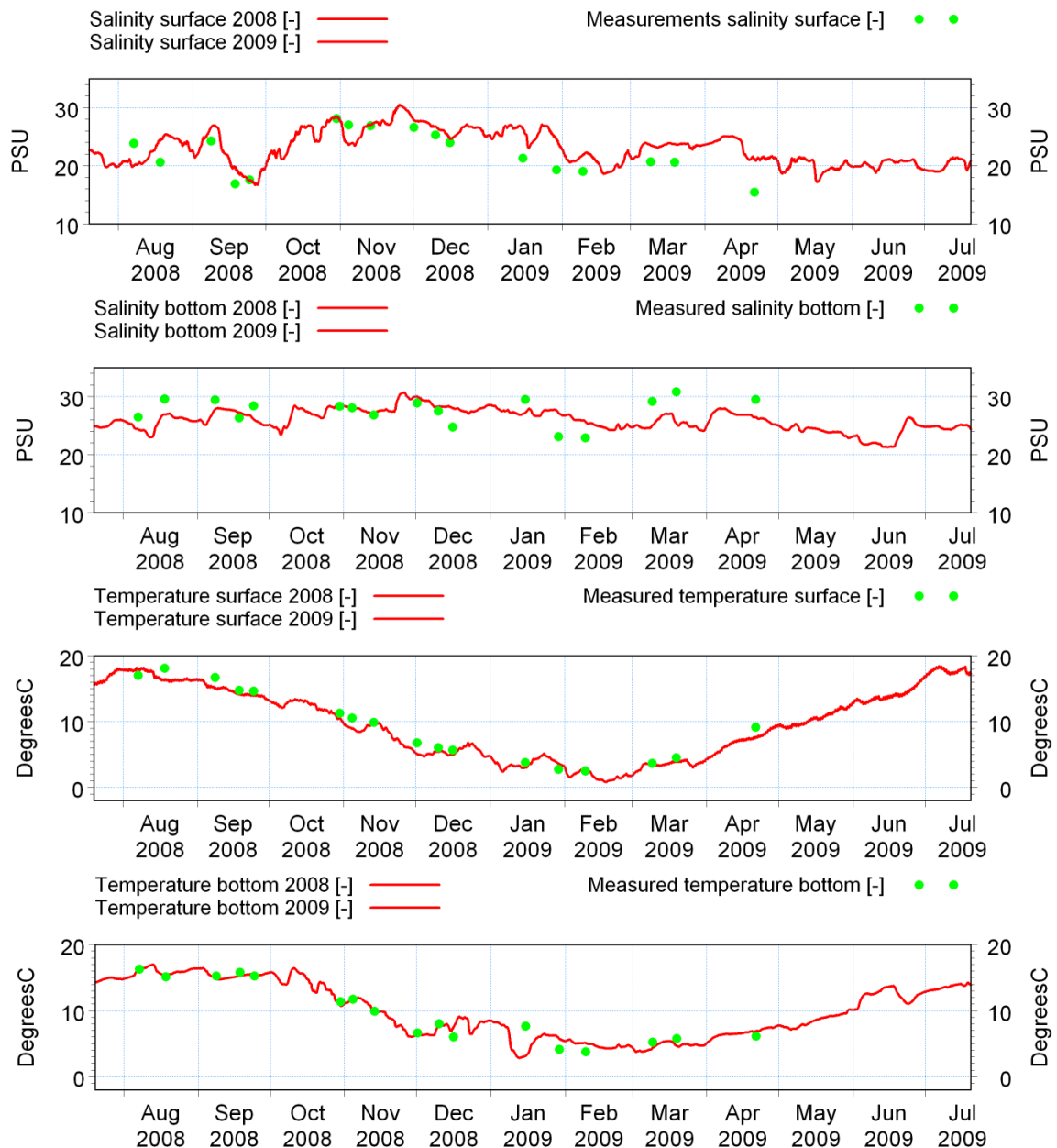
Figure 3-18   Comparison of measured and modelled salinities and temperatures in Aalborg Bugt, applying the BANSAI model.

3.2.3.2   **Regional wave model**

DHI has been involved in numerous studies of wave conditions in the North Sea, Kattegat and the Baltic Sea and has an operational wave model covering the area shown in Figure 3-19.

The wave model is based on DHI's numerical wave model, MIKE 21 SW, developed by DHI. MIKE 21 Spectral Wave Model is a third generation spectral wind-wave

model. The model simulates the growth, decay and transformation of wind generated waves and swells in offshore and coastal areas.

MIKE 21 SW solves the spectral wave action balance equation. At each mesh point, the wave field is represented by a discrete two-dimensional wave action density spectrum. The model includes the following physical phenomena:

- Wave growth by action of wind
- Non-linear wave-wave interaction
- Dissipation by white capping
- Dissipation by depth induced wave breaking
- Dissipation due to bottom friction
- Refraction due to variation in the water depth
- Wave-current interaction

The regional model is based on an flexible mesh which enables a high resolution of grid cells in the area of interest and a coarser mesh in areas where a less detailed solution is sufficient.

All boundaries in the model are closed. Nothing comes through and all variables go down to zero when reaching the boundary.

The model is forced by times series of 2D wind defined by u,v-components at 10m. The wind 2D file has a 1 hour time step. Wind data are available at DHI for the North Sea from 1979 to date (supplied by DMI (1979-1997), VEJR2 (1997-2007), Storm (2008-present)).
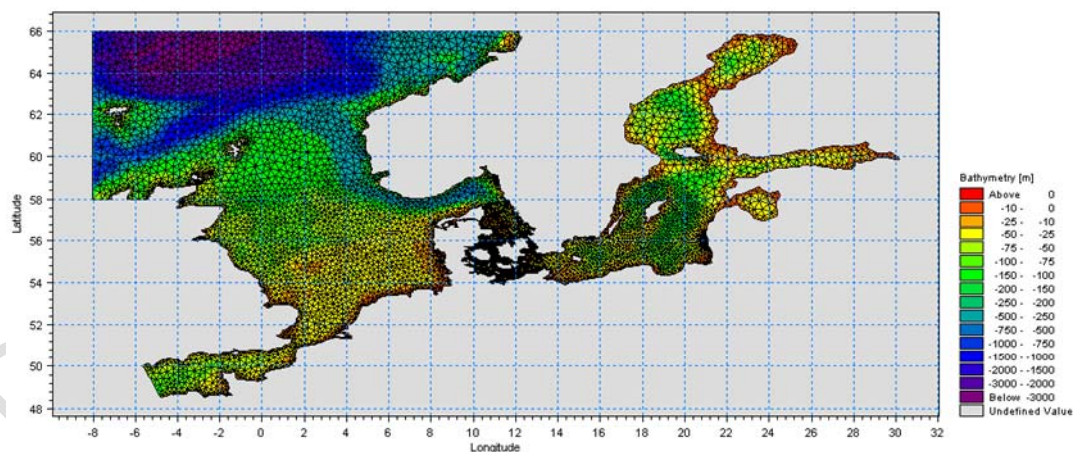
Figure 3-19   The area covered by DHI's operational wave model.

The regional wave model is often calibrated for the area of interest if data are available. A regional model setup, which was previously used in a study in the vicinity of Anholt (north of Læsø in the northern part of Kattegat /13/), has been applied. The

mesh in the regional model near the Anholt Wind Farm was refined as shown in Figure 3-20 for the present study.
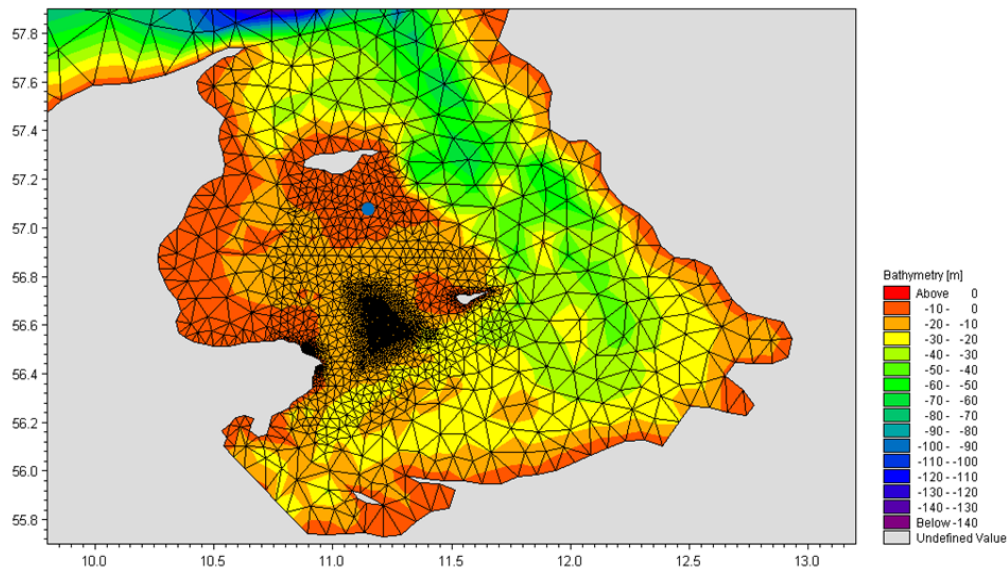
Figure 3-20   Zoom of mesh in regional wave model. The comparison of measured and modelled wave height has been carried out at the location indicated in blue.

The model was calibrated in /13/ and within this study a comparison of measured and modelled wave heights south of Læsø at the location indicated in blue on Figure 3-20 was carried out to check the validity of the model with the refined mesh. The comparison is shown in Figure 3-21. The significant wave height (H_{m0}) shown in the figure represents approximately an average of the largest 1/3 of the waves at a given time.

The modelled wave heights compare well to the measured data, all storm events and major peaks are taken into account by the model. To quantify how well the model conforms to the measurements, a number of statistical values are evaluated. These statistical values or quality indices are as follow:

- BIAS: average difference between modelled and measured values (mean error)

- Absolute mean error: average of the absolute difference between modelled and measured values (real mean error)

- Correlation coefficient: it reflects the degree to which the variation of the measured value is reflected in the variation of the modelled value.
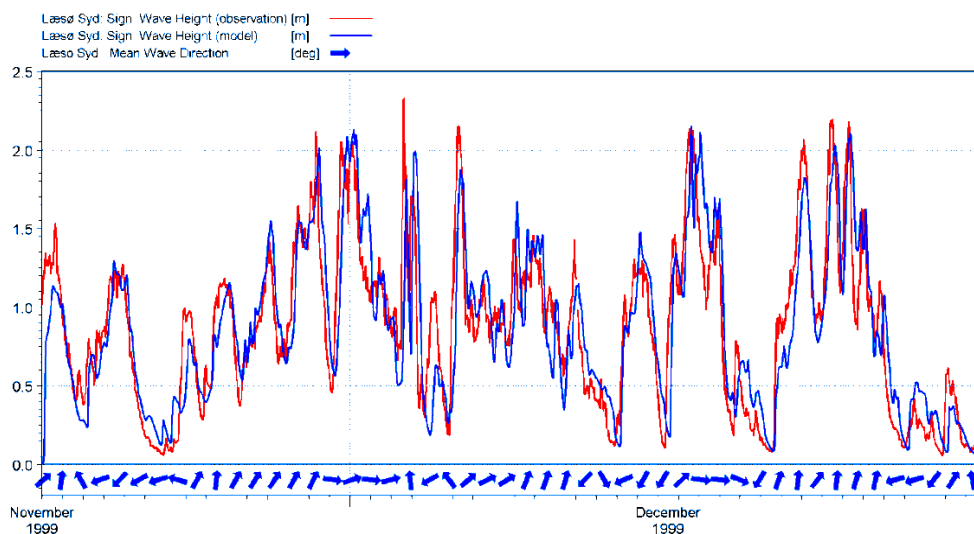
Figure 3-21   Comparison between the modelled and the observed values from the significant wave height at the extraction point shown in Figure 3-20. Measurements by DHI for ELSAM, 1999.

Table 3-1   Quality indices for significant wave height

Quality Index	Læsø Syd buoy
Mean (m)	0.79
BIAS (m)	0.002
Absolute mean error (m)	0.20
Correlation Coefficient	0.86

Although the BIAS value is almost null the absolute mean error shows an average difference of +20 cm indicating that the wave heights in average are predicted with an accuracy of 20 cm. It has to be noted that these two quality indices are measured in absolute values and should be compared to the wave height at Læsø Syd.

The correlation coefficient of 0.86 indicates an acceptable correlation over this time series.

The comparison shows that results from the regional wave model are very close to field data in a location very close to Anholt Wind Farm. In /13/ more calibration/validation results are shown.

3.2.4   Current, water level and stratification conditions

The flow through the Kattegat is governed by meteorology, the air pressure, tide, and the runoff from land. Depending on these parameters a salinity and/or tempera-

ture front will be travelling back and forth in the Kattegat. A front is defined as an area where water masses with different characteristics in salinity/temperature meet.

This is shown in a schematic way in Figure 3-22. The freshwater input from the rivers causes the waters of the estuary of the Baltic Sea to be less saline and hence less dense than the saltier waters of the North Sea. These water masses 'meet' in the Kattegat and the Danish Belts (The Oresound, The Great Belt and the Little Belt). The lighter (less saline and/or warmer) water overlays the denser water masses and causes the stratification in the water column.
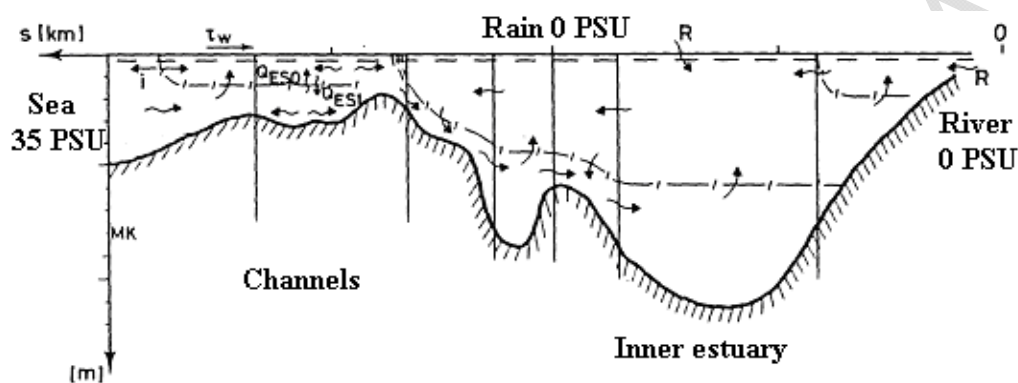
Figure 3-22   Schematical sketch of current conditions in Kattegat and the Belts between the North Sea and the estuary of the Baltic Sea. Figure from /14 /

3.2.4.1   **Methods**

The analysis of the current, water level and stratification conditions is based on analysis of numerical modelling results. The baseline conditions are described and form the basis for the further analysis of the impact due to a wind mill farm in the area.

The current and stratification conditions are studied from two different perspectives:

1. An analysis of the current conditions in a representative year. For this analysis, a 3D flow model is applied since the flow in the study area in the main part of the year is stratified.

2. An analysis of current conditions during selected rough weather situations with strong speeds. These events are denoted 'Storms' in this report (although the wind speeds are less than characterizing the technical definition of storms, wind speeds >24.5 m/s). For this analysis, a 2D depth integrated flow model is applied since the stirring effect from waves causes the water column in these situations to be well mixed. A 2D model is hence sufficient to describe the horizontal flow field in these situations.

1. leads to an analysis of the typical annual current conditions in and near the development site and is used in Chapter 3.2.4 to study the impact of the wind mill park on the annual mean current conditions and on the stratification conditions. The outcome of the calculations of the annual current conditions in the baseline situation is furthermore input to water quality modelling and input to calculations of annual sediment transport rates at selected positions in the development site.

2. is carried out to investigate the severe current conditions. The purpose of this is to make sure that the storm conditions are adequately represented in the mapping of the baseline conditions as well as in the further analysis of the impact of the wind mill park on the flow conditions. During an average year some storm conditions will occur. However, during a single year critical storms from all the most critical directions do not occur. Severe storm conditions are therefore selected from a 10-year period and calculated separately. This ensures that the storm conditions are represented in the analysis carried out to estimate the maximum extent of the area of influence of the wind mill park on the current climate. Specifically it is required to investigate if the wind mill park can lead to any significant impact on the current conditions as far away as near the shorelines of Djursland and Anholt.

The water level conditions are described based on work presented in /10/.

3.2.4.1.1 Methodology for 3D modelling of annual current and stratification conditions

The approach for simulation of the annual conditions is described briefly in the following. The model setup and the selection of the representative year chosen for the numerical modelling of the annual current conditions are described. Further details are included in Appendix A.

<u>Short description of the model and the setup</u>

The numerical modelling of the annual flow conditions are based on the best model setup and data for the area of Kattegat available for DHI. DHI has several numerical 3D flow models running covering the North Sea, Kattegat and the Belt Sea and the Baltic Sea – these models are referred to as regional models. Each of these models has individual strengths. With the purpose of water quality modelling, the best model is the socalled BANSAI model (/12/). This model setup has been reused in the numerical modelling carried out in this study. A local model has hence been set up with the same model setup as the BANSAI model applying boundary condition from the regional model.

The BANSAI model has a resolution of 3 nautical miles. The local model applied has this resolution in the outer mesh but by use of the nesting technique this is downscaled by a factor 9 to a resolution of app. 600 m in the area of interest where the wind mills are located. An overview of the bathymetry and the nestings used is given in Figure 3-23.

The distance between the wind mills is 600 m – 700 m which means that there will be approximately one wind turbine in each cell in the model area.

Hydraulically a wind turbine is an obstacle that partly blocks the water and partly imposes a hydraulic resistance in the form of a drag. Locally the blocking effect is causing main impacts, but on a larger scale the increased hydraulic resistance is the most important factor, which potentially could reduce the flow through the wind farm and divert it around the area. A grid scale of 600 m is fully sufficient to model the hydraulic resistance from the wind farm; however, to include the blocking effect would require a grid spacing less than 5-10 m. The local effects are assessed by a desk study.
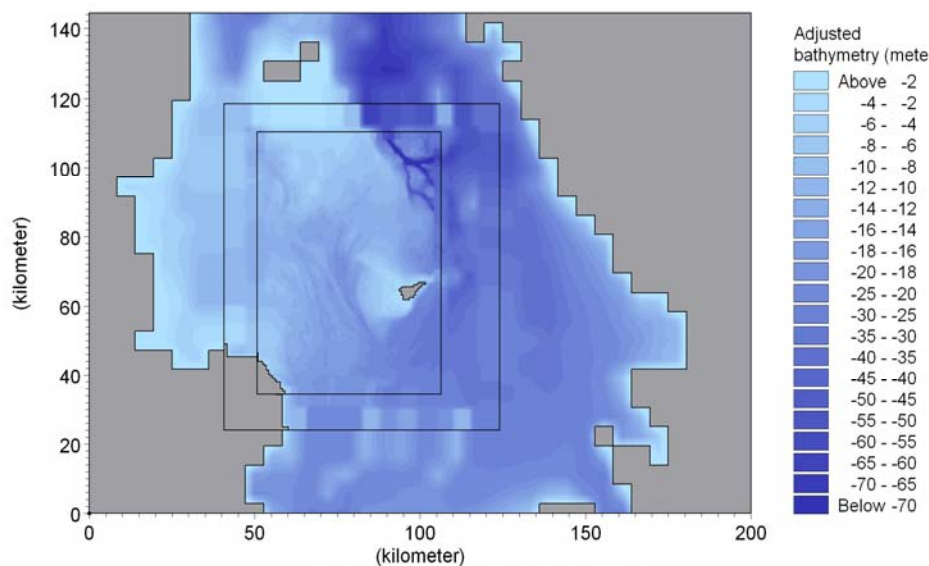
Figure 3-23   Applied bathymetry squares are areas of decreasing grid size. Finest resolution is 617.33m.

The system has three boundaries. The Oresound, the southern Kattegat, and north of Læsø. All boundaries are forced with data extracted from the BANSAI model. The northern boundary and the southern Kattegat boundary are forced with salinity, temperature and fluxes. The Oresund boundary is forced with surface elevation temperature and salinity.

Initial fields of elevations, salinity and temperature came from the BANSAI model.

The meteorological forcings came from the VEJR2 in the form of numerically simulated wind, temperature, insolation and precipitation. The runoff data are statistical values. For further information on the model forcings please see /12/ or see Appendix A.

The most important settings are given in Table 3-2.

Table 3-2   Main model settings for the local 3D hydrodynamic model applied in the base-
             line simulations

Parameter	Value
Simulation mode	Non hydrostatic
Number of nestings	3
Number of layers	35
Vertical grid spacing	2m
Grid spacing area 1	3 nautical miles (5556 m)
Grid spacing area 2	1 nautical mile (1852 m)
Grid spacing area 3	1/3 nautical mile (617 m)
Simulation period	01/01/2005 -01/01/2006
Timestep	60 sec
Boundary southern Kattegat	Transfer files from BANSAI model (Flux based)
Boundary northern Kattegat	Transfer files from BANSAI model (Flux based)
Boundary Oresund	Transfer files from BANSAI model (Elevation based)
Heat exchange included	Yes
Precipitation	2D map (resolution 3 nautical miles, 5556 m)
Air temperature	2D map (resolution 3 nautical miles, 5556 m)
Wind	2D map (resolution 3 nautical miles, 5556 m)

The model was validated against data from the original BANSAI model. The model
reproduced the original model results very well. For further details on the model
setup and validation see Appendix A.

3.2.4.1.2 **Methodology for 2D modelling of storm conditions**

Short model description and setup

The hydrodynamic modelling under storm conditions has been carried out using
DHI's numerical hydrodynamic model, MIKE 21-FM HD. This model describes the
depth-integrated current, driven by a combined forcing, which may comprise forces
induced by wave breaking, tide and wind by solving the depth-averaged equations of
continuity and momentum.

The extent of the domain, the bathymetry and the mesh which have been used for
the modelling of the storm conditions are shown on Figure 3-24. The modelled area
extends from immediately south of Læsø to the southern boundary defined by the
spit of Odden and the southern tip of Djursland. A flexible mesh composed of ap-
proximately 101,000 triangular elements, the resolution of which increase gradually

from 1,800 m at the boundaries to 50 m at the wind farm location has been created. The resolution in the proximity of Djursland and Anholt has been set to 800m in order to describe carefully the impact of the wind mills on wave and current conditions near the shorelines at Djursland and Anholt.

The mesh does not resolve the very local effect on the currents. The minimum element size is about 50 m and the cone of the wind mill foundations for the 2.3 MW wind mills is 5-14 m across the water depth. The local effects take place within a few diameters of the wind mill foundation and are described further in 3.3.2.2.1. Outside this local zone near each wind mill foundation, the variations in the flow (and wave fields) are smaller and the mesh is fine enough to describe the variations in the flow (and wave) field in the gaps between the wind mills and in the area surrounding the wind farm.

The driving forces applied in the model consist of time- and spatially varying wind forces and Coriolis force. At the north and south boundaries, time series of fluxes have been applied, whereas the boundary condition at the Øresund's entrance has been defined in the form of a time varying water level. Bed friction has been included by means of a Manning number formulation. Contribution of the wave-induced current due to gradients in radiation stresses over the domain during the storm conditions has also been investigated and described in Appendix A. The impact from the radiation stresses on the current field has shown to be insignificant.

The input to the 2D model has been extracted from DHI's model 'Vandudsigten', a 3D regional model covering the North Sea, the Kattegat and the Baltic Sea. Vandudsigten is a validated model and the numerical 2D model developed in this project has been calibrated against 'Vandudsigten'.

The main settings for the model are summarized in Table 3-3. Further details regarding the model setup and validation are described in Appendix A.
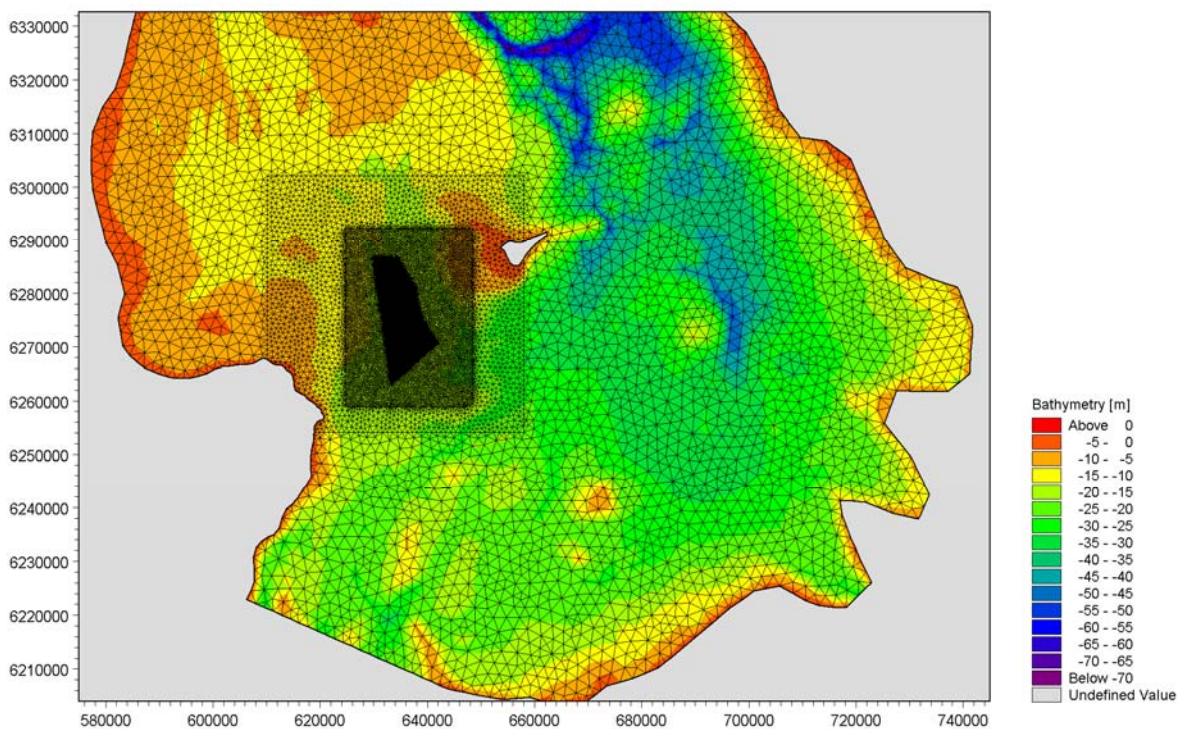
Figure 3-24   Bathymetry and mesh of the entire domain created for the modelling of storm conditions. The horizontal coordinates system is UTM-32 (WGS84).

Table 3-3   Main model settings for the numerical 2D hydrodynamic model applied in the simulation of the storm conditions.

Parameter	Value
Mesh size – coarsest mesh	1800 m
Mesh size – finest mesh	50 m
Simulation periods	25/11/1999-04/12/1999 (Storm 1) 13/01/2000-20/01/2000 (Storm 2) 18/12/1999-28/12/1999 (Storm 3) 26/10/2000-04/11/2000 (Storm 4)
Maximum time step	60 s
Boundaries	3 boundaries: Boundary 2: South of Læsø Boundary 3: Between the spit of Odden and the southern tip of Djursland Boundary 4: Øresund
Flood and dry	Included
Water density	Barotropic
Horizontal eddy viscosity for-mulation	Smagorinsky - Smagorinsky coefficient set to 0.28

Parameter	Value
Bed resistance	Calibrated 2D Manning no. map. Roughly varying as: M=35 $m^{1/3}$/s: 0-10m water depth M=41 $m^{1/3}$/s: 10-15m + above 25 water depth M=50 $m^{1/3}$/s: 15-25m water depth M=60 $m^{1/3}$/s: selected areas, 10-20 m water depth
Coriolis forcing	Varying in the domain, it is obtained from the geographical latitude of the model
Initial conditions	Surface elevation extraction from the model 'Vandudsigten'
Wind forcing	Spatial and time varying wind from Vejr2 (resolution 3 nautical miles = 5556 m). The wind forcing is calculated with a wind friction factor varying between 0.0013 and 0.0024 for wind in the range of 7 -25m/s
Wave radiation stresses	not included
Boundary conditions	Boundary 2: time series of flux based on the depth integration of the current speed extracted from the model 'Vandudsigten' Boundary 3: time series of flux based on the depth integration of the current speed extracted from the model 'Vandudsigten' Boundary 4: time varying water level

Choice of storm events

Four storm periods have been selected based on statistical analyses of time series of hindcast wind and surface current. The time series have been extracted from the DHI's 3D regional model, ´BANSAI' at (642018E; 6265325N (UTM-32), see Figure 3-37 further below in the report) at the southern limit of the wind farm area for the period 1998 to 2008.

The corresponding wind rose, scatter diagram and return period of extracted hindcast wind speed are shown on Figure 3-25, Table 3-4 and Figure 3-26, respectively. The return period indicates how frequent on average a given wind speed occurs. It can be seen that the typical wind directions are from the sector ESE to WNW and the wind speed exceeds 20 m/s in less than 0.1% of the time. The current rose for depth averaged current speeds in Figure 3-27 clearly points out that the current at the future location of the wind mills is oriented in the N-S axis and is predominantly north-going. The depth averaged current speeds reach a magnitude of about 1 m/s.

Four storms events were selected based on the previous information. They were chosen as severe combinations of wind and current in order to study the impacts of the wind farm in situations with high waves and strong current.

Each storm period covers 3 days and is characterized by a fairly constant wind speed and direction. In Figure 3-28 to Figure 3-31, the time series of the wind and current

conditions during the four selected periods are shown, while in Table 3-5 and Table 3-6 the main characteristics of the wind and current for each storm are summarized.

Storm 1 represents a very strong wind condition. The wind blows from west with a speed that exceeds 15 m/s during 20 hours. The peak wind speed is 23.8 m/s which correspond to a return period of 10 years (c.f. Figure 3-26). Within this event, the current reaches a maximum of 0.6 m/s and the mean flow direction is directed to-wards the south.

Storm 2, 3 and 4 have peak wind speeds between 18 m/s and 20 m/s. This type of storm occurs 1-3 times in an average year (see Figure 3-26). Storms 2 and 3 have been chosen as they combine wind and current coming from the same direction as the main axis (N-S) of the wind farm. Storm 2 is characterized by wind of medium intensity coming from N-NW combined with a high south-directed current. The peak wind speed is 18.4 m/s; it occurs with a return period of half a year and the maxi-mum current speed is 1.1 m/s. For storm 3 the wind coming from the South is slightly stronger; it reaches 20.3 m/s and occurs on average once every year. The corresponding current is directed towards the north with a peak of about 0.9 m/s. For these two storms the current and the wind pattern are clearly strongly corre-lated.

For Storm 4, the combined effect of a strong wind blowing from SSW reaching 19.7 m/s and a strong north-directed current have been selected in order to determine the effect of the wind mills on wave and current at the western coast of Anholt.
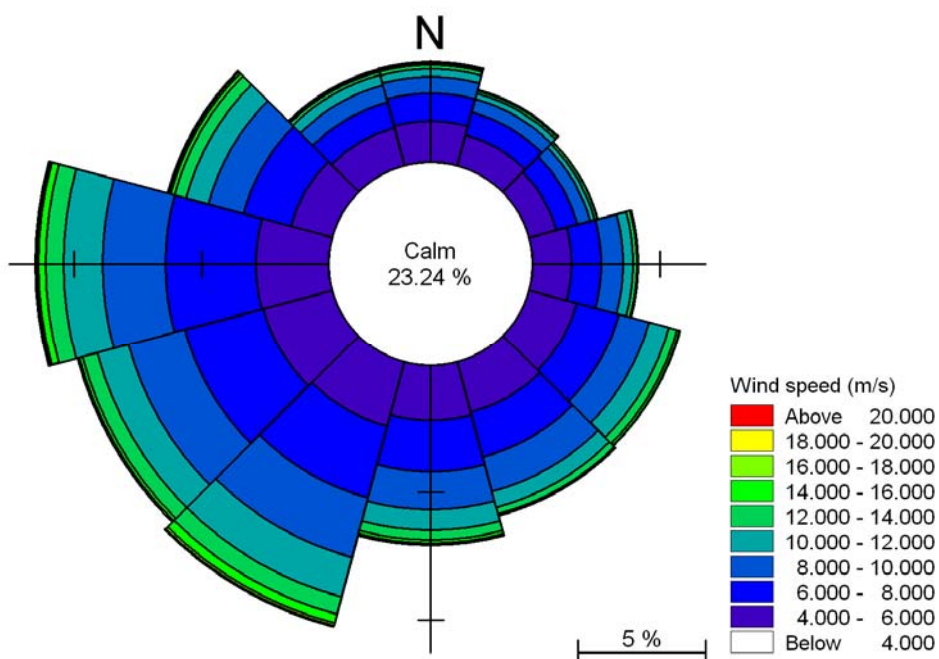
Figure 3-25   Hindcast wind (model data from VEJR2) covering the period from 1998 to 2008 extracted at (642018E; 6265325N (UTM-32 (WGS84))) just south of the project area. Directions are defined as "coming from".

Table 3-4   Scatter diagram for hindcast wind data 1998-2008 at (642018E; 6265325N (UTM-32 (WGS84))) indicating the duration in percent of the year of each combination of wind direction (by sector of 30°) and speed. Directions are defined as "coming from".

|	<10 m/s	10-12m/s	12-14m/s	14-16m/s	16-18m/s	18-20m/s	20-22m/s	22-24m/s	>24 m/s
N	5.025	0.344	0.164	0.083	0.031	0.015	0.001		
NNE	4.422	0.227	0.100	0.056	0.007	0.001			
ENE	4.165	0.200	0.106	0.009	0.006				
E	5.562	0.382	0.157	0.034	0.003	0.009			
ESE	6.920	0.793	0.353	0.099	0.028				
SSE	7.267	0.654	0.275	0.062	0.009				
S	7.702	0.847	0.385	0.120	0.050	0.027	0.003		
SSW	10.111	1.628	0.743	0.380	0.100	0.039	0.001	0.004	
WSW	10.417	1.257	0.592	0.138	0.079	0.011	0.003	0.002	
W	10.843	1.536	0.715	0.284	0.078	0.037	0.011	0.009	
WNW	6.932	0.908	0.458	0.179	0.071	0.031	0.012	0.003	0.003
NNW	4.999	0.427	0.152	0.074	0.025	0.003			
Σ	84.363	9.202	4.200	1.519	0.488	0.174	0.032	0.019	0.003
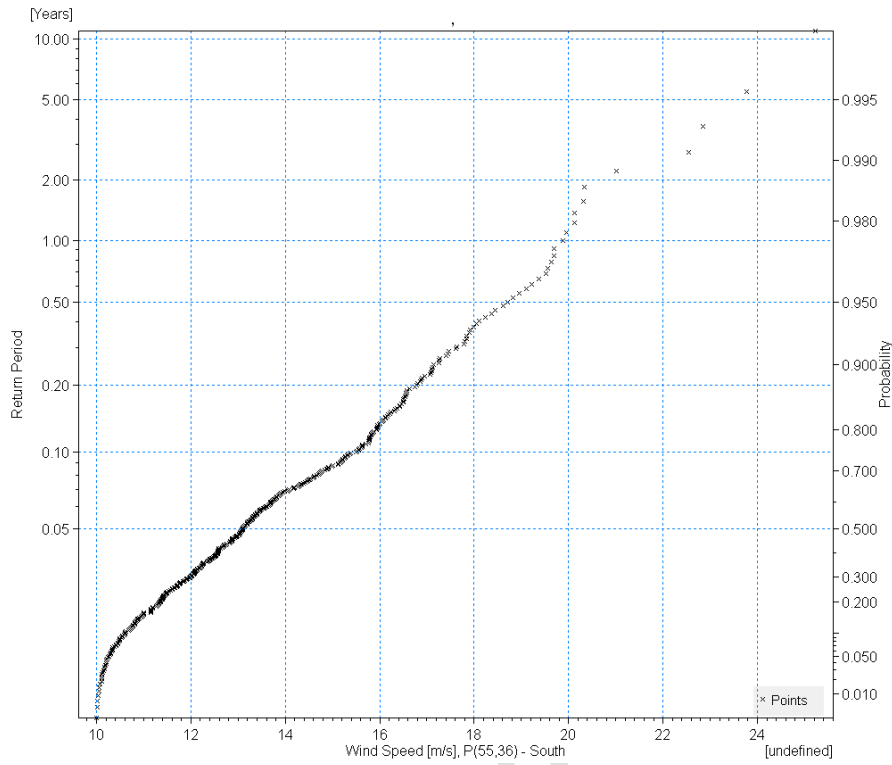
Figure 3-26   Return period for modelled wind speeds at (642018E; 6265325N (UTM-32 (WGS84))).
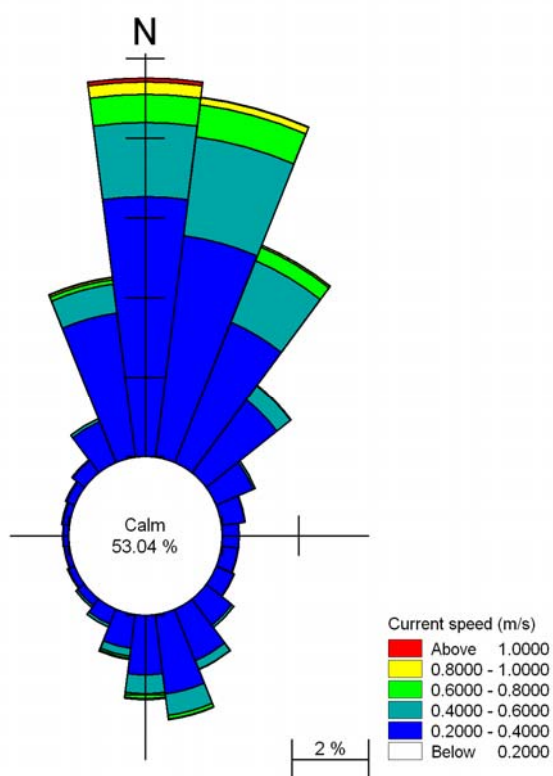
Figure 3-27   Hindcast surface current covering the period from 1998 to 2008 extracted at (642018E; 6265325N (UTM-32 (WGS84))) from DHI's Vandudsigten 3D regional model. Directions are defined as "going to".
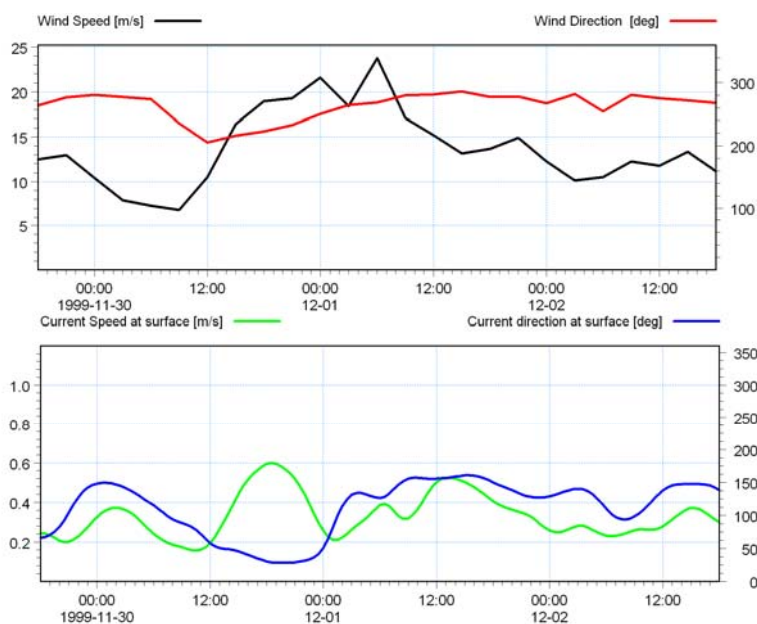
Figure 3-28   Hindcast wind speed and direction (up), surface current speed and direction (down) for **Storm 1** at (642018E; 6265325N (UTM-32 (WGS84))). Directions are defined as "coming from" for the wind and "going to" for the current.
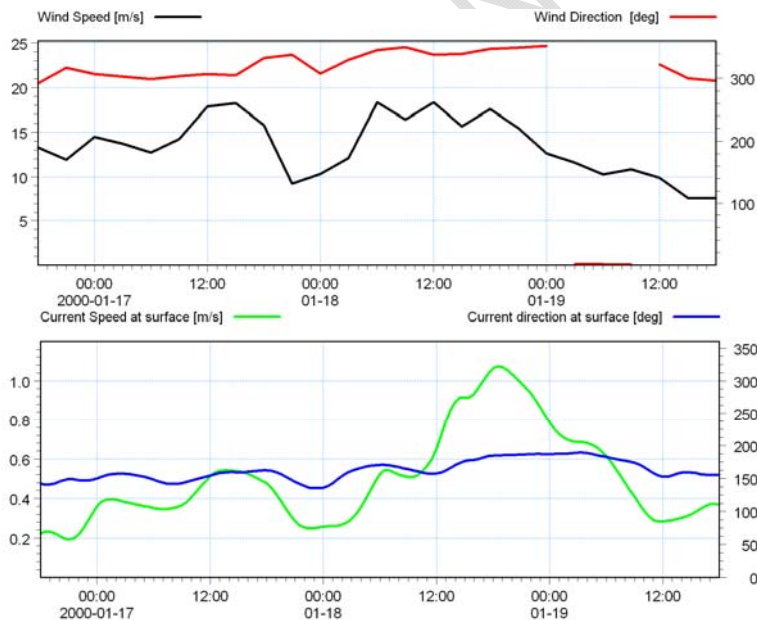
Figure 3-29   Hindcast wind speed and direction (up), surface current speed and direction (down) for **Storm 2** at (642018E; 6265325N (UTM-32 (WGS84))). Directions are defined as "coming from" for the wind and "going to" for the current.
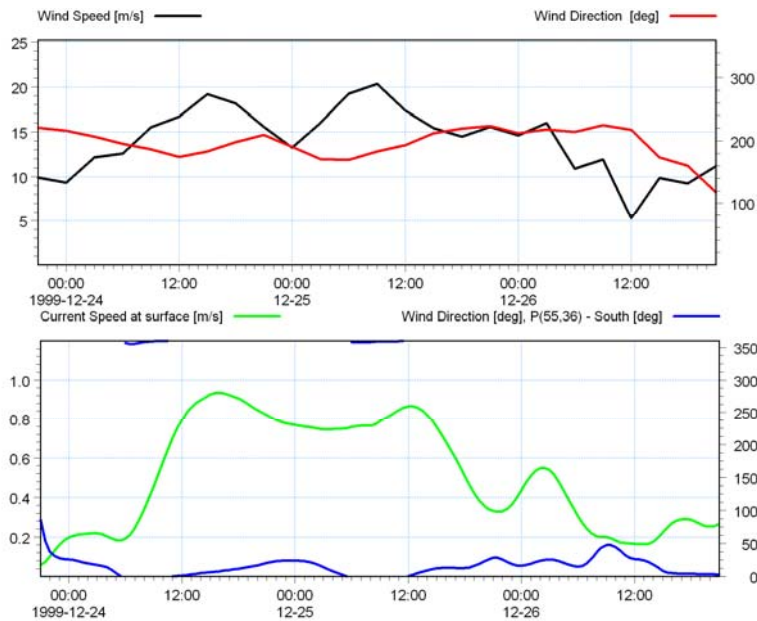
Figure 3-30   Hindcast wind speed and direction (up), surface current speed and direction (down) for **Storm 3** at (642018E; 6265325N (UTM-32 (WGS84))). Directions are defined as "coming from" for the wind and "going to" for the current.
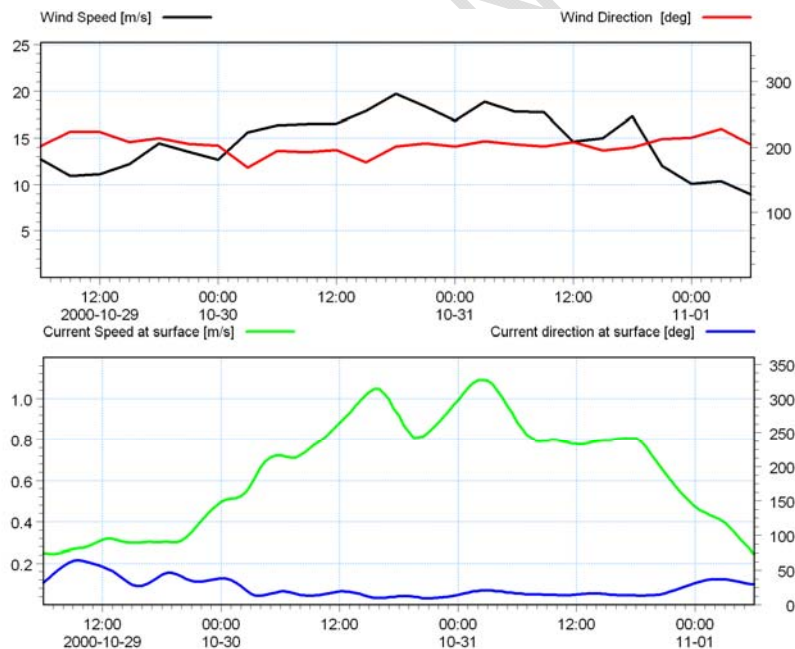

Figure 3-31   Hindcast wind speed and direction (up), surface current speed and direction (down) for **Storm 4** at (642018E; 6265325N (UTM-32 (WGS84))). Directions are defined as "coming from" for the wind and "going to" for the current.

Table 3-5   Characteristics of the wind during the four selected storms (hindcast wind speed and direction extracted at (642018E; 6265325N (UTM-32 (WGS84))). Directions are defined as "coming from".

Period	Peak wind speed (m/s)	Wind direction at peak wind speed (degN)	Average wind speed (m/s)	Average wind direction (degN)
Storm 1: **Strong wind from W** **Medium South-directed current** 29/11/1999 18:00 AM 02/12/1999 18:00 AM	23.8	268.2	13.7	262.1
Storm 2: **Medium-strong wind from NW-N** **Strong South-directed current** 16/01/2000 18:00 AM 19/01/2000 18:00 AM	18.4	345.2	13.5	327.2
Storm 3: **Strong wind from S** **Strong North-directed current** 23/12/1999 21:00 AM 26/12/1999 21:00 AM	20.3	183.0	14.0	195.4
Storm 4: **Strong wind from SSW** **Strong North-directed current** 29/10/2000 06:00 PM 01/11/2000 06:00 AM	19.7	201.1	14.7	202.4

Table 3-6   Characteristics of the surface current during four selected storms (hindcast surface current speed and direction extracted at (642018E; 6265325N (UTM-32 (WGS84))). Directions refer to "going to".

Period	Peak current speed (m/s)	Average current speed (m/s)	Average current direction (degN)
Storm 1: **Strong wind from W** **Medium South-directed current** 29/11/1999 18:00 AM 02/12/1999 18:00 AM	0.6	0.3	115.3
Storm 2: **Medium-strong wind from NW-N** **Strong South-directed current** 16/01/2000 18:00 AM 19/01/2000 18:00 AM	1.1	0.5	168
Storm 3: **Strong wind from S** **Strong North-directed current** 23/12/1999 21:00 AM 26/12/1999 21:00 AM	0.9	0.5	11.3
Storm 4: **Strong wind from SSW** **Strong North-directed current** 29/10/2000 06:00 PM 01/11/2000 06:00 AM	1.1	0.6	19.9

3.2.4.2   **Tides and water levels**

Water level variations due to tide in Kattegat are relatively small. The tidal variation at Århus is shown in Figure 3-32 during a period of one month. It appears that the tidal range during spring tide is about 0.5m and decreases to be in the order of 0.2 m during neap tide.

Under severe weather conditions, water level variations increase significantly. Statistical analyses of the water level variations were carried out in /10/ based on model data from the period1979 to 2007. Results showed for example that the 50 year return period high water level is approximately 1.5m MSL and the low water level for the 50 year return period is about -0.8 m MSL in the north-eastern part of the project area (see Table 3-7). The return period is describing the <u>average</u> period of time between events.
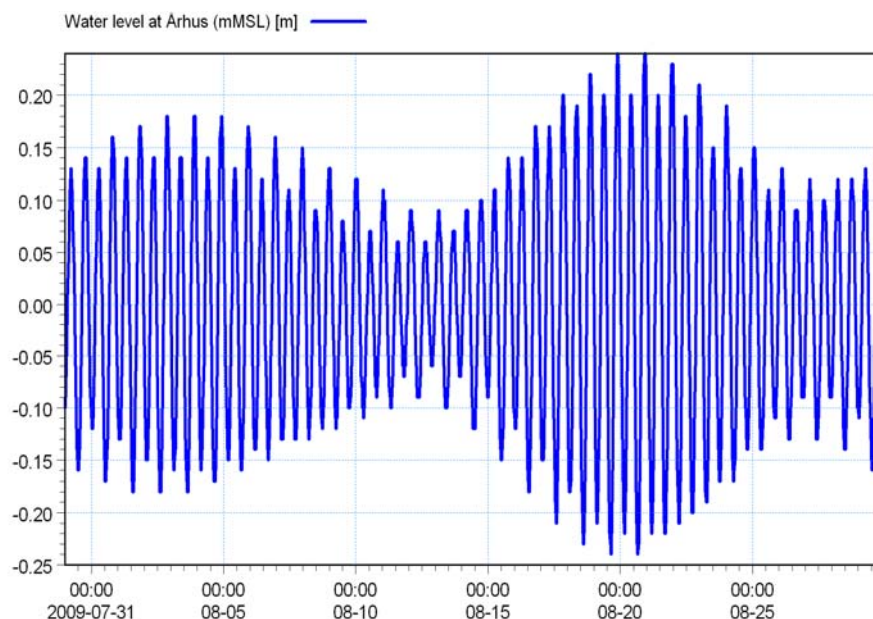
Figure 3-32   Tidal water level variation over one month period at Århus – C-MAP predictions. The water level variation is presented relative to MSL.

Table 3-7   Extreme water level analysis based on modelled Metocean data (1979-2007). From /10/.

	Extreme value for return period (yrs)		
	25	**50**	**100**
HW (mMSL)	1.41	1.53	1.66
LW (mMSL)	-0.78	-0.83	-0.88

3.2.4.3 Annual current and stratification for the baseline situation

The area where the wind mills are situated is by nature very dynamic with regards to temperature, salinity and currents. To get an overview of the salinities, temperatures and currents the hydrodynamics from the simulated representative year are analysed.

Time series of salinities, temperatures and currents for the years 2004-2008 from the regional model (see Appendix A) show an increased mixing in the winter months due to higher frequency of storms and a stronger stratification in the calmer summer months. A salinity and temperature front exists mainly in the summer time. This front moves back and forth depending on the meteorological conditions.

In Figure 3-33 cross sections of the modelled salinity profile modelled in the refined local model through the project area is given for a typical situation in the summer (upper figure) and for a typical situation in the winter (lower figure). The plot shows

the high concentrations in the northern end (the left side) of the plot and the low concentrations in the southern end (the right side) of the plot. The stratification is clearly seen to be much stronger in the summer time compared to the winter time.
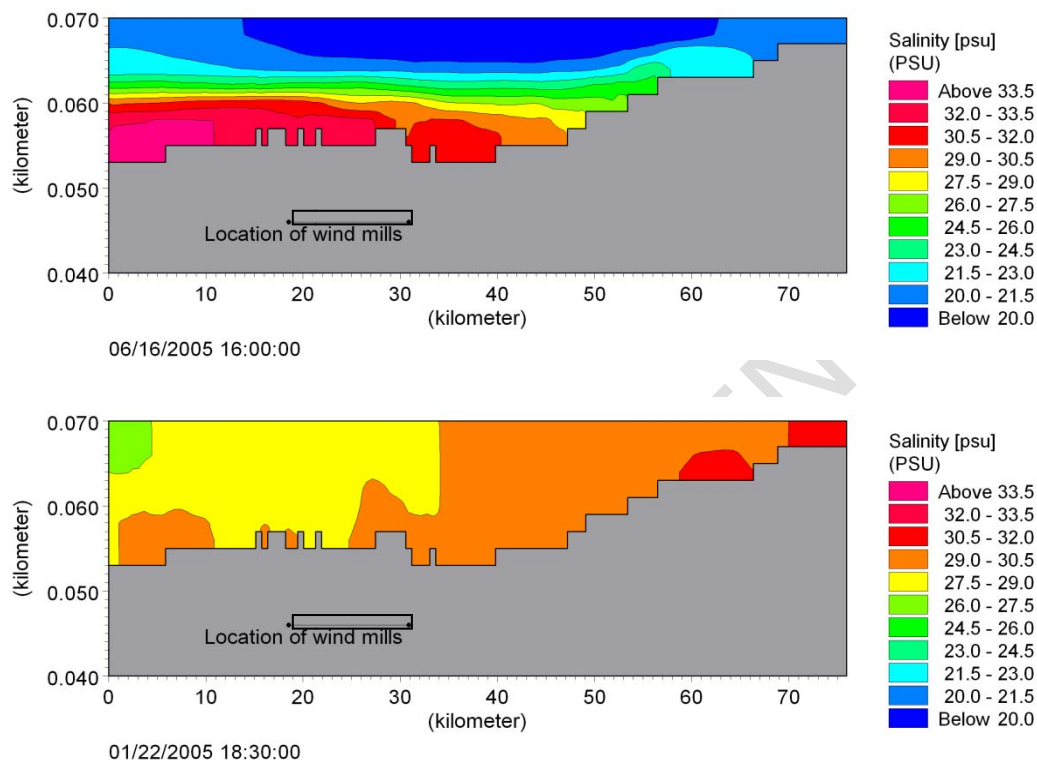
Figure 3-33   Cross sections of salinity through the project area for summer period (upper) and winter period (lower). Model results from the local model. Note that Skagerrak (north) is towards the left in the figure and south is towards the right. Location of cross section indicated in Figure 3-37.

The flow fields show that in periods large eddies are formed in the Kattegat. These eddies may form in all parts of the Kattegat but are observed especially just south and north of Anholt. Some of them become almost stationary over longer periods of time. Examples of typical surface flow patterns are seen in Figure 3-34. Current roses for the northern (location 1, see Figure 3-37) and the southern (location 2) Kattegat are given in Figure 3-35 for the surface as well as the near bottom flow.
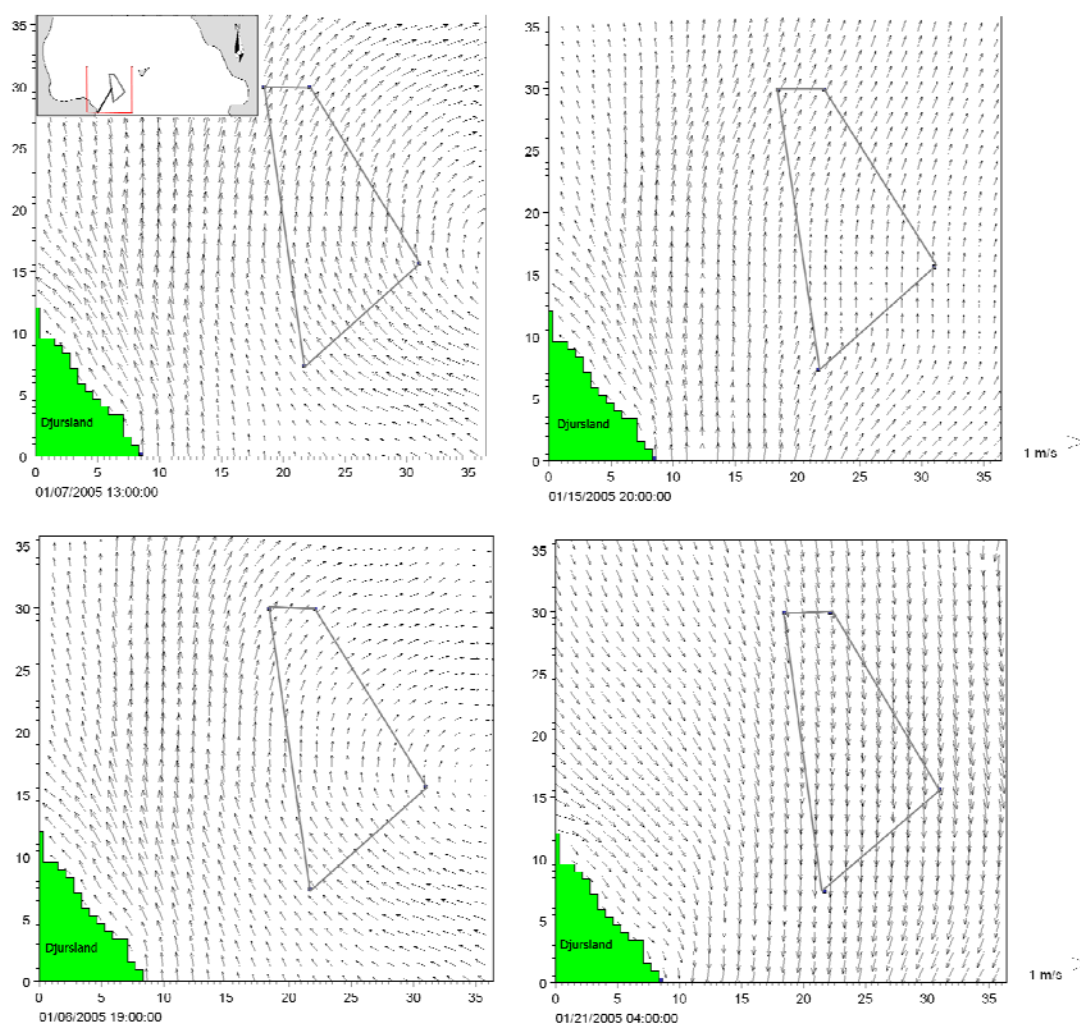
Figure 3-34   A variation of typical surface current patterns from 2005. Model results from the local model.
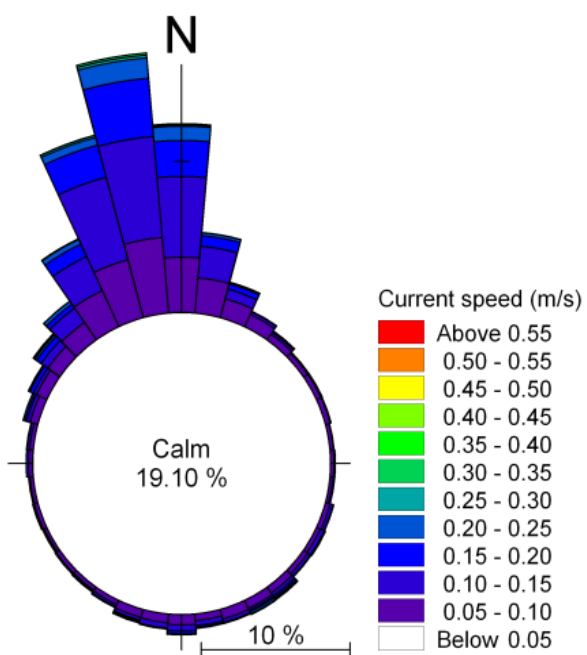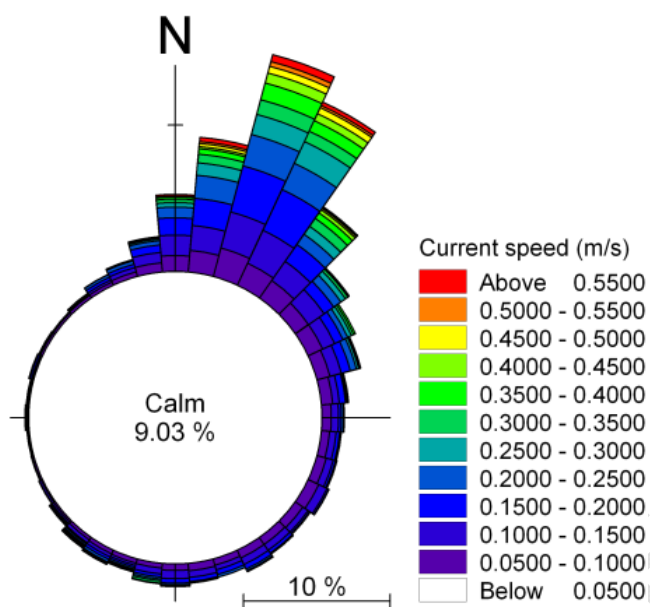
Figure 3-35   Modelled current roses at the surface for location 1. Upper is surface and lower
               is bottom. Geographical locations are shown in Figure 3-37.
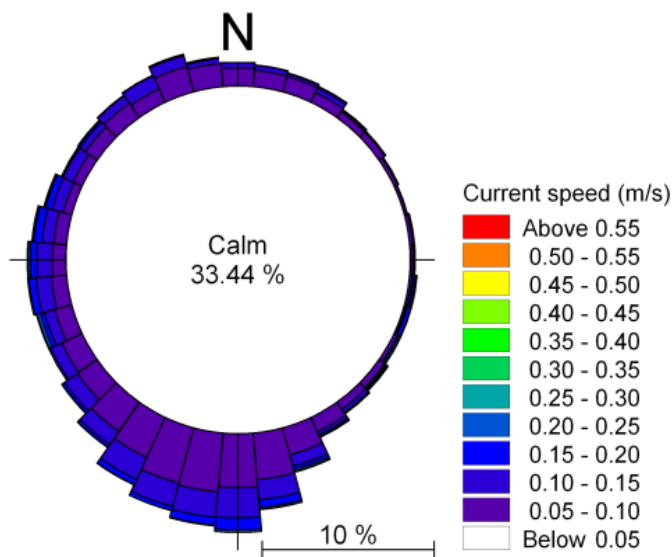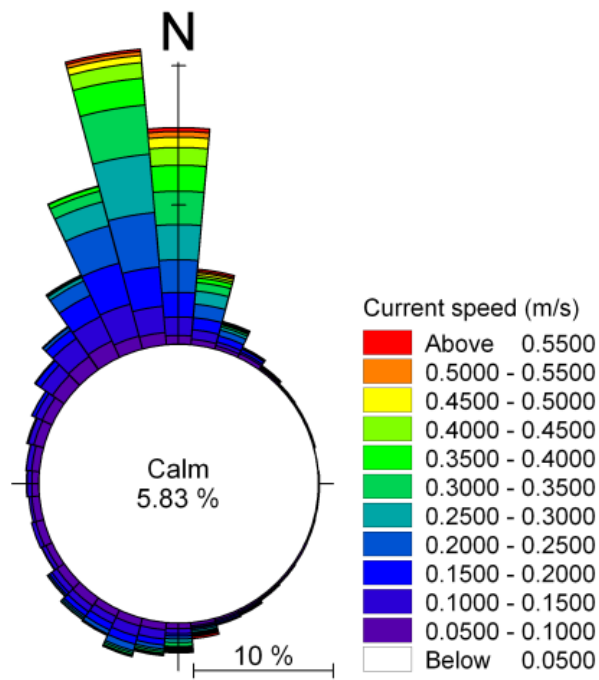
Figure 3-36   Modelled current roses at the surface for location 2. Upper is surface and lower
                is bottom. Geographical locations are shown in Figure 3-37
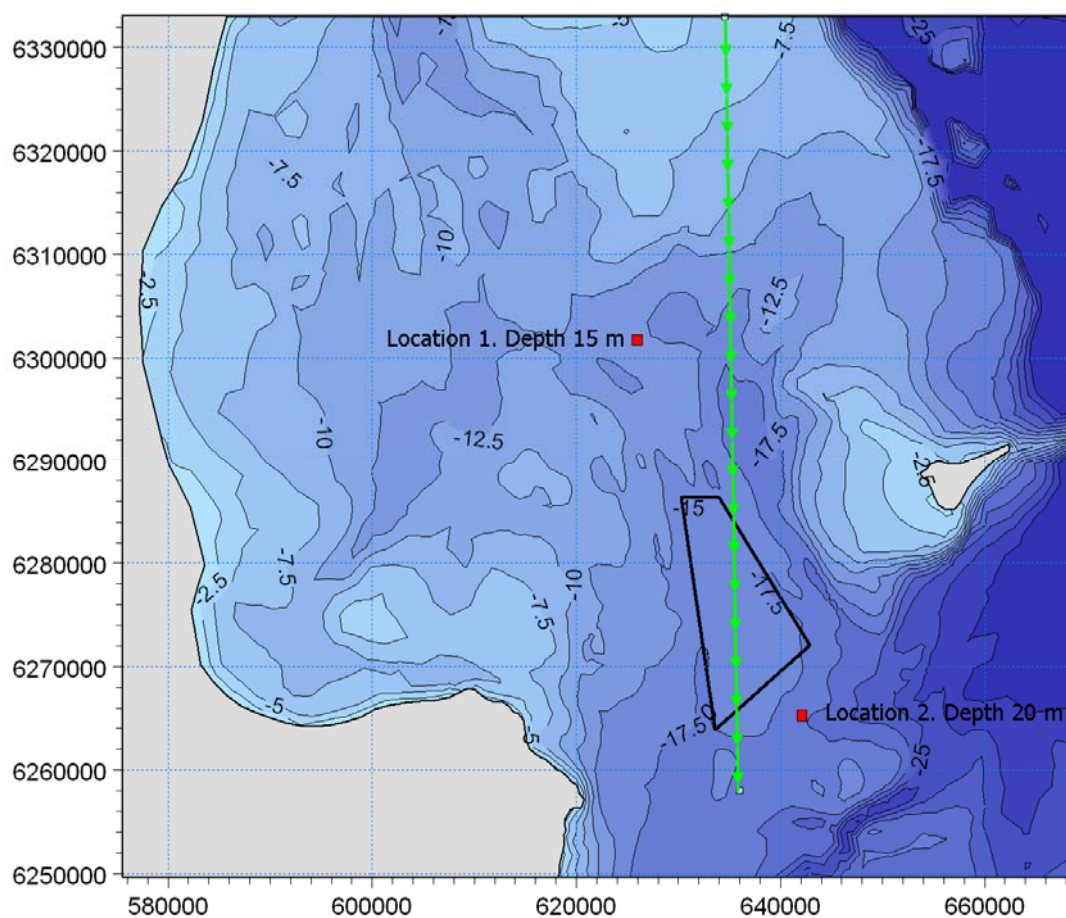
Figure 3-37   Locations of current data illustrated in Figure 3-35 and of vertical cross section for summer and winter profile for salinity in Figure 3-33.

The statistical properties for location 1 and 2 in 2005 are given in Table 3-8 to Table 3-11.

Table 3-8 Statistical properties for modelled currents from the local model in 2005 at location 1

Location 1	% of time where current is towards the north	% of time where current is towards the south	Maximum current velocity	Mean current velocity	Maximum northbound current velocity	Maximum southbound current velocity	Total number of current direction changes (N/S)
Surface	69.5	30.5	0.9	0.2	0.9	0.8	324
Bottom	53.9	46.1	0.4	0.1	0.3	0.4	616

Table 3-9 Statistical properties for modelled currents from the local model in 2005 at location 2

Location 2	% of time where current is to-wards the north	% of time where current is to-wards the south	Maxi-mum current velocity	Mean cur-rent veloc-ity	Maximum northbound current ve-locity	Maximum southbound current veloc-ity	Total number of cur-rent direc-tion changes (N/S)
Surface	66.3	33.7	1.0	0.2	1.0	0.9	348
Bottom	37.7	62.3	0.4	0.1	0.4	0.4	630

Table 3-10 Statistical properties for modelled salinity and temperature from the local model in 2005 at location 1

Location 1	Max salinity	Min salin-ity	Mean salin-ity	Mean tempera-ture winter	Mean tempera-ture spring	Mean tempera-ture summer	Mean tem-perature autumn
Surface	29.6	10.5	19.2	3.6	5.3	16.5	13.1
Bottom	30.2	20.9	25.2	5.7	6.6	15.5	14.6

Table 3-11 Statistical properties for modelled salinity and temperature from the local model in 2005 at location 2

Location 2	Max salinity	Min salin-ity	Mean salin-ity	Mean tempera-ture winter	Mean tempera-ture spring	Mean tempera-ture sum-mer	Mean tem-perature autumn
Surface	25.5	9.6	16.7	3.6	5.0	16.3	13
Bottom	33.7	23.1	28.9	7.0	8.2	11.8	13.2

The variation in the currents across the area is also illustrated by current roses of depth-averaged currents in five locations in the project area as shown in Figure 3-38. The five locations are the four corners of the project area and a central posi-tion. The variation in the current speeds is small. The current directions are slightly more north-westerly in the eastern part of the project area.
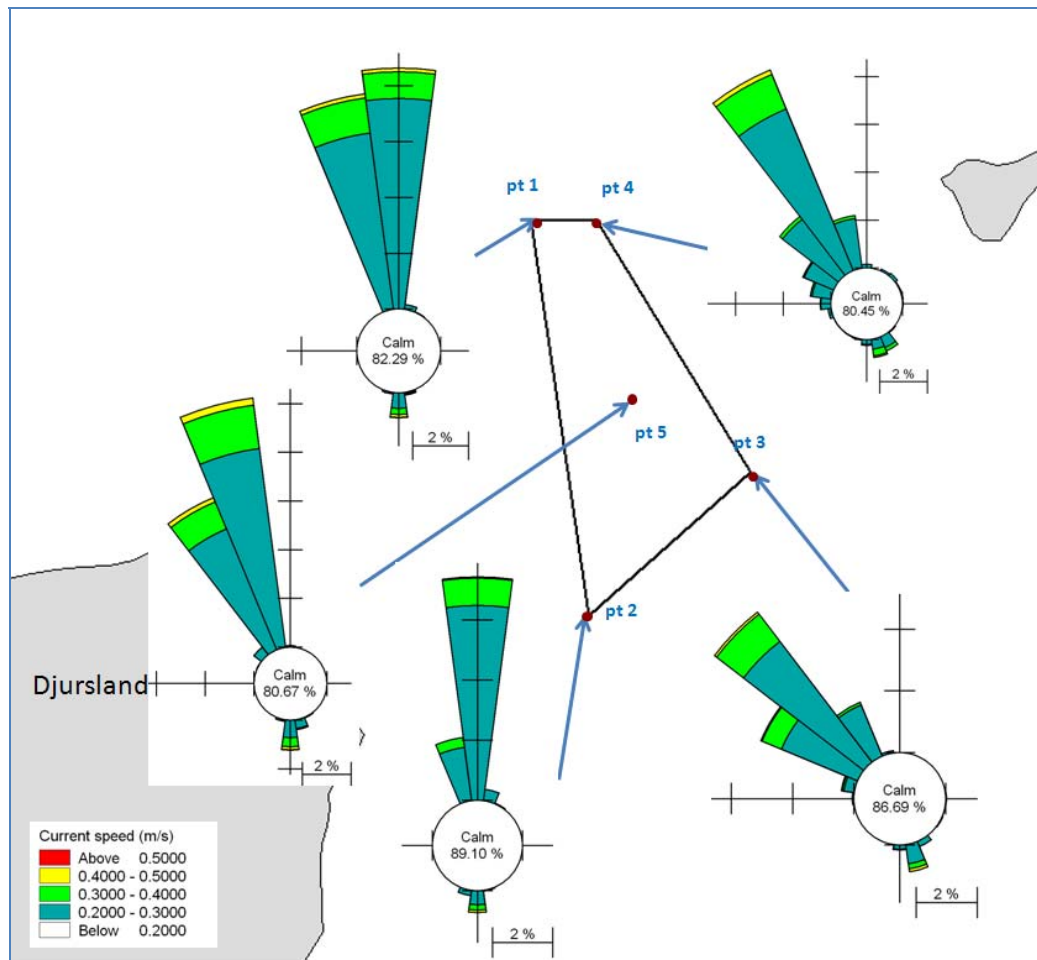
Figure 3-38   Modelled depth-averaged current conditions (from the local model, grid resolution approximately 600 m) in each corner of the project area and in a central location.

3.2.4.4   **Current conditions during selected storm weather events for the baseline situation**
Examples of the flow field during the storm conditions defined previously (cf. section 3.2.4.1) are presented in this section. The flow fields are from the 2D depth-integrated numerical model. In Figure 3-39 to Figure 3-42 the instantaneous current fields at the maximum intensity in the area of interest are shown for each storm. The Anholt wind farm area is outlined in black.

Storm 1, 3 and 4 are characterised by a north-going flow forced by a wind coming from south-west (Storm 1 and 4) and south (Storm 3). For Storm 1, the depth-averaged current intensity is generally low and decreases slightly towards the north from 0.4 to 0.3 m/s in the wind farm area. During Storm 3 and 4 the current concentrates in the east of the wind mill farm area corresponding to the deeper area located approximately 20 km south-west of Anholt. This flow pattern results in an

increase of the current speed from 0.5 to 0.6 m/s from west to east in the area of interest.

Similarly during Storm 2, the flow is directed towards the south mainly due to the south-going wind and converges towards the deeper area located south-west of An-holt resulting in an increase of the current speed from 0.45 to 0.6 m/s from west to east at the wind farm location.
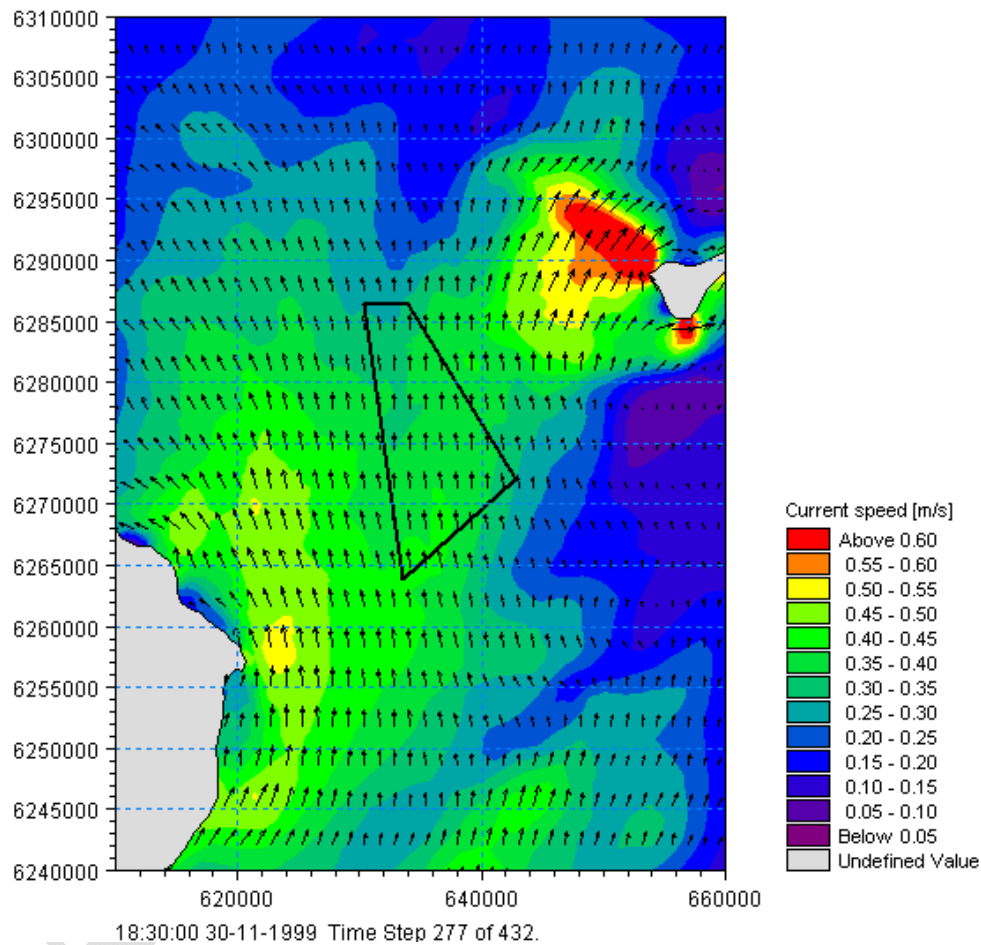
Figure 3-39   Maximum instantaneous current speeds in the project area during Storm 1. The project area is outlined in black.
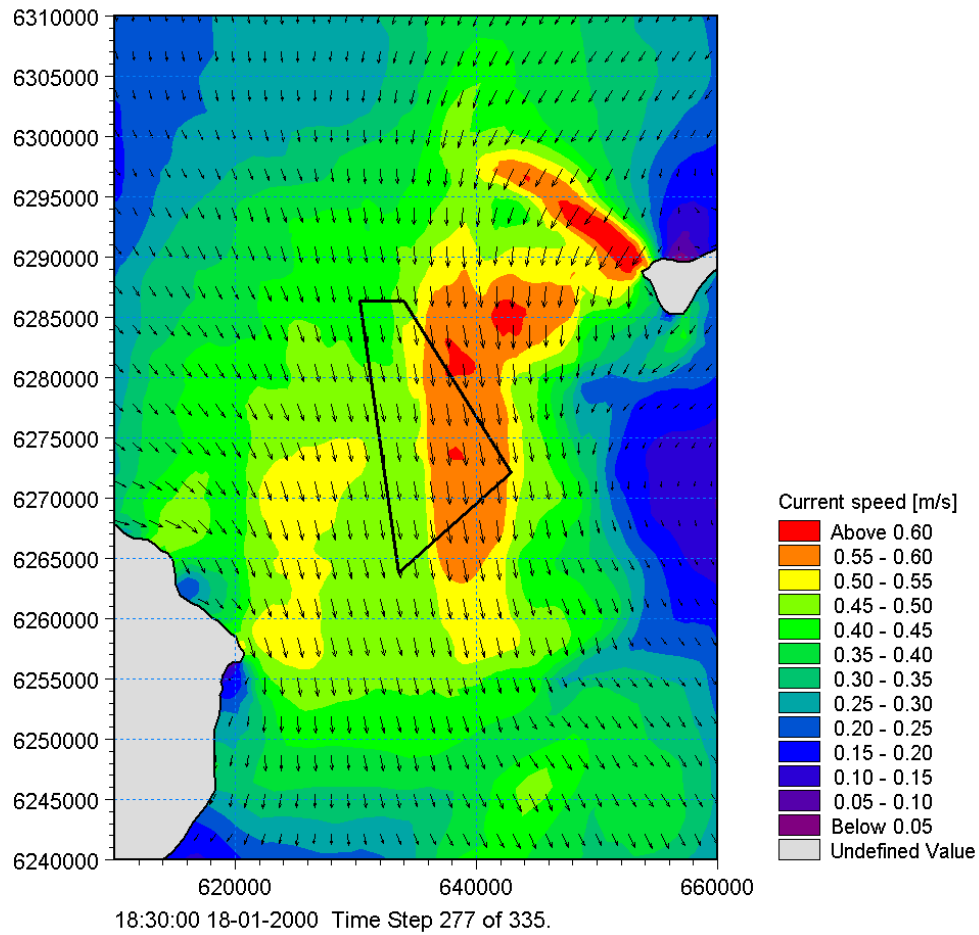
Figure 3-40   Maximum instantaneous current speeds in the project area during Storm 2. The
               Anholt wind farm area is outlined in black.
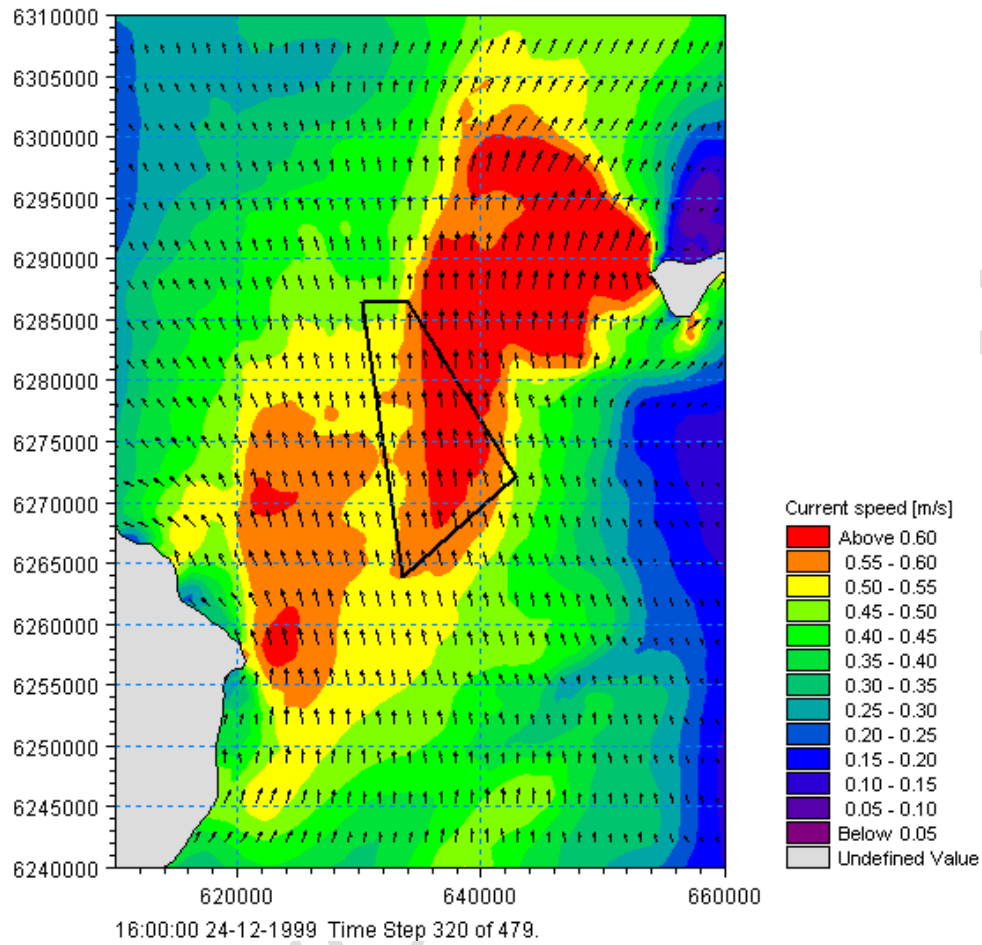
Figure 3-41   Maximum instantaneous current speeds in the project area during Storm 3. The Anholt wind farm area is outlined in black.
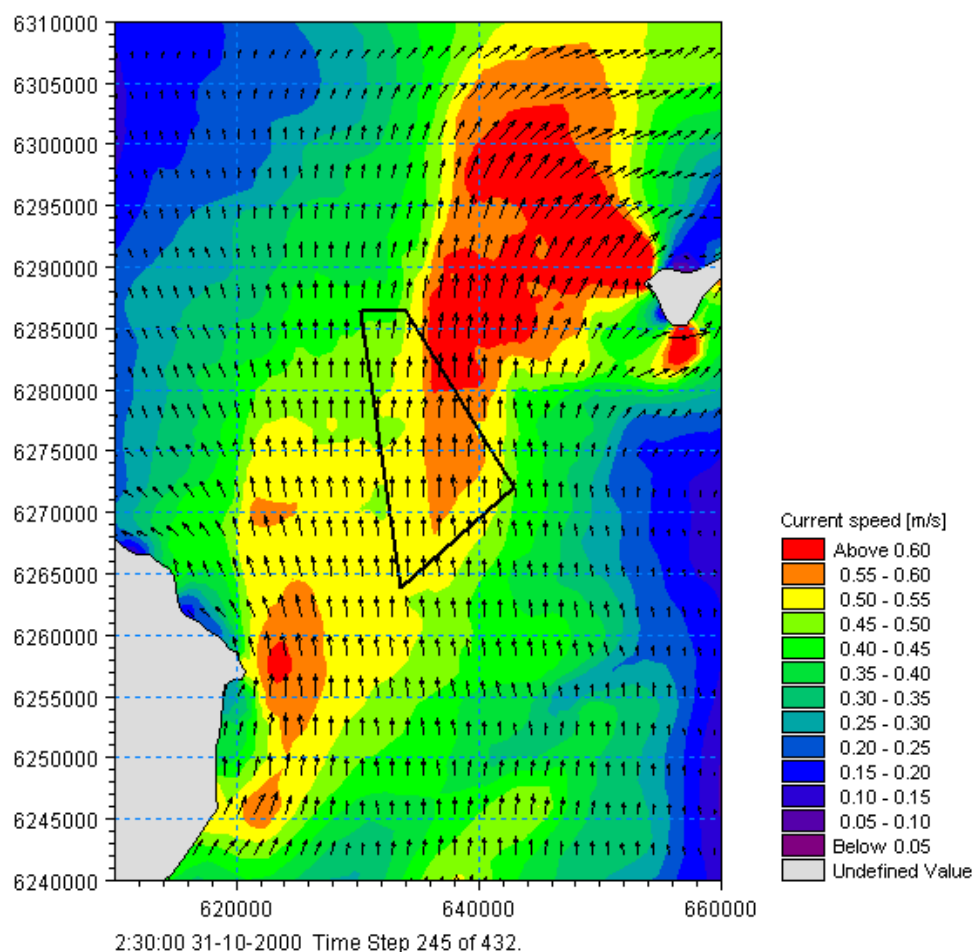
Figure 3-42   Maximum instantaneous current speeds in the project area during Storm 4. The Anholt wind farm area is outlined in black.

3.2.5   Wave conditions

The waves in the project area of Anholt Offshore Wind Farm are primarily determined by the combination of the wind field and the fetch limitation due to the limited distance to land areas such as Djursland to the W-SW, Læsø to the N, Anholt to the E and further away to Skagen, Sweden, The spit of Odden and Samsø.

Severe wave conditions are mostly experienced in connection with the passage of travelling depressions. Determination of design conditions for waves, water levels and currents require long time series and is not a part of this report – this analysis is included in /10/.

Methods

The baseline description of the wave conditions in the study area are based on analysis of results from numerical modelling carried out as a part of this study.

The wave conditions are studied from two different perspectives:

1. An analysis of the annual wave climate in a representative year.

2. An analysis of wave conditions during selected storm weather situations.

1. leads to an overall description of the typical annual wave climate conditions in and near the development site and in Chapter 3.3 to study the impact of the wind mill park on the annual wave climate. The outcome of the calculations of the annual wave conditions in the baseline situation are furthermore input to estimations of annual sediment transport rates in selected positions in the development site.

2. is carried out to investigate the severe wave conditions. The purpose of this is to make sure that the storm conditions are adequately represented in the mapping of the baseline conditions as well as in the further analysis of the impact of the wind mill park on the wave conditions. During an average year, some storm conditions will occur. However, during a single year critical storms from all the most critical directions do not occur.

Severe storm conditions are therefore selected from a 10-year period and calculated separately. This ensures that the storm conditions are represented in the analysis carried out to estimate the maximum extent of the area of influence of the wind mill park on the wave climate (in Chapter 3.3) by comparing the baseline situation with the situation including the wind mills. Specifically it is required to investigate if the wind mill park can lead to any impact on the wave conditions near the shorelines at Djursland and Anholt.

3.2.5.1.1 **Annual wave climate - modelling methodology**

Short model description and setup

The wave climate in and near the development site was modelled with DHI's numerical wave model, MIKE 21-FM SW. This model has been developed by DHI and used in numerous studies on waves. MIKE 21-FM Spectral Wave Model is a third generation spectral wind-wave model. The model simulates the growth, decay and transformation of wind generated waves and swells in offshore and coastal areas.

The geographical area of the model as well as the bathymetry and the flexible mesh are depicted in the lower part of Figure 3-43. The model obtains input from a larger regional wave model covering the entire North Sea and the Kattegat. The regional model was presented in Section 3.2.3 and details are provided in Appendix B.

The main part of the domain is covered by a grid size about 1 km^2; the main areas of interest are covered by a very fine grid about 0.005 km^2 equivalent to 100m length. To make a smooth transition from the coarser mesh to the very fine mesh a couple of cells surround those areas. Note that as the 3D regional model is defined in the geographical coordinates, the local model has been defined in the same coordinate system.

Due to its relative small scale and to have a reasonable computation time, the wave model is run with the so-called decoupled parametric formulation and a quasi-stationary solution technique. This method can be used over relatively small domains such as the Anholt Wind Farm project area, where the travel time for the waves across the computational domain is small (order of 1 hour). This approach is a very fast computational numerical method and allows high spatial resolution and simulations of long time series. The downside to this approach is that sea states of combined swell waves and wind waves are not represented well with this method. Waves in this part of Kattegat, however, are dominated by fetch-limited wind waves and swell is not important for waves in the project area.

The most important model parameters are shown in Table 3-12. Details of the model setup as well as the validation of the model are described in Appendix B.
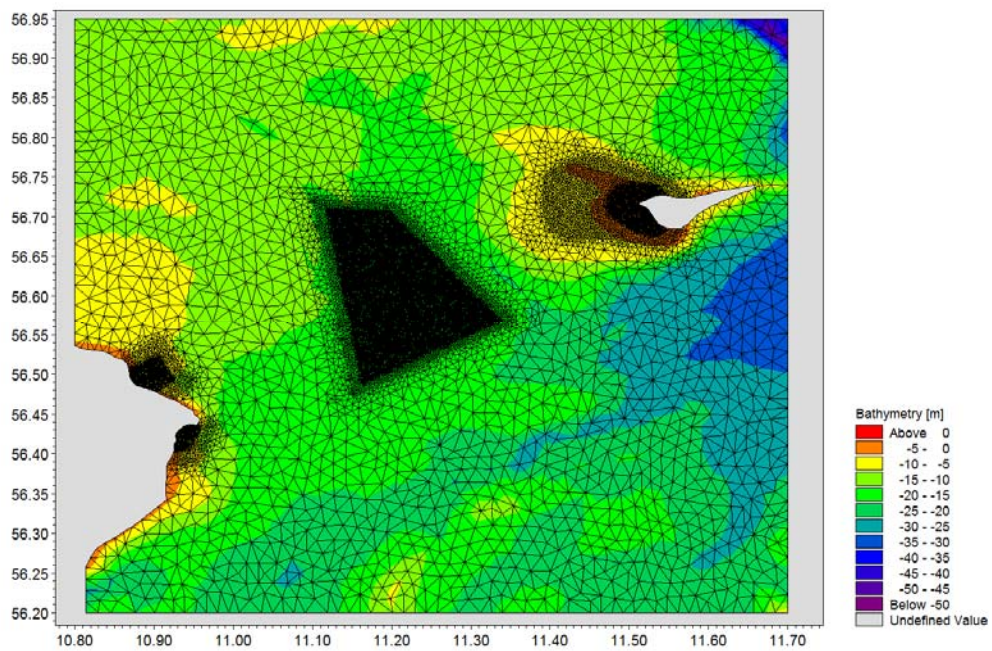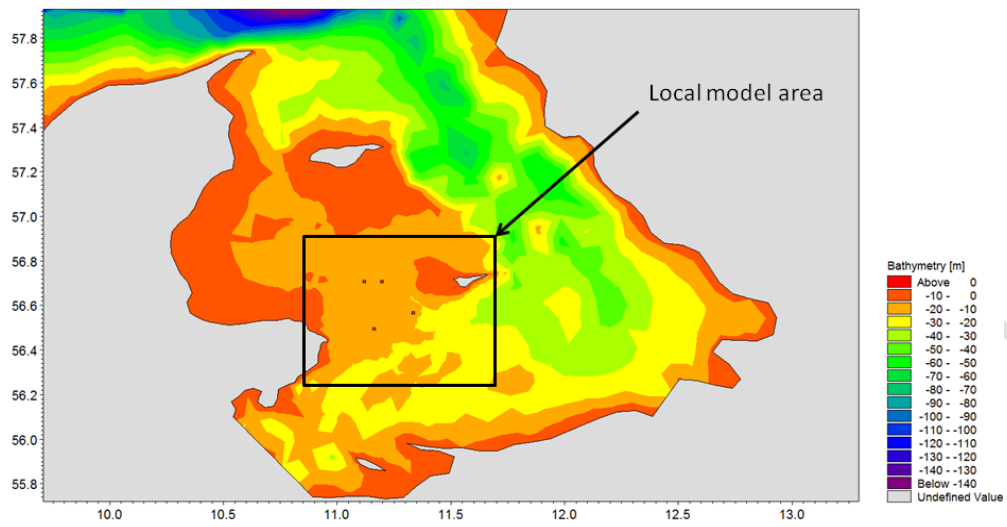
Figure 3-43   Geographic area of local wave model is covering the development site and extents to include the nearby coastlines. The resolution of mesh is finest in the area of the development site and near the coast.

Table 3-12   Model settings for the local wave model in the baseline simulations. Further details in Appendix B

Parameter	Value
Simulation mode	Decoupled parametric, quasi stationary formulation
Mesh size – coarsest mesh	$1\ km^2$
Mesh size – finest mesh	$5 \cdot 10^{-3}\ km^2$
Simulation period	01/01/2005 -01/01/2006
Boundaries	South-west, south, east, north, north-east
Boundary conditions	H_{m0}, T_p, MWD and directional spreading from reg. model
Wind forcing	2D map (VEJR2)
Wind formulation	Shore Protection Manual (1984)
Bottom friction	$1 \cdot 10^{-5}$
Wave breaking, depth-induced	$\gamma=0.8$, $\alpha=2$
Wave breaking, steepness	$\alpha=4$

3.2.5.1.2   **Wave conditions during selected storm conditions - modelling methodology**

Short model description and setup

The geographical extent of the wave model is slightly different in these simulations compared to the simulations of the annual wave climate to be able to include the output from the simulations (the wave forcing) in the flow field calculations of the storm events. The importance of the wave-induced current has been investigated by including radiation stress field resulting from the wave modelling under storm conditions in the 2D hydrodynamic model (cf. Section 3.3.2.2). The hydrodynamic and wave model have therefore been setup using the same geographical extent and horizontal coordinate system (UTM-32(WGS84)) (cf. Figure 3-24). The set up of the model is otherwise identical to the wave model generated for calm weather conditions.

Choice of modelling periods

Please refer to Section 3.2.4.1 for a description of the selected storm conditions.

3.2.5.2   **Annual wave conditions for the baseline situation**
The waves in the project area are wind generated waves. The wind in the period 1998-2007 based on model data from VEJR2 is from directions between south-east and north-west as seen in Figure 3-25.

The most common wind directions are from south-west to west. An example of a modelled wave field in the local model from November 2005, where the wind direction in the project area was 236° (south-west), is illustrated in the upper part of Figure 3-44. The figure shows the distribution of wave heights in the local model area. The wave heights are shown as the so-called significant wave height. The significant wave height (trough to crest) represents approximately an average of the largest 1/3 of the waves at a given time.

The wind speed at the time shown in the upper part of Figure 3-44 is 13 m/s, which can be characterized as a medium-strong wind speed. The statistical analysis of the wind speed and directions was shown in Table 3-4. From this table it can be derived that wind speeds of 13 m/s are exceeded in about 4.5% of the time in an average year, corresponding to about two weeks in total.

The lee effect from Djursland is clearly seen. In the wind mill area the wave height is limited due to this lee effect as seen when comparing with the wave heights in the area south of Anholt, where the fetch for the waves to grow is larger for this direction.

The statistical analysis from Table 3-4 shows that the strongest wind speeds are from directions between west and north-west. Such a situation is shown in the lower part of Figure 3-44. In this situation from December 2005, the wind direction is from WNW in the project area. In this case, Djursland is not restricting the wave heights from this direction in the wind mill area. The fetch from the WNW is much longer causing higher waves in the wind mill area, but also the wind speed is higher in this event than for the event shown in the upper figure (16 m/s versus 13 m/s in the upper figure).

The influence of the distance to land (fetch) on wave height at different locations in the project area is illustrated in Figure 3-45. The figure shows wave roses in the four corners of the project area and in the centre. The lee effect from Djursland is clearly limiting the wave heights from south-western directions in all five locations, but most pronounced in the south-western corner nearest land. The lee effect of Anholt is much smaller, but is seen most clearly in the north-western location. It should be noted that not only the fetch is influencing the wave heights, but also local and regional depth-variations.
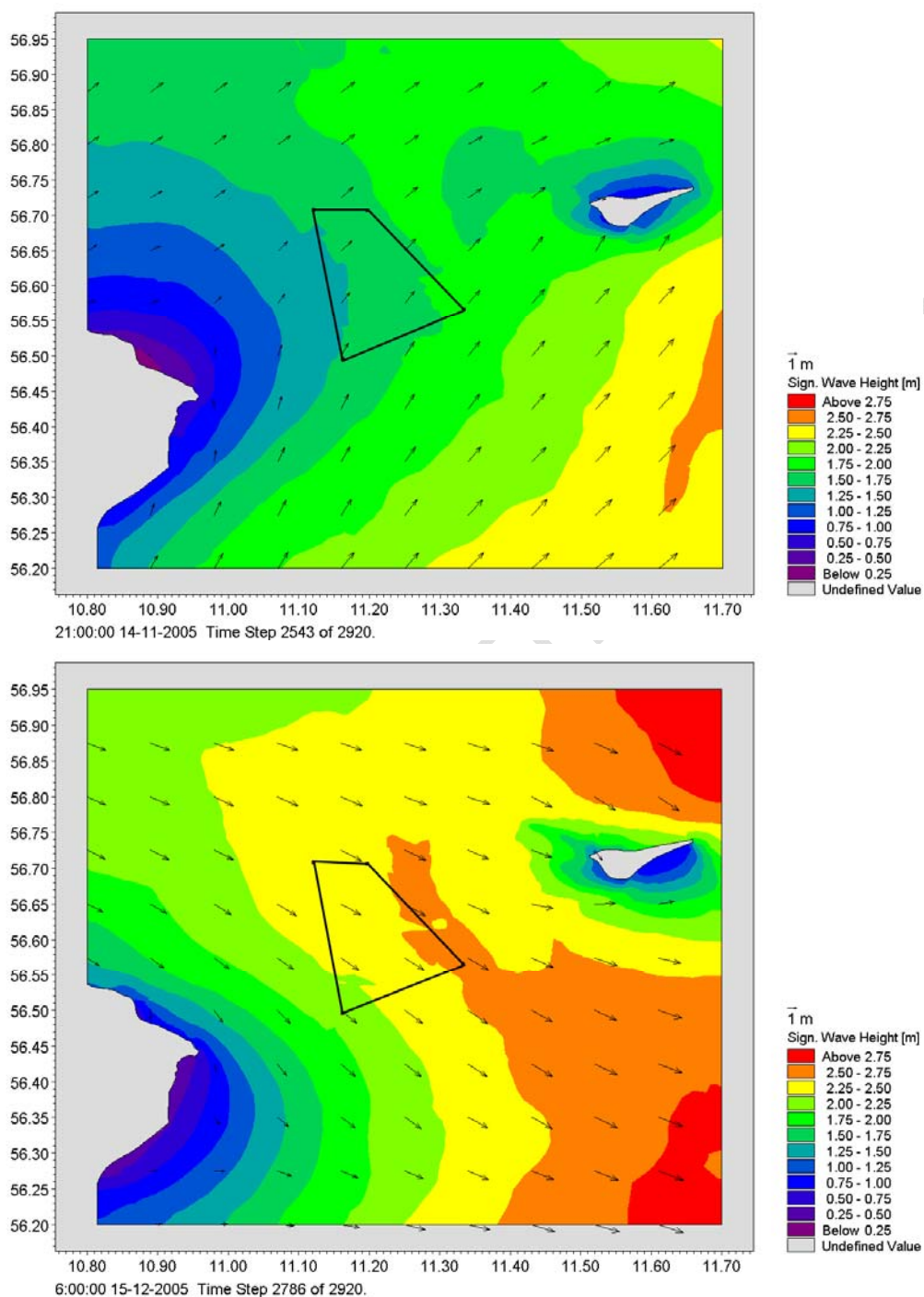
Figure 3-44   Example of modelled wave fields for two characteristic wind directions (local model, grid resolution approximately 100m). Upper figure: example of waves with a wave direction of approx. 220 degr. N in the wind mill area. Wind speed is 13 m/s and wind direction is 236 degr. Lower figure: example of waves with

a wave direction of approx. 300 degr. N in the wind mill area. Wind speed is 16m/s and the wind direction is 292 degr. N.
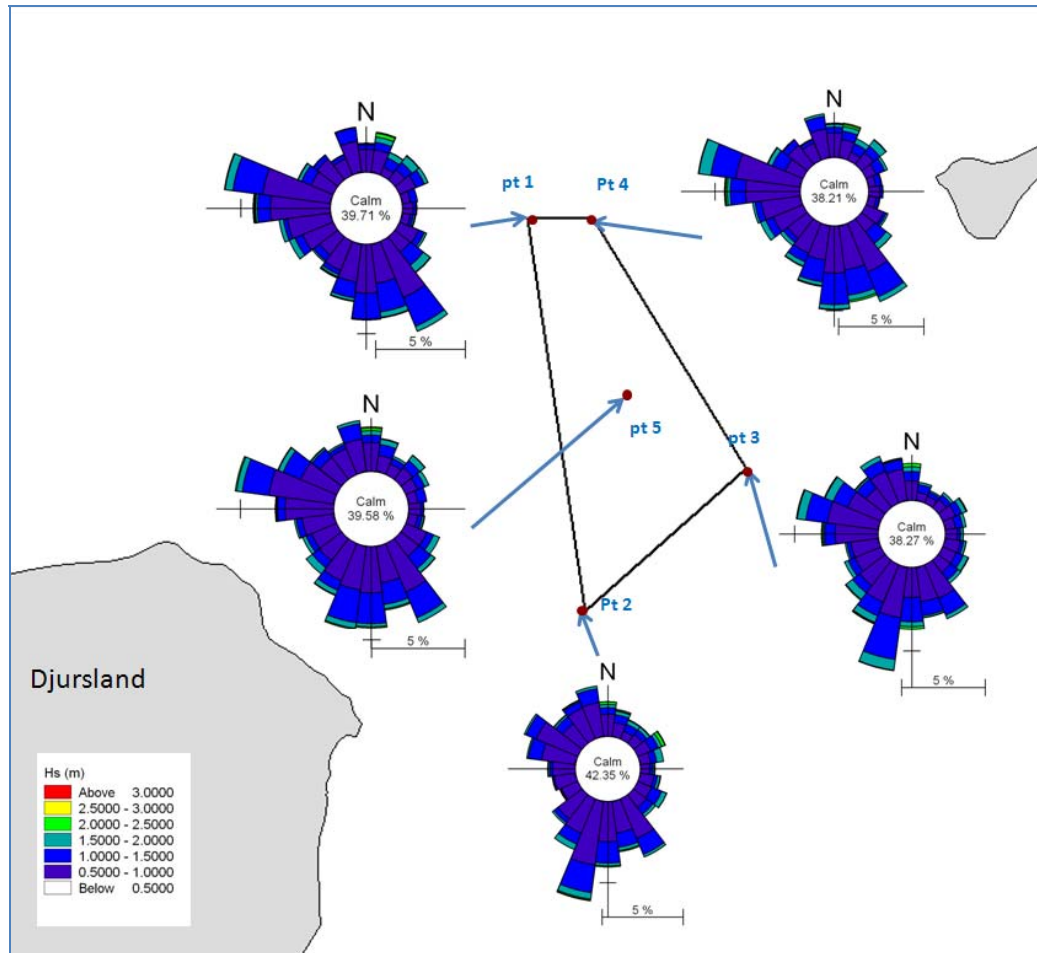
Figure 3-45   Modelled wave conditions from the local wave model (grid spacing in the project area of about 100 m) in the four corners of the project area and in the centre. Baseline conditions.

3.2.5.3   **Wave conditions during selected storm weather conditions for the baseline situation**
The wave field at the time step corresponding to the peak wind speed of each storm under the four selected storm conditions (cf. Section 3.2.4.1) are illustrated in Figure 3-46 to Figure 3-49.

Storm 1 (see Figure 3-46) is characterised by a wind coming from west (268.2°N at the peak). Due to varying fetch limitations caused by the presence of Djursland, a slight variation can be felt in the significant wave height field from north to south within the project area of Anholt Offshore Wind Farm. At the peak of Storm 1, the

very strong wind speed of 23.8 m/s leads to waves propagating towards 277°N with a significant height varying from south to north from 2.5 to 3m, respectively.

Regarding storm 2, the combination of wind coming from 345.2°N with a maximum wind speed of 18.4 m/s and a fetch of about 60km (from the island of Læsø to the north of the project area) results in relatively uniform waves characterised by a significant wave height of 2.5m coming from a direction of about 350°N at the future wind farm. This is seen in Figure 3-47.

For Storm 3 and 4 presented in Figure 3-48 and Figure 3-49, as the wind is coming from 182°N and 201.1°N, respectively, waves grow over a fetch of about 80 km and reach Anholt wind farm with a wave height varying between 2.6-3 m (Storm 3) and 2.4-2.8 m (Storm 4) from west to east. Their incoming direction is about 175°N for Storm 3 and 183°N for Storm 4.

6:00:00 01-12-1999 Time Step 102 of 186.
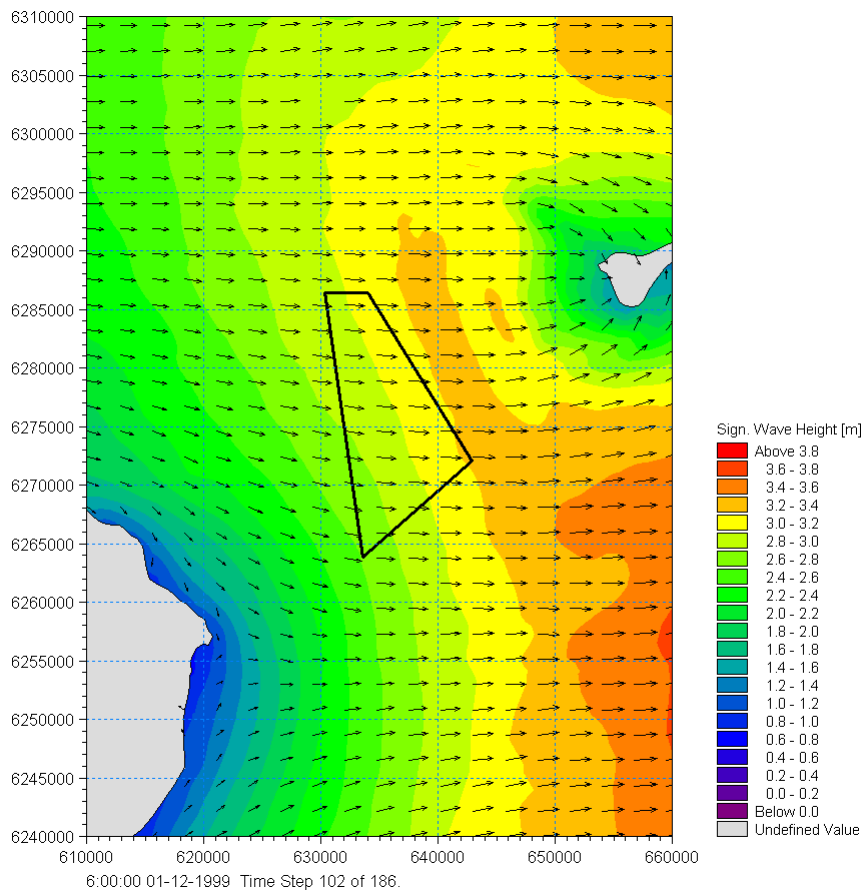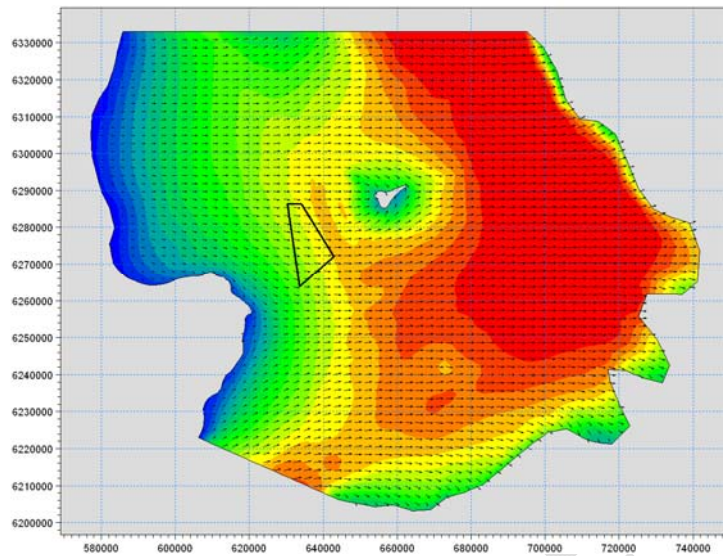
Figure 3-46   Instantaneous wave field over the entire model (up) and zoomed (down) at Anholt wind farm extracted at the peak wind speed defining Storm 1. The Anholt wind farm project area is outlined in black.

6:00:00 18-01-2000 Time Step 108 of 191.
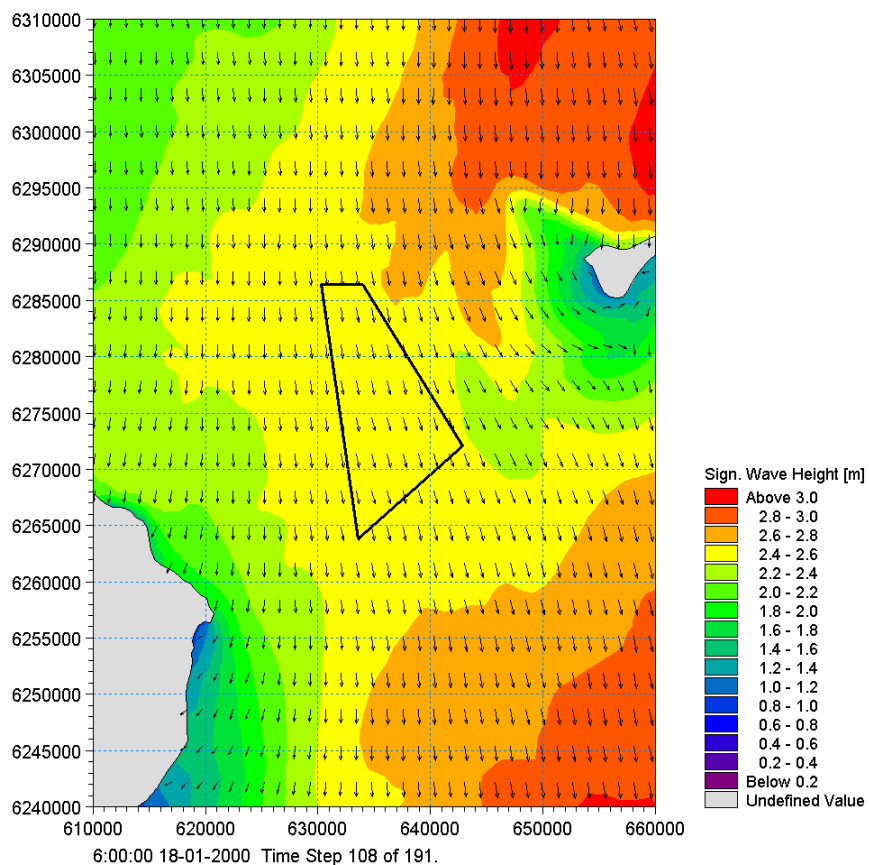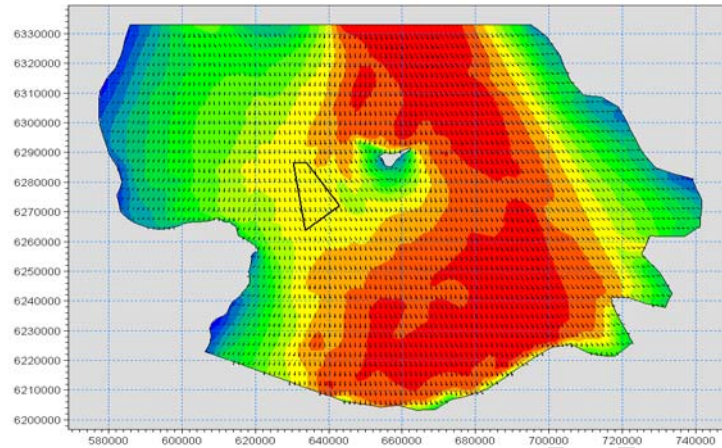
Figure 3-47   Instantaneous wave field over the entire model (up) and zoomed (down) at Anholt wind farm extracted at the peak wind speed defining Storm 2. The Anholt wind farm project area is outlined in black.
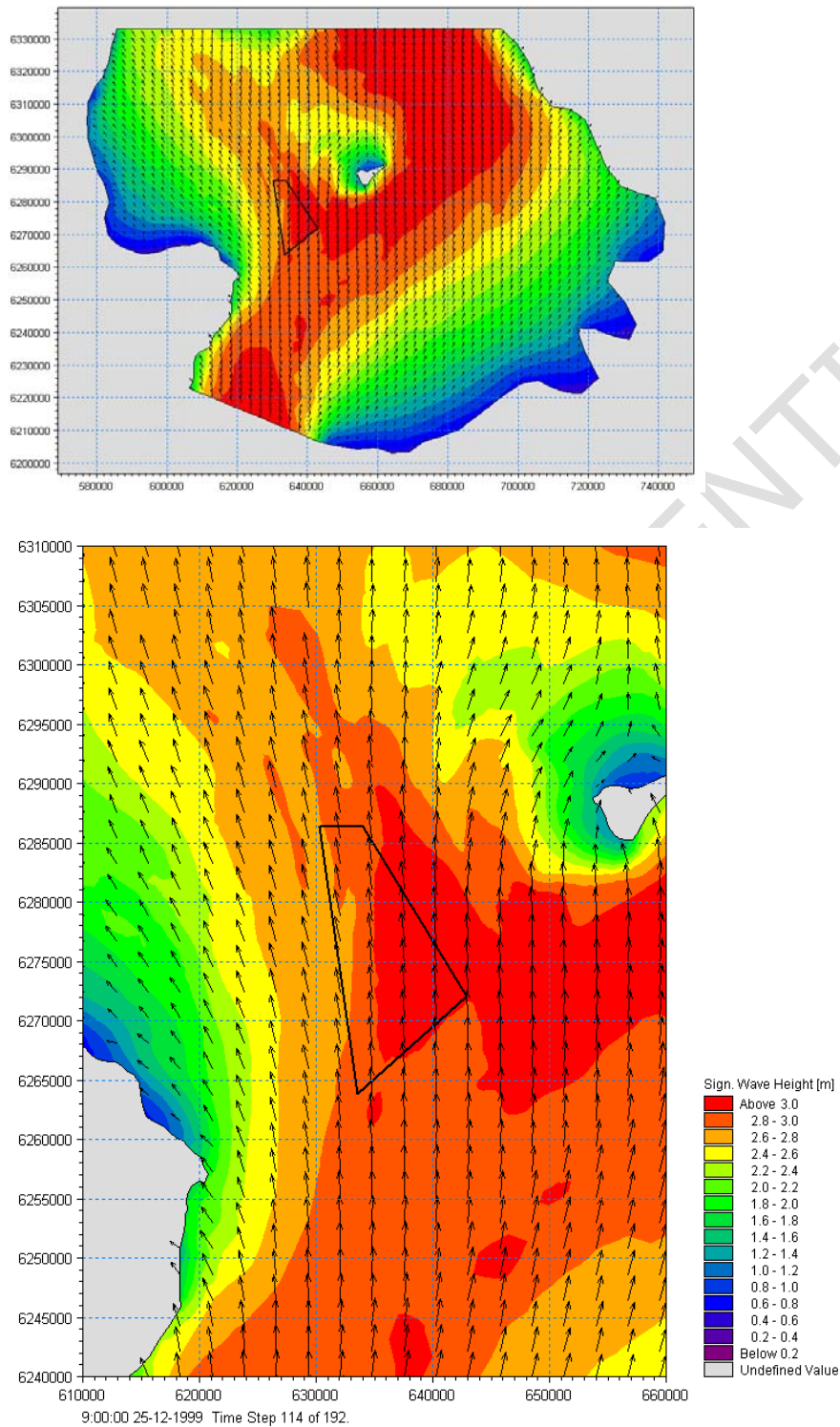
Figure 3-48   Instantaneous wave field over the entire model (up) and zoomed (down) at Anholt wind farm extracted at the peak wind speed defining Storm 3. The Anholt wind farm project area is outlined in black.
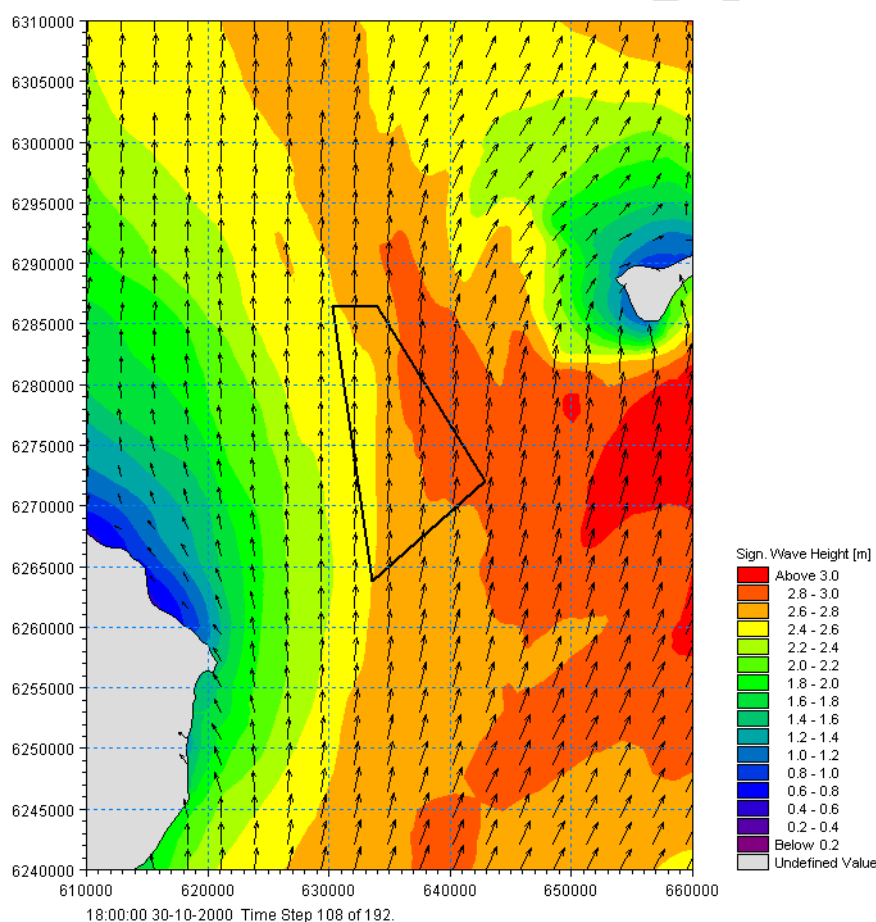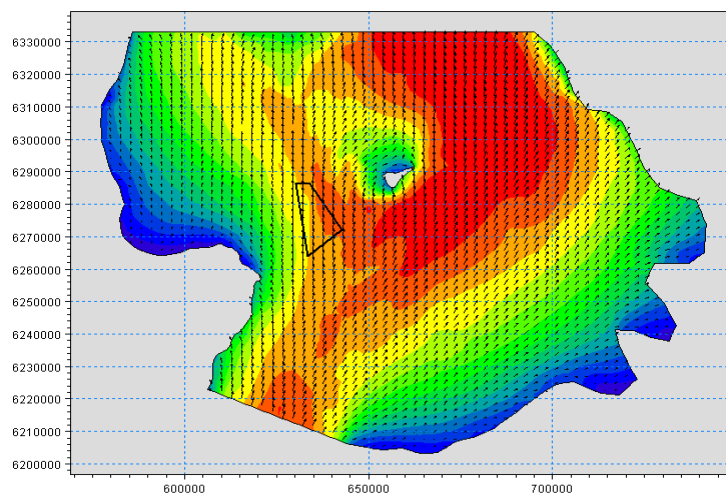
Figure 3-49   Instantaneous wave field over the entire model (up) and zoomed (down) at Anholt wind farm extracted at the peak wind speed defining Storm 4. The Anholt wind farm project area is outlined in black.

3.2.6 Water quality conditions

This section describes the water quality in the project area under baseline conditions (year 2005). Because monitoring data covering water quality do not exist for the project area a calibrated ecological model covering a larger area (e.g. entire Kattegat, see Figure 2-1) was established to resolve the spatial and temporal variability in the project area. The baseline conditions are used as a yardstick to evaluate the permanent changes in water quality following establishment of a wind park (two alternative layouts), and temporal effects related to earth works.

3.2.6.1 Methods

The ecological model used in this study consists of an eutrophication model describing the pelagic system with 13 state variables, and seven state variables describing the exchangeable N and P pools in the sediment (/14/ and /15/). The pelagic system includes phytoplankton, described in terms of their concentration of carbon (C), nitrogen (N) and phosphorus (P), chlorophyll-a, zooplankton, detritus (C, N & P), inorganic nutrients (dissolved inorganic nitrogen—DIN & PO_4–P), total N and P nutrients (including dissolved organic N and P compounds) and dissolved Oxygen (DO). Due to the depth in the project area benthic vegetation (i.e. macroalgae) is poorly developed or not existing and accordingly benthic vegetation is not included in the model. In addition to state variables a large suite of derived variables such as water transparency / Secchi depth is modelled and stored during the modelling process. Benthic organisms are not modelled explicitly, but are included as a forcing in the water quality model. Filter-feeding bivalves constitute on average 93% of the entire biomass of benthic invertebrates in the project area (/7/) and their filtering activity can exert a significant grazing loss on phytoplankton. Their effect is included in the model by imposing a filtration loss on phytoplankton and detritus in the near bed model layer according to the filtration capacity calculated from length distribution and total biomass of the different species. Because bivalves are not included as a state-variable they do not participate directly in nutrient cycling and accordingly, 50% of filtered algae (C,N,P) are returned as inorganic solutes to the near-bed layer and 50% are entered into the detritus pool subject to sedimentation and remineralisation. Figure 3-50 shows the state variables and processes for carbon (C) for the pelagic system.

1. Production, phytoplankton
2. Sedimentaion, phytoplankton
3. Grasing
4. Extinction
5. Excretion, phytoplankton
6. Extinction, zooplankton
7. Respiration, zooplankton

8. Mineralisation of detritus
9. Sedimentation of detritus
10. Mineralisation of sediment
11. Accumulation in sediment
12. Exchange with surrounding waters
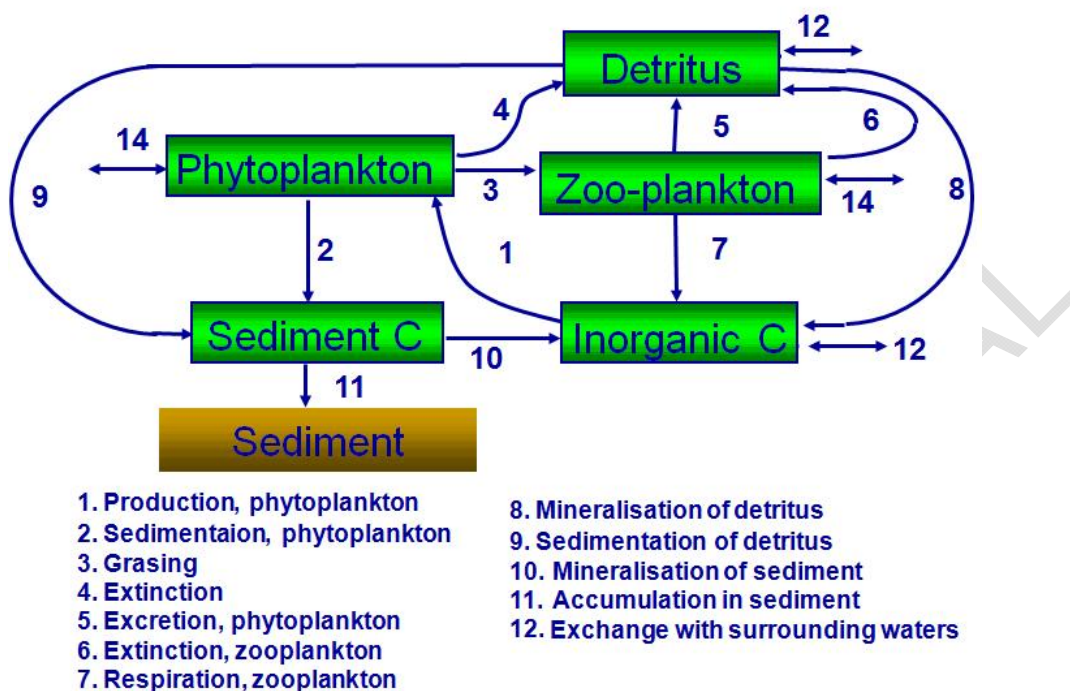
Figure 3-50   Schematic diagram showing state variables and processes for carbon in the model established to simulate water quality.

The water quality model was built using the generic equation solver ECOLab that functions as a module in the MIKE 3 simulation software and ECOLab is linked to the advection-dispersion term of the hydrodynamic flow models (see Section 4.2.3), so that transport mechanisms based on advection-dispersion are seamless integrated in the ECO Lab simulation.

Forcings and boundary conditions of the water quality model follows the line of the forcings and boundaries of the hydrodynamic model (see Section 3.2.4.1) but in addition including values for all pelagic state variables at boundaries (Øresund, Southern Kattegat and north of Læsø) and nutrient concentrations in freshwater loads (monthly basis) in addition to atmospheric loads. Boundary values are forced with water quality data extracted from the BANSAI model.

3.2.6.2   Baseline water quality conditions

The ecological model was calibrated (7 stations: Anholt E, Fladen, Fornæs, Gniben, Kullen, Læsø, Aalborg Bugt) against measured data of total N and P, chlorophyll, transparency (Secchi Depth) covering the model year 2005 and for long-term averages (2000-2007) including primary production in Kattegat. Results from the NOVANA monitoring station Aalborg Bugt are shown below. This station constitutes the station closest to the project area where the data cover is good. An extensive set of

calibration data and figures is shown in Appendix C. Model calibration involves a series of procedures such as minor adjustments in process parameters to allow as many as possible state variables to simulate observations at as many stations as possible. Besides matching observations across the years a proper seasonal behaviour of the model is mandatory, e.g. timing and magnitude of spring bloom and the associated reductions in inorganic nutrients should match with the observed bloom etc.

During the calibration process the goodness-of-fit of the model was estimated as the total difference between simulated and measured values as the root mean square error (RMSE):

$$RMSE = \frac{100}{\overline{O} * n} \sqrt{\left(\sum_{i=1}^{n} [(P_i)] - O_i \right)^{\wedge}2}$$

where n is the total number of observations, $\overline{O}$ is the mean of the observed values Oi, and Pi represents the simulated values. The lower the value of RMSE is, the beter the model fits to the observed data. RMSE was calculated for stations, depths and parameters if at least 6 yearly measurements were available for 2005.

The average of RMSE was lowest for Secchi Depth (=24), followed by tot-N (32), tot-P (38), NOx (56) and Chla (58). This range also reflects the sequence in calibration that initially focuses on nutrients, followed by Chla and oxygen.

After calibration the water quality model was able to simulate observations in water quality parameters in sufficient detail and with acceptable minor deviations from measured values in 2005 and within the long-term monthly range defined by 5% and 95% percentiles. The percentiles were calculated based on 8 years data of monitoring (2000-2007). In the examples from Aalborg Bugt only chlorophyll at the surface deviates systematically from long-term monthly means (Figure 3-53), while all other variables were in good accordance with observations.
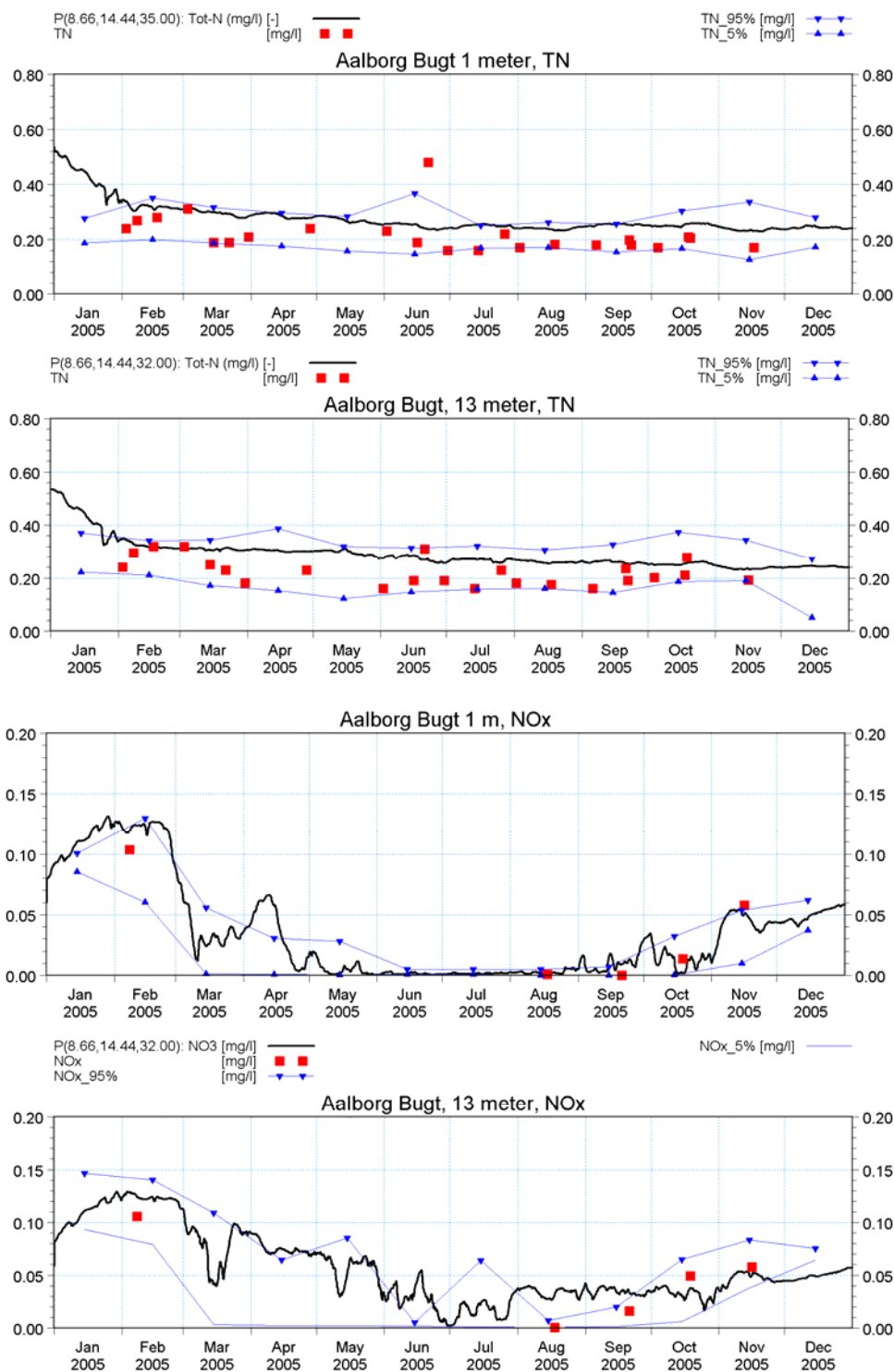
Figure 3-51   Concentration of total nitrogen (TN) and NOx-N in Aalborg Bugt at surface and at bottom (13 m). Modelled (black line), measured in 2005 (■) and 5 and 95% percentiles covering 2000-2007.
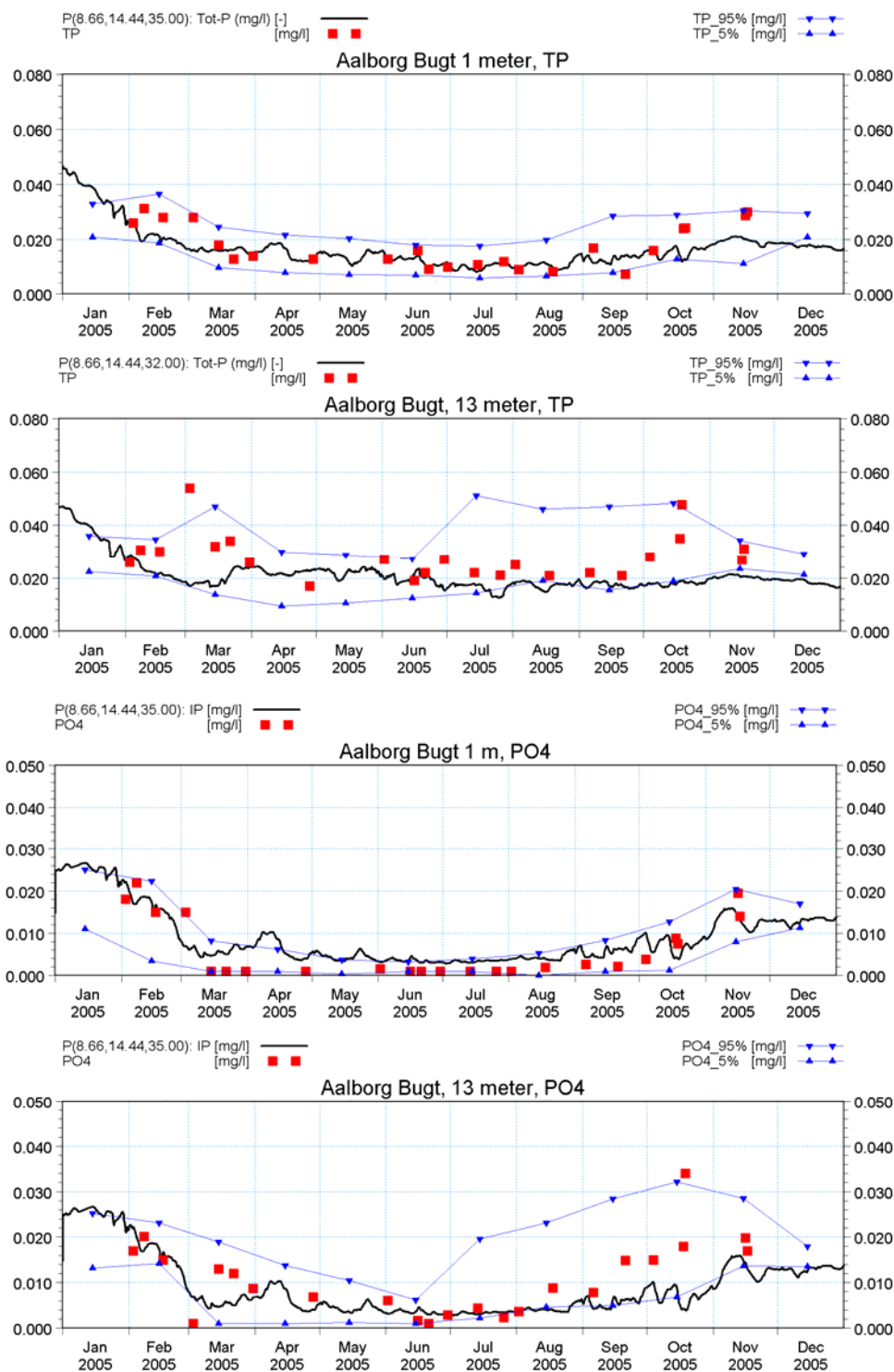
Figure 3-52   Concentration of total phosphorus (TP) and PO_4 -P in Aalborg Bugt at surface and at bottom (13 m). Modelled (black line), measured in 2005 (■) and 5 and 95% percentiles covering 2000-2007.
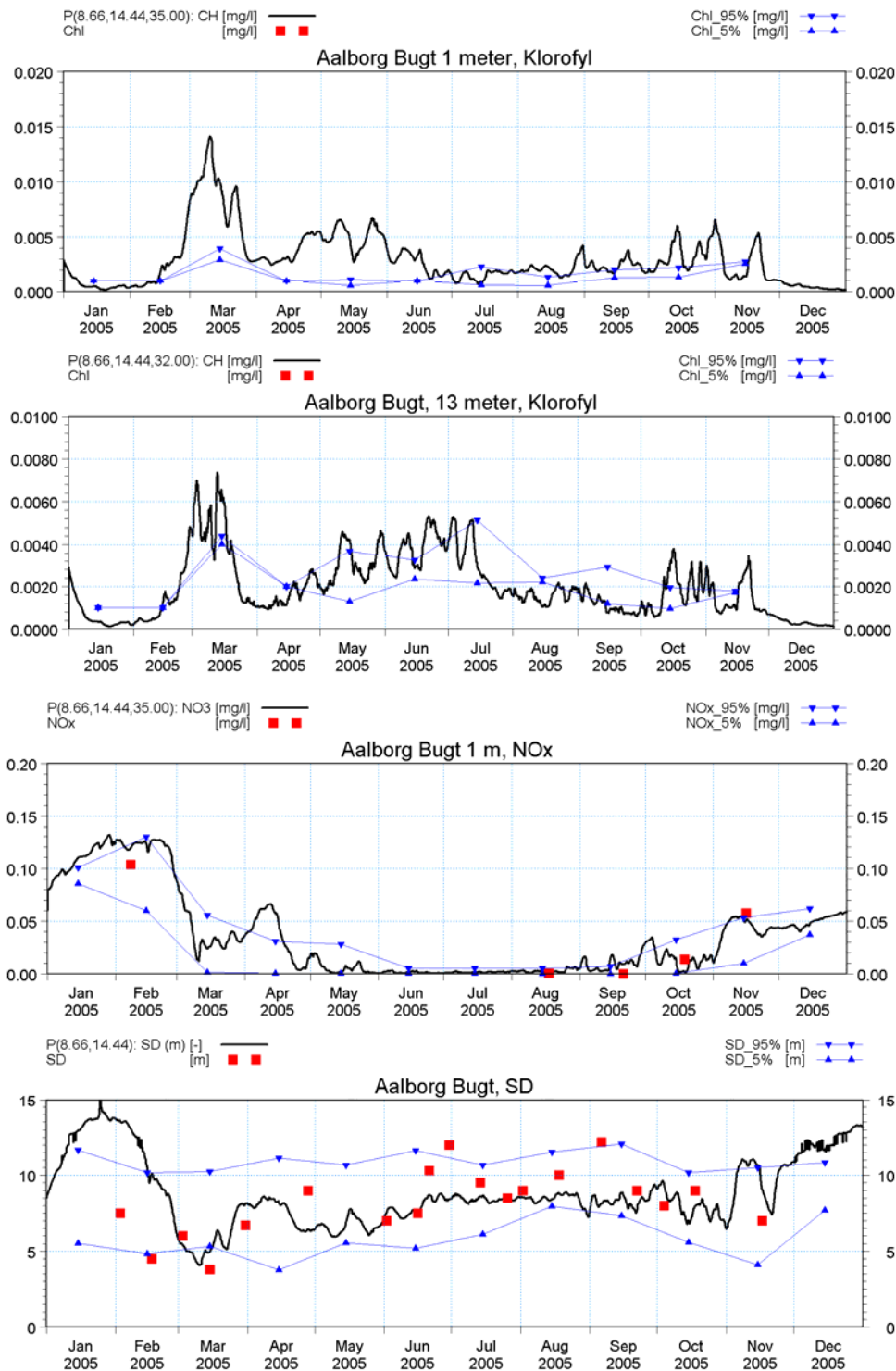
Figure 3-53   Concentration of Chlorophyll, NOx –N and Secchi Depth (SD) in Aalborg Bugt at
surface and at bottom (13 m). Modelled (black line), measured in 2005 (■) and
5 and 95% percentiles covering 2000-2007.

An overview of the modelled salinity and water quality in the central project area is depicted in Figure 3-54.

The depth in the central project area varies between 14 and 16 m and density stratification occurs at 10-12 m during larger parts of the year except during winter when the water column is fully mixed. A secondary pycnocline develops regularly at 4-5 m during summer and autumn.

Concentration of inorganic nutrients (NO_3, PO_4) accumulates in the water column during winter but nutrients are exhausted in surface waters during early spring when phytoplankton blooms. During summer and autumn smaller surface blooms occur in concert with the establishment of the secondary pycnocline. Another characteristic feature is smaller phytoplankton blooms around the primary pycnocline at 10 m. Concentration of inorganic nutrients increases from October onwards through winter when primary production becomes light limited.

The transparency of the water column measured as Secchi depth varies between 4 and 9 m during the productive period which indicates that light intensity at seabed probably is too low for benthic primary production.

Concentration of oxygen rarely falls below 6 mg/l in the central project area and the durations with low oxygen are short. In these areas the oxygen conditions must be regarded as good. During periods with strong density stratification there is risk for oxygen deficiency at shallower areas (near the Jutland coast) because the height of bottom water below pycnocline is limited. The low oxygen content will be exhausted rapidly by the benthic respiration.
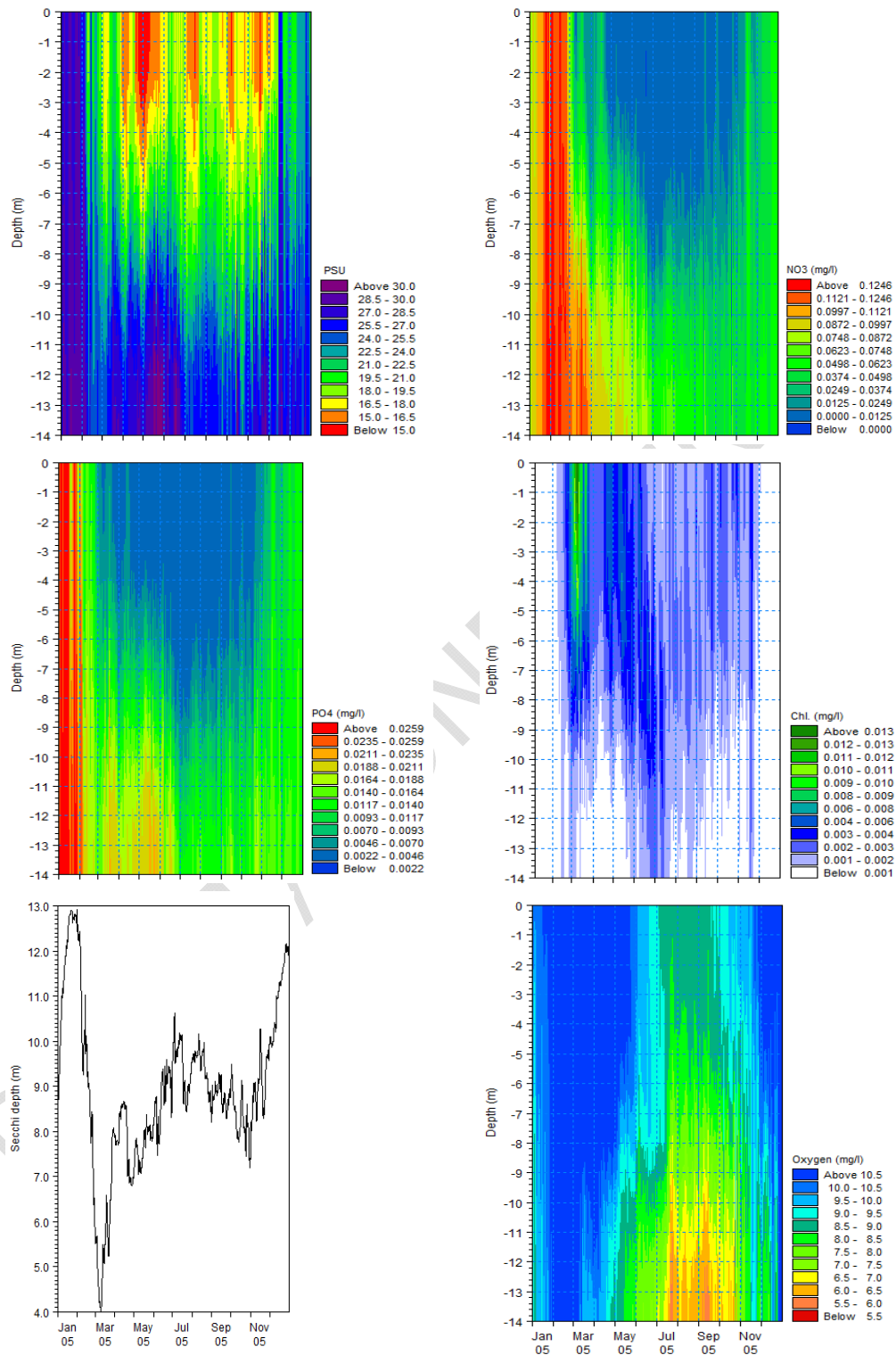
Figure 3-54   Isopleths of salinity, nitrate, phosphate, chlorophyll-a, Secchi depth and oxygen concentration in the central project area. Modelled data.

The spatial variation in pelagic primary production in the entire Kattegat is shown in Figure 3-55 and a detailed distribution of primary production covering the local model area is shown in Figure 3-56.
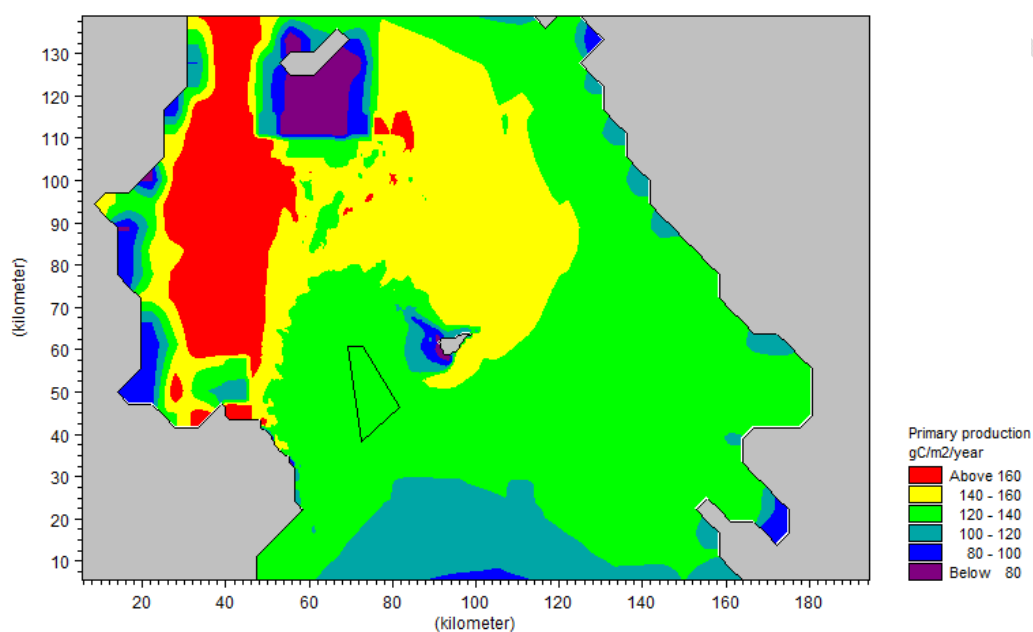
Figure 3-55   Modelled yearly (2005) pelagic primary production (g C/m^2/y) in the Kattegat.

Within the Kattegat the depth integrated primary production peaks along the 10-13 m depth curve in Aalborg Bugt as a result of intense mixing between surface and bottom water bringing nutrients up in the photic zone (Figure 3-55). At shallow waters, e.g. along coasts and South of Læsø pelagic primary production is low. Instead, benthic vegetation such as Eelgrass south of Læsø dominates production, but these processes are not modelled as benthic vegetation practically is absent in the wind park area.
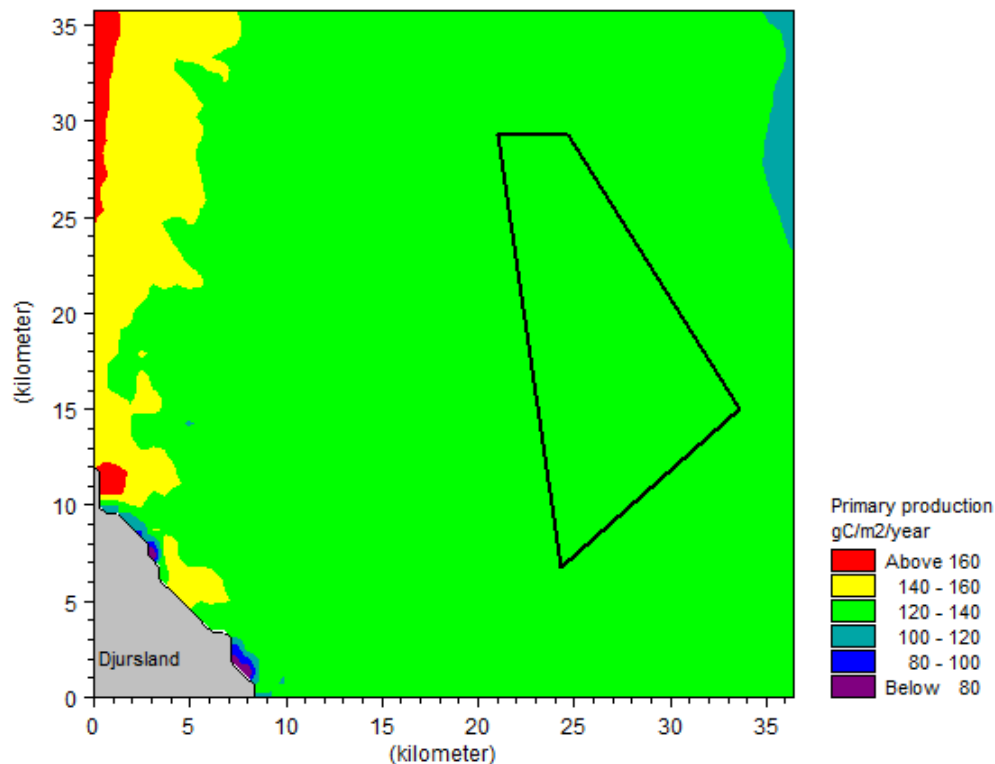
Figure 3-56   Modelled yearly (2005) pelagic primary production (g C/m^2/y) in the local model area.

3.2.7 Coastal morphology

The present state and the stability of the shorelines of Anholt and Djursland are described. The stability of the shorelines is influenced by the waves and if the near shore waves are affected by the wind farm, the shorelines may erode or accrete differently from today. The impact assessment is carried out in Section 3.3.6.

3.2.7.1 Methods

A coastal inspection of relevant sections of the shorelines of the island of Anholt and Djursland was carried out by DHI on May 12-14 2009. The descriptions of the coastal processes are based on the coastal inspection and literature on the issue.

3.2.7.2 Anholt

Anholt has undergone to drastic morphological changes since the end of the last (Weichsel) glacial period. Today the island is dominated by glacial deposits (moraine till and possible melt water deposits) which rise to heights of 20-30 m at the west end of the island. The original glacial deposits have extended much further to west of the present coastline, but the prevailing westerly winds have caused significant erosion and the eroded material has been transported towards the east along the north and south coast and have been deposited to form the large east part, ørkenen ('The

Desert'), of the island. Anholt has been the subject of considerable interest by geo-morphologists; as an example Figure 3-57 shows a diagram by A. Schou demon-strating the relation between the formation of the island and the resulting dominant wind direction, the thick arrow.

Fig. 11. Vindvirkeresultant for Anholt, indtegnet i morfologisk Skitse af Oen. A. Glaciallandskab. C. Marint Forland.

Direction-resultant of windwork for the isle of Anholt combined with a morphological sketch of the island.
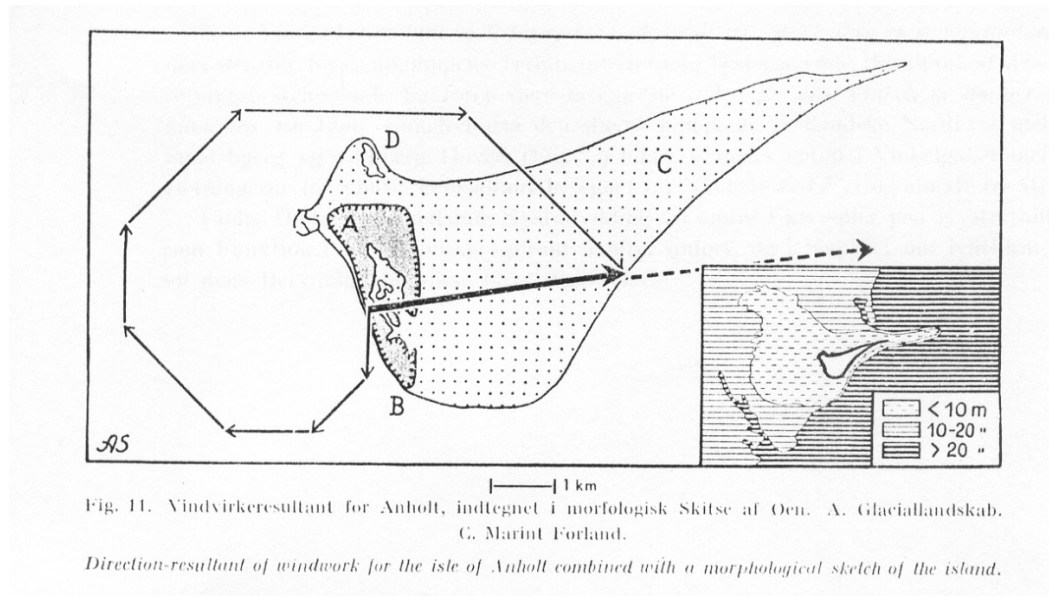
Figure 3-57   The resulting dominant wind direction, according to Schou /17/.

In Figure 3-57 A is the glacial landscape, while C is Ørkenen consisting of originally marine deposited but now mostly wind-blown sand. The west coastline has under-gone continuous erosion and steep cliffs are found between points A and B. The eroded sand has been transported both to the north and south, but the construction of the harbour in the years 1899-1902 (near point A) has blocked a considerable part of the sand transported to the north. As a result the sand has deposited south of the harbour where the coast has advanced to form a wide sandy beach, see Figure 3-58.

Figure 3-58   The wide sandy beach immediately south of the harbour.

On the north coast east of the harbour a cuspate foreland (D in Figure 3-57) has formed, which is built up by sand coming from the west as well as from the nearest part of the coast east of the foreland where it shelters for the waves coming from west. Historically the foreland has been more pronounced and tends to shift towards east which is associated with coastal erosion to the east of the harbour. The shifting of the cuspate foreland and the coastal erosion has occurred during the entire 20th century and is probably caused or intensified by the construction of the harbour, which has blocked for supply of sand coming from south to the cuspate foreland.

Figure 3-59   The coast east of the harbour. View of the eroding coast from the harbour, the coast at the camping ground and the eroding coast further to the east.

The accumulating beach south of the harbour consists of fine sand. Further to the south the coast is eroding and the beach consists more of shingles and stones. The erosion is not very pronounced and the high cliffs are covered by vegetation and do not appear to be subject to frequent slides. The beach changes from being stony to sandy at the south coast (Sønderstrand).

Figure 3-60   The west coast. The coarse stone covered beach. The cliff showing no signs of slides, and the more sandy beach furthest to the south.

The coast along the gently curved coast Pakhusbugt facing towards southeast varies slightly in character, Figure 3-61. At places at the western part it is in a dynamic equilibrium, maybe weakly erosive, the dune front shows signs of erosion but is presently being rebuilt by windblown sand. At places at the central part the coast is accretive and a new belt of dunes is under formation. At the east part the coast is again in dynamic equilibrium or weakly eroding. At places the beach is supplied by windblown sand from the land side coming out through cuts in the dunes. The sand coming from land is more yellow than the beach sand. The coast ends in a spit (Totten) which extends several km to the east and is build up by sand supplied from the coast along the Pakhusbugt as well as the north coast.

The lighthouse is placed at the east end of the north coast. The coast at the light-house is eroding and the lighthouse is protected by groynes and a breakwater.
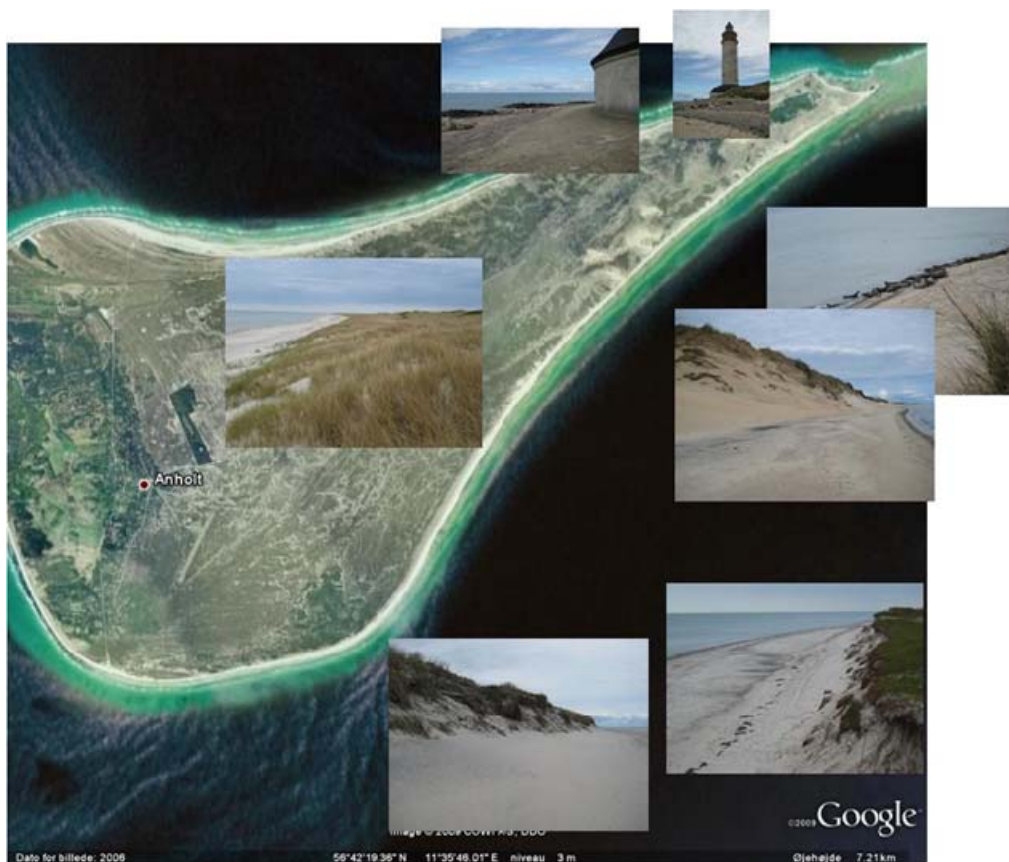
Figure 3-61   The coast at the west part of the island. From bottom: dune fronts with signs of erosion. A new belt of dunes. Yellowish sand blown out from the interior, and at the top the Lighthouse placed at the east end of the north coast with groynes at the coast.

The coastal evolution is dominated by the longshore sediment transport also known as the littoral drift. The littoral drift is driven by the incoming waves. When waves approach the coast at an angle the breaking waves drive a longshore current in the surf zone near the shoreline. The current in combination with the waves transport sand along the coast in the direction determined by the angle of the incoming waves relative to the coastline. The intensity and even the direction of the transport vary according to the changing wind conditions, but the resulting mean transport direction is well defined by the prevailing wind conditions.

The main paths of transport are shown in Figure 3-62. The system is robust in the sense that the transport directions and the areas of erosion and accretion are well defined.

Figure 3-62   The main paths of longshore transport.

3.2.7.3   Djursland

It is argued by Schou (1960) /18/ that the peninsula of Djursland exists partly because of uplift of the substratum between fault lines and that it is a horst formation of the bedrock where resistant Cretaceous (or Danian) limestone has withstood erosion by the ice during the glacial periods.

The coast of Northern Djursland is illustrated in Figure 3-63. The coastline is irregular. At some sections it consists of steep or even vertical cliffs of limestone or moraine till. The cliffs are subject to erosion and hardest parts of the eroded material have been transported to the shingle beaches between the protruding cliffs. The coastline has thus a characteristic 'festoon' form. At some locations the protruding coastline is protected by shallow submarine ledges of limestone /19 /. The north coast is an open wide sandy beach which is not subject to erosion. To the south the coastal section under consideration ends at the port of Grenå. The approximate locations of two landfall points under consideration for the power cable from the wind mill farm are also shown in Figure 3-63.
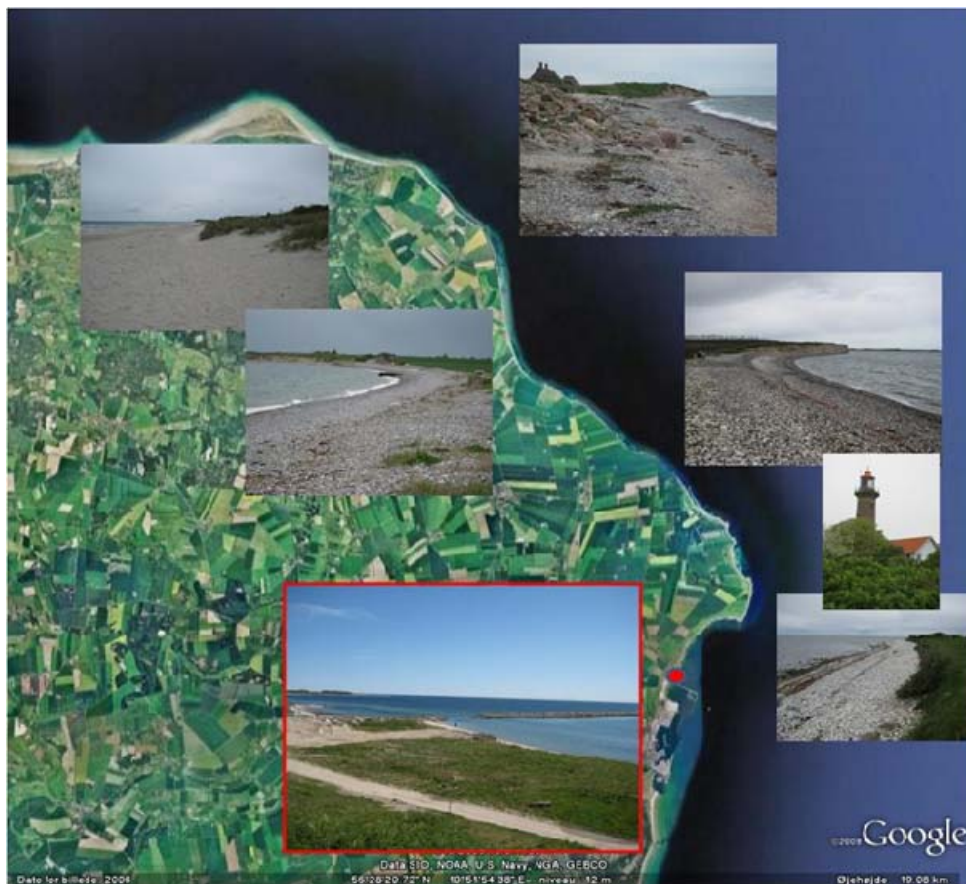
Figure 3-63   The coast of Northeast Djursland. Approximate landfall location: Grenå Nord marked with red.

Schou (1960) (/18/) distinguishes between different types of recent coastlines as illustrated in Figure 3-64. In this context the types VI and VIII are of interest.

Section VI which includes the location of the Port of Grenå is described in /18/ as simplified coast (in Danish: 'udligningskyst'), where the coastline to a large degree has been smoothed out by the incoming waves and adjusted to the dominant wave direction. Kolindsund (VII in Figure 3-64) formed a strait in at the time of the Litorina Sea (approx. 5000-7000 years B:P.) where the relative sea level was up to 5 m higher than present. The entrance was closed by a series of beach ridges, which grew out from the south side of the entrance. The construction of the Port of Grenå has affected the coastline, possibly by increasing the erosional pressure to the coast north of the harbour, while the coast immediately north of the harbour structures is now protected from waves coming from southeast; here the coast will tend to turn to face the incoming waves from northeast which is associated with a local tendency for accretion.
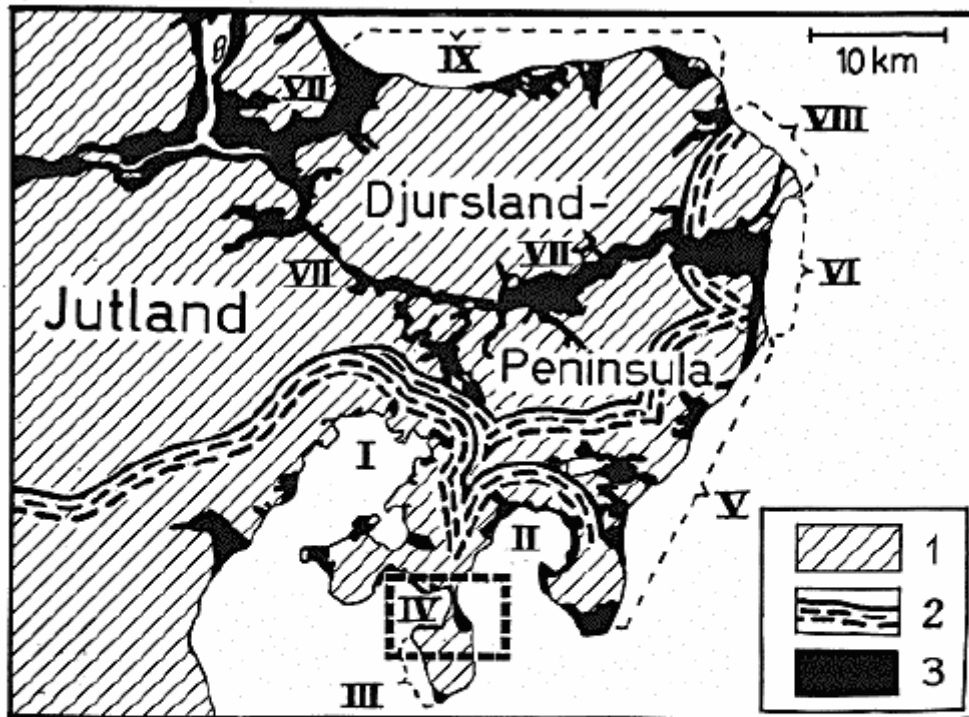
Fig. 2. *Geomorphological map of the Djursland peninsula.*

1. Young moraine landscape, Würm/Weichsel glaciation.
2. Marginal moraines.
3. Coastal plains formed by marine accumulation combined with up-heaval of land (3—5 m.) and re-clamation. The frame indicates the area shown in fig. 3 C.

I. The bay of Kalvö Vig.
II. The bay of Æbeltoft Vig.
III. The totally simplified cliff shore-line of Helgenæs.
IV. The bay of Begtrup Vig.
V. The mature simplified festoon-shaped east coast.
VI. The totally simplified east coast.
VII. The earlier "fossil" shorelines of the strait of Kolindsund.
VIII. The limestone cliffs.
IX. The old simplified north coast.

Figure 3-64   Geomorphological map of Djursland from /18/.

Section VIII is dominated by the limestone cliffs. The abrasion plane in front of the cliffs is almost covered with cobbles and boulders originating from overlying moraine which has fallen as the cliff has eroded and from flint released from the eroding lime-stone. North of the 10 m high limestone cliff of Karleby Klint this coastal type ends in a depression at Gjerild Bugt. The low lying coastline of Gjerring Bugt has a length of approximately 1.5 km. Behind it is a low-laying flat area extending up to 2 km from the coast which has been sea bed when the Litorina sea stood 3-5 m higher than the present sea level. The adjacent northern shoreline at the boundary between VIII and IX is a moraine cliff, Gjerrild klint, which rises to more than 20 m.

3.2.8 Geomorphology and sediment transport

In the following the mobility of the sea bed in the project area is investigated. The wind turbines will have an impact on the currents and waves and could potentially have an influence on the sea bed mobility and hence the geomorphology in the area. Due to the combinations of the water depth being in the order of 15-20 m and the relative small current speeds and waves in the project area, the mobility of the sea bed is found to be small. Modifications to the mobility due to the wind farm are expected to be insignificant except for very locally around the wind turbine foundations.

The order of magnitude of the sea bed mobility in this area is therefore of most interest in connection with analysing the risk of scour around the wind mill foundations as well as estimating the backfilling rates of excavated holes in the construction phase or in case the wind mill foundations are removed/partly removed in the decommissioning phase.

The sea bed mobility depends on the combination between local sediment characteristics, and the wave and current conditions in the area of interest.

Waves mainly increase the turbulence near the bed and influence the pick-up rate at the bed. The waves also keep the sediment in suspension in the water column. The current also is the main transport mechanism.

The sea bed mobility is quantified by estimations of annual sediment transport rates.

3.2.8.1 Methods

Annual sediment transport rates have been estimated at five locations pt1 to pt5 shown in Figure 3-65. The five locations correspond to the delimitation and the central point of the wind farm. These five points cover the variation in the non uniformity of the sediment characteristics (see Section 3.2.2) and in the wave and current climates within the project area.

The transport rates have been calculated using the module LITSTP of DHI's model system LITPACK. The model and the model setup are described below.
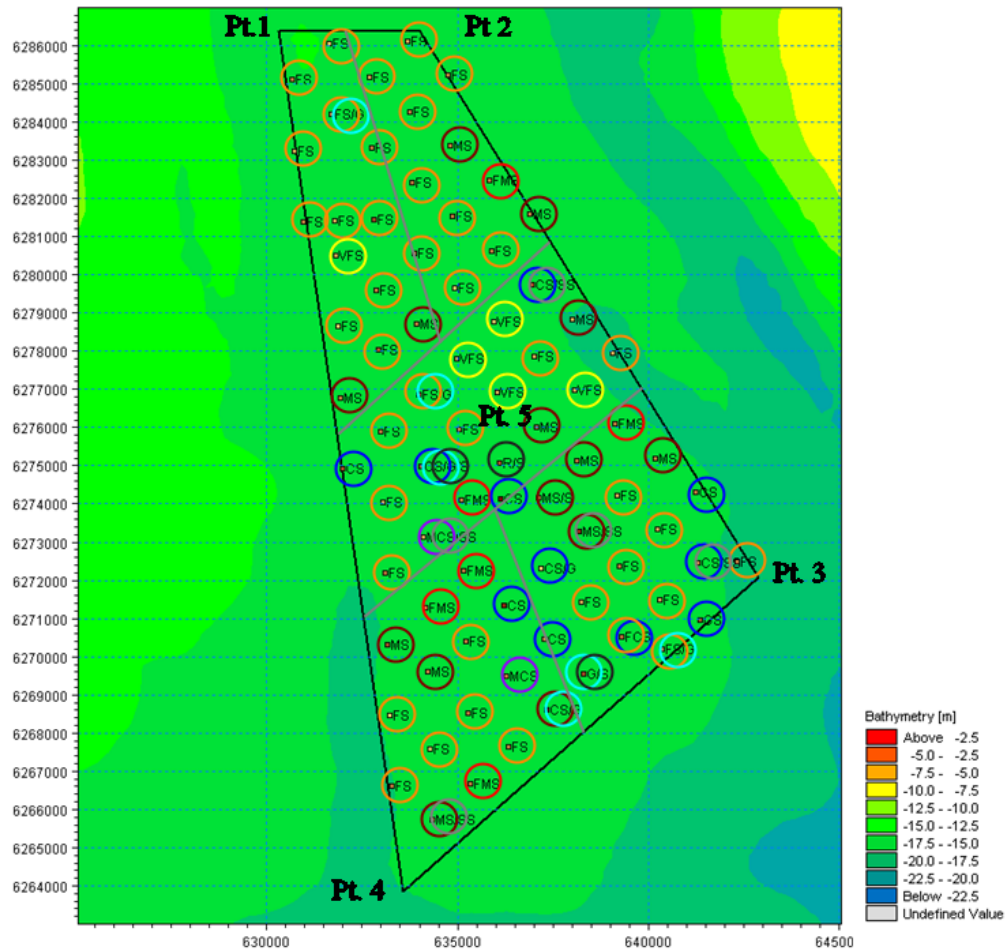
Figure 3-65   Annual sediment transport rates have been calculated in Pt. 1-5. The character-
               istics of the surface sediment samples (collected by DHI /7/) within the five
               boxes defined in the figure are applied in the calculations of annual sediment
               transport rates. Wave and current conditions in pt1 to pt5 are applied.
               VFS(yellow circle): very fine sand, FS(orange): fine sand, MS(brown): medium
               sand, FMS (red): fine to medium sand, CS(blue): coarse sand, MCS(purple):
               medium to coarse sand, SS(grey): small stones, S(black): stones, G(light
               blue): gravel, R: rocky bottom. The depth contours are shown by the colour
               coding on the right.

Short model description and setup

The sediment transport is calculated through two components: the bed load, which
corresponds to grains rolling and jumping along the bed, and the suspended load,
which represents sediment carried in the water column.

The bed-load is calculated from the instantaneous forcing from currents and waves on the sea bed, the so-called bed shear stress. Time-varying suspended sediment concentration is determined from the settling velocity and the vertical turbulent exchange.

LITSTP includes a detailed description of the turbulent boundary layer under combined waves and current and the turbulent generated by wave breaking. Temporal and vertical variations of shear stresses, turbulence and sediment concentration are resolved. The time evolution of the boundary layer due to combined wave/current motion is solved by means of the integrated momentum approach of Fredsøe. The force balance includes contributions from the near bed wave orbital motion, force associated with wave breaking (gradient of radiation stresses) and the sloping water surface.

Numerically modelled depth averaged current conditions and wave conditions for 2005 were previously illustrated at the five points in Figure 3-38 and Figure 3-45, respectively. These hindcast annual wave climate and hydrodynamic conditions were used as input to the LITSTP calculations. The main settings for the model setup are included in Table 3-13.

Sediments are treated as non-cohesive in LITSTP, which represents the characteristics of the surface sediments in the project area well. The sediment is characterised by the median grain size (d_{50}) and the geometric standard deviation ($\sigma = \sqrt{d_{84} / d_{16}}$) in the numerical model. σ is related to the uniformity of the sediment samples. A large value of σ indicates that a wide range of grain sizes are found in the sample, while a small value of σ indicates that the grain sizes of the individual grains are close to the median grain size.

The sediment characteristics in the area of each of the five points are summarized by dividing the project area into five boxes as shown in Figure 3-65. Within each box, the mean, the minimum and the maximum of d_{50} and σ are found. These are summarized in Table 3-14 to Table 3-18 together with the sediment characteristics of each of the sea bed samples in each of the boxes.

Sediment transport rates have then been calculated at pt1 to pt5 for four combinations of d_{50} and σ, combining the minimum and maximum values of d_{50} with respectively the minimum and maximum of σ. It should be stressed that the transport rates are calculated assuming that the bed in the area is entirely covered by sediment characterized by the given σ and d_{50}. Potential erosion resistant layers below the sand layer are thus not taken into account.

Table 3-13   Model setup for LITSTP for calculations of annual sediment transport rates

Parameter	Value
Water Depth	times series extracted from the 3D local hydrodynamic model described in section 5.4.1.1 at 5 points pt1-pt5
Wave climate	times series of Hrms/ Tz/ MWD extracted from the local wave model described in section 5.5.1.1 at 5 points pt1-pt5
Current climate	times series of current speed and direction extracted from the 3D local hydrodynamic model described in section 5.4.1.1 at 5 points pt1-pt5
Spectral description of wave	Irregular
Wave breaking formulation	Battjes & Janssen (1978) - γ1=1.0 and γ2=0.8
Wave theory	Stokes 1st order
Streaming process	Included
Undertow process	Included
Sediment description	Graded sand caracterised by d_{50} and σ defined above
Fractions of sediment	10
Relative sediment density	2.65
Water temperature (used for the determination of the fall velocity of each fraction of sediment)	10°C
Critical Shields parameter	0.045
Description of bed concentration	Formulation of Zyserman & Fredsøe (1994)
Ripples effect	excluded
Bed slope effect	excluded

Table 3-14   Sea bed sample characteristics (d_{50} and σ) within the box representative of pt1. Extreme and mean values of d_{50} and σ are indicated as well. Samples were collected carried out by DHI in the spring 2009 /7/.

Sample nb	d_{50} (mm)	σ
A1	0.32	1.40
A2	0.28	1.43
A3	0.30	1.43
B1	0.25	1.30
B2	0.38	1.35
BX3	0.29	1.52
B4	0.30	1.45
B5	0.25	1.30
C2	0.32	1.37
C3	0.46	1.57
C4	0.32	1.46
D4	0.32	1.46
average	0.32	1.42
min	0.25	1.30
max	0.46	1.57

Table 3-15   Sea bed sample characteristics (d_{50} and σ) within the box representative of pt2. Extreme and mean values of d_{50} and σ are indicated as well. Samples were collected carried out by DHI in the spring 2009 /7/.

Sample nb	d_{50} (mm)	σ
C1	0.29	1.45
D1	0.30	1.44
D2	0.36	1.48
D3	0.31	1.45
E1	0.32	1.44
E2	0.33	1.42
E3	0.30	1.42
F1	0.38	1.56
average	0.32	1.46
min	0.29	1.42
max	0.38	1.56

Table 3-16   Sea bed sample characteristics (d_{50} and σ) within the box representative of pt3. Extreme and mean values of d_{50} and σ are indicated as well. Samples were collected carried out by DHI in the spring 2009 /7/.

Sample nb	d_{50} (mm)	σ
G5	0.30	1.53
G6	0.25	2.41
H3	0.38	N/A
H4	0.53	N/A
H5	0.27	1.44
H6	0.47	N/A
I1	0.27	1.60
I2	0.39	1.65
I3	0.29	1.52
I4	0.30	1.76
I5	0.37	1.68
J1	0.36	1.76
J2	0.27	1.47
J3	0.28	1.67
J4	0.36	1.67
K1	0.31	1.90
K2	0.38	3.10
K3	0.40	2.37
L1	0.34	1.85
average	0.34	1.83
min	0.25	1.44
max	0.53	3.10

Table 3-17   Sea bed sample characteristics (d_{50} and σ) within the box representative of pt4. Extreme and mean values of d_{50} and σ are indicated as well. Samples were collected carried out by DHI in the spring 2009 /7/.

Sample nb	d_{50} (mm)	σ
C9	0.44	1.58
C10	0.24	1.48
C11	0.39	1.69
D9	0.31	1.60
D10	0.36	1.52
D11	0.22	1.36
D12	0.28	1.60
E8	0.32	1.52
E9	0.32	1.53
E10	0.38	1.81
E11	0.30	1.55
F7	0.53	1.84
F8	0.35	2.16
F9	0.32	1.67
G7	0.33	1.73
G8	0.73	N/A
average	0.36	1.64
min	0.22	1.36
max	0.73	2.16

Table 3-18   Sea bed sample characteristics (d_{50} and σ) within the box representative of pt5. Extreme and mean values of d_{50} and σ are indicated as well. Samples were collected carried out by DHI in the spring 2009 /7/.

Sample nb	d_{50} (mm)	σ
B6	0.31	1.47
B7	0.48	2.29
C5	0.41	3.18
C6	0.36	1.52
C7	0.26	1.54
C8	0.38	1.58
D5	0.31	1.75
D6	0.31	2.44
D7	0.44	N/A
D8	0.26	N/A
E4	0.22	1.25
E5	0.30	1.50
E6	0.33	1.64
E7	0.37	1.45
F2	0.33	1.46
F3	0.22	1.36
F4	0.26	1.40
F5	0.48	N/A
FX6	0.62	1.80
G1	0.37	1.43
G2	0.45	2.55
G3	0.28	1.53
G4	0.39	N/A
H1	0.28	1.76
H2	0.28	1.52
average	0.35	1.74
min	0.22	1.25
max	0.62	3.18

3.2.8.2   **Sea bed mobility – estimations of annual sediment transport rates**
The calculated sediment transport rates at pt1 to pt5 for the four different sediment combinations of the grain size and grading are shown in Figure 3-20 (net transport) and Table 3-20 (gross transport, i.e. the absolute mobility rate). An example of a calculated time series of sediment transport rates is shown in Figure 3-66 together with the modelled current speeds and wave heights.

The initiation of movement of sediment depends on the combined waves/currents motion. If the sediment is coarse, the combined forcing from waves and currents has to be strong whereas finer particles are more mobile. The friction on the sea bed, however, also increases with grain size. The transport rates are consequently strongly related to combination of wave and current climates as well as sediment characteristics (d_{50} and σ). No significant variations in the wave climate or currents are found across the area.

In the northern part at locations 1 and 2, the calculated sediment transport rates are very small. Net transport rates are smaller than 0.5 m^3/m/year and gross rates are smaller than 1 m^3/m/s. The sediment in this part is finer and more homogeneous than the sediments in the central and southern part.

In the central and southern part, pt. 3-5, the sediment transport rates calculated in this area are still very small, but slightly higher than the transport rates calculated in the northern part. The transport rates for the maximum grading coefficient, σ_{max}, are most likely exaggerated, in particular for the small minimum d_{50}. Under such combinations, sand fractions smaller than 0.063mm which is the limit for non cohesive sediment, are included in the sediment transport calculation. A small grain size is combined with a small grading coefficient in the present data set; however, the results are included here to cover the variation in the sediment characteristics.

Also for the combination of the maximum d50 and maximum grading in points 3-5, the transport rates seem exaggerated. The simplified parameterization of the sediment grain sizes in the samples causes the inclusion of very fine sediments in calculations of transport rates in the areas with a high grading coefficient. These fine sediments are not found in the sediment samples to such a degree. These numbers are hence included in parenthesis.

Estimations of the upper values of the annual and net and gross sediment transport rates in the project area are summarized in Figure 3-67 and Figure 3-68, respectively.

To conclude, sediment transport rates in the project are expected to be low, in the order of a couple of m^3/yr/m which is a good indication that the seabed mobility is relatively low under the existing situation. Due to the small variations in the water depth over the area and the expected small transport rates, the seabed is found to be quite stable. Local variations in the bed level up to, say 0.1 to 0.2 m may be associated with the formation and migration of small bed forms like wave or current ripples.

Table 3-19   Net sediment transport rates (m^3/m/year) calculated at pt1 to pt5 for four combinations of σ and d50. Rates in parenthesis are not realistic, please refer to text.

Location	min d50	max d50

	min σ	max σ	min σ	max σ
pt1	0.05	0.28	0.02	0.04
pt2	0.02	0.04	0.01	0.03
pt3	0.18	(13.79)	0.08	(9.41)
pt4	0.1	2.07	0.05	0.3
pt5	0.13	(25.61)	0.02	(17.01)

Table 3-20   Gross sediment transport rates (m^3/m/year) calculated at pt1 to pt5 for four combinations of σ and d50. Rates in parenthesis are not realistic, please refer to text.

| Location	min d50		max d50	
	min σ	max σ	min σ	max σ
pt1	0.29	0.72	0.11	0.33
pt2	0.10	0.19	0.06	0.11
pt3	0.27	(17.55)	0.1	(12.66)
pt4	0.36	4.19	0.05	1.2
pt5	0.39	(33.04)	0.04	(24.89)
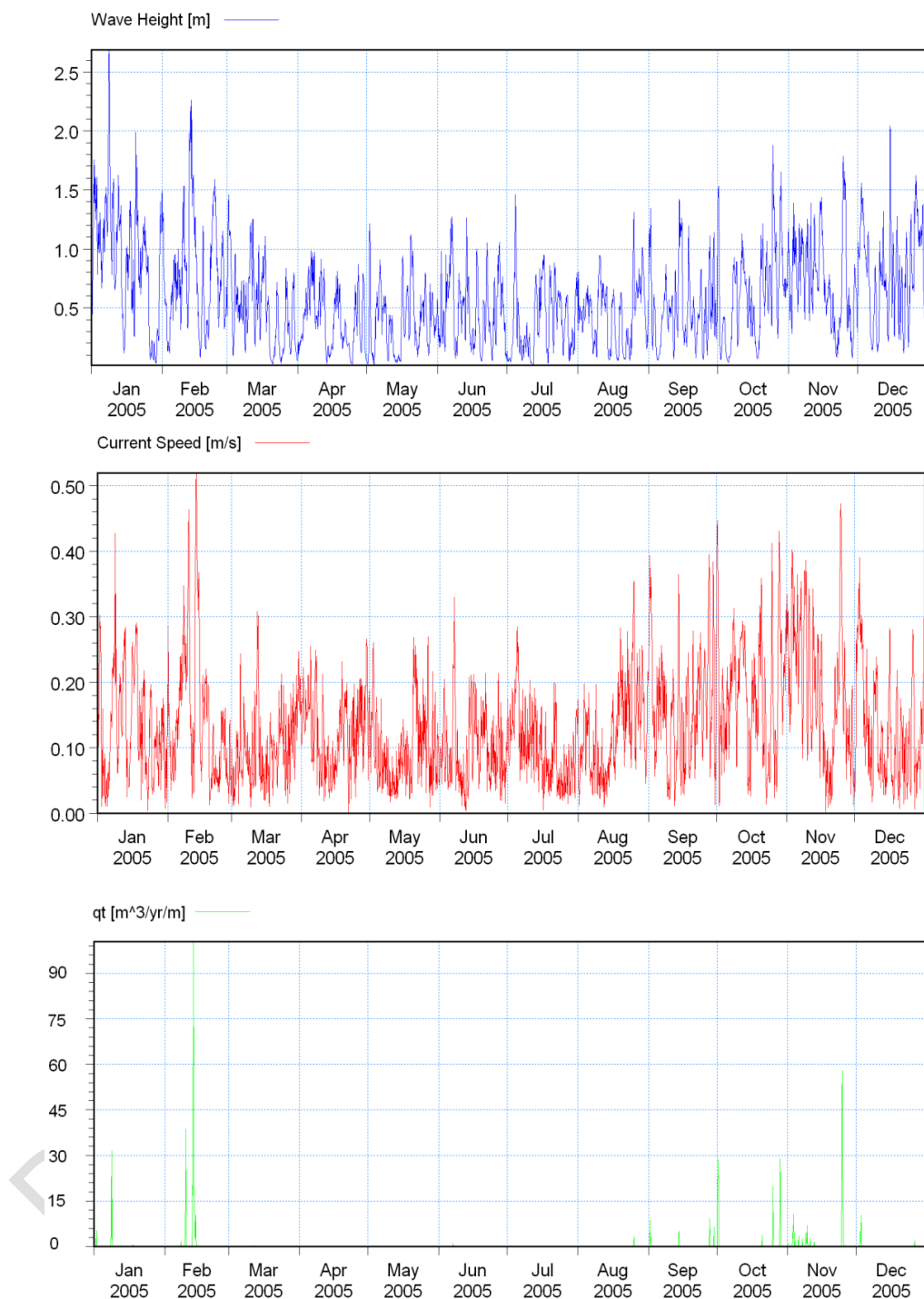
Figure 3-66   Time series of calculated sediment transport rates (lower figure) in pt 1 and modelled wave heights (upper figure) and current speeds (middle figure). Transport occurs only during events with high waves and/or strong currents.
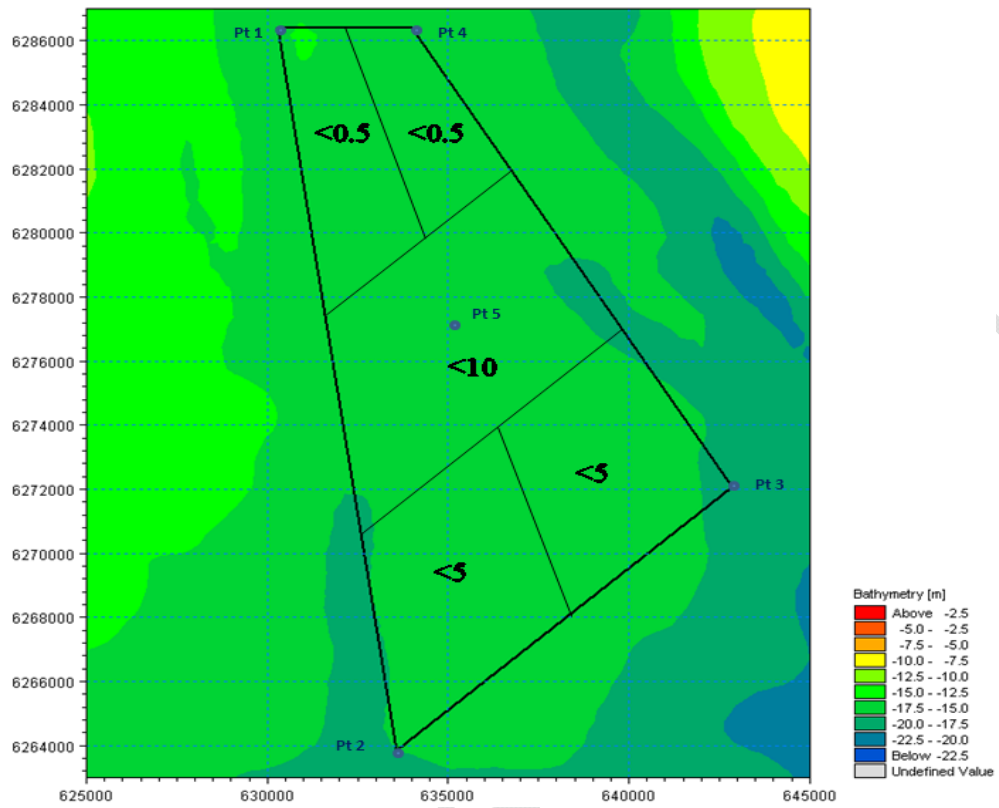
Figure 3-67   Estimations of net transport in m^3/m/year based on calculations.
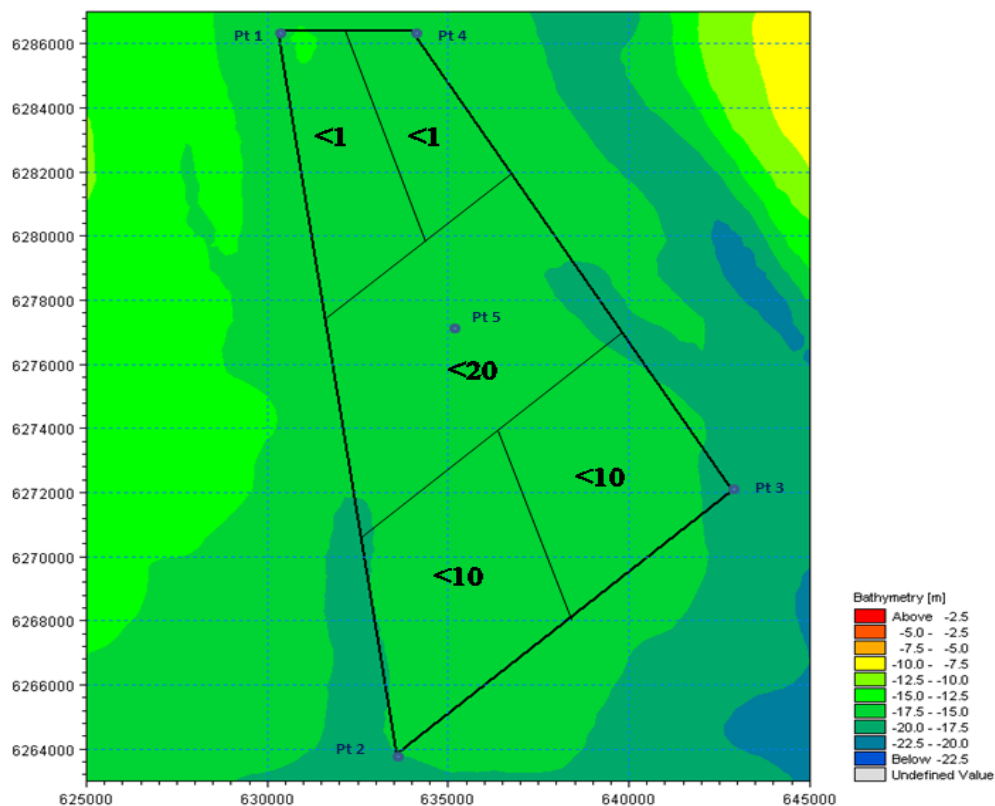
Figure 3-68   Estimations of gross transport in m^3/m/year based on calculations.

3.3   Environmental impacts

The environmental impacts on hydrography (currents and waves), water quality, geomorphology and coastal morphology associated with the planned Anholt Offshore Wind Farm are described in this chapter. Sediment spreading due to dredging activities and the risk of scour around the wind turbine foundations are also investigated. The issues listed are treated in separate subchapters below for the construction phase and the operational phase, respectively.

3.3.1   Method for impact assessment

The methodology used to assess the environmental impacts is described within each of the subchapters. Every subchapter will be accompanied by a conclusion at the end of the section that includes a table with an assessment of the different variables and an evaluation of the overall significance of the impacts, see Table 3-21. The criteria and methodology of the assessment are described in further details in /34/.

The environmental impact assessment is based on evaluation of a worst case scenario with respect to the specific choice of foundations, number and size of wind turbines etc. given the limitations in the project description /1/. The worst case scenario could in theory be different for each of the issues studied; however, the combination

of 174 2.3 MW wind turbines on gravity foundations turns out as the worst situation for each of the issues. Further details and discussion are included in the subchapters.

Table 3-21 Criteria used in the environmental impact assessment for the off-shore wind park.

Intensity of effect	Scale of effect	Duration of effect	Overall significance of impact[1]
No	Local	Short-term	No impact
Minor	Regional	Medium-term	Minor impact
Medium	National	Long-term	Moderate impact
Large	Transboundary		Significant impact
[1]: Evaluation of overall significance of impact includes an evaluation of the variables shown and an evaluation of the sensitivity of the resource/receptor that is assessed.			

3.3.2 Influence on currents and stratification

When a pile group (or a wind mill park) is placed in steady currents it will impact the current pattern. The impacts can be divided in two based on the influenced area. An impact very near the foundations, which is due to the increases in velocities around the individual foundations and the generation and dispersion of turbulence in the near vicinity of the individual wind turbines and a regional impact due to the flow resistance of the wind farm causing some water to be diverted around the farm. In the project area, the water column is stratified in the main part of the year. The effect very near the foundations may result in an increased mixing of the water column, weakening the stratification behind the foundations. These effects are the topic of this task.

3.3.2.1 Method for impact assessment

The impact of the wind mill farm on the current field can be divided into *effects felt only very near the foundations* (within a distance from the wind turbine corresponding to 1-2 times the diameter of the foundations) and *regional effects* felt in an area of a scale corresponding to the size of the wind farm area.

The effects very near the foundations are caused by the changes in the current and pressure field in the immediate vicinity of the wind mill foundation when the flow is forced around the foundation. These changes can cause:

1. eddies on the sides and behind the wind mill foundations

2. increases in the velocity in the immediate vicinity of the foundations due to contraction of streamlines

In addition to changes in the velocity field, also more mixing of the water column may take place reducing the strength of a possible stratification. These modifications occur very near the wind mill foundations and their impacts are insignificant further away than approx. 1-2 foundation diameters away from the individual wind mills. The distance between the wind mills is in the order of 40-100 foundation diameters,

so these effects do not change the overall current pattern in the wind mill farm and in the surroundings.

The effects very near the foundations are analysed by a desktop study including theory from available literature and experience from previous studies at DHI.

The regional effects are changes on the current field due to the increased resistance the foundation imposes on the overall current field. These effects impose a change in the current field within the wind mill farm area and in the surrounding area of the wind mill farm.

The regional effects of the wind mills are assessed by analysing results from the numerical models developed to describe the baseline conditions (see Section 3.2.4). These models are modified to include the impact of the wind mills on the flow field and the impacts are assessed by comparing results from the baseline calculations and the calculations with the modified set ups including the wind mills. The developed 3D flow model is applied to evaluate the impact on the annual conditions for the selected representative year (2005). The mesh size in the 3D model in the project area is 600 m. By experience it is known that the regional effects in the flow field takes place within distances in the order of the size of the wind farm from the wind farm, i.e. in the order of 10 km. The grid spacing of the local model is 1/3 nautical mile (approximately 600 m) and is sufficient to describe the expected variations to the general flow field in the area.

The developed 2D flow model is applied to assess the modifications to the flow field during storm conditions. This model has a minimum grid spacing of about 50 m within the project area. This small grid spacing was chosen to be able to test the influence on the wave forces on the flow field in the storm conditions. The wave forces have shown to have insignificant influence on the current field.

In the numerical models the wind mills are implemented at their individual locations in the form of an increased drag to include the hydrodynamic resistance from the wind mills. The drag is calculated piecewise for each component/geometry in the design and included in the local drag calculations – this is illustrated schematically in Figure 3-69. That means that the individual effects of the bottom plate, the cone and the cylinder at the top are included. The cone is included as a cylinder as shown with the mean diameter of the cone. This approach is used in both 2D and 3D.

The sources of impact and the potential impacts on the currents and stratification are summarized in Table 3-22.
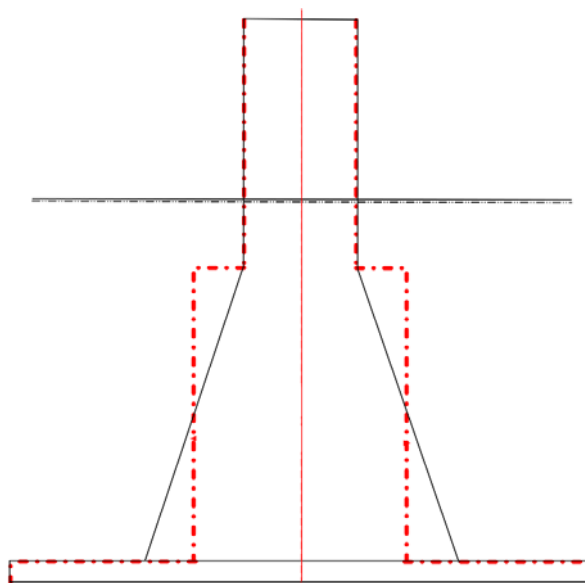
Figure 3-69   Schematic drawing of how the hydraulic resistance of the foundations is included in the numerical models.

Table 3-22   Project activities and sources of impact and potential impacts on the current and stratification

Project Activity	Sources of potential impact	Potential environmental impact
Operational phase		Environmental impact parameter affected /target of impact
Structures (foundations and piles)	Hydraulic resistance and blocking of the water flow Increased mixing of the water column near the foundations	Areas with decrease/increase of the current speeds Weakening of the stratification and modified salinities/temperatures Water quality Benthic fauna Benthic habitat

Selection of worst case scenarios of wind farm setup for modelling
The impact assessment for the current conditions is based on analysis of numerical modelling results of two scenarios selected as a combination of:

1) the type of foundation (monopile and concrete gravity base, see Section 3.1 and /1/)

2) the number and size of mills (174 pieces of 2.3 MW wind turbines or 80 pieces of 5 MW wind turbines, see Section 3.1 and /1/)

3) the wind farm layout (geographical position of wind mills, north-south going rows or arcs, see Section 3.1 and /1/)

The two worst case scenarios selected for numerical modelling are found to be the 174 pieces of 2.3 MW wind turbines on gravity base foundations for the two layouts considered in /1/.

The evaluation of the worst case scenarios is based on the reasoning below.

The effects very near the foundations and regional effects increase with the blocking effect the wind mill foundations impose on the current field. Of the two types of foundations the gravity base will clearly have the highest impact on the flow, due to the larger cross sectional area these foundations have regardless of the choice of the size of the mills across the water depth compared to the monopiles.

The gravity foundation increases with the size of the mill. The preliminary design parameters for the gravity base from /1/ are shown in Table 3-23. The gravity foundations to consider for the numerical modelling were agreed with Rambøll and are shown in Figure 3-70 for the small 2.3 MW turbines and the 5 MW turbines, respectively. For the small 2.3 MW wind turbines the width of the gravity base applied in the modelling is slightly smaller (14 m) than the upper limit in Table 3-23 (up to 20 m).

The foundations for the 2.3 MW mills in Figure 3-70 have a total cross sectional area (below MSL) of 288 m^2 (327 m^2 with the width of the gravity base as in Table 3-23) on a characteristic water depth of 17 m. Installation of 174 units of these wind turbines is required to reach the 400 MW limit of the maximum capacity /1/. The total cross sectional area is hence 50112 m^2. The individual gravity foundations for 5 MW wind turbines in Figure 3-70 have a cross sectional area of 368 m^2 and 80 mills of this type are required in case the larger wind mills are chosen for the wind farm. The total cross sectional area for these mills is hence 29440 m^2. The total cross sectional area blocking the hydrodynamic field is therefore a factor of 1.70 larger for the combination of smaller foundations and larger number of wind mills than for the combination of larger foundations and fewer wind mills.

The regional hydrodynamic effect does not only depend on the blocking area, but also on the incoming flow velocities and the ratio between the diameter of the foundation and the distance between the wind turbines – this is explained in more details below. However, the difference between this ratio for the small and the large foundations is small. The total blocking area is hence the dominant factor and the combination of the smaller foundations and the larger number of mills is evaluated as being

the worst case scenario in comparison with the larger size but smaller number of mills for the hydrodynamic impacts.

The wind farm layout for the small wind mills is shown in Figure 3-71 and Figure 3-72. If the distance between mills are small enough that the effect on the current due to the first mill is felt at the next downstream mill, the number of mills in the current direction is important for the total impact. However, the differences between the two configurations considered in this work are small.

The two worst case scenarios are hence chosen as the combination shown in Table 3-24.

Table 3-23   Preliminary design parameters for gravity base from the project description /1/.

GRAVITY BASE	Smaller Turbine (174 units)	Larger Turbine (80 units)
Shaft Diameter	Up to 5.0 m	Up to 5.5 m
Width of Base	Up to 20 m	Up to 25 m
Concrete weight per unit	Up to 2000	Up to 3000
Total Concrete weight (t) , 174/80 turbines	Up to 350.000	Up to 240.000
BALLAST		
Type	Sand or equivalent	Sand or equivalent
Mass per unit (m3)	Up to 6000	Up to 9000
Total mass (m3) , 174/80 turbines	Up to 1000.000	Up to 700.000
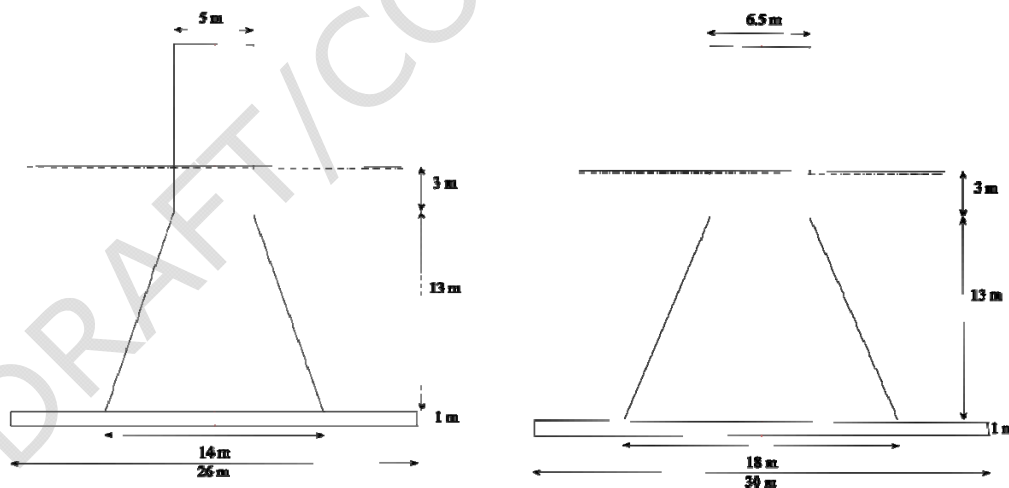
Figure 3-70 Gravity base for 2.3 MW (left) and 5 MW (right) wind turbines as considered for the modelling tasks. The smaller foundations (left) are applied in the numerical modelling.

Table 3-24   Worst case scenarios used in the numerical modelling

Scenario	Foundation	Mill size/no. of mills	Configuration of mills
Scenario 1	Gravity base	2.3 MW/174 units	Layout 1

| Scenario 2	Gravity base	2.3 MW/174 units	Layout 2
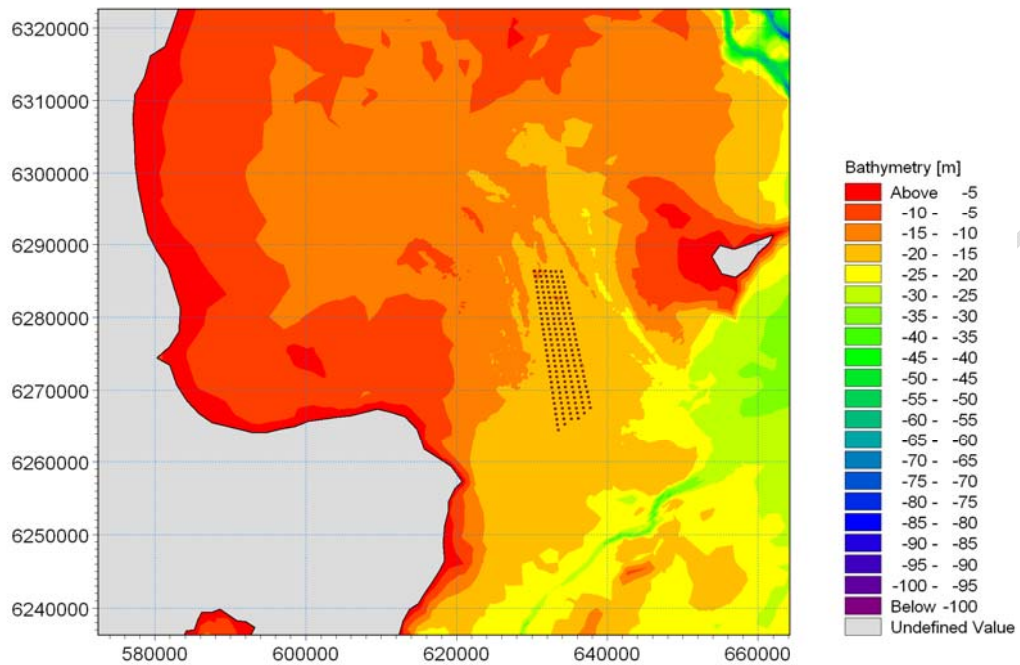
Figure 3-71   Configuration of wind farm for Scenario 1 with 2.3 MW wind turbines.
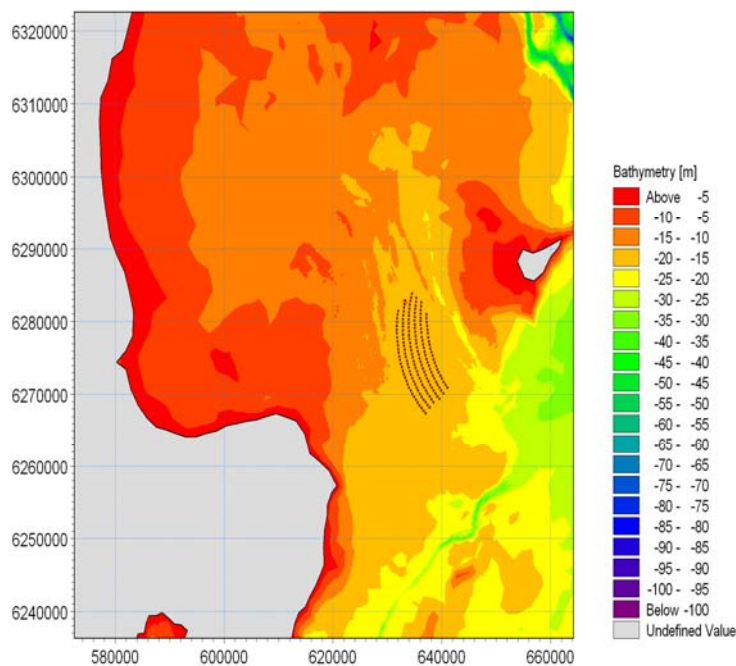

Figure 3-72   Configuration of wind farm for Scenario 2 with 2.3 MW wind turbines.

3.3.2.2 Impacts during the operational phase

3.3.2.2.1 Impact on current conditions during calm weather conditions — 3D modelling

Effects very near the foundations

The problem of pile groups placed in steady currents has been investigated by various researchers. The general finding is that depending on the gap ratio there may be both an impact very near the foundations (within a distance of 1-2 diameters of the foundations) and regional effect on the current patterns and subsequently on the scour patterns. For this study the focus will be on the current patterns. The effect very near the foundations is caused by the immediate presence of the pile, or in this case the wind mill. The result is an increase in velocities in the immediate vicinity of the wind mill. This will be felt 1-2 diameters away from the mill. This is called contraction of streamlines. The result is also the formation of the so called horse shoe vortex. This is a rotation of the water that will form at the base of the wind mill due to the transverse pressure gradient. This rotation is the one that cause scour if no protection is present. This will also be felt 1-2 diameters away from the wind mill. Finally, the presence of the wind mill will induce vortex shedding or lee wake vortices. This is a form of turbulence that will form on the sides of the wind mill and travel downstream while shifting rhythmic from side to side. These are the three effects that cause an impact very near the foundations of the wind turbines. An overview of these effects is given in Figure 3-73.
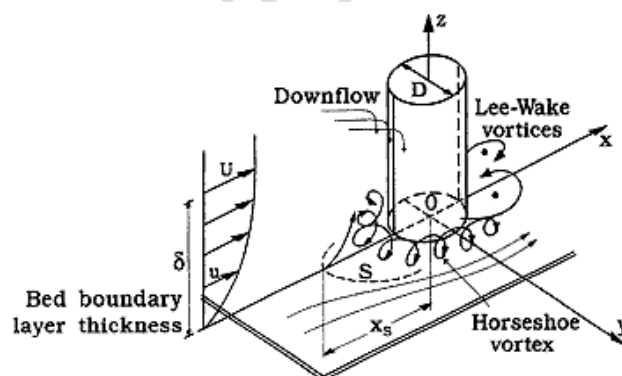

Figure 3-73   Overview of mechanisms very near the foundations of the wind turbines (From /33 /).

Naturally, the formation of vortices will also lead to increased mixing in the vicinity of the wind mills. Therefore an impact on the flow of salinity, temperature and nutrients

must be expected in the immediate vicinity of the wind mills. Tests conducted at DHI indicate that approximately 5% of the produced turbulent kinetic energy at the wind mill is going to increased mixing across the interface. This is the energy dissipated due to the three mechanisms shown in Figure 3-73.

The changes in salinity (or temperature) due to the increased mixing can be evaluated by carrying out calculations of the possible mixing of the water column based on calculation of 1) the energy available for mixing, 2) the energy required for mixing and 3) volumetric considerations depending on the flow speed and the depths of respectively the more saline/cooler lower layer and the less saline/warmer upper layer. Detailed calculations are given in Appendix A.

In Figure 3-74 results showing the modified salinity in the upper and lower layer respectively at a distance of one wind mill diameter downstream from the wind mill foundations. The salinities obviously depend on the upstream salinities in the upper and lower layer and in Figure 3-74 the results are shown for two variations of these salinities. The thicknesses of the upper/lower layers are assumed as 12 m and 5 m, respectively. The travelling time for a water volume to pass through the area where mixing occurs is reduced for higher current speeds; however, the energy input available for mixing is higher for higher current velocities. Results show that mixing increases with higher current velocities. When the current speed is less than 0.4 m/s – 0.5 m/s, no significant mixing effect is seen and for all practical purposes mixing can be neglected in this regime. For current velocities higher than approximately 0.5 m/s mixing may cause the salinities to change with about 0.2-0.3 PSU. The results also show that mixing of the full water column is a function of how strong the stratification is but even for relatively weak stratifications (2.5 PSU) the full mixing is not achieved. The current speed is assumed to be uniform across the water depth. The exceedance frequencies for surface current speeds in 2005 at a location near the wind mill park are given in Table 3-25. The current speed exceeds 0.4-0.5 m/s only about 2-5% of the time, hence significant mixing occurs only in 2-5% of the time during an average year. Note that if the depth averaged velocity was considered the number would be even smaller.

The change in salinity due to mixing is highest for the lower layer, since the lower layer thickness in this example is smaller than the thickness of the upper layer.

Figure 3-75 shows similar results as Figure 3-74, but with thicknesses of the upper/lower layer of respectively 5 m and 12 m, i.e. in this case the upper layer is thinner than the lower layer. In this situation the salinity change for the upper layer is higher than the salinity change for the lower layer.
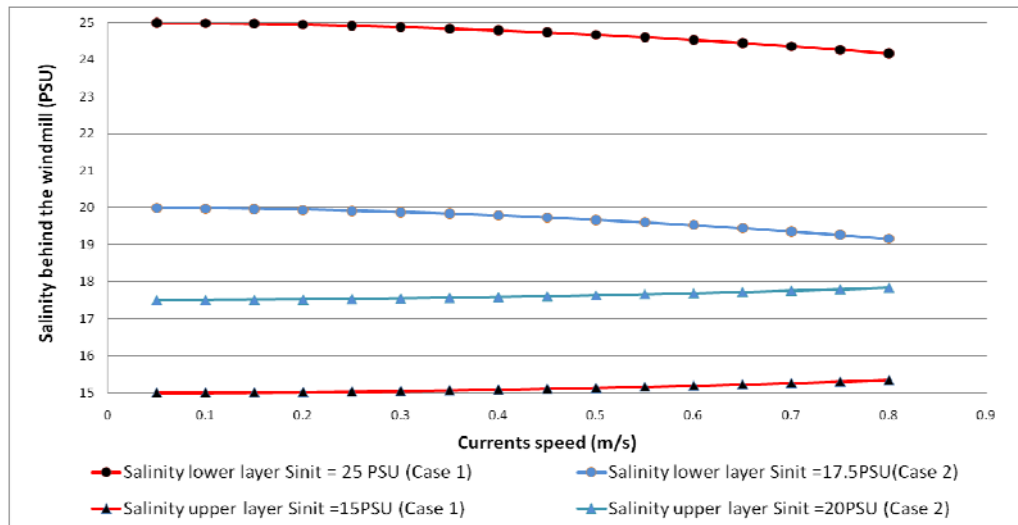
Figure 3-74   Salinity downstream of the wind turbine at different current speeds. S_{init} is the salinity upstream of the wind mill, the thickness of the lower layer is 5 m and the upper layer is 12 m. The diameter considered is 15 m.
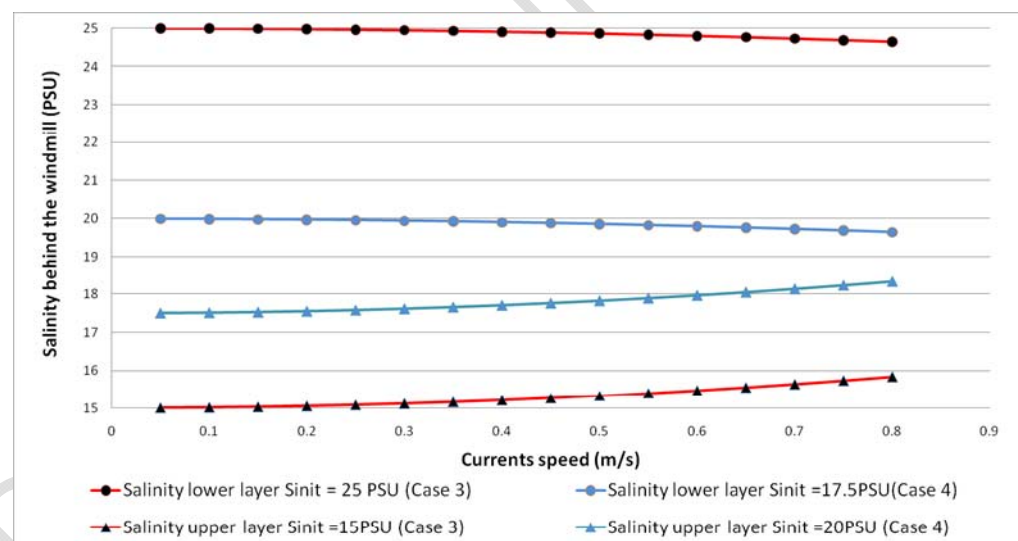
Figure 3-75   Salinity downstream of the wind turbine at different current speeds. S_{init} is the salinity upstream of the wind mill, the thickness of the lower layer is 12 m and the upper layer is 5 m. The diameter considered is 15 m.

Table 3-25   Exceedance of current speeds at the surface near the wind mill park (from modelling presented below).

Current speed	0	0.05	0.1	0.15	0.2	0.25	0.3	0.4	0.5	0.6	0.7	0.8

| Time of year in % where current speed is exceeded	0.00	9.05	30.30	51.15	68.90	80.41	86.92	94.65	97.82	99.40	99.99	100.00

In the case where significant mixing is present it is relevant to consider how far downstream the effect is felt. Downstream of the foundations the impacts spread out in a fan or plume. There is no exact formula for this but from /3/ it is known that the width of the plume (y) is proportional to:

$$y = a\sqrt{x} + b$$

In which y is the plume width, x is the distance downstream and a and b are constants. If we assume that the width of the plume at x = 0 is equal to the diameter of the wind mill, then b is equal to the diameter. If it is also assumed that the plume initially expands with 10 degrees downstream (figure of experience) then a can be determined to be 0.35. The width of the plume can then be written as:

$$y = 0.35\sqrt{x} + D \quad \text{(m)}$$

where x is measured from the edge of the wind mill foundation and y is the full width of the plume. In Figure 3-76 the development of the width of the wake is given. It should be noted that this is probably a conservative estimate because the plume will most likely expand faster in the area near the pier.

The lesson from this is that if the flow is unidirectional downstream the plume will form a narrow band that is slowly diluted. 600 m downstream the volume will have doubled and the effect has been reduced by a factor of two. Similarly at 1200 m, the effect has been reduced by a factor of three.

The conclusion is that mixing effects at the wind mills will occur only for 2-5% of the time during high current events (above 0.4-0.5 m/s), where changes in the salinities in the order of 0.2-0.5 PSU can occur temporarily in the near vicinity of the wind turbines (corresponding to a distance downstream the wind turbine of about 1-2 diameters of the foundation). The impact will be felt in a narrow but slowly expanding band downstream and will reduce with the distance from the wind turbine.

Regional effects

The regional effects are different from the effects in the immediate vicinity of the wind turbine foundations. These are changes which impact the current speeds and flow pattern in the wind farm area and in the area around the wind farm due to the hydraulic resistance caused by the wind mills. On a larger scale than corresponding to 1-2 diameters of the foundations around each individual foundation, contraction and/or divergence of streamlines can take place due to the extra roughness caused by the presence of the wind mills.

The impact is dependent on the size and shape of the wind mill foundations and the distance between the wind mills compared to the radius of the wind mills. On one hand, if the wind mills are placed right next to each other, the wind mill park will act as one pile where the diameter is equal to the diameter of the group. On the other hand, if the wind mills are placed very far from each other, the wind mills will act individually without any group effect. Sumer et. Al. /37/ investigated this effect for the purpose of determining the scour in pile groups. They demonstrated that not only the distance between the piles but also the formation or layout of the piles played a role. They concluded that the less organized the piles were located, the higher was the combined resistance from the piles. However, from their study it was shown that if the distance between the piles was 4 diameters or more then the flow in the middle of the sections between the piles would be practically unchanged (change in flow velocity of less than 5%).

In the Anholt wind farm distances around 600 m are planned and the diameter of the foundations varies between 5 m (upper part of the water column) and 14-18 m (lower part of the water column). That gives a ratio G/D of 40 – 100 between the diameters (D) and the gaps between the wind mills (G). Based on this, the main flow should be virtually unaffected. If one does a calculation based on the geometry of the wind mills and a water depth of 17m and a distance between the mills of 600 m then one gets to the conclusion that a gravity foundation for a 2.3 MW wind mill

block around 1.4% of the cross section between the centre of one foundation to the centre of the neighboring foundation. The calculation can be found in Appendix D.

The park acts as an extra roughness or a partial blockage of the overall current field. The blocked water volume is forced around the park which leads to a decrease in the flow inside the park and an increase in flow velocities on the sides of the park. In the following sections modelling results will show the extent of this impact.

Time series of the simulated baseline surface flow velocities at five locations within and near the project area and the velocity difference between the baseline and Scenario 1 and 2 are shown in Figure 3-77 to Figure 3-79. The velocity changes are seen to have an order of magnitude up to approximately 1 cm/s and the maximum velocity changes occur when flow velocities are high.

The flow in Kattegat is very dynamic with many eddies forming and disappearing. Short term effects (hours) of the wind mill park include vortices being shifted slightly in space. These are not interesting from a practical point of view due to their very short duration and still minor influence on the current speeds.

The annual mean changes in the surface flow velocities during the year modelled with the 3D flow model, 2005, are presented in Figure 3-80 - Figure 3-83. From a biological point of view the annual mean changes are the most interesting. The changes are in each computational cell evaluated as:

$$annual\ mean\ velocity\ change = \overline{u_{modified}(t) - u_{baseline}(t)}$$

The largest impact is expected at the surface where the flow velocities are significantly higher than at the bottom. The flow resistance at the bottom is smaller even though the geometry of the mills is larger at the bed.

The annual average velocity change for Scenario 1 is presented in Figure 3-80 (change in the north-south going velocity component) and in Figure 3-81 (change in the east-west going velocity component) for the surface flow.

The main flow direction is north-south. The results in Figure 3-80 show very small effects with average velocity changes less than 1 – 2 mm/s and in most areas even lower. The mean surface velocity changes are very small and insignificant compared to the mean flow velocity, which for the surface flow is in the order of 0.2 m/s.

The results also show that these very small velocity changes caused by the increased roughness due to the wind mill park lead to a slight diversion of the flow. This is the reason for the decrease in the north-south going currents at the wind mill park and the increase at the sides of the wind mill park. Note that a small effect is seen on the eastern side of Anholt indicating that some flow is diverted this way.

The annual mean velocity changes for the east-west going component are shown in Figure 3-81. The general flow direction is in the north-southerly direction; however,

in periods large eddies form and these eddies are affected by the presence of the wind mill park. The reason for the patterns seen in Figure 3-81 is therefore partly that the pattern of the eddies changes slightly and partly that the dominating flow is slightly shifted towards east as explained above.

The corresponding mean velocity changes for Scenario 2 are presented in Figure 3-82 and Figure 3-83. The results show that the impacts on the north-south going velocity component as well as the east-west going velocity component are very similar to the ones found for Scenario 1, i.e. very small.
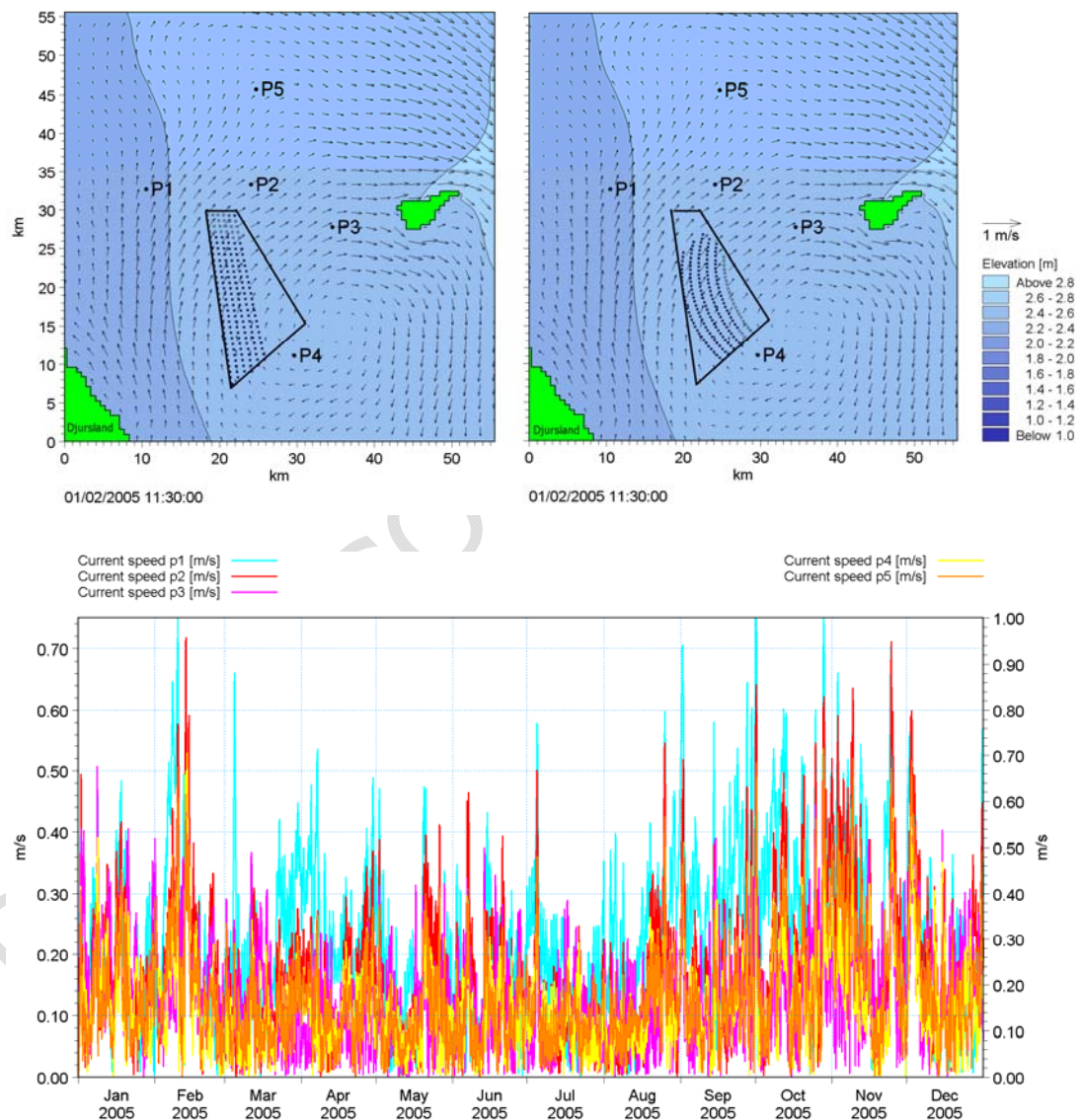
Figure 3-77   Modelled current speeds in the Baseline situation (local model, grid size approximately 600 m) are shown at five locations, P1-P5, within and near

the project   area. Deviations in current speeds in Scenario 1 and Scenario 2 are shown in Figure 3-78 and Figure 3-79.
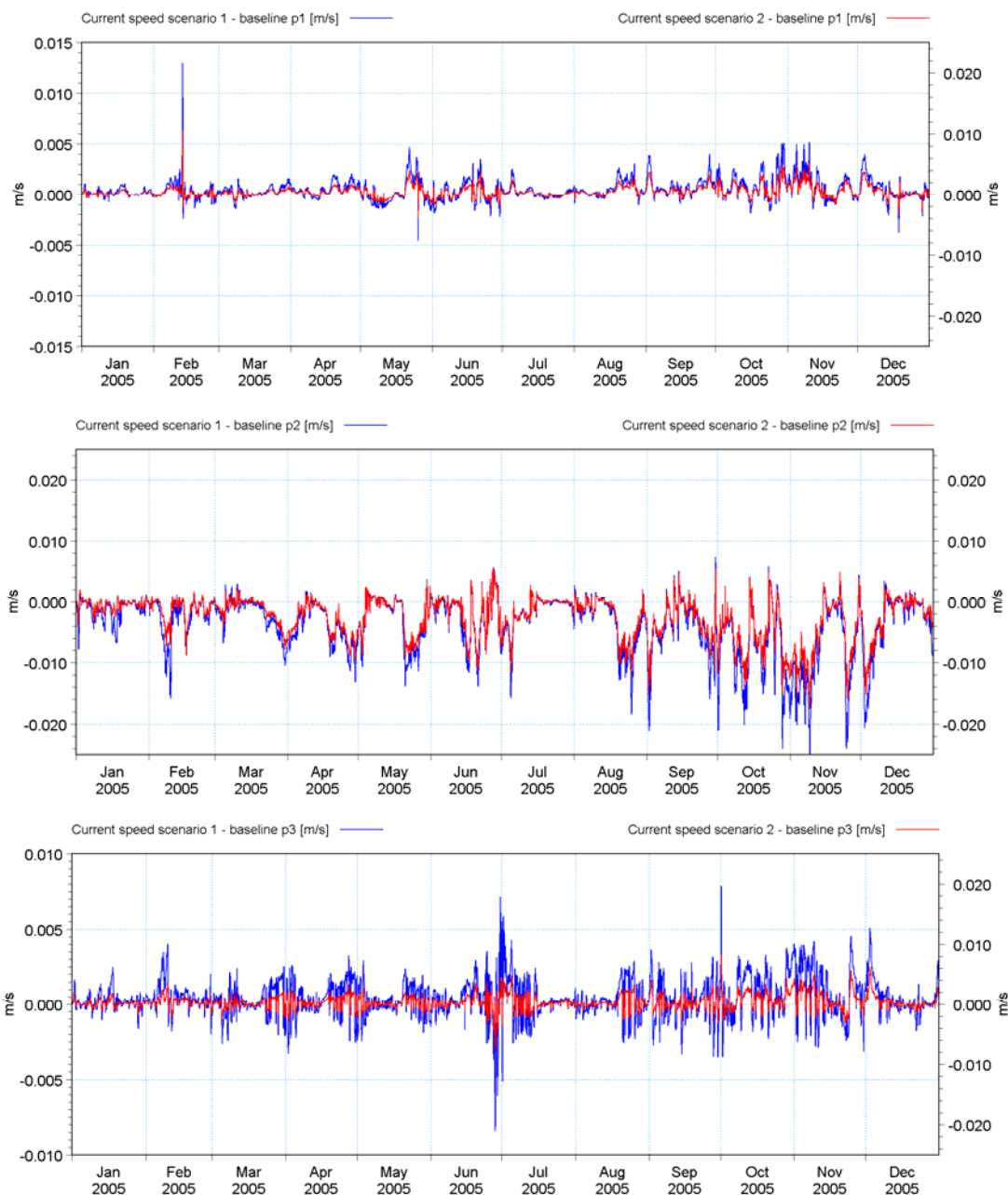
Figure 3-78   Modelled current speeds and deviations in current speeds (local model, grid size approximately 600 m) at locations P1, P2 and P3 as defined in Figure 3-77.
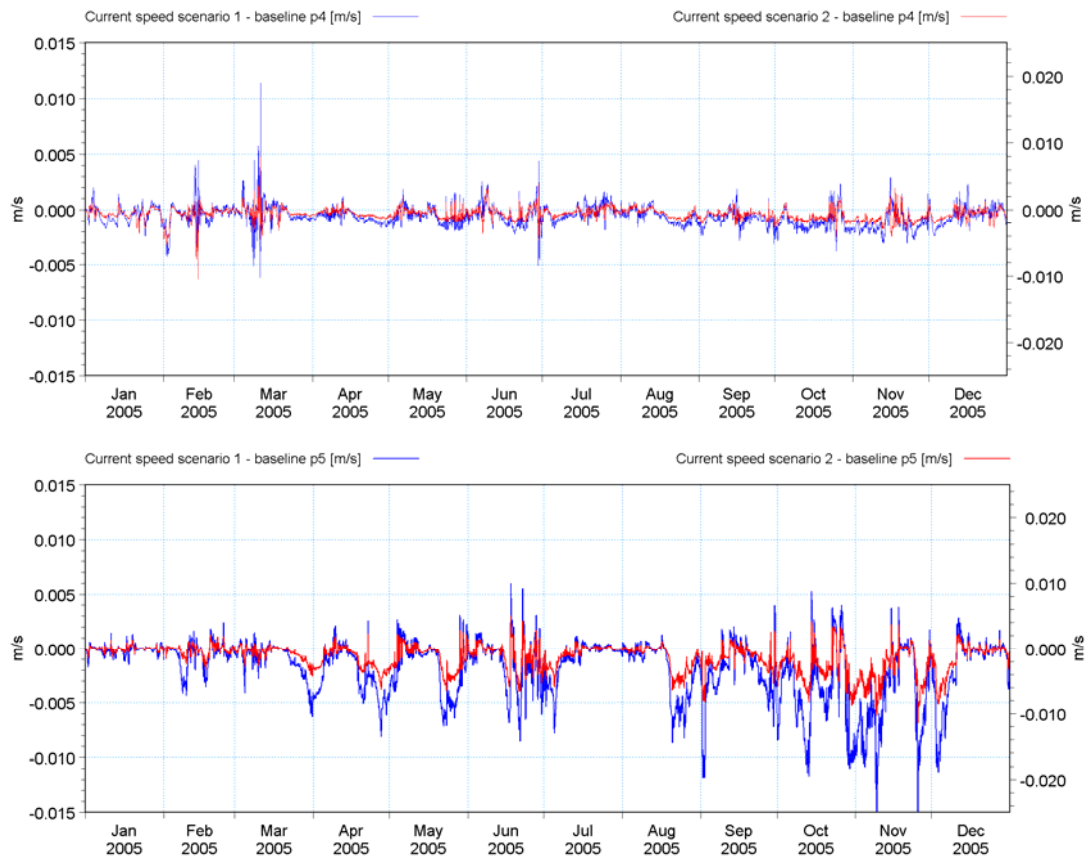
Figure 3-79   Modelled current speeds and deviations in current speeds (local model, grid size approximately 600 m) at locations P4 and P5 as defined in Figure 3-77.
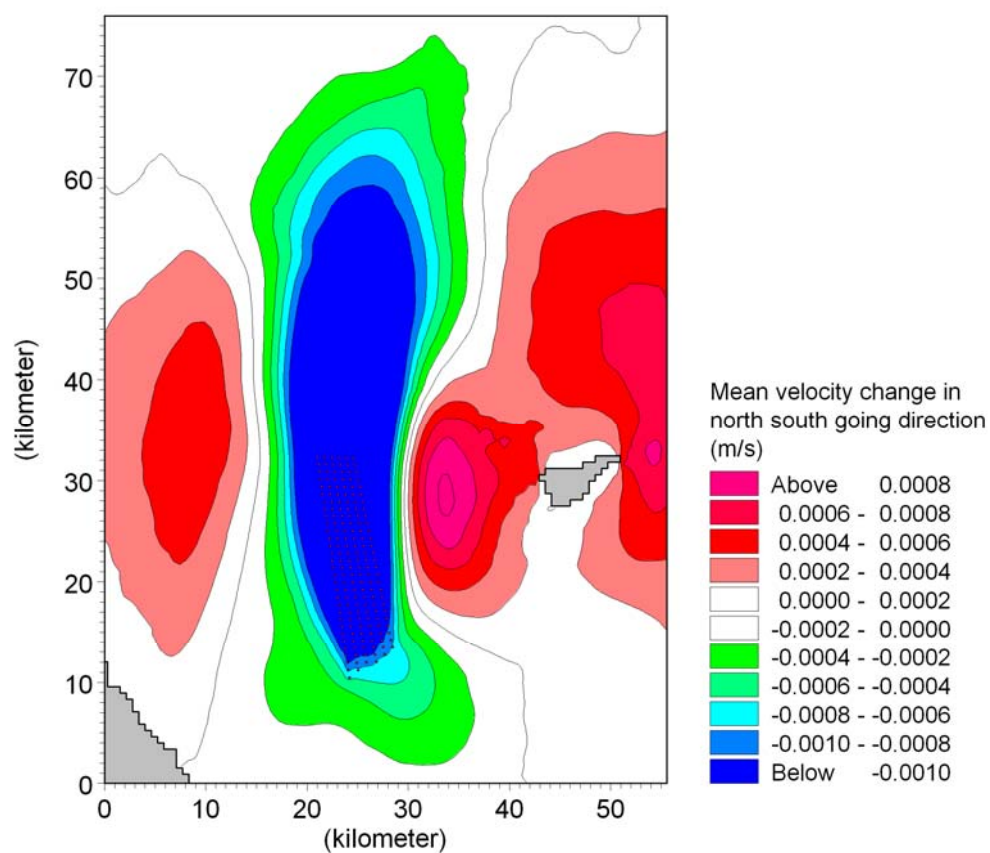
Figure 3-80   Annual mean surface velocity changes for the north-south going velocity component in 2005. Model results from the local 3D model (grid spacing approximately 600 m). Green-blue colours indicate a velocity reduction and red colours indicate an increase in current velocity.
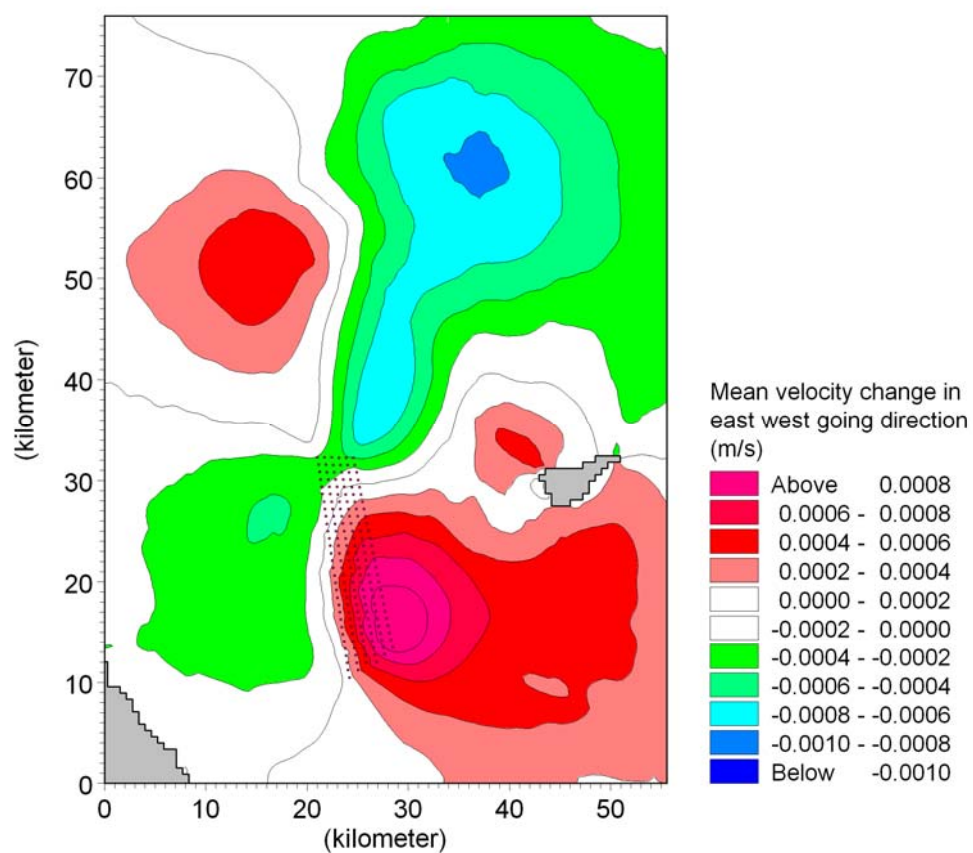
Figure 3-81   Annual mean surface velocity changes for the east-west going velocity compo-
nent in 2005. Model results from the local 3D model (grid spacing approxi-
mately 600 m). Green-blue colours indicate a velocity reduction and red colours
indicate an increase in current velocity.
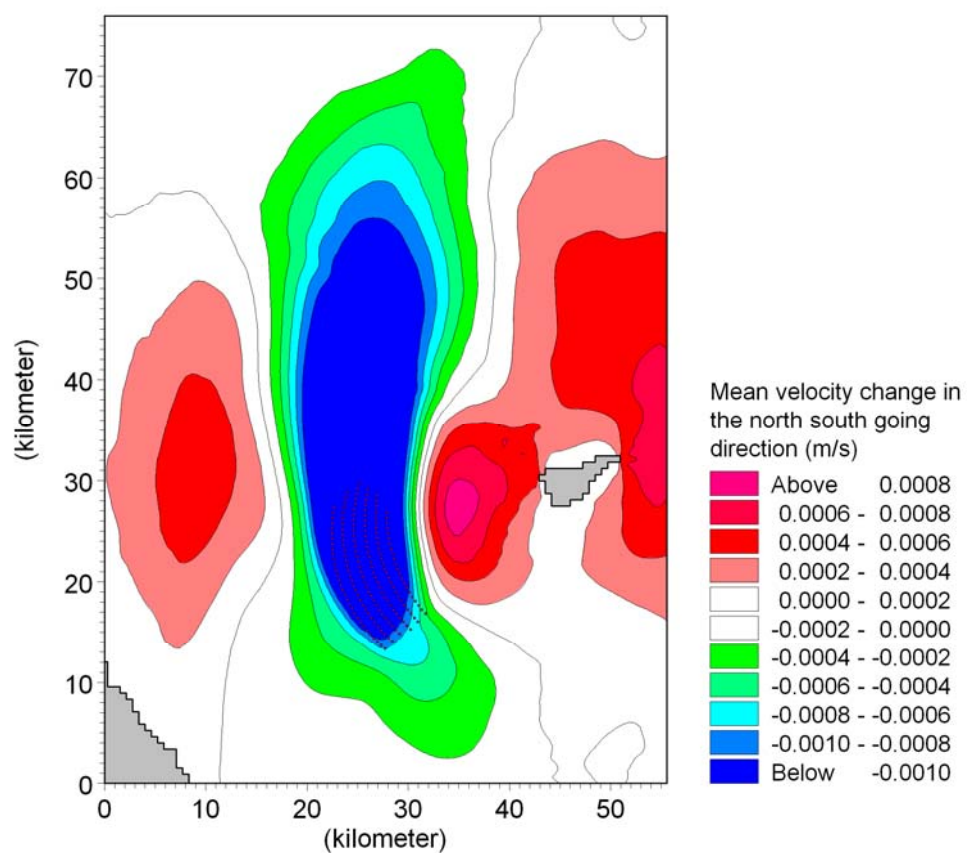
Figure 3-82 Annual mean surface velocity changes in the north-south going velocity compo-
nent 2005. Model results from the local 3D model (grid spacing approximately
600 m). Green-blue colours indicate a velocity reduction and red colours indi-
cate an increase in current velocity.
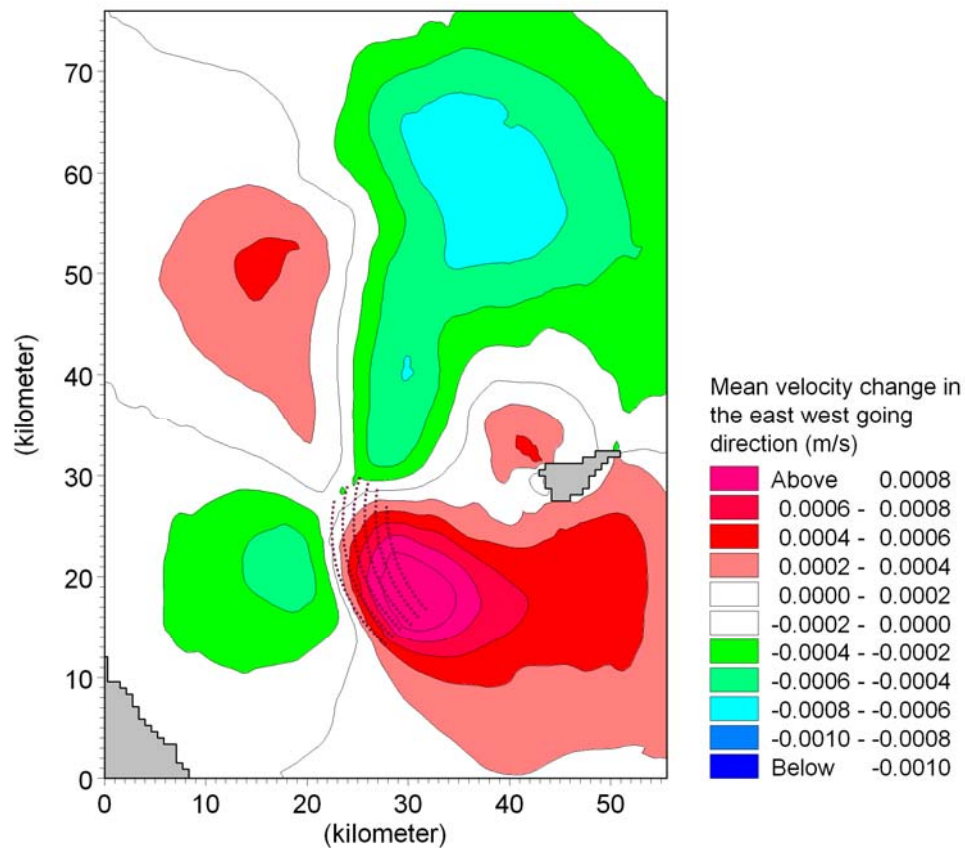
Figure 3-83   Annual mean surface velocity change for the east-west going velocity compo-
               nent in 2005. Model results from the local 3D model (grid spacing approxi-
               mately 600 m). Green-blue colours indicate a velocity reduction and red colours
   indicate an increase in current velocity.

3.3.2.2.2 **Impact on current conditions during storm conditions – 2D modelling**
The influence of the wind farm on the current field in selected storm conditions is
shown in this section for the two worst case scenarios. For each storm, the local 2D
hydrodynamic model presented in Section 3.2.4.1 has been applied.

Figure 3-84 to Figure 3-91 show the differences in the current field calculated during
each storm situation between the baseline situation and the situations including Sce-
nario 1 and 2 of the wind farm layout, respectively. The current fields shown in the
figures are at the peak of each storm period, defining 'the peak' as the time when
the strongest current speeds are seen within the project area in the baseline situa-
tion. The calculated flow fields for the baseline conditions at the given times were
shown in Section 3.2.4.4 (baseline description) in Figure 3-39 to Figure 3-42.

A reduction of about 0.01 m/s corresponding to about 2% in the current speed is
seen up to 5 km from the border of the wind farm area. Changes to the current

speeds higher than 0.001 m/s (corresponding approximately to 0.2% of the current speed in the baseline situation) are not seen further away than approximately 15-20 km downstream the wind farm in the flow direction, as seen in Figure 3-86 to Figure 3-91. The area of influence of the wind farm for Storm 1 is small due to lower flow intensity (0.3-0.4 m/s) in the area of interest compared to the other situations where the depth-integrated current reaches 0.45-0.6 m/s.

The dampening effect on the flow is largest nearer to the wind mills. This impact is seen more clearly than in the annual flow conditions studied with the local 3D flow model (Figure 3-80-Figure 3-83) simply due to the refined mesh in the local 2D model.

The impact on the flow speed clearly accumulates when more wind turbines are present along the flow direction. The current directions at the peak of Storm 1 (Figure 3-84) and Storm 2 (Figure 3-86) are almost parallel to the main axis N-S of Scenario 1 of Anholt wind farm leading to an increase in the flow dampening for each wind turbine in the flow direction. As the flow is not intense for Storm 1, this effect remains small. It is, however, more pronounced during Storm 2 due to the presence of a higher current parallel to the wind farm. During Storm 3, the largest instantaneous current is higher than during Storm 2 but more oblique to the main axis of the park; therefore the dampening effect is comparable.

The two eastern rows of wind mills tend to have slightly more effect on the current due to the presence of a higher current in this area (cf. Section 3.2.4.4). For the same reason Scenario 2 has generally a slightly stronger effect on the current field than Scenario 1, since the higher currents are located in the eastern area, where wind turbines are only located in Scenario 2 (see Section 3.2.4.4). Furthermore, the distance between the wind turbines in the rows is smaller in Scenario 2 than in Scenario 1, which results in a stronger combined effect in scenario 1. The area influenced by Scenario 2 is wider than for Scenario 1 due to its curved shape.

The area of influence is concentrated in the axis of the wind farm. The impact of the wind farm at the peak of the four storms are similar to the impacts found during the annual flow conditions evaluated with the 3D local model: the flow resistance from the wind mill foundations acts to dampen the flow speeds in the area of the wind mills and is compensated by a slight increase in flow velocities to the east and west of the wind farm, respectively. This pattern is observed at the peak of Storm 2-4.

During Storm 1, the modelled flow direction reverses from WSW to S in a short time span causing the pattern of the velocity differences to be slightly more complex than described above. Approximately three hours prior to the peak of the storm, the current comes from WSW. The impact of the hydraulic resistance from the wind turbines at this time is therefore to reduce the flow speed in the area of the wind farm inducing, for continuity reasons, increased flow speeds south of the wind farm. The area of the reduced flow speeds turns towards the east and north as the flow reverses towards the north and disappears with time. This explains the slightly different impact area in the flow field in Storm 1 in Figure 3-84 and Figure 3-85 than in the

other storm events. These do not show this pattern simply because the current direction is fairly constant around the peak of the storms (see Figure 3-28 to Figure 3-31).
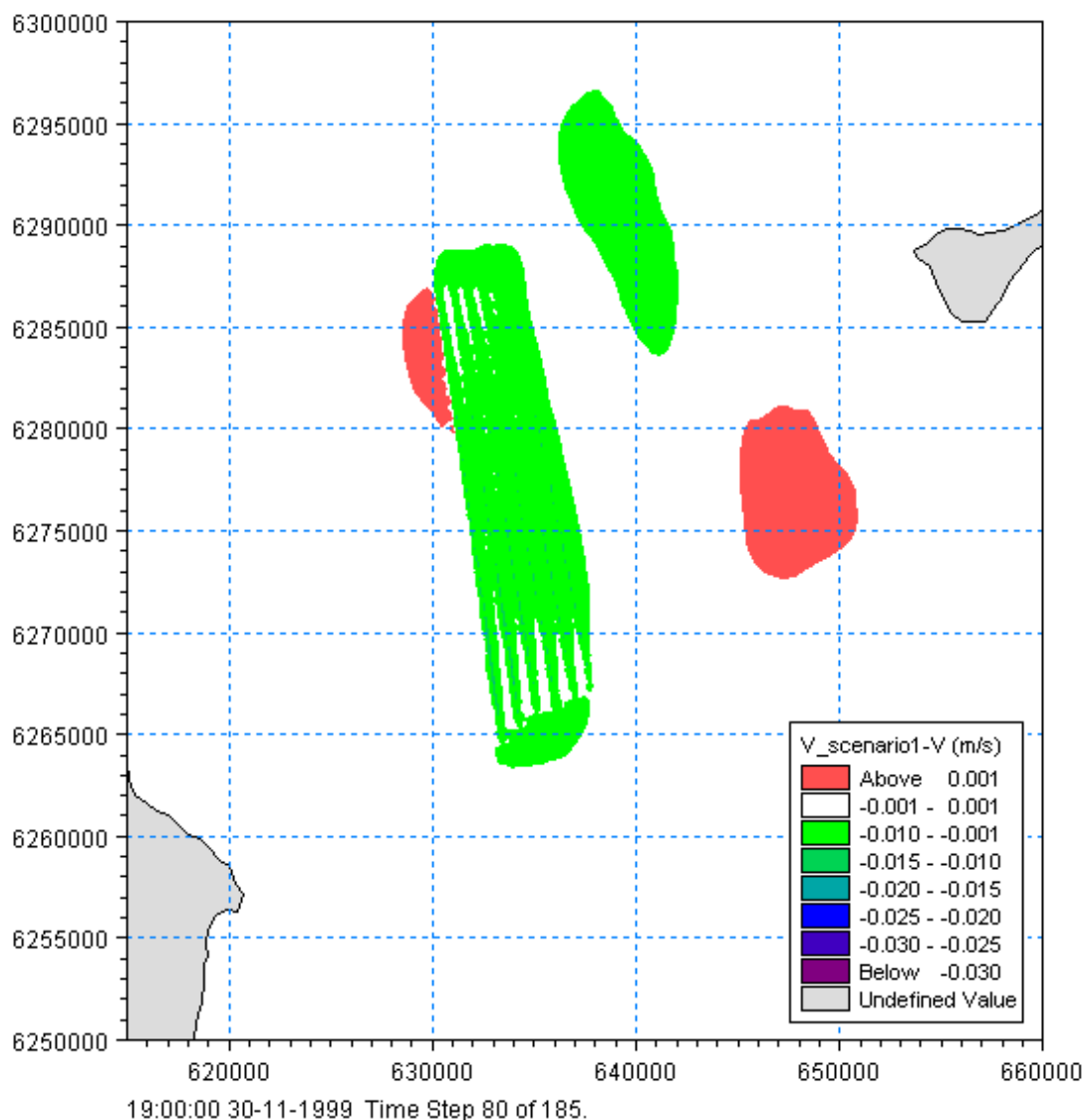
Figure 3-84   Difference in the current speed during Storm 1 (south-going depth-averaged current) between the baseline and Scenario 1 at the time step corresponding to the most severe current speed. Model results from local 2D flow model (smallest grid spacing approximately 50 m). Green-blue colours indicate a velocity reduction and red colours indicate an increase in current velocity.
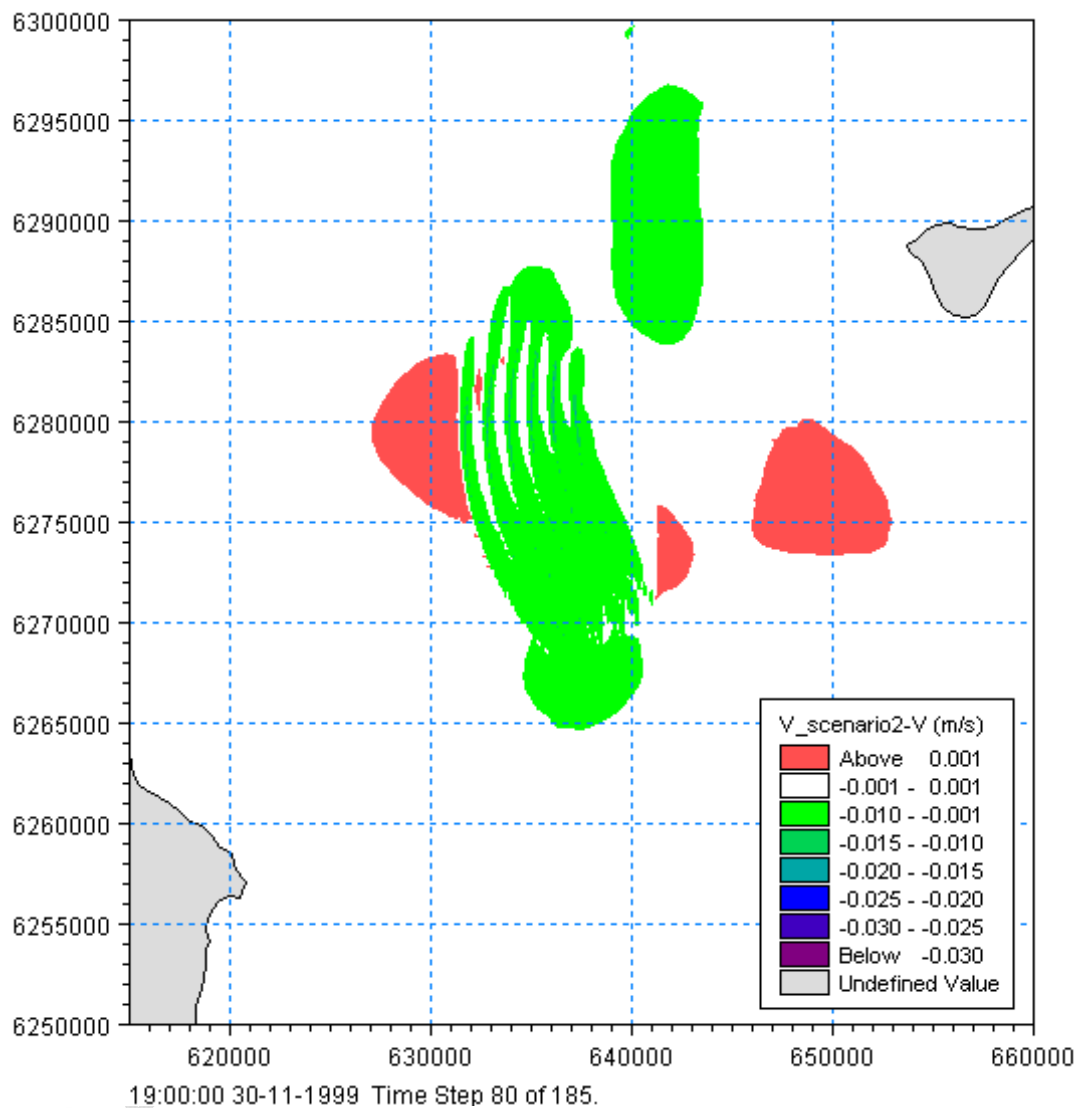
Figure 3-85   Difference in the current speed during Storm 1 (south-going depth-averaged current) between the baseline and Scenario 2 at the time step corresponding to the most severe current speed. Model results from local 2D flow model (smallest grid spacing approximately 50 m). Green-blue colours indicate a velocity reduction and red colours indicate an increase in current velocity.
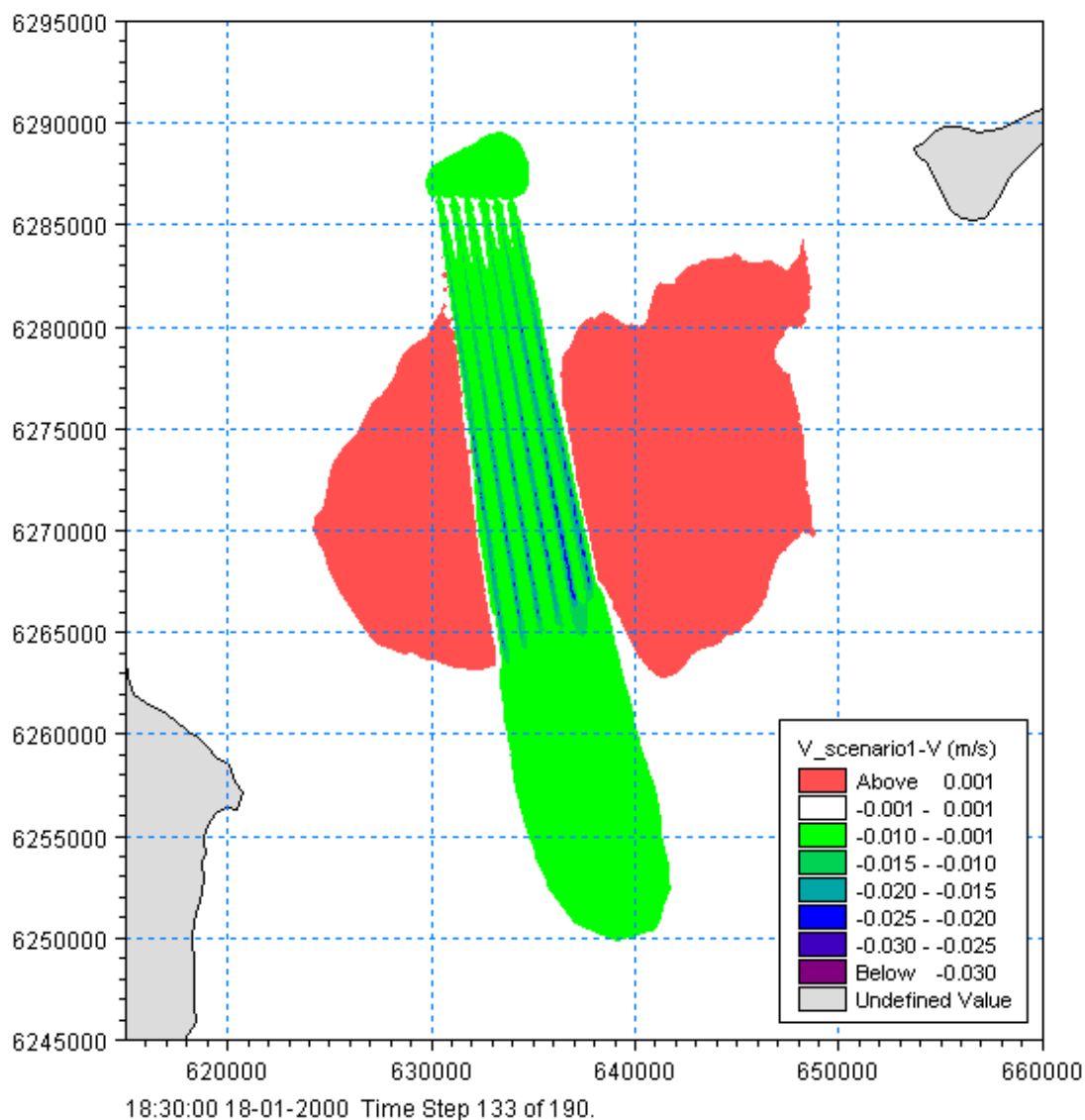
Figure 3-86   Difference in the current speed during Storm 2 (south-going depth-averaged current) between the baseline and Scenario 1 at the time step corresponding to the most severe current speed. Model results from local 2D flow model (smallest grid spacing approximately 50 m). Green-blue colours indicate a velocity reduction and red colours indicate an increase in current velocity.
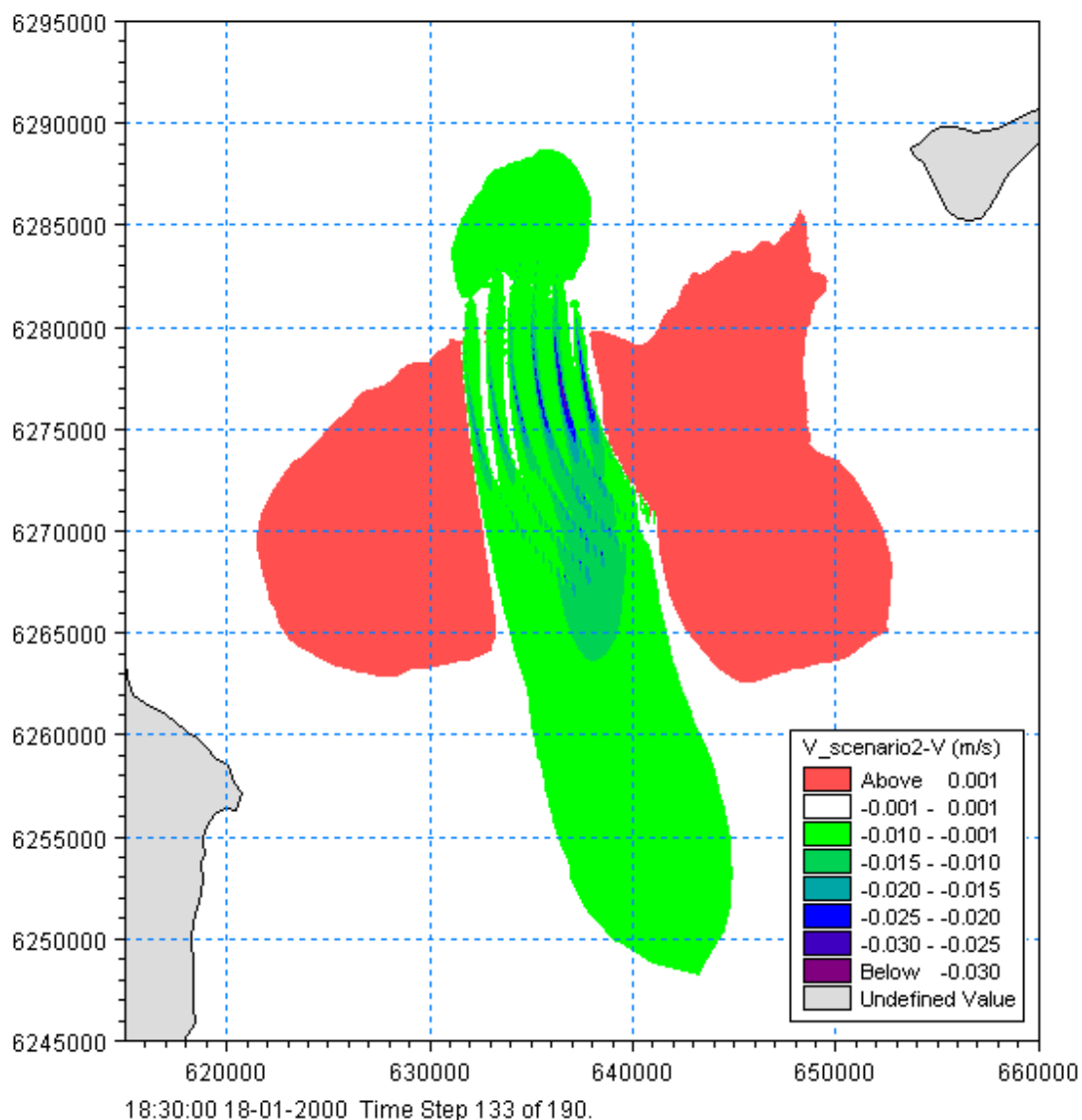
Figure 3-87   Difference in the current speed under Storm 2 (south-going depth-averaged current) between the baseline and Scenario 2 at the time step corresponding to the most severe current speed. Model results from local 2D flow model (smallest grid spacing approximately 50 m). Green-blue colours indicate a velocity reduction and red colours indicate an increase in current velocity.
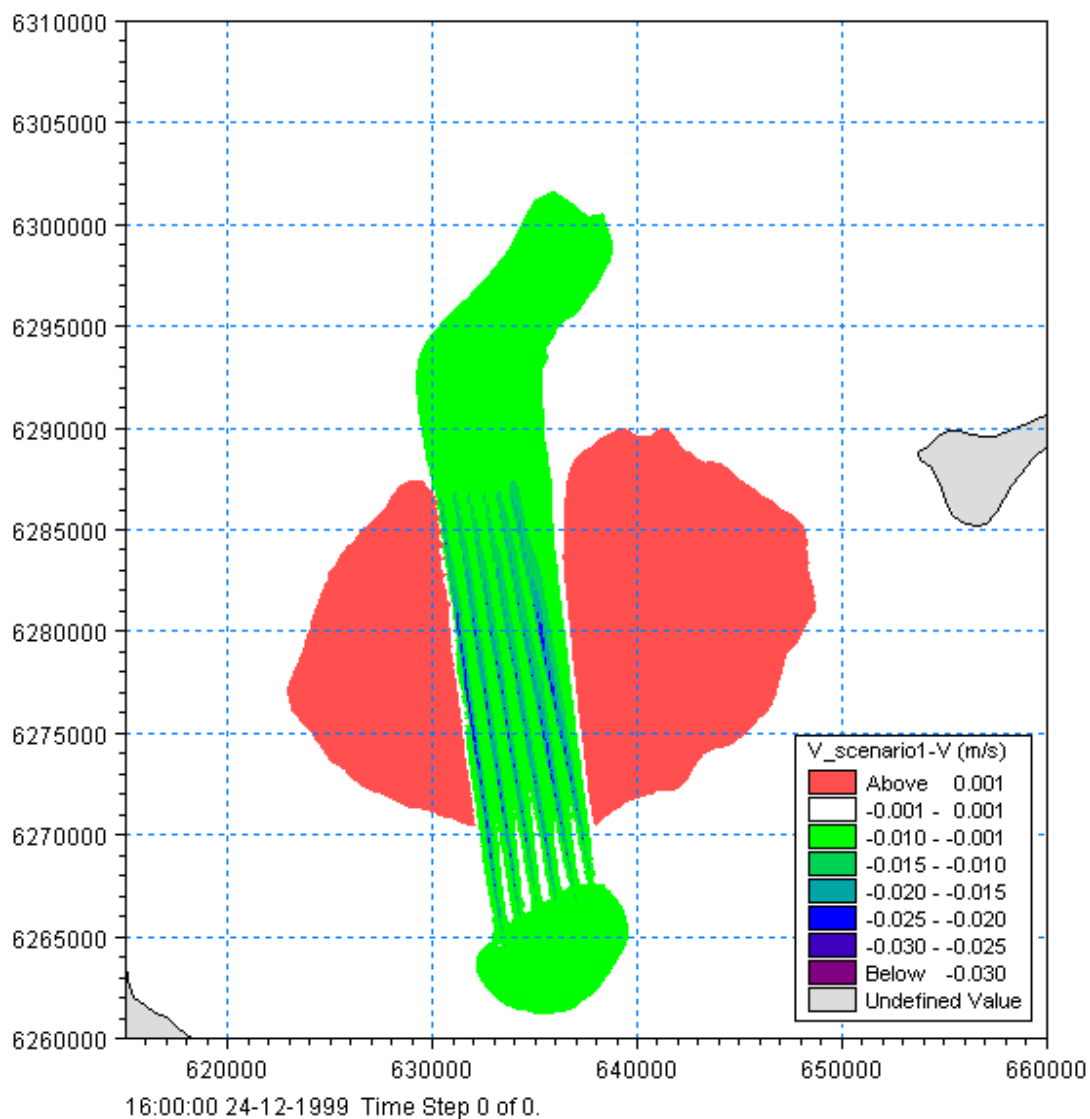
Figure 3-88   Difference in the current speed during Storm 3 (north-going depth-averaged current) between the baseline and Scenario 1 at the time step corresponding to the most severe current speed. Model results from local 2D flow model (smallest grid spacing approximately 50 m). Green-blue colours indicate a velocity reduction and red colours indicate an increase in current velocity.

16:00:00 24-12-1999 Time Step 0 of 0.
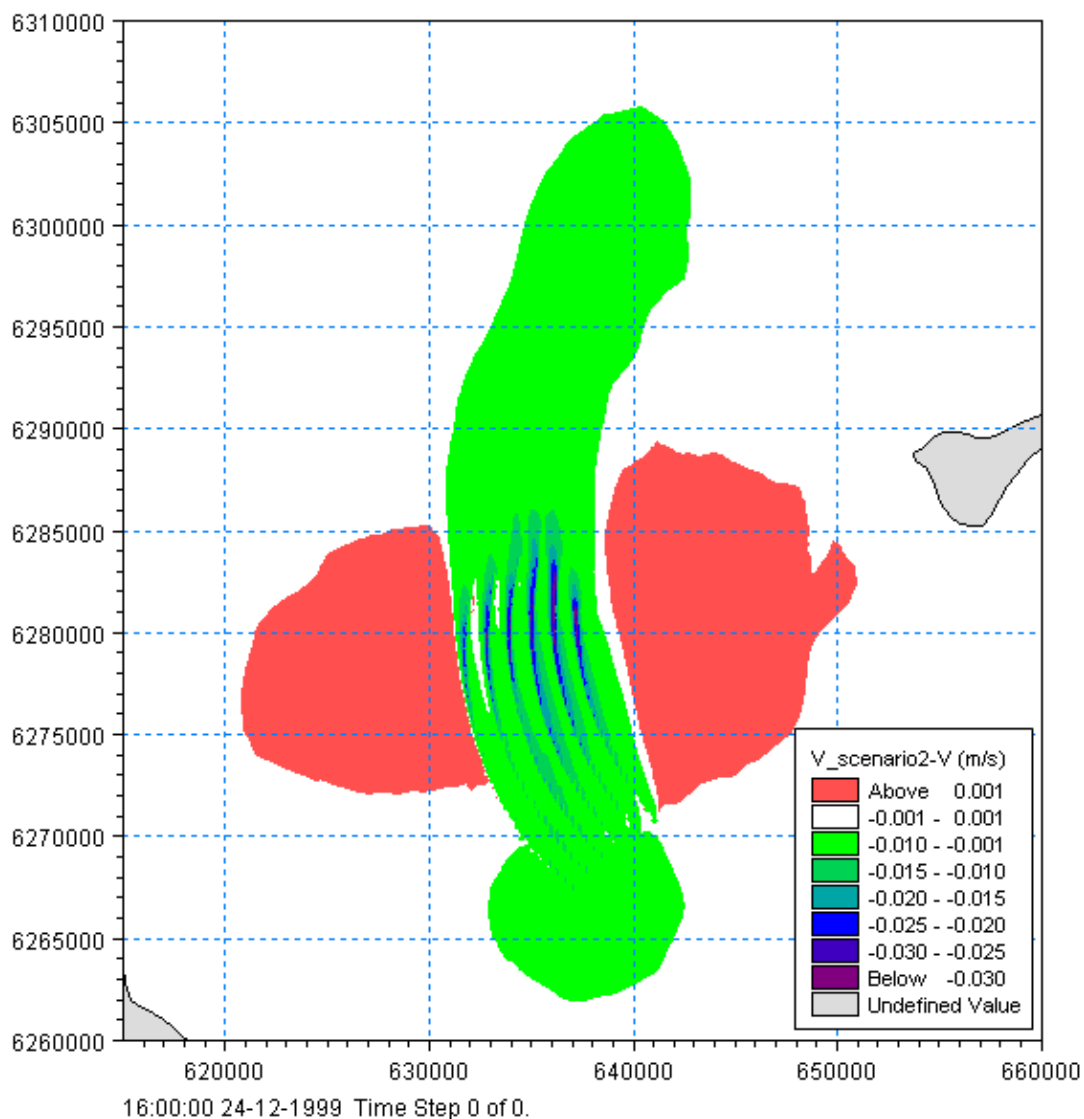
Figure 3-89   Difference in the current speed during Storm 3 (north-going depth-averaged current) between the baseline and Scenario 2 at the time step corresponding to the most severe current speed. Current toward the north. Model results from local 2D flow model (smallest grid spacing approximately 50 m). Green-blue colours indicate a velocity reduction and red colours indicate an increase in current velocity.
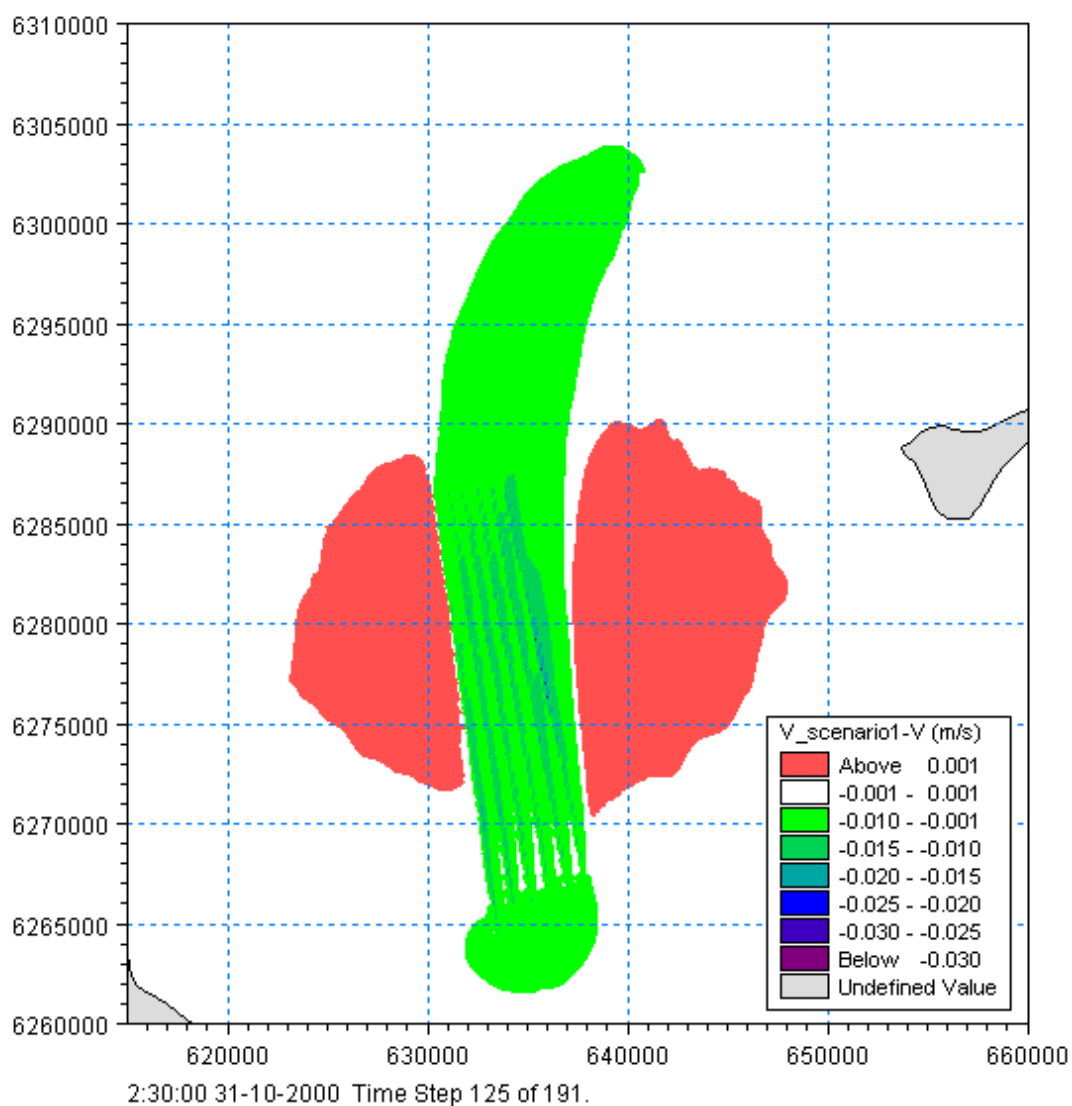
Figure 3-90   Difference in the current speed during Storm 4 (north-going depth-averaged current) between the baseline and Scenario 1 at the time step corresponding to the most severe current speed. Model results from local 2D flow model (smallest grid spacing approximately 50 m). Green-blue colours indicate a velocity reduction and red colours indicate an increase in current velocity.
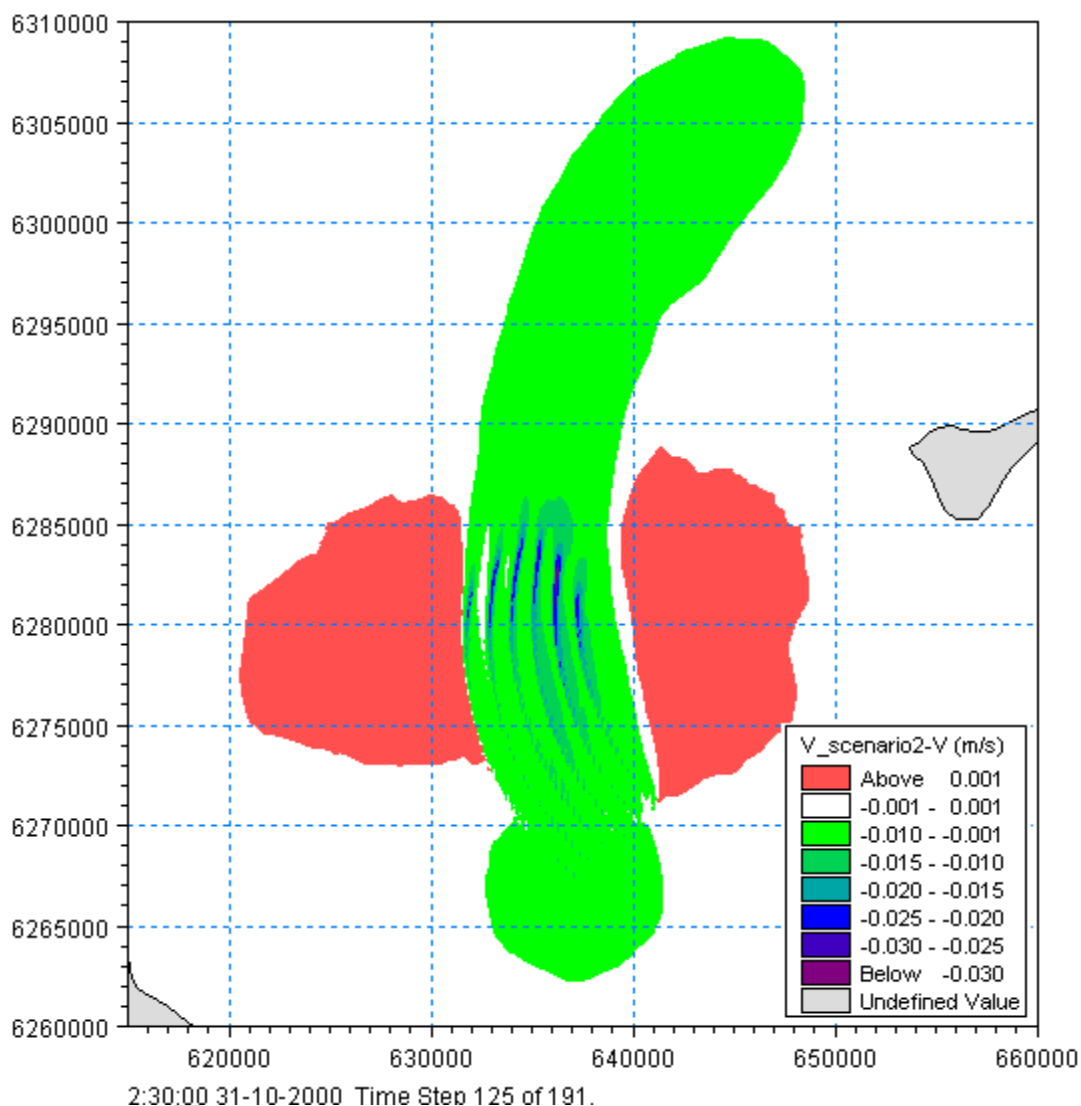
Figure 3-91   Difference in the current speed during Storm 4 (north-going depth-averaged current) between the baseline and Scenario 2 at the time step corresponding to the most severe current speed. Model results from local 2D flow model (smallest grid spacing approximately 50 m). Green-blue colours indicate a velocity reduction and red colours indicate an increase in current velocity.

3.3.2.3   Conclusions regarding impact assessment on currents and stratification during the operational phase

The stratification is expected to be weakened slightly downstream from the individual wind turbines due to increased turbulence. During normal flow conditions the effect will be very small. At high flow speeds occurring only 2-5% of the time, differences up to 1 PSU are found in the calculations at a distance of one gravity base diameter

from the foundations. At the next downstream wind turbine (approximately 600 m), the effect is reduced by a factor of two.

The largest impacts on the current speeds are found for the largest current speeds, which are typically connected to storm events. Reductions in the current speed larger than 2% are limited to an area within approximately 5 km from the wind farm area. Smaller increases in the flow speeds are expected primarily east and west of the wind farm.

During the entire 2005, the annual mean velocity changes at the surface were in the order of 0.0008 m/s. These changes are minor.

The impacts were slightly higher for Scenario 2 than for Scenario 1, but minor for both scenarios.

Table 3-26   Summary of impacts on currents and stratification during the operational phase

Impact	Intensity of effect	Scale/geographical extent of effect	Duration of effect	Overall significance of impact
Impact on mixing and stratification	Minor	Local	Long-term	Minor
Impact on current pattern and velocities	Minor	Regional	Long-term	Minor

3.3.3 Sediment spill due to dredging operations in the construction phase
In the construction phase up to 174 wind turbines will be erected in the project area. Sediment spill is expected during the construction when the cables between wind turbines are being jetted and – in case of gravity foundation – when the foundation area will be dredged down to layers capable of supporting the foundations.

During this operation a portion of the fine material in the bed will be spilled into the environment. The fate of this material is the topic of this section.

3.3.3.1 Method for impact assessment
Sediment spill due to the construction of Anholt Offshore Wind Farm is assessed by studying the sedimentation and spreading of sediment due to dredging in the construction phase. Simulations are carried out by assuming a realistic day-by-day dredging schedule, where the dredgers move around in the wind farm and dredge holes for the foundations and the cables to be laid out. According to the project description /1/, gravity foundations are expected to be filled with sand from an offshore source to provide ballast. It is assumed that this sand is washed during mining and therefore does not contain any fines (clay, silt).

The project activities causing sediment spill are summarized in

Table 3-27 together with the potential environmental impacts of the activities.

The material spilled into the water is tracked until the dredging operation is finished. As long as the sediment is in the water column, the concentration of sediment is increased in the areas where the sediment drifts to. The spreading is governed by the current speed and direction, the turbulence and the settling velocity of the sediment. When the particles fall to the bed, they may later be eroded if the hydrodynamic conditions are strong enough to erode them from the sea bed.

Increased concentration of suspended solids can be seen as a deterioration of water quality along with increased concentration nutrients and phytoplankton and reduction in dissolved oxygen. Actual levels of suspended solids that may cause harm to the environment will vary depending on the background concentration. Hence, while 5 mg/l will be detrimental to most coral reefs, an additional concentration of 50 mg/l will have no effects in e.g. Yangtze River because background concentrations often exceed 500 mg/l. Therefore, published criteria for suspended solids vary by orders of magnitude and several criteria also consider duration of exposure to increased concentration (/22/,/23/,/24/). Hence, for practical purposes the concentration levels obtained in the present report are evaluated against three different effect criteria somewhat based on published evidence from environments comparable to the Kattegat, but it must be stressed that these are not to be taken as firm criteria for the project area.

The three criteria are:

1. Plume visibility (2 mg/l)
2. Potential effect on fish (10 mg/l)
3. Effect on diving birds (15 mg/l)

The first criteria (2 mg/l) constitute the limit when the plume is visible in the water provided that ambient concentration is much lower. However, such low concentration will have very limited impacts unless it occurs in very clear water. On the other hand concentrations above 10 mg/l in the water column have been found to have impact on the perception volume for some species of predatory fish and affecting their capture of prey. At higher concentration (above 15 mg/l) predation by diving birds may be affected.

Table 3-27   Project activities during the construction of the planned wind park, sources of   impact, and potential impacts on sediment spill

Project Activity	Sources of Potential impact	Potential environmental impact
Construction phase		Environmental impact parameter affected /target of impact
Dredging for foundations	Sediment spreading and sedimentation	Water Quality

		Benthic fauna
		Benthic habitat
		Fish
Dredging for cables between wind turbines	Sediment spreading and sedimentation	Water Quality
		Benthic fauna
		Benthic habitat
		Fish

3.3.3.1.1 Selection of worst case scenarios for sediment spreading simulations

The worst case scenarios for sediment spreading are selected by considering the dredging volumes required for the different scenarios.

The impact assessment for sediment spreading is carried out for two combinations of the following:

1) The type of foundation (monopile and concrete gravity base, see Section 3.1 and /1/)

2) The number and size of mills (174 units of 2.3 MW wind turbines or 80 pieces of 5 MW wind turbines, see Section 3.1 and /1/)

3) The wind farm layout (geographical position of wind mills, north-south-going rows or arcs, see Section3.1 and /1/)

The two worst case scenarios selected for the sediment spill calculations are found to be the 174 units of 2.3 MW wind turbines on gravity base foundations for the two layouts considered in /1/.

The evaluation of the worst case scenarios is based on the reasoning below.

The sediment spill in the construction of a wind farm depends mainly on the volumes of sediment that are handled. Foundation by monopiles does not require any dredging. Choosing gravity foundations hence cause larger volumes of sediment dredging and therefore larger sediment spill rates. The larger number of smaller wind turbines requires a larger total volume of dredged material. No obvious differences can, prior to calculations, be identified between Layout 1 and Layout 2. The two worst case scenarios are hence chosen as the combination shown in Table 3-28.

Table 3-28   Worst case scenarios used in the spill calculations

Scenario	Foundation	Mill size/no. of	Configuration of

		mills	mills
Scenario 1	Gravity base	2.3 MW/174 units	Layout 1
Scenario 2	Gravity base	2.3 MW/174 units	Layout 2

3.3.3.1.2 **Dredging volumes and soil properties**

Geologically the sea bed in the wind mill area consists of layers of mud and sand. The main part of the upper layer of the sea bed is sand as described in Section 3.2.2; however, below this sandy upper layer, the geotechnical investigations /26/ reveal that in some areas a layer of soft grey mud or clay extending to between 6 m and 10 m is found. This clay will have to be removed before constructing the foundations.

The geotechnical investigations were not completed at the time of carrying out this work. The volumes required to be removed is therefore based on a first assessment by Rambøll of the results from the geotechnical surveys. It is hence assumed that the area can be categorized in three different cases related to the volumes that have to be removed before foundations can be placed. These are denoted Case A, B, and C., and are defined in Figure 3-92.
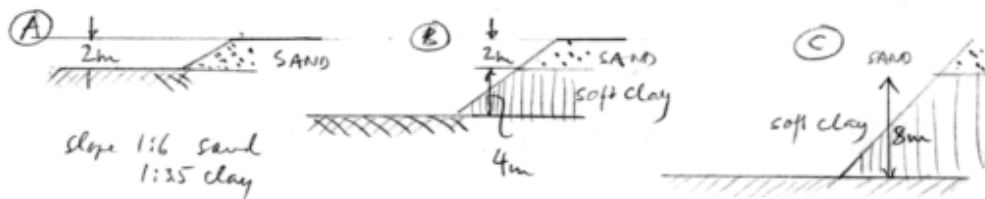
Figure 3-92   Rambølls classification (personal communication) of the sea bed in the wind
farm area in Cases A, B and C, depending on the depths and materials to be
removed before gravity foundations can be placed.

The spatial distribution in % of the project area between the three cases is given in
Table 3-29. The distribution of the wind turbines is assumed to be placed evenly over
the three sea bed types. 80% of the wind turbines are hence assumed to be located
on the sea bed corresponding to Case A, 10% are placed in an area corresponding to
Case B and 10% are placed in an area corresponding to Case C.

The soft clay is found in narrow bands within the wind farm area. It is therefore as-
sumed in the dredging operation that the first 8 wind mills are located in sandy areas
denoted as 'Case A', and that the next wind turbine is a Case B and the next is a
Case C and then it repeats itself. The assumed geographical distribution of Case A, B
and C are illustrated in Figure 3-93.

Table 3-29   Distribution of soil properties according to Rambøll

Type of sea bed where foundation is placed	Found at % of founda-tions
Case a (Sand)	80%
Case b (Sand top 2 m, mud 2 m-6 m)	10%
Case c (Sand top 2 m, mud 2 m-10 m)	10%
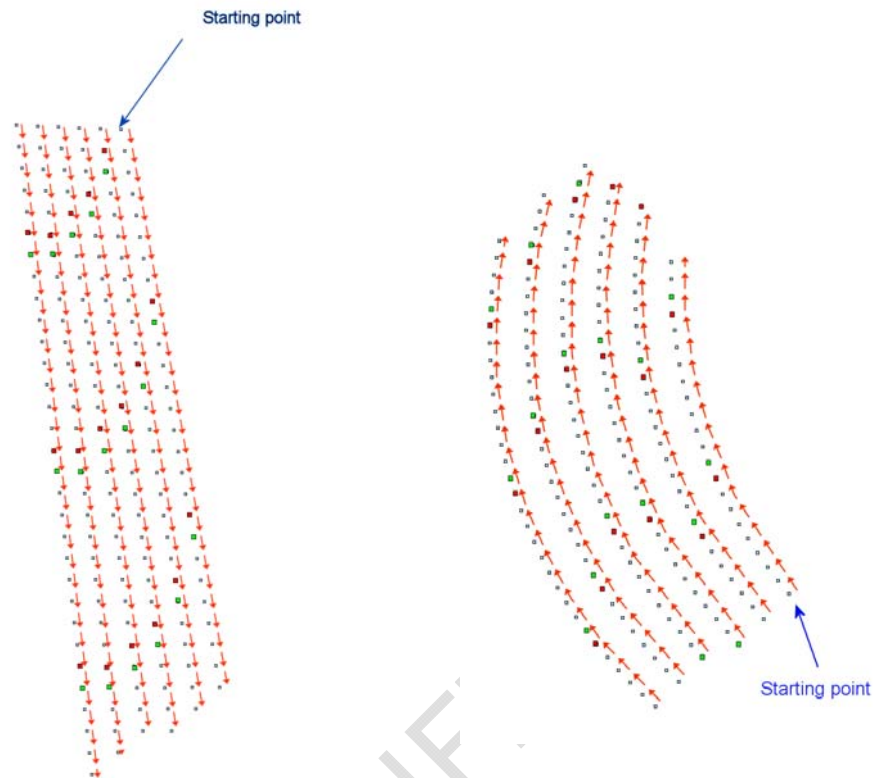
Figure 3-93   Dredging pattern Scenario 1 (left) and Scenario 2 (right). Blue markers at wind
               turbine positions indicate Case A dredging scheme, red markers indicate Case B
               and green marker indicate Case C.

The volumes to be dredged for the foundations can be found in Table 3-30.
These numbers were provided by Rambøll (personal communication).

Table 3-30   Volumes required for dredging for foundations for each of the Cases A, B and C as specified by Rambøll (personal communication).

Type of sea bed where foundation is placed	Volume sand (Top 2 m)	Volume clay (Below 2 m)
Case a (Sand)	1700 m^3	-
Case b (Sand top 2 m, mud 2 m- m)	6700 m^3	5000 m^3
Case c (Sand top 2 m, mud 2 m-10 m)	13500 m^3	18000 m^3

The bulk densities are assumed to be 2650 kg/m^3 for sand with a porosity of 0.4 and 1600 kg/m^3 for mud.

The cables are to be buried by water jetting at a depth of 1.2 m (personal communication, Rambøll) below the surface and will hence only be buried in the top sandy layer. The volume of the impacted area is approximately 1.5 m^3/m, see also Table 3-31.

The jetting operations will follow the north-south-going lines only connecting each line in one point.

Table 3-31   Volumes of sea bed affected when burying the cables

Cables	Volume of sand affected when the cables are laid down. [m3/m]
Cables between wind turbines	1.5

Properties of the sand

On average the first two metres of the soil are assumed to consist of sand in all three Cases A, B and C. Available information at the time of carrying out this study was sieve analysis from Borehole BH07 and short descriptions of the sediment samples from boreholes BH2, BH4, BH5 and BH10 (personal communication, Rambøll). The locations of the boreholes are given in Figure 3-94.
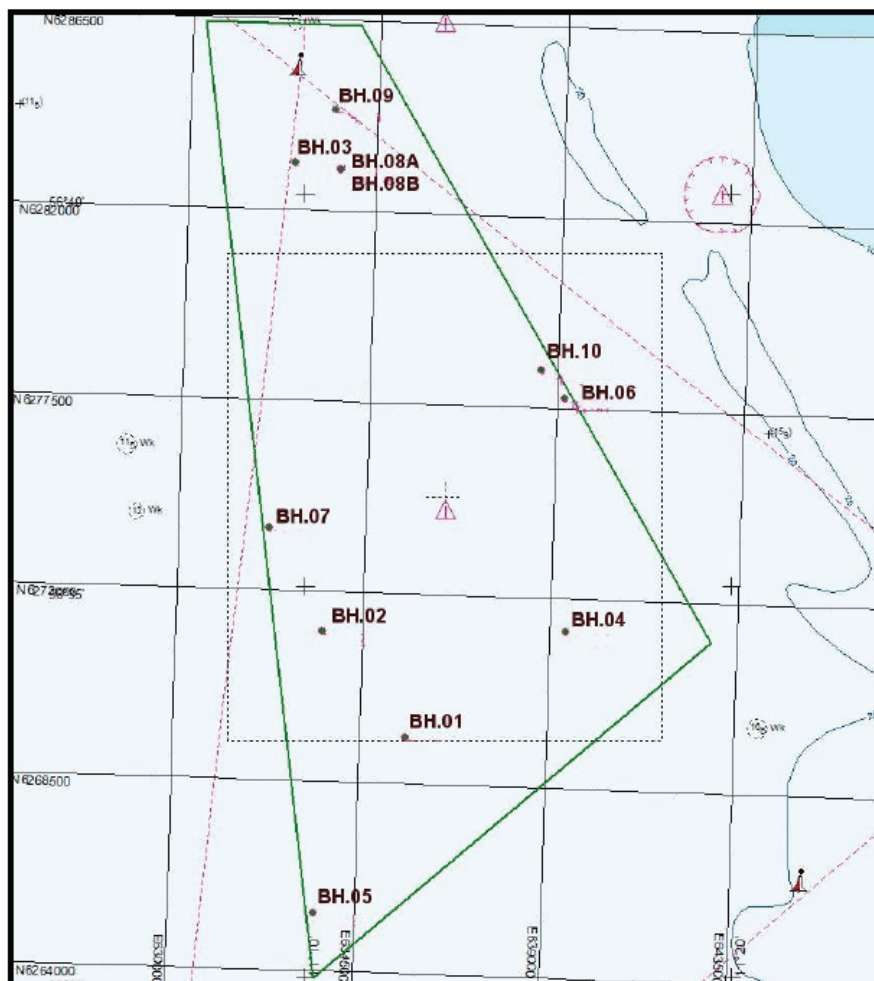
Figure 3-94   Location of boreholes from geotechnical investigations by GEO /26/.

The physical property of the sand is exemplified by the grain size distribution curve for Boring Sample No BH 07/2 from 2 m below the sea bed in Borehole 07, see Figure 3-95.

The table embedded in the figure:

| Boring/Sample No.:		BH.07 / 13	BH.07 / 14	BH.07 / 19	BH.07 / 2	BH.07 / 9
Curve		O	⊗	▲	△	⊘
Geology		SAND TILL	SAND TILL	CLAY TILL	SAND	SAND
Medium grain size d_{50} (mm)		0.114	2.14	0.05	0.233	0.0488
Uniformity coeff. d_{60} (mm) / d_{10} (mm)		0.146/0.0017 = 86.9	5.02/0.0517 = 97.1	0.0998/ =	0.339/0.0303 = 11.19	0.0717/0.0042 = 17.11
Plasticity index $W_L - W_P = I_P$ (%)		- =	- =	22.3- 10.6 = 11.7	- =	- =
Activity I_P(%) / ler(%) = I_A		/10.8 =	/3.5 =	11.7/23.0 = 0.51	/4.8 =	/7.0 =
CaCO$_3$ (%)						
Specific gravity d_s						2.69
Note						

Figure 3-95   Sieve analysis from borehole BH 07 in the geotechnical survey. The borehole is located at 17m depth in the western part of the potential wind mill area. For information, see geotechnical report by GEO /26/. The sample number indicates the depth below the surface. The one at interest is number 2 indicating 2 m below surface.

The grain size distribution curve shows that the main part of the sample is sand (grain sizes between 0.063 mm and 2 mm) and that the sample has a median diameter (d_{50}) of about 0.22 mm. The sand is generally classified as medium to coarse with shell fragments. Other boreholes like boreholes BH02 and BH04 indicate coarser materials whereas borehole BH10 indicates slightly finer material in the top layers /26/. This indicates some spatial variation in the grain size distribution in the top layer.

Assuming a typical settling velocity of the sand fraction of approximately 2 cm/s (/27/), the sand will settle out quickly and very near the dredger. Hand calculations indicate a maximum travelling distance of about 200-300 m under strong current conditions. Sand is hence not considered in the simulations of sediment spreading. The top layer contains some fines which are carried much further away. From the grain size distribution curve it is seen that about 11% of the soil has a grain size below 0.063 mm, which characterizes sediment with silty or clayey properties. However, boreholes 2 and 4, which are located in other parts of the potential wind mill area, indicate coarser materials. To accommodate this spatial variation a percentage

of material less than 0.063 mm of 10% is adopted. In the simulations of the dredging operation it is hence assumed that when dredging from the top (sandy) layer, 10% is fines.

Properties of the clay

No exact grain size distribution is available for the clay. It is assumed that the clay in the deeper parts does not contain any sand and has 100% in the silty and clayey fractions.

3.3.3.1.3 **Assumption regarding equipment**, **dredging patterns**, **and dredging rates**
There are two types of dredging operations involved in the present project: dredging for wind mill foundations and jetting for cables.

As prescribed by Rambøll the dredging for foundations is expected to be carried out using a backhoe dredger and barges. The barges will be available in such a number that the backhoe can dredge continuously 24 hours a day, 7 days a week. The average dredging rate is assumed to be 3200 m^3/day. In case of a sandy bed (Case A), the dredging will take about half a day per foundation, but at locations where the sea bed is as in Case C, the dredging for a foundation will take more than 10 days.

Dredging for cables will be done differently. This operation will be done by jetting. For this process the water from the jet will fluidize and wash the soil in a triangular shape above the cable. For this process it is assumed that the cabling between two wind turbines can be placed in a day.

The dredging is assumed to start in the corner and follow the north-south-going lines. For Scenario 1 the dredging advances from north to south one line at a time and proceeding in lines of wind turbines from east to west as shown in the upper part of Figure 3-93. For Scenario 2 the dredging starts in the south-eastern corner and the dredger moves from south to north, proceeding in lines of wind turbines from east to west as illustrated in the lower part of Figure 3-93.

The dredging for cables is assumed to start 6 months after the dredging for foundations has started. This means that the cable laying will be finished slightly after the dredging for foundations.

3.3.3.1.4 **Spill volume rates**
The spill pattern will vary depending on the choice of equipment. For a backhoe the spill is assumed to happen in three different ways:

1. At the bottom when the bed is disturbed due to the grab.

2. In the water when the grab is moved up towards the surface.

3. At the surface when the water runs out of the grab and when the water drains off the barge.

Based on experience from other projects and from the literature the spill rates in percentages of the volumes dredged are chosen as given in Table 3-32 (/28/, /25/).

Table 3-32   Spill percentages for backhoes dredging for foundations

Dredging for foundations	Spill rates in percentage of the volume dredged
Spill at bottom	1 %
Spill in midwater	0.5 %
Spill at surface	1.5 %
Total	3%

In the process of jetting the cables into the sea bed, the spill is assumed to be 20% of the affected volume, since the sand is never lifted away from the bottom. Physically what happens is that the water used for the jetting process will create an excess pressure at the jet. Due to this excess pressure the water will try to exit and this can only happen through the soil above. The soil above is therefore lifted slightly while streaming water passes. And thus fine materials can be washed out and released at the soil surface. The sand particles are too big and too heavy to be part of this process. They might be lifted slightly of the bed but they will settle immediately after the jet has passed. Sand is therefore not considered in this process. A sketch of the entire process can be seen in Figure 3-96.
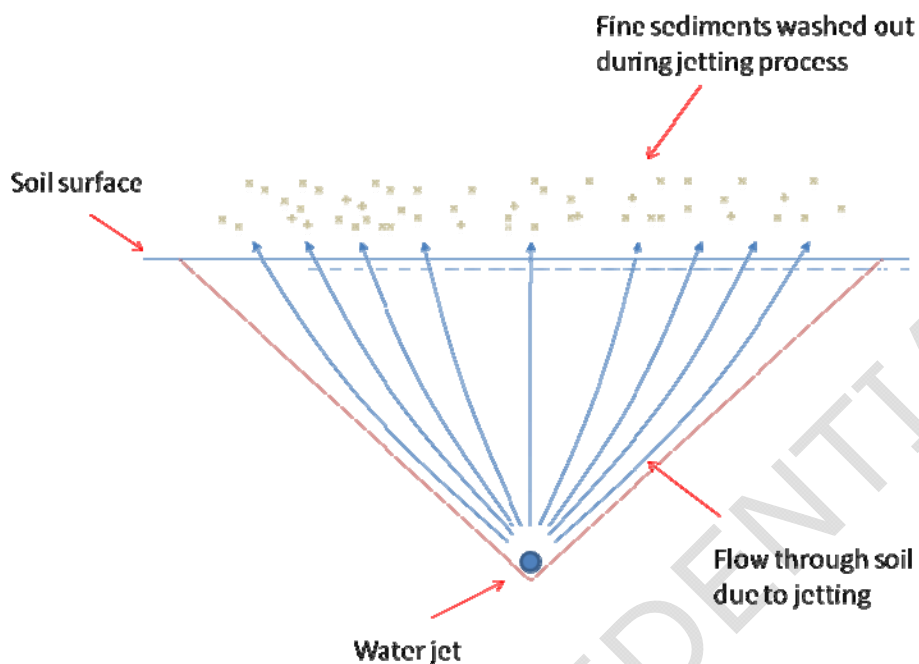
Figure 3-96   Sketch of the water jetting effect

The spill is hence only assumed to consist of 20% of the fines in the sand, which means that in total 2% of the total mass is spilled.

Table 3-33   Spill percentages for water jetting the cables into the seabed

Jetting of the cables	Spill rates in percentage of the volume affected by jetting
Spill at bottom	2 %

An overview of the total spill rates is given in Table 3-34.

Table 3-34   Assumptions of total spill rates at different locations in the water column for different types of sea bed, Cases A, B and C.

	Spill percentage	Spill Kg/h (Dredging in sand)	Spill Kg/h (Dredging in mud)
Backhoe, spill at bottom (Case A)	1 %	190.8	-
Backhoe, spill in midwater (Case A)	0.5 %	95.4	-
Backhoe, spill at surface (Case A)	1.5 %	286.2	-
Backhoe, spill at bottom (Case B)	1 %	190.8	2133.3
Backhoe, spill in midwater (Case B)	0.5 %	95.4	1066.7
Backhoe, spill at surface (Case B)	1.5 %	286.2	3200
Backhoe, spill at bottom (Case C)	1 %	190.8	2133.3
Backhoe, spill in midwater (Case C)	0.5 %	95.4	1066.7
Backhoe, spill at surface (Case C)	1.5 %	286.2	3200
Spill during water jetting (sand)	2 %	1073.3	-

The total amounts spilled for each type of sea bed are given in Table 3-35.

Table 3-35   Total spill of fines

	Total spill pr foundation/cable between two wind turbines in tones	Number of wind turbines assumed located in this type of sea bed	Total spill in tones
Case A	7	140	1021.7
Case B	270	17	4569.0
Case C	920	17	15673.0
Cables	25 (per cable)	174 (stretches of cables)	4350.0
Total			25613.7

3.3.3.1.5 **Short description of numerical model and model setup**

The applied model is a so-called particle model (PA). This model follows the path of a number of particles released at the source point under the influence of currents, settling velocities dispersion and other parameters. The particles/substances simulated may be a pollutant of any kind, conservative or non-conservative, for example suspended sediment particles, inorganic phosphorus, nitrogen, bacteria and chemicals. The pollutant is considered as particles being advected with the surrounding water body and dispersed as a result of random processes. To each particle a corresponding mass is attached. This mass can change during the simulation as a result of decay or deposition.

The basic Lagrangian type approach involves no other discretisations than those associated with the description of the bathymetry of the model area and wind, current and water level fields. This concept has several advantages e.g. eliminating of numerical dispersion associated with finite differencing phenomena, and computer requirements are limited. For more information see /29/.
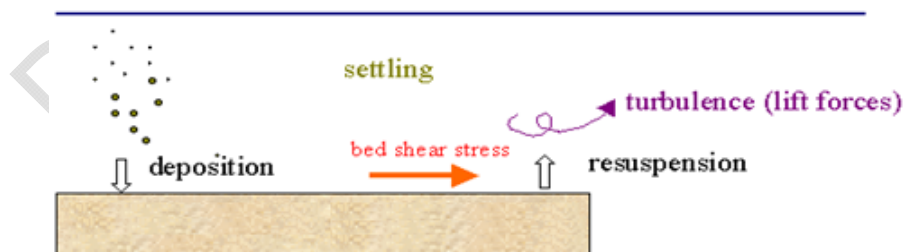

Figure 3-97   Physical processes included in the particle model.

The model is setup for a sufficiently long period of time to cover the entire dredging operation. With the given dredging rate for the wind mill foundation it will take 303 days to dredge for this. At the same time water jetting for the cables is going on.

This operation takes one day pr. Mill or 174 days. The start and end times of the simulations are given in Table 3-36.

Table 3-36   Simulation periods

	Start date	End date	Total time
Dredging for cables	1 June 2005	21 November 2005	174days
Dredging for founda-tions	1 January 2005	31 October 2005	303 days
Total simulation pe-riod	1 January 2005	1 December 2005	334 days

The spill occurring during dredging for foundation was split in 3 sources. A fourth source represented the dredging for cables. The spill rates and dredging procedures are given in Section 2. The sources files will follow the dredging order shown in Figure 3-93 and use the spill rates given in Table 3-32 and Table 3-33. All operations will be continuous as they move from location to location. It is assumed that all equipment is active 24 hours a day. The most important settings regarding sediment properties are given in Table 3-37.

Table 3-37   The main model settings in the sediment spreading simulations

Model settings	Value
Time step	300 s
Type of particle	Mud
Settling velocity	0.0005 m/s
Critical shields parameter	0.1
Grain size	20µ

The most important settings are the settling velocity and the critical shields parameter. No measurements are available for either of these parameters. In reality the fine sediments will flocculate and different flocculation sizes will be available in the water column at the same time. Since no data is available the settling velocity is chosen as a normal mean value for fine sediments based on DHI experience. When evaluating the results one should consider the possibility that some of the finest fractions may travel slightly further than the results show due to lower settling velocities. The critical Shields value is chosen slightly bigger than the one usually applied for sand

(0.045) because mixtures of mud and sand tend to increase erosion resistance significantly.

3.3.3.2   **Impacts during the construction phase**
In the following the results for the simulation of the dredging operations will be presented. In general the operation leaves a narrow plume which is advected around by the currents. The dredger is only located at the same position for a relatively short period of time and thus the accumulated result is the sum of a moving point source creating a narrow plume.

With regards to the concentration levels in the water column the general environmental criterion is the visibility of the water. This is evaluated with respect to the three specific criteria specified in Section 3.3.3.1:

1. Plume visible (2 mg/l)

2. Effect on fish (10 mg/l)

3. Effect on diving birds (15 mg/l)

In Figure 3-98 the sedimentation patterns are given for Scenario 1. The results show very low sedimentation rates over a large area. The locations of where maximum sedimentation is seen in the wind mill area is consistent with the spill locations. Sedimentation due to the dredging operations are up to about $250 g/m^2$, but mostly below $100 \ g/m^2$ within the wind farm. This corresponds to less than 0.25 mm in thickness. Outside the wind farm area the sedimentation is mostly below $25 \ g/m^2$ except for small patchy areas. The total impact area is approximately 15 km times 35 km with with some smaller patches outside. Of these approximately $25 \ km^2$ are found to be impacted by a deposition higher than 100 g/m2 and approximately 1 km^2 by a deposition higher than $250 \ g/m^2$. The sizes of the impacted areas are nearly independent of the layout.

Monitoring after the construction of Nysted Offshore Wind farm showed no changes of the overall sediment composition after the dredging operations; however, at some measuring points close to the construction area, the content of silt/clay was increased after the earthworks.
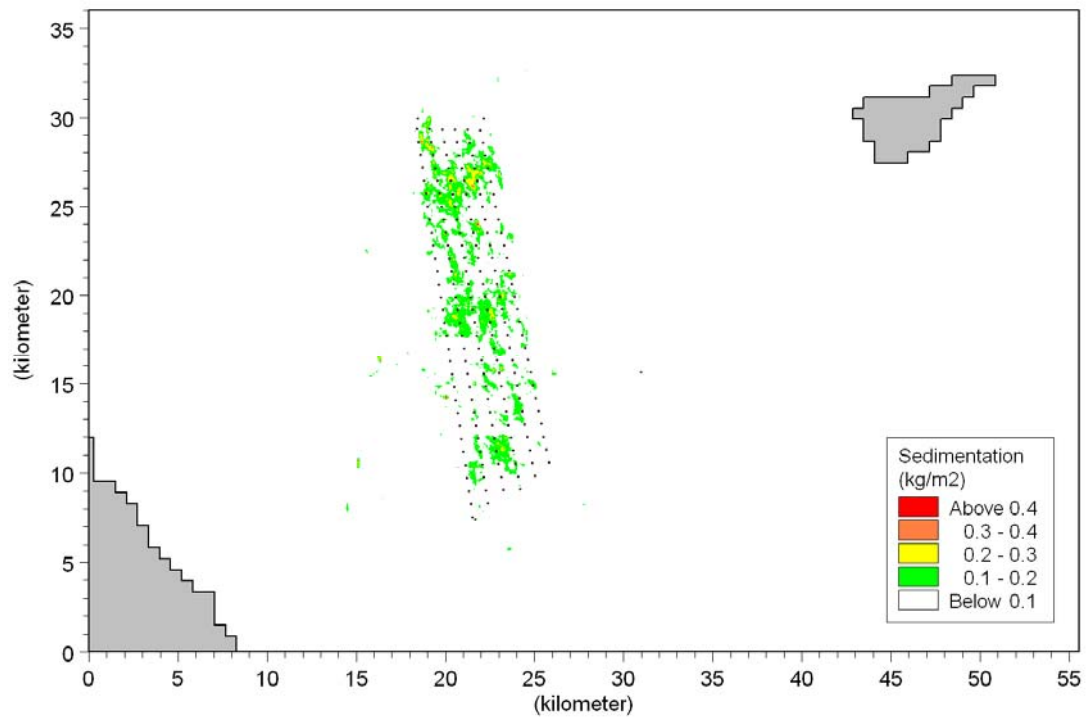
Figure 3-98   Deposition pattern after dredging operation for Scenario 1. Model results from
the sediment spreading calculations.

For Scenario 2 the final deposition pattern is given in Figure 3-99. The results are
similar to those found for Scenario 1, however with a slight tendency for larger areas
with higher deposition in the wind mill park. It is also noted that the overall impact
area is slightly smaller and that more patches are seen to the south-east consistent
with the flow pattern (eddy) found here.

As for Scenario 1 the maximum deposition rates found are approximately 0.250
kg/m^2 corresponding to less than 0.25 mm.
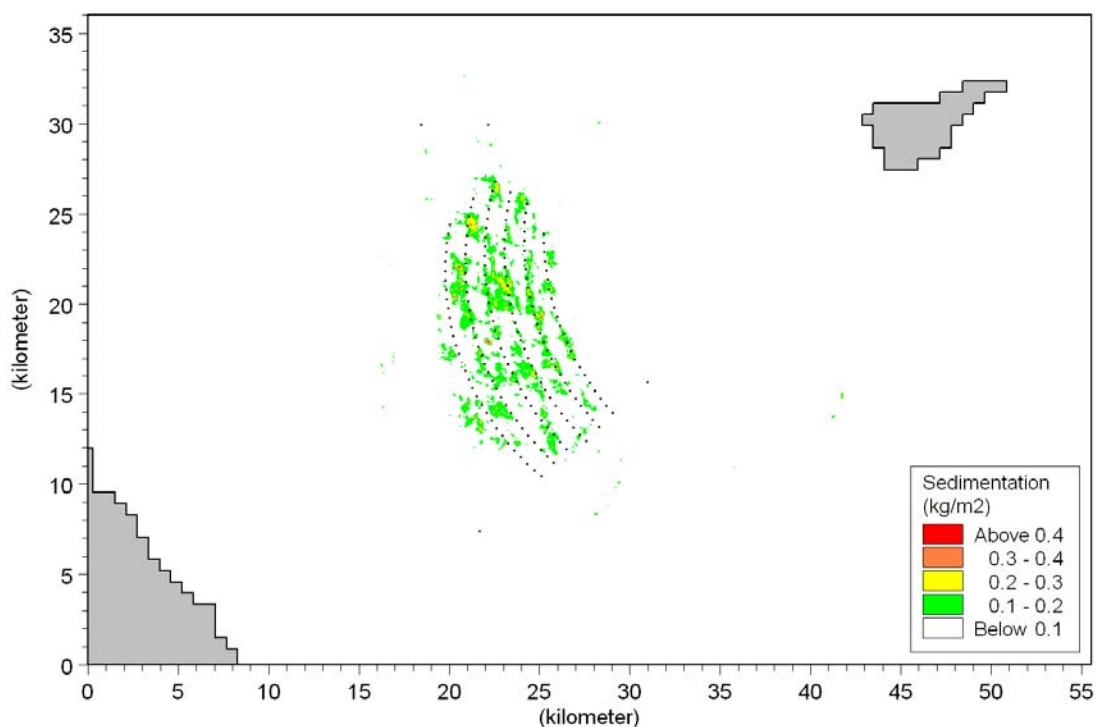
Figure 3-99   Deposition pattern after dredging operation for Scenario 2. Model results from
                   the sediment spreading calculations.

When evaluating the deposition patterns it is important to emphasize that temporarily the deposition rates may be higher at some positions. However, this is a temporary effect that will be removed by the currents over time.

Based on the above it can be concluded that the deposition of fines from the dredging work will not be a problem because the material is spread over a very large area and therefore the deposition rates will be very low.

The maximum depth averaged concentrations occurring at each computational point are given in Figure 3-100 and Figure 3-101.
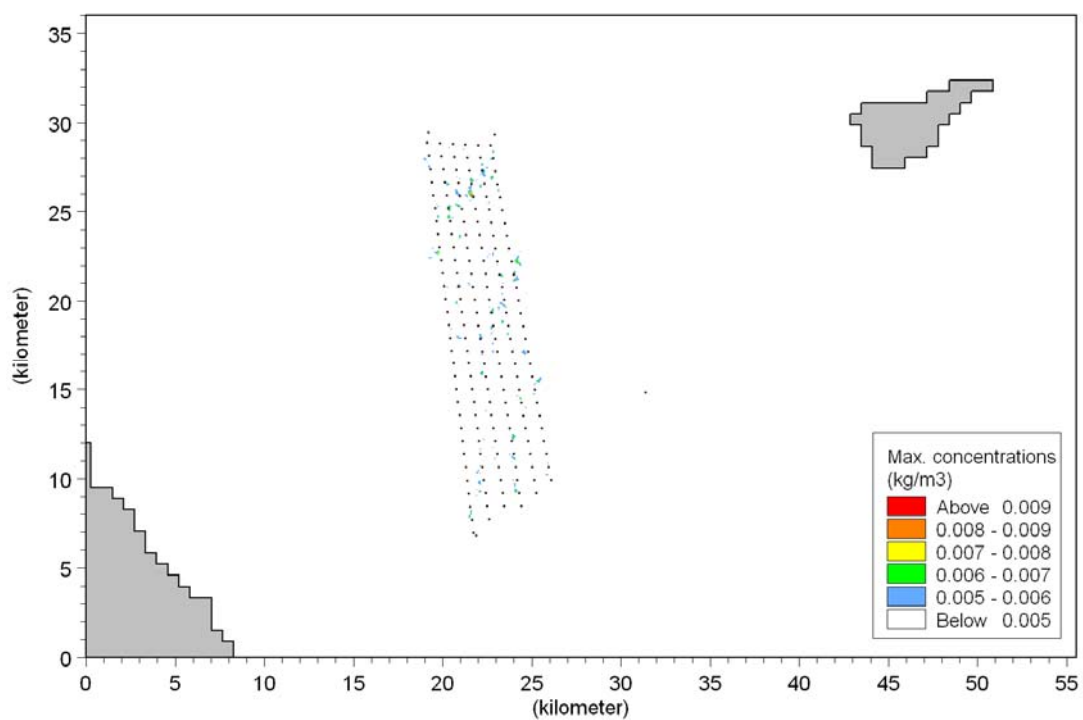
Figure 3-100   Maximum concentration for Scenario 1 during the dredging operation. Model results from the sediment spreading calculations.
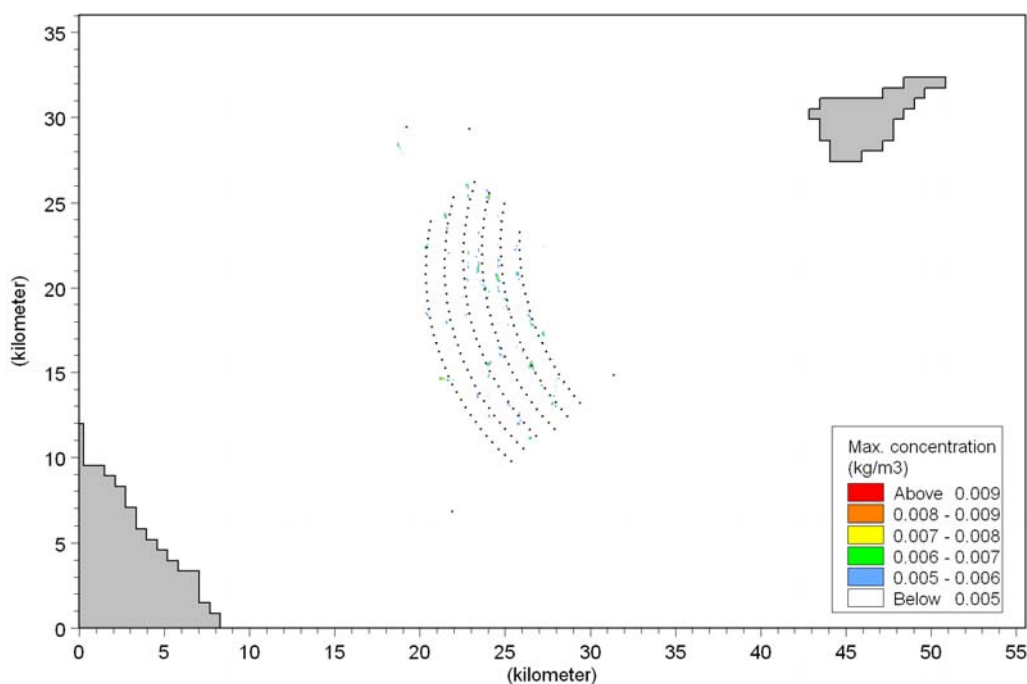
Figure 3-101   Maximum concentration for Scenario 2 during the dredging operation. Model
                results from the sediment spreading calculations.

Results show that depth averaged concentrations rarely exceed 5 mg/l and therefore
the fish and bird criteria are never exceeded. Note the long bands appearing in the
figures. These are individual plumes. This illustrates the random nature of the
spreading. For both scenarios the maximum concentrations are just below 10 mg/l
occurring near the dredging operations. There is no general difference in the levels
between the two scenarios except that the plumes from Scenario 1 extend further to
the north whereas for Scenario 2 the plumes tend to travel further to the south-east.
Given the low maximum concentrations it is relevant to evaluate the time during
which the visibility limit (2 mg/l) and the effect criteria for fish (10 mg/l) is ex-
ceeded. The latter is included to illustrate the maximum values and the exceedence
times for these. This is done in Figure 3-102 to Figure 3-105.
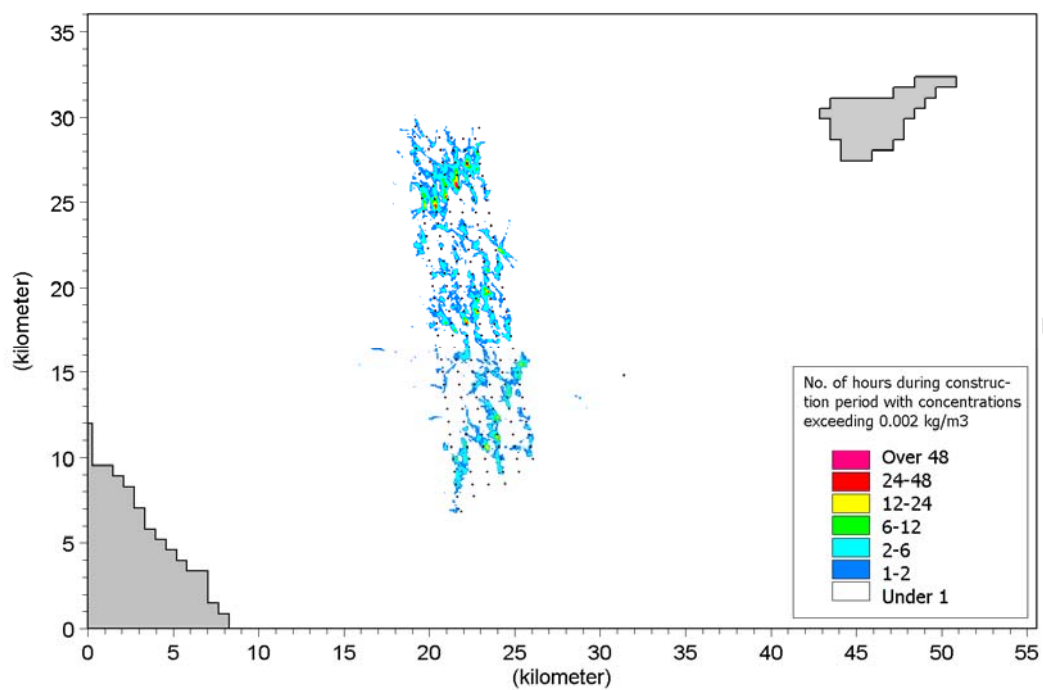
Figure 3-102   Number of hours during the dredging operation (334 days) where the concen-
tration exceeds 2 mg/l for Scenario 1. Model results from the sediment spread-
ing calculations.
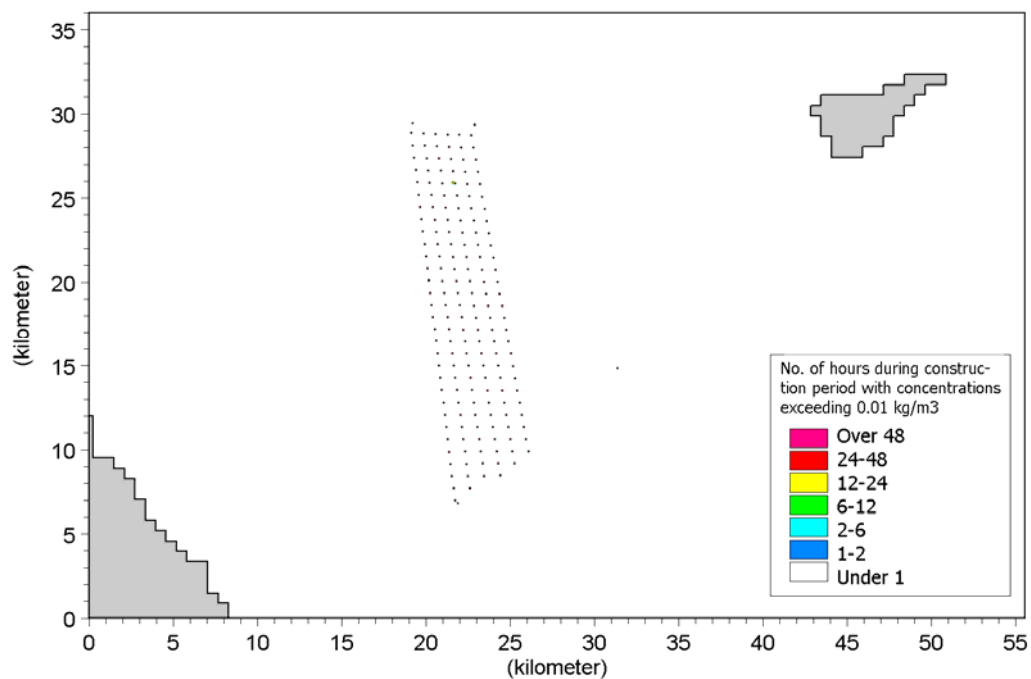
Figure 3-103   Number of hours during the dredging operation (334 days) where the concen-
                tration exceeds 10 mg/l for Scenario 1. Model results from the sediment
                spreading calculations.
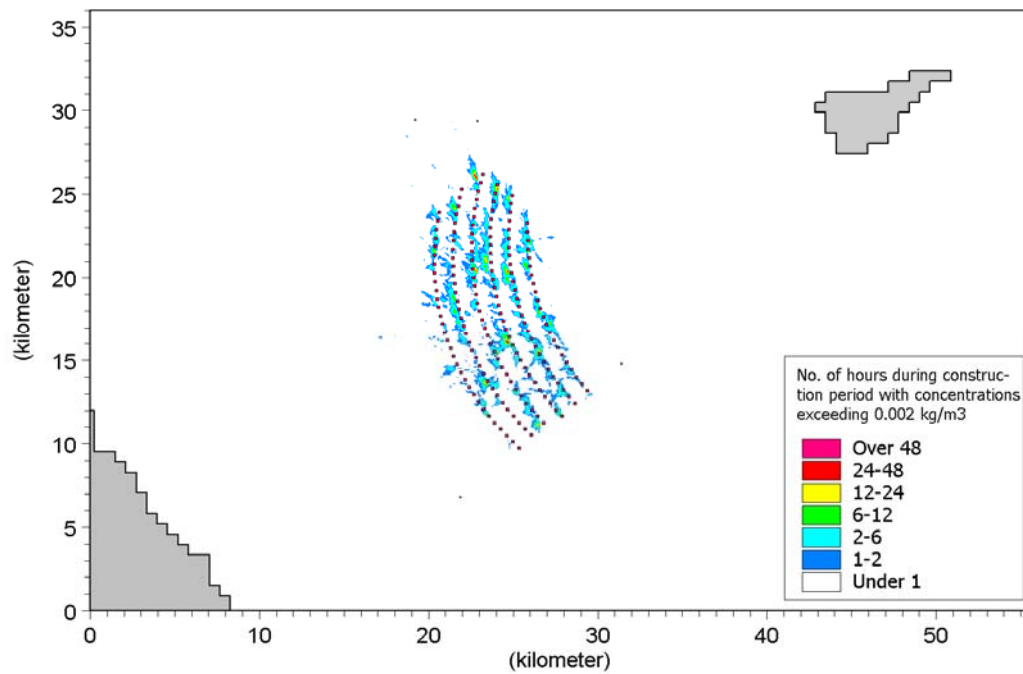
Figure 3-104   Number of hours during the dredging operation (334 days) where the concen-
tration exceeds 2 mg/l for Scenario 2. Model results from the sediment spread-
ing calculations.
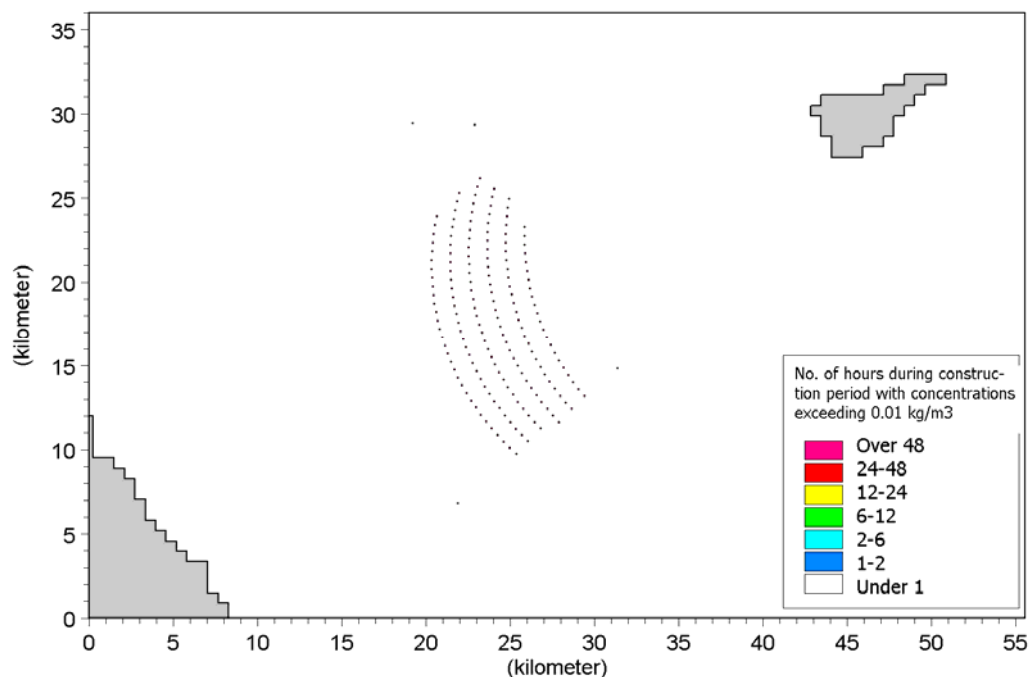
Figure 3-105   Number of hours during the dredging operation (334 days) where the concen-
               tration exceeds 10 mg/l for Scenario 2. Model results from the sediment
   spreading calculations.

Results show that the visibility limit is only exceeded very locally (not outside the
project area) and for very short periods of time - in most cases less than a day. 5
mg/l is only exceeded at the foundations and only very shortly (< 1 hour). There is
no significant difference between the two layouts in terms of impact. In both cases
the impacts are very small and local. Further away the plumes will not be visible.

It should be noted that the present calculations only relate to sediments with a di-
ameter less than 64 microns. Sand will also be spilled. However, the sand will have a
much larger settling velocity and will thus settle in the immediate vicinity of the
dredging operation. Deposition of sand should therefore be expected in the vicinity of
the operation but away from the operation no impact is expected.

The overall conclusion is that very locally there will be a minor effect of dredging,
however, on the large scale there will be little or no effect. The plume from the op-
erations will be visible and the impact area will be large. However, the impact of both
sedimentation and the concentration from the plumes will not be significant.

3.3.3.3   **Summary regarding impacts due to spill during the construction phase**
           Two probable dredging schemes representing the two worst case scenarios for
           dredging have been simulated: one for each of the two scenarios outlined in Table
           3-28. The simulations were carried out using a numerical 3D PA-model.

Results showed very small impacts. Depth-averaged concentrations were always below 10 mg/l which is the impact criteria for fish. The visibility limits (2 mg/l) were only exceeded in short periods in the order of magnitude of hours or days.

The sedimentation was spread over a very large area but with very small amounts. The deposition was calculated to be less than 1 mm everywhere and in most cases much smaller. Largest sedimentations were seen in the wind mill area.

No significant differences between the two wind mill scenarios were observed. In both cases the observed impacts were small.

Table 3-38   Summary of impacts on sediment spreading during the construction phase

Impact	Intensity of effect	Scale/geograp-hical extent of effect	Duration of effect	Overall signifi-cance of impact
Increased concentra-tions of sediments in the water column	Minor	Regional	Short term	Minor impact
Sedimentation on the sea bed	Minor	Regional	Short term	Minor impact

3.3.4   Dampening of waves due to the wind mill park

When the waves interact with the wind mill foundations, spreading of the wave en-ergy will take place. Furthermore, above the water surface the wind mill pile and wind turbine act as resistance to the wind so that wind speeds within and on the leeside of the wind farm are reduced. Both of these processes cause reductions in the wave heights in the area of the wind mill farm. These impacts are analysed in this chapter. Section 3.3.4.3 concludes the impacts on waves from the Anholt Off-shore Wind Farm in the operational phase.

Only the impacts in the operational phase are assessed. The impacts on the waves are so small that the temporal construction phase is irrelevant to study.

The impact on the waves from the wind park may have indirect effects on the coastal morphology on the coasts of Anholt and Djursland and on the local geomorphology. Waves cause increased stirring of the water column and help to mobilize the sea bed sediments. The possible effects of changes to sediment transport rates along the coasts and in the wind park area due to changes in the waves are assessed in Sec-tion 3.3.6 (Coastal morphology) and Section 3.3.7 (sea bed morphology), respec-tively.

3.3.4.1   Method for impact assessment

When the waves collide with the wind mill structure, a part of the wave energy will be reflected and a part of the energy will be diffracted around the foundation. This effect is denoted the *reflection/diffraction effect* in the following. The physical proc-esses of reflection and diffraction are well known and happen around all offshore structures, such as bridge piers, offshore platforms, and breakwaters. The impacts of

reflection and diffraction on the wave dampening have also been studied for other wind mill parks, among others Horns Rev and Nysted.

The input of the wind energy to the wave generation process within and on the lee-side of the wind farm is reduced due to the blocking effect of the pile and wind turbine acting on the wind passing the wind farm. This effect is denoted the *wind effect* in the following. The reduction in wind speed near the surface has until recently not been very well known and hence the reduction in wind energy input to the wave generation process have not been included previously in similar studies. However, measurements carried out by Risø /36 / show that the wind speed reduction within and on the lee side of the wind farm is significant and results from an ongoing development at DHI have revealed that this process may have a similar impact on the waves as the process of reflection/diffraction.

These two effects are the main processes which will alter the wave field within and near the wind farm. This is summarized in Table 3-39.

Friction and separation also reduces the wave energy. Separation is the process, where the flow very near the surface/foundation detaches from the surface due to a too large angle between the surface/foundation and the main flow direction. Based on experience, however, friction and separation are known to be insignificant compared to the other effects.

The impacts of the waves due to reflection/diffraction are analysed by numerical modelling. The methodology is described in Section 3.3.4.1.1. The wind effect is analysed by analysing previous generic analyses as described in Section 3.3.4.1.2.

The impact assessment is carried out for two worst case scenarios with regard to the layout of the wind park. The selection of these scenarios is carried out in Section 3.3.4.1.3.

Table 3-39   Project activities during the operation of the planned wind park and the sources of impact.

Project Activity	Sources of potential impact	Potential environmental impact
Operational phase		Environmental impact parameter affected /target of impact
Structures (foundations and piles)	Structures (foundations and piles) blocking and spreading the wave energy	Dampening of waves
Structures (piles and wind turbines)	Structures block the wind in and downstream the wind farm	Dampening of waves

3.3.4.1.1 Methodology of assessing the impacts of reflection/diffraction effects on the wave field

The wave energy flux is proportional with the square of the wave height. The change of the wave height and hence the energy flux due to reflection/diffraction effects is hence depending on:

- water depth

- wave period for the incoming waves

- the shape and size of the foundation

- the number of mills and the distance between the wind mills

In order to quantify the wave height changes a 3-step procedure has been used:

1. Detailed calculations of the wave climate around a single wind mill foundation

2. The results are parameterised

3. The change in wave climate over the entire power plant area is calculated with the numerical wave model.

The detailed calculations of the wave climate around a single wind mill foundation are carried out with WAMIT. WAMIT is a panel method that finds the diffracted wave field for an arbitrary shaped structure, based on potential wave theory. Reduction actors in the wave energy flux due to blocking effect of the individual wind mill foundations are calculated depending on the water depth, wave period and shape/size of

foundation. These reduction factors are parameterized to equivalent 'blocking widths', Ref$_m$. This means that the impact of the individual wind mill foundation on the wave field corresponds to all the incoming energy over these equivalent widths being reflected. The equivalent 'blocking widths' are input to the numerical wave model such that the transmitted wave energy is altered at each position of the wind mills.

The details of this procedure are included in Appendix B. An example of how foundations are included in WAMIT is shown in Figure 3-106.

The modifications to the wave field due to the Anholt Offshore Wind Park due to the reflection/refraction effect are based on comparison of results from numerical calculations of the baseline situation as described in Section 3.2.5 with results from numerical modelling applying the same numerical model, which is modified to include the wind mills in the model setup based on the above methodology.
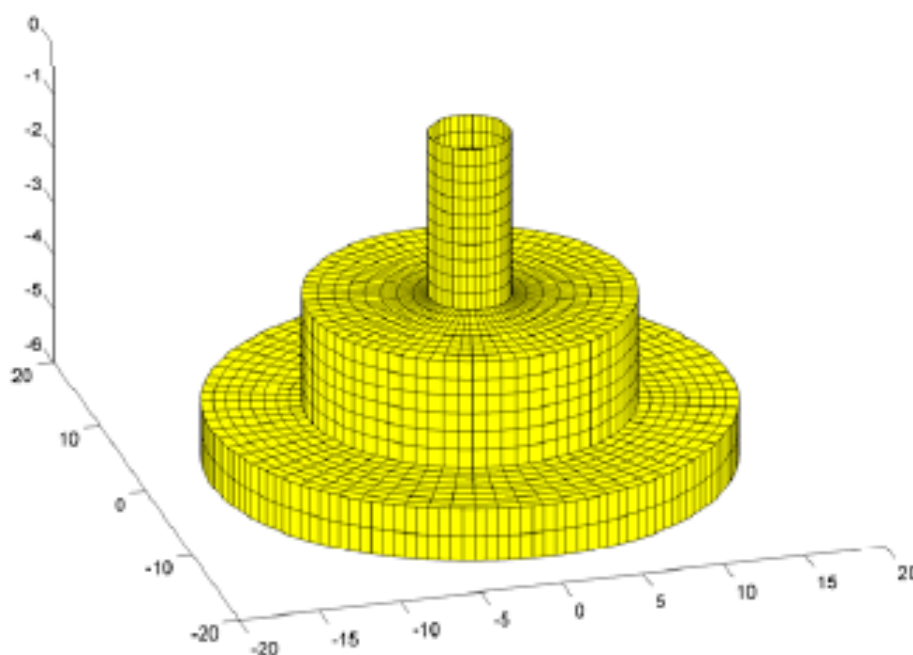
Figure 3-106   Example of how the foundation is included in WAMIT in a situation with 6 m of water depth and the scour protection layer included in the model (the lower layer).

3.3.4.1.2   **Methodology of assessing the impacts of wind effect on the wave field**
Knowledge on the modifications to the wind field in a wind farm has until recently been restricted to the impact on the wind speeds at hub height since this is impor-

tant for energy production. Knowledge on reductions in the wind speeds near the water surface within and in the lee zone of a wind farm is new. Risø have carried out radar measurements of the water surface undulations which can be related to the reduction of surface shear stress.

The impacts of this modified energy input to the wave generation input and the wave field have therefore only recently been investigated. In an ongoing research project at DHI detailed calculations of the modified wave field is carried out for different wind speeds, wind park configurations, fetches etc.

Detailed calculations of the effects in the specific case of Anholt Offshore Wind Farm have not been included as part of this study. It was decided to carry out initial estimations of the impacts of the reduction in wind speeds on the wave heights based on results from the research project. Only if results from this initial study showed that the wave dampening due to the wind effect were believed to be large enough to possibly cause any critical impacts on the coastal morphology (at Anholt or Djursland) or on the geomorphology in the area, should detailed site specific calculations be carried out. Analysis of results showed this was not required.

3.3.4.1.3 **Selection of worst case scenarios of wind farm setup for modelling of waves**
The impact assessment for the wave conditions are based analysis of numerical modelling results of two scenarios selected as a combination of:

1) the type of foundation (monopile and concrete gravity base, see section **Error! Reference source not found**. and /1/)

2) the number and size of mills (174 units of 2.3 MW wind turbines or 80 units of 5 MW wind turbine, see Section 3.1 and /1/)

3) the wind farm Scenario (geographical position of wind mills, north-south going rows or arcs, see 3.1 and /1/)

The two worst case scenarios selected for the wave calculations are found to be the 174 units of 2.3 MW wind turbines on gravity base foundations for the two layouts considered in /1/ base on the following considerations.

The reflection and diffraction effect increase with the blocking effect the wind mill foundations impose on the wave field. Of the two types of foundations the gravity base will clearly have the highest impact on the waves, due to the larger cross sectional area these foundations have regardless of the choice of the size of the mills across the water depth compared to the monopiles. The wind effect is not depending on the type of foundation.

The gravity foundation increases with the size of the mill. The foundations for the 2.3 MW mills have a total cross sectional area of 288 m^2 on a characteristic water depth of 17 m and installation of 174 of these are planned. The summarized total cross sectional area is hence 50112 m^2.The individual gravity foundations for 5 MW wind

mills have a cross sectional area of 368 m^2 and 80 mills of this type will be installed in case the larger wind mills are chosen for the wind mill farm. The summarized total cross sectional area for these mills is hence 29440 m^2. The total cross sectional area blocking the wave field is therefore a factor of 1.70 larger for the combination of smaller foundations and larger number of wind mills than for the combination of larger foundations and fewer wind mills. The reflection/diffraction effect does not only depend on the blocking area, but also on the relationship between the wave characteristics (wave period/wave length) and the diameter of the foundation. However, the difference between the diameters of the foundations for the small and the large foundations are small and the D/L-relationship for the two foundations, where D is the diameter of the foundation and L is the wave length are nearly the same. The total blocking area is hence the dominant factor and the combination of smaller foundations and larger number of mills is evaluated as being the worst case scenario in comparison with the larger but fewer number of mills for the reflection/diffraction effect.

The same reasoning can be followed in evaluating whether the smaller/large number or larger/fewer number of mills will be the worst case scenario with regard to the wind effect. The differences in height of the pile and size of the wind turbine between the 2.3 MW and the 5 MW mill are relatively small and the blocking effect the wind mills impose on the wind is hence larger for the smaller/large number of wind mills.

The wind farm configurations for the small wind mills are shown in Figure 3-71 and Figure 3-72. If the distance between mills are small enough that the effect on the waves due to the first mill is felt at the next downstream mill, the number of mills in the wave direction is important for the total impact. Also the geographical location of the wind mills can be important if there are local variations in the wave field in the area considered for placing the wind mills. The differences between the two configurations considered in this work are small from the perspective of impact of the waves.

The two worst case scenarios are hence chosen as the combination shown in Table 3-40

Table 3-40   Worst case scenarios used in the numerical modelling of waves

Scenario	Foundation	Mill size/no. of mills	Configuration of mills
Scenario 1	Gravity base	2.3 MW/174 units	Layout 1
Scenario 2	Gravity base	2.3 MW/174 units	Layout 2

3.3.4.2   Impacts on wave conditions during the operational phase

The impacts of the wind farm on waves are described for the reflection/diffraction effect and the wind effect separately since the impacts have been assessed by different means as described above. The combined effects are summarized in the end of this section.

3.3.4.2.1 **Impacts from reflection/diffraction effects – annual wave conditions**
The equivalent blocking widths, Ref_m, as calculated by WAMIT are shown in Figure 3-107. As described above the equivalent blocking width is a measure for the reduction in the energy flux passing each individual wind mill due to reflection and diffraction of the waves. The impact is largest for the short periodic waves. Waves with higher wave period (and a larger wave length) pass relatively undisturbed through the wind farm. Typical wave periods in the area of Anholt Offshore Wind Farm are between 3 and 7 s. With a decreasing water depth the gravity foundations take up a relatively larger part of the cross sectional area and the equivalent blocking width is therefore larger for the smaller water depths.

The impact on the wave heights are illustrated in Figure 3-108 - Figure 3-110. In Figure 3-108 and Figure 3-109 the wave heights at a given time in 2005 (8 January at 3 am) are approximately 1.5 m in the wind farm area. The wave heights are shown for the baseline situation, scenario 1 and scenario 2. By comparing the pictures for the three situations it is seen that the distribution of wave heights in the area are affected very little by the wind mills.

Figure 3-110 shows the differences in the wave heights between respectively the baseline situation and scenario 1 in the upper figure and the baseline situation and scenario 2 in the lower figure. The differences are in the order of 1-2 cm between the rows of wind mills and less than 0.5 cm or about 0.3% of the incoming wave height approximately 10 km away.

The maximum dampening ratios of the incoming wave height in each computation cell are shown in Figure 3-111 for Scenario 1 in the upper figure and for Scenario 2 in the lower figure. The dampening ratio is defined as:

$$Dampening \; ratio = \frac{H_{s,scenario} - H_{s,baseline}}{H_{s,scenario}}$$

The computational cells or grid cells were previously illustrated in Figure 3-43. For each cell the dampening ratios are calculated every 3rd hour through 2005, and the maximum reduction is selected. Figure 3-114 are combining these maximum wave height reductions in one figure.

The maximum reductions in wave heights are less than 3% between the wind mill rows. This is consistent with the order of magnitude of the wave dampening found in the assessment of Horns Rev I and Nysted Offshore Wind Farms (/30/ and /31/). Very near the wind mill foundations the reductions in the wave heights may be larger. These very local effects are not resolved in the mesh (mesh size approximately 100 m), but they are irrelevant from the perspective of an EIA. These local effects are only relevant for design purposes.

The reductions in the wave heights due to reflection/diffraction do not exceed 1% at distances larger than 10 km from the wind park. Near the coast of Anholt and

Djursland, the calculations show that the impacts on the wave heights are insignificant.
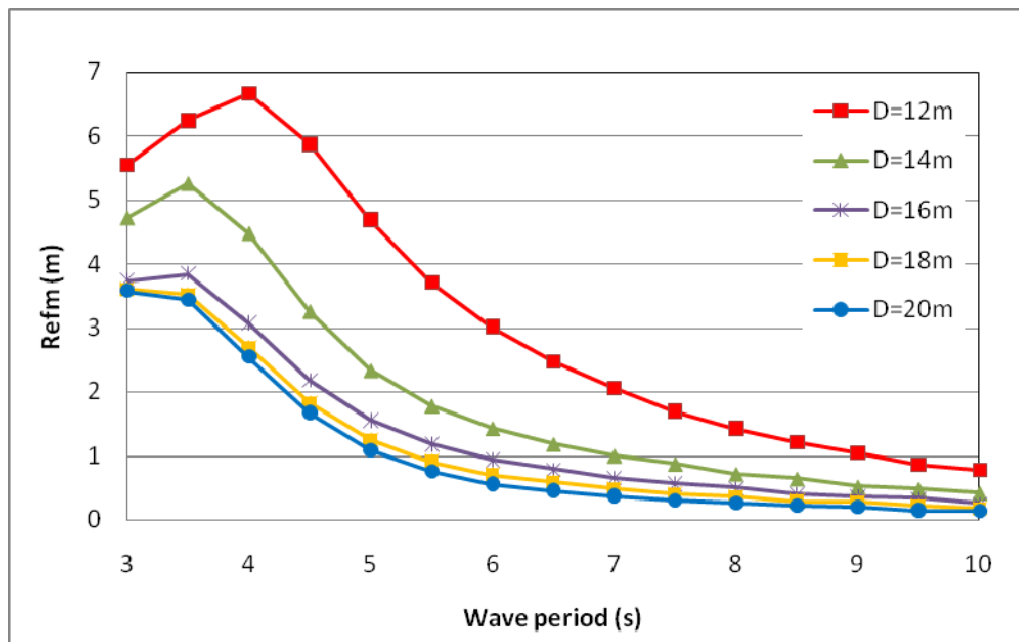

Figure 3-107   Equivalent blocking widths, Ref$_m$, as calculated by WAMIT for gravity base foundations for 2.3 MW mills.
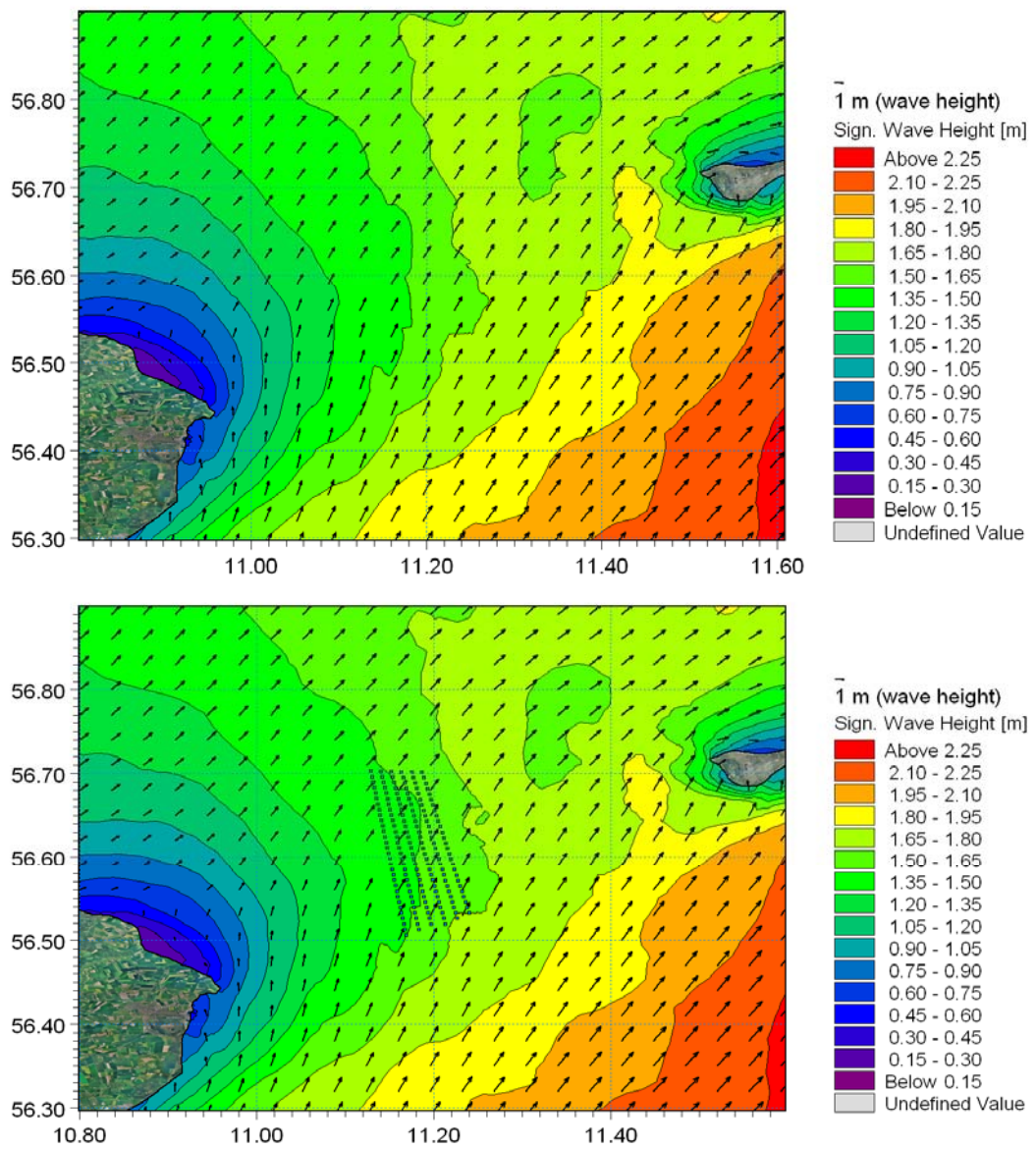
Figure 3-108   Example of wave height distribution for the baseline conditions (upper) and Scenario 1(lower figure).
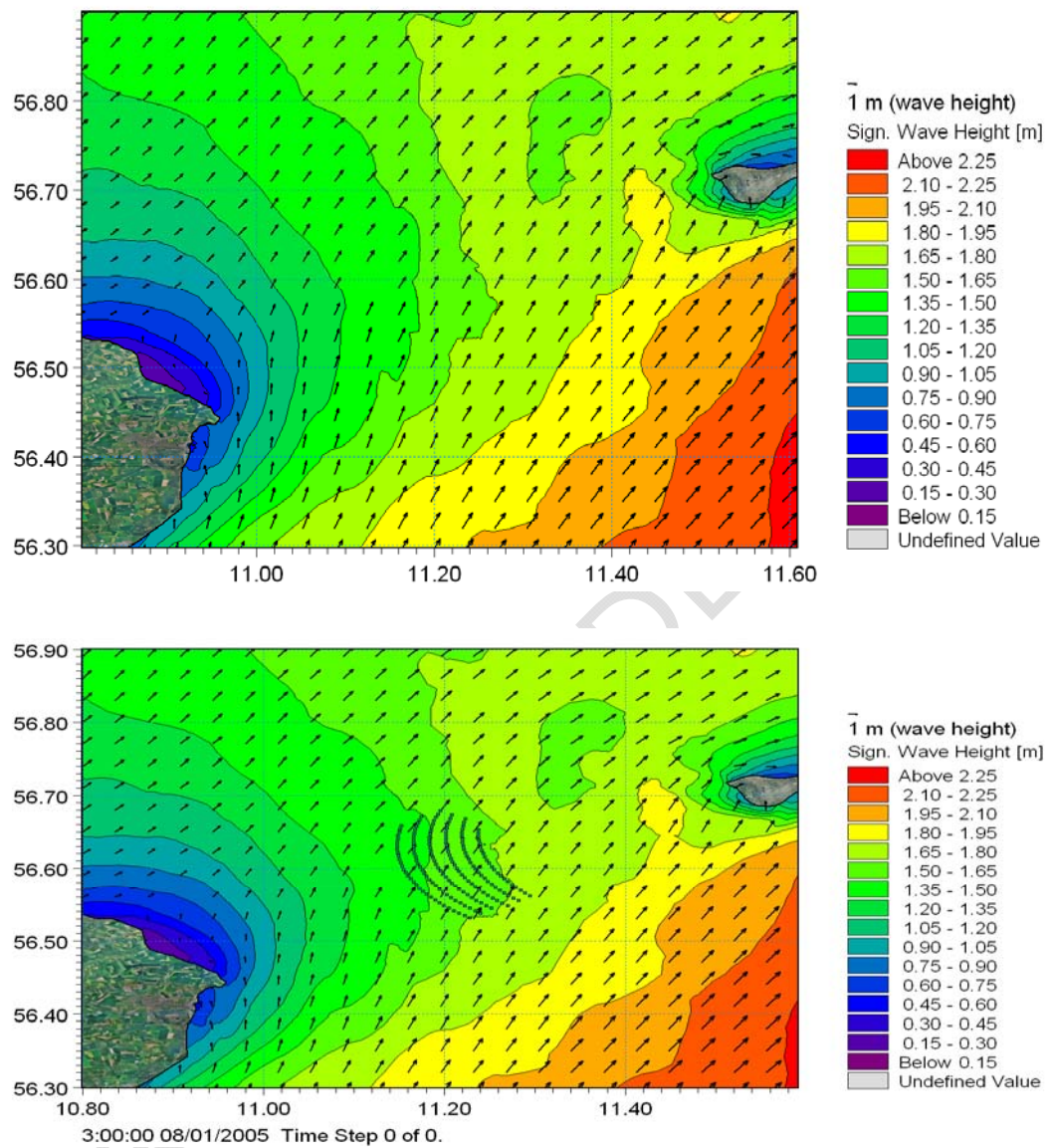
Figure 3-109   Example of wave height distribution for the baseline conditions (upper) and Scenario 1(lower figure).
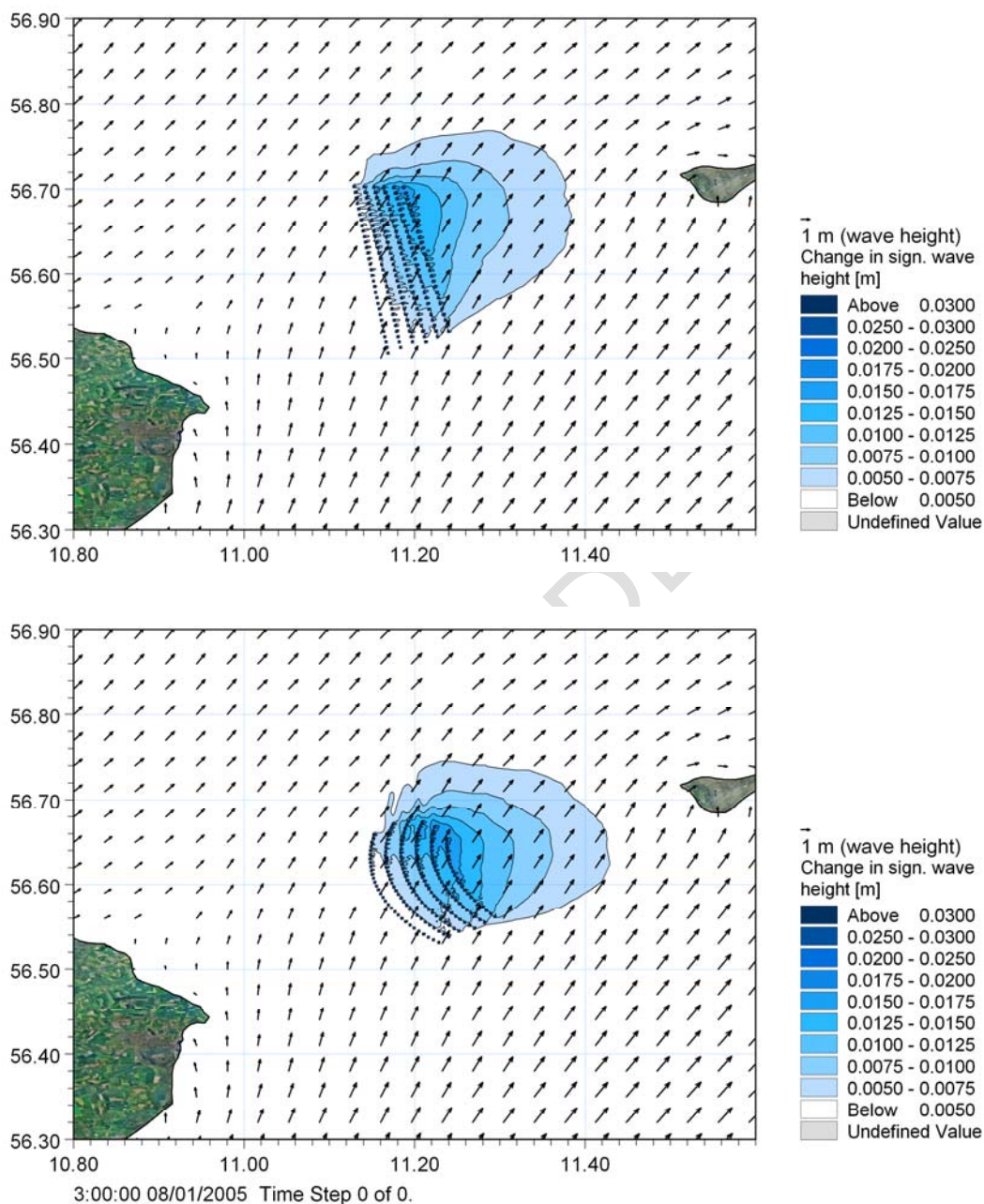
Figure 3-110   Difference in significant wave heights between baseline and Scenario 1 (upper
figure) and baseline and Scenario 2 (lower figure) for the selected time step.
Wave height distributions are shown in Figure 3-108. Vectors are showing the
wave heights and directions of wave conditions for the baseline situation. The
significant wave heights in the project area are approximately 1.5 m at the
time.
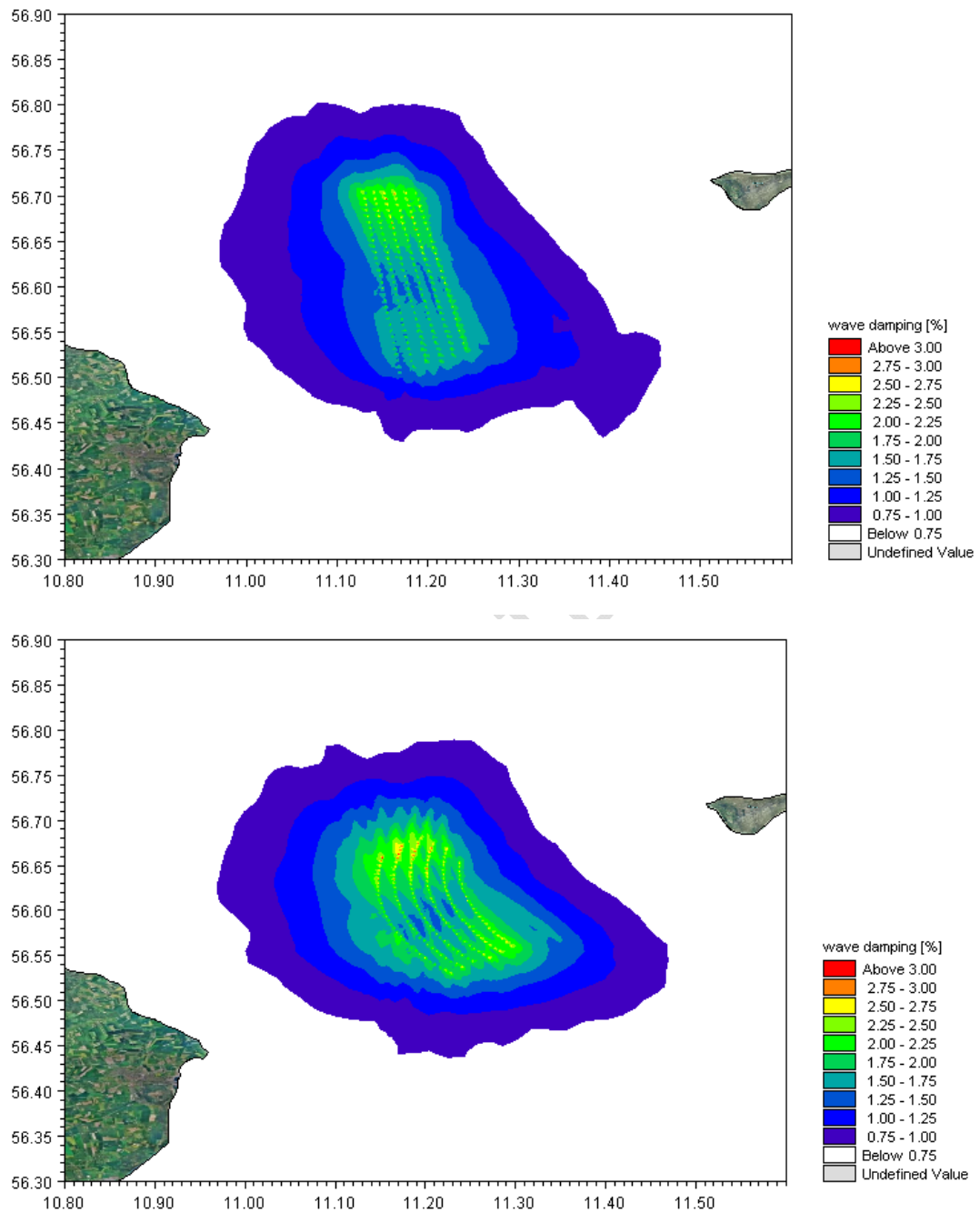
Figure 3-111 Model simulations of the dampening of the waves due to reflection/refraction due to an offshore wind farm between Anholt and Djursland. Colour scale indicates the dampening in % of the incoming wave height in the project area for the un-disturbed situation. The shown values are the maximum dampening coefficient in each computational mesh element (see mesh in Figure 3-43) throughout 2005. Only situations with incoming wave heights above 1 m centrally in the wind farm area are considered.

Impacts from reflection/diffraction effects – storm conditions

For each of the four storms described in Section 3.2.4.1, the impacts of the wind farm on the wave conditions have been assessed. The wave field during selected storms (c.f. section 3.2.4.1.2) has been simulated for the two worst case scenarios outlined in Table 3-24 and results are compared to the baseline simulations of the same storm conditions. The equivalent blocking widths, Ref_m, corresponding to the reduction in the energy flux passing the individual wind mills as shown in Figure 3-107 are applied in the modelling.

Figure 3-112 to Figure 3-119 show the wave dampening calculated during each storm for respectively scenario 1 and 2. The chosen time step for the illustration corresponds to the peak of each storm, i.e. the most severe wind. The wave fields for the baseline condition at the given time were shown in Figure 3-111 to Figure 3-114. The corresponding characteristics of the waves are shown in Table 3-41 for each storm.

Table 3-41   Characteristics of the wave field describing the peak of each storm within Anholt wind farm area.

Period	H_s at peak	Mean wave direction at peak
Storm 1: **Strong wind from W** **Medium South-directed** **current** 29/11/1999 18:00 AM 02/12/1999 18:00 AM	2.6 to 3.1m from west to east	277°N
Storm 2: **Medium-strong wind from NW-N** **Strong South-directed current** 16/01/2000 18:00 AM 19/01/2000 18:00 AM	2.5m	353°N to 347°N from NW to SE
Storm 3: **Strong wind from S** **Strong North-directed current** 23/12/1999 21:00 AM 26/12/1999 21:00 AM	2.7 to 3m from west to east	170°N to 178°N from NW to SE
Storm 4: **Strong wind from SSW** **Strong North-directed current** 29/10/2000 06:00 PM 01/11/2000 06:00 AM	2.5 to 2.9m from west to east	185°N to189°N from NW to SE

The wave dampening results indicate clearly that the influence of the wind farm is almost insignificant on the high waves during storms. Their effect can be felt in the immediate vicinity of the wind mills resulting in a dampening of maximum 1% of the

waves which corresponds to a maximum decrease of 3 cm of the wave height. Wave heights are reduced by 0.5% 1-2km downstream of the wind farm for each scenario. The reason for the relatively smaller impact on the waves in the storm situations than in the annual wave climate is correlated to the results in Figure 3-107. The larger waves with the higher wave periods have a smaller equivalent blocking width than shorter-period waves. The large waves in typical storm situations hence pass more undisturbed through the wind farm.

For Storm 1, the effect of the wind mills in term of area of influence and dampening intensity is extremely low for both scenarios. Westerly waves loose 0.5% of their height at the eastern part of the wind farm for both scenarios. It can be seen that Scenario 2 seems to have a slightly higher effect on the waves. The waves are incoming with a direction of 277°N which is 7° off compared to the axis W-E of Scenario 1. Therefore each wind mill may act individually and their effect will not be accumulated in the wave direction whereas this may be the case for Scenario 2 due to its curved shape.

Under Storm condition 2, waves are incoming from the north with a direction almost parallel to the wind mill rows in the layout in Scenario 1 and the area where the highest dampening of the wave heights (less than 2 cm) is seen is located south of the wind farm. The width of influence of the wind mills on the waves is narrow whereas it is more spread for Scenario 2 due to its shape.

Concerning Storm 3 and 4, the patterns are almost the same. The highest influence is seen NW and NE of the wind farm for Storm 3 and 4, respectively, due to the accumulating effect when the wave direction is nearly parallel with the rows of wind turbines. The area of influence of the wind mills is about 1-2 km downstream the wind farm.
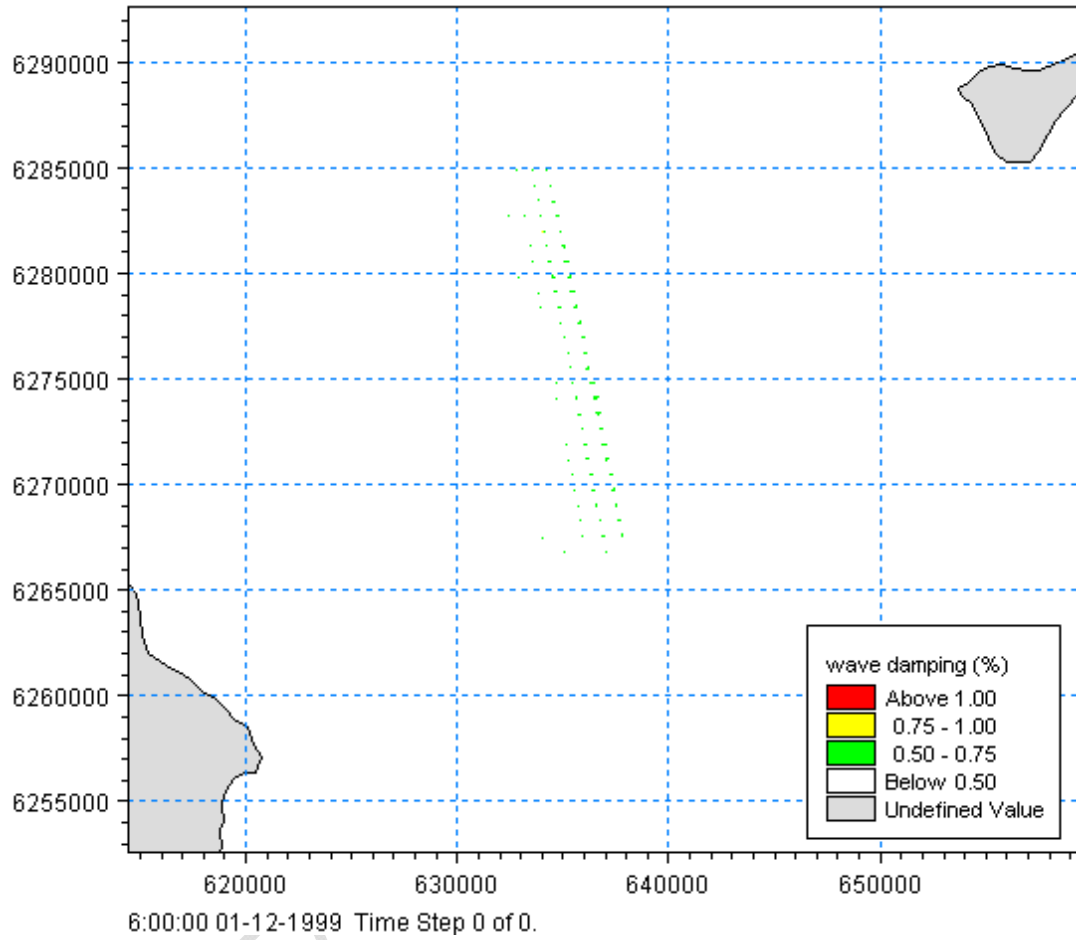
Figure 3-112　Instantaneous wave dampening field (in %) at the peak of Storm 1 for Scenario 1.

6:00:00 01-12-1999 Time Step 0 of 0.
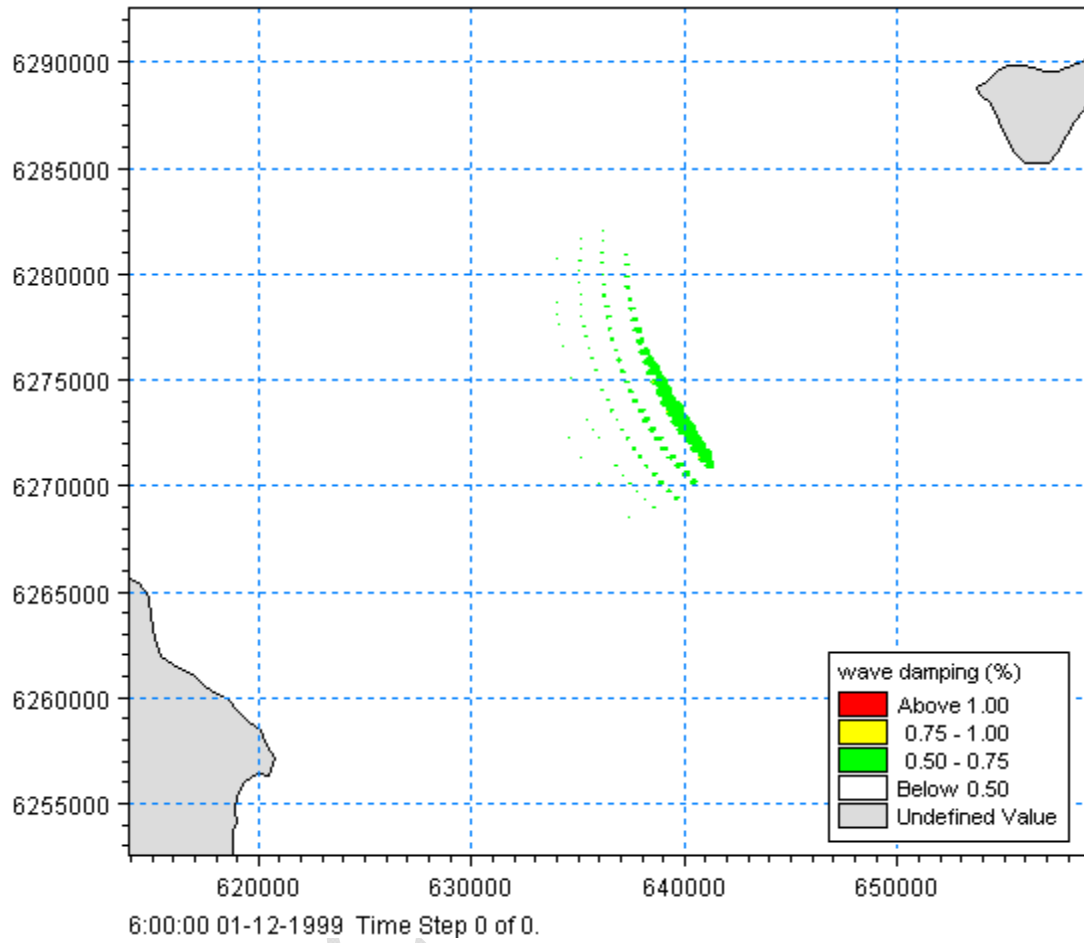
Figure 3-113 Instantaneous wave dampening field (in %) at the peak of Storm 1 for Scenario 2.
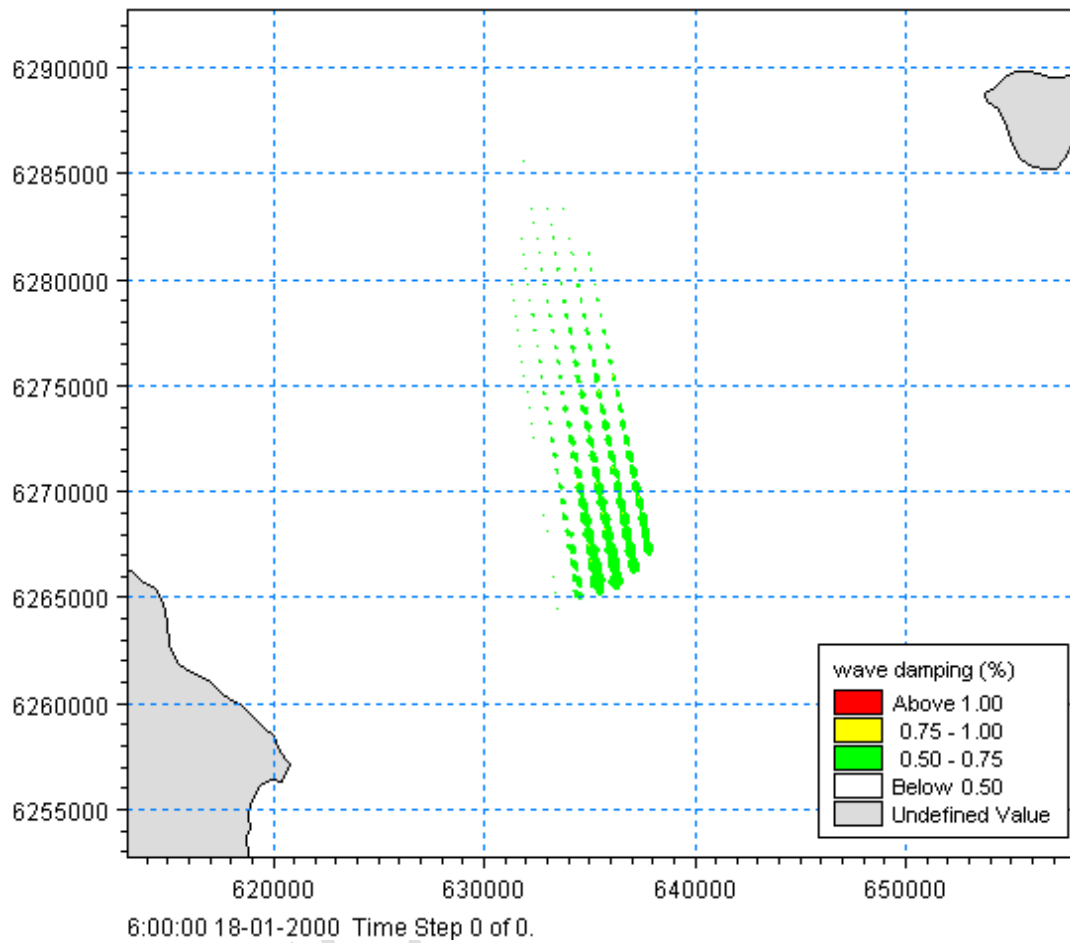
Figure 3-114 Instantaneous wave dampening field (in %) at the peak of Storm 2 for Scenario 1.
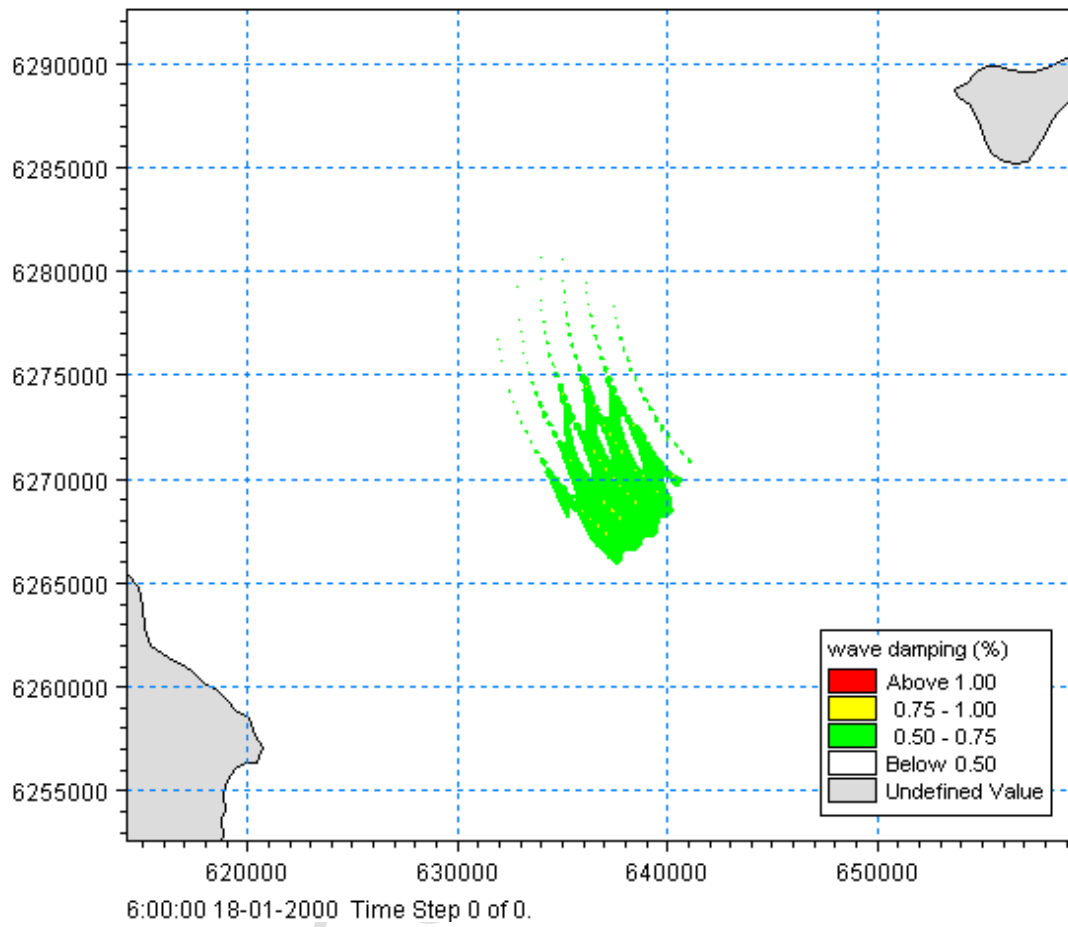
Figure 3-115 Instantaneous wave dampening field (in %) at the peak of Storm 2 for Scenario 2.

9:00:00 25-12-1999 Time Step 0 of 0.
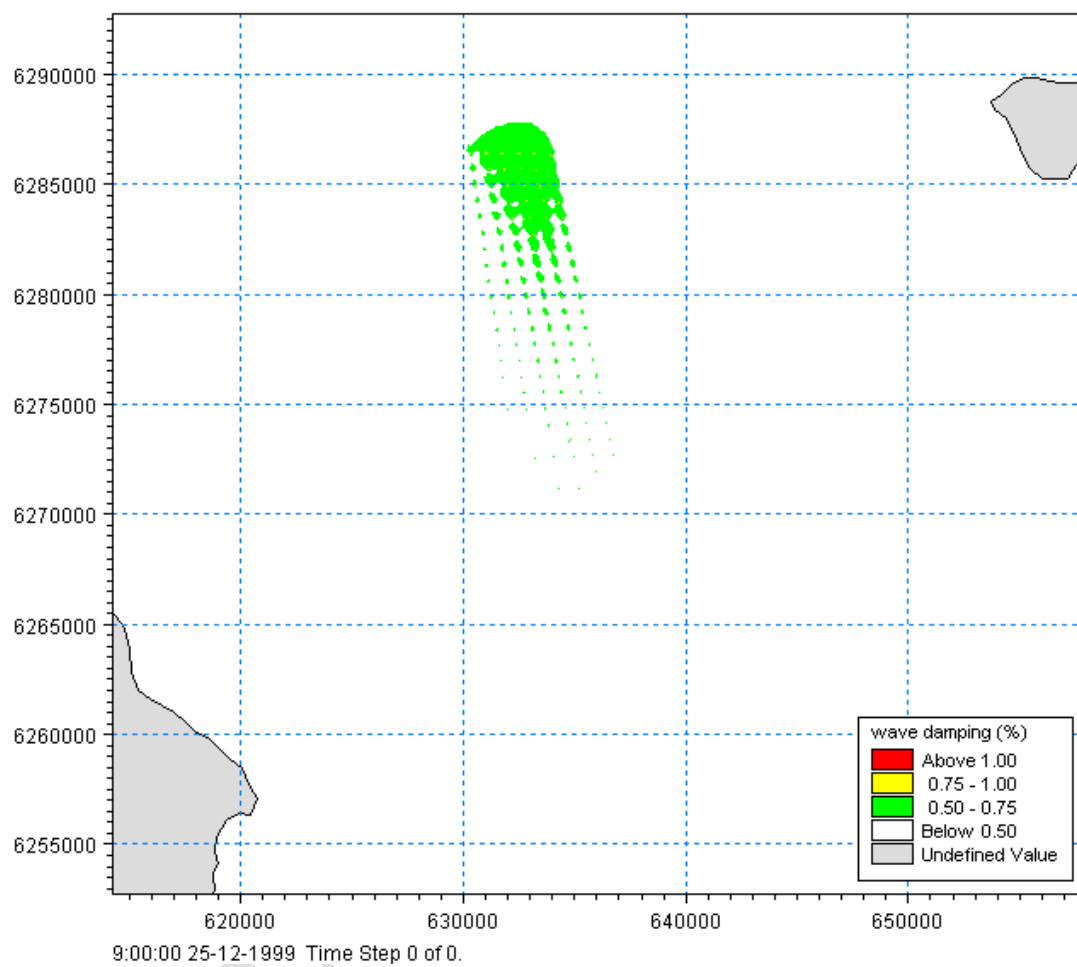
Figure 3-116 Instantaneous wave dampening field (in %) at the peak of Storm 3 for Scenario 1.

9:00:00 25-12-1999 Time Step 0 of 0.
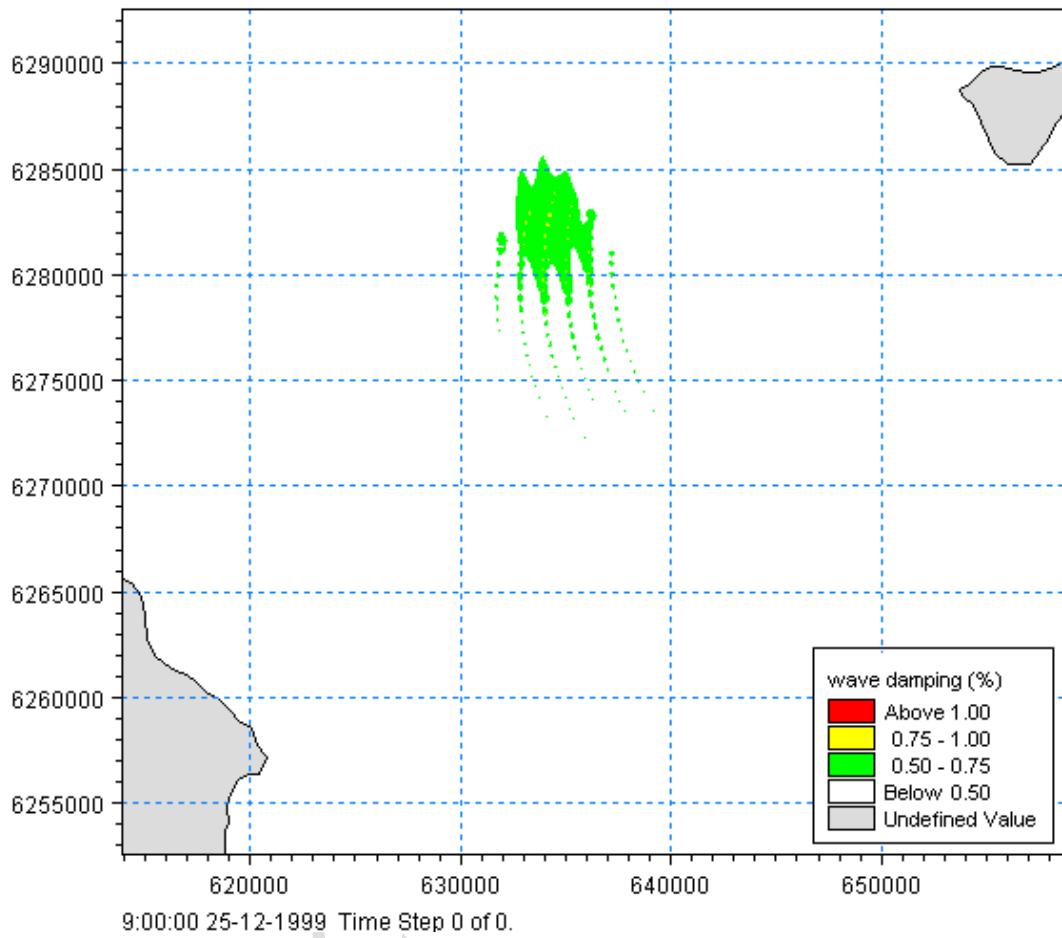
Figure 3-117 Instantaneous wave dampening field (in %) at the peak of Storm 3 for Scenario 2.
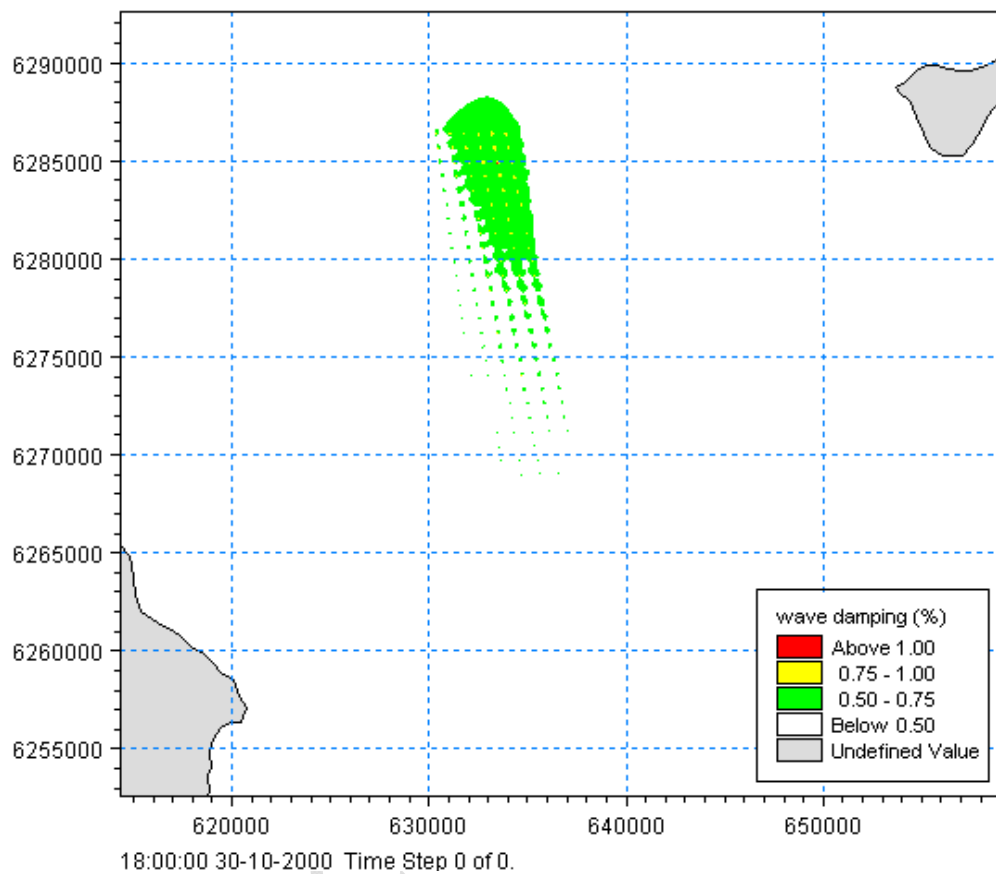
Figure 3-118 Instantaneous wave dampening field (in %) at the peak of Storm 4 for Scenario 1.
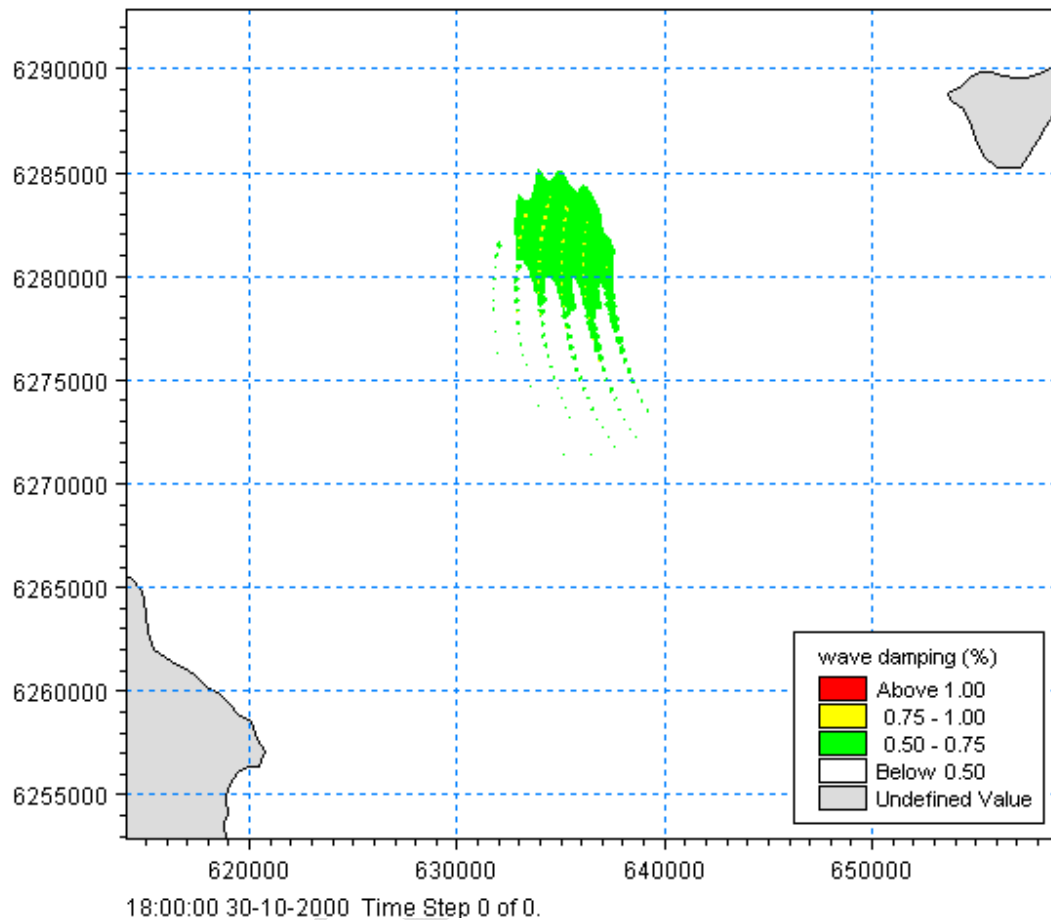
Figure 3-119 Instantaneous wave dampening field (in %) at the peak of Storm 4 for Scenario 2.

3.3.4.2.3 **Impacts from wind effects on the wave conditions**

Generation of wind waves is governed by the surface shear stress on the water surface due to the wind, the fetch, the depth and the duration of the storm. Wind turbines change the wind field inside and downstream an offshore wind farm, and therefore reduce the shear stress at the water surface. For moderate stretches this mechanism has in an ongoing development project by DHI shown to have a similar order of magnitude as the reflection of waves from the wind turbine foundation. For short fetches the mechanism might be the dominant one. The fetch from Djursland to the offshore wind farm is in the order of 20 km, the width of the wind farm is in the order of 6 km and the distance from the wind farm to Anholt is in the order of 20 km. This is relatively short compared to the size of the wind farm.

Results from previous generic analyses give some indication of the magnitude of the reduction. The analyses were carried out with the spectral wave model MIKE21 SW. A comparison of the key numbers applied in the generic analyses and for the Anholt

Offshore Wind farm are supplied in Table 3-42. Only the impacts near the coasts of Djursland and Anholt are assessed.

Table 3-42   Comparison of key numbers for Generic case and Anholt Offshore Wind farm

Parameter	Anholt Offshore Wind Farm	Generic case
Free fetch from land to wind farm (km)	Approx. 20	10
Width of wind farm in wind direction (km)	Approx. 6	5.5
Width of wind farm perpendicular to wind direction (km)	Approx. 20	3.7
Distance between wind turbines (m)	700-1500	600

Figure 3-120 shows the area of the wind farm as the area with the very fine mesh in the upper panel. The wind direction is from west to east in the example. The width of the wind mill park in the example is 5.5 km which compares well with the width (west to east) of the layouts of the wind mills in the two worst case scenarios outlined in Table 3-40, where the widths are approximately 6 km. Wind turbines are located with a distance between turbines of approximately 600 m, which also corresponds well with the distance between mills in the selected worst case scenarios studied. A relative map of the shear stress distribution in the calculated example is shown in the lower panel of Figure 3-120. The maximum reduction of the shear stress is 10 % at the lee side of the wind farm.
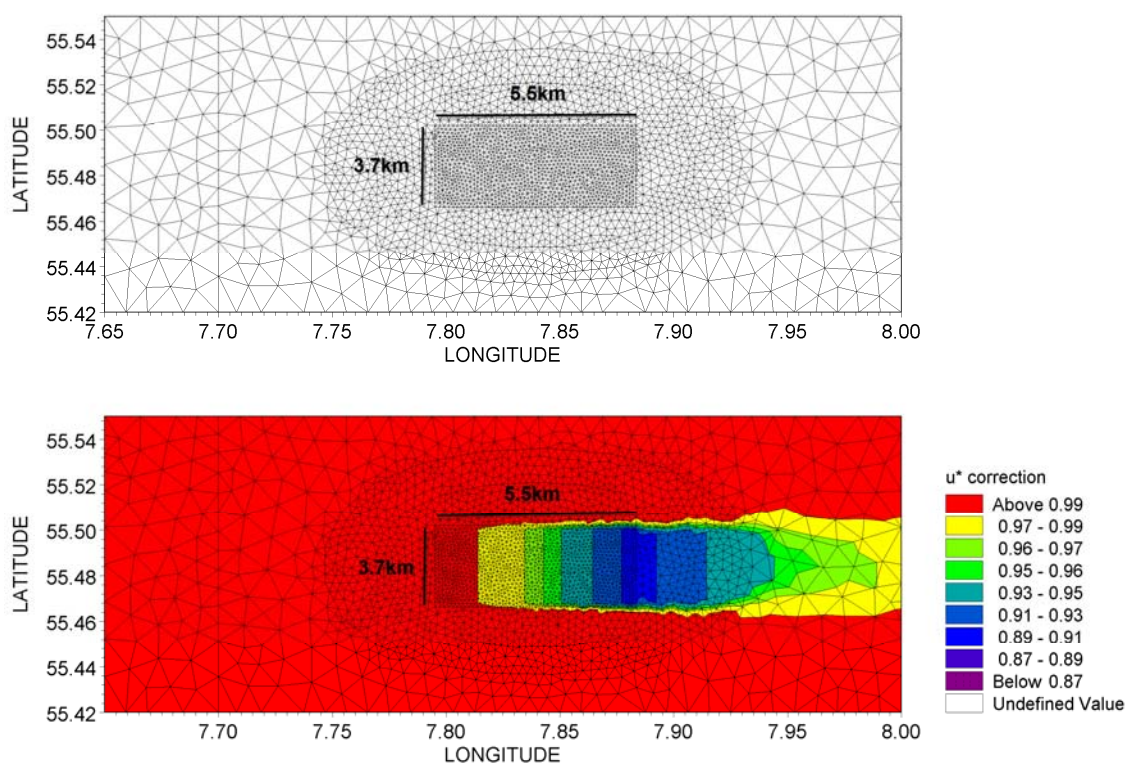
Figure 3-120   The computational grid for the MIKE21 SW calculation (upper panel) and the relative map of the shear stress (lower panel)

Figure 3-121 shows the wave field in a case with the free wind speed U_{10} = 20 m/s and a free fetch of 10 km. U_{10} is the wind speed in a height of 10 m above the surface. The change in the wave height on the lee side is found to be in the order of 2% approximately 5 km downstream from the wind park. A similar figure is found when the wind speed is reduced to 10 m/s (Figure 3-122). Therefore a reduction of the wave height of 2% at Anholt is considered to be conservative for the waves coming from SW to W. On the edges of the influenced area the reduction will be smaller due to directional spreading and spreading of wave energy. This effect is larger, the further away from the wind park. In the calculated example the wind park has a N-S extension of only 3.7 km compared with approximately 20 km in Scenario1 and 2 and the influence of directional spreading is smaller centrally downstream the wind park.

The estimates of wave dampening near the coasts of Anholt are based on the above considerations a reduction up to 1 % for waves from 270°, up to 1-2 % for waves from 247.5°, and up to 1 % for waves from 225°. The reductions in wave heights are expected to be insignificant for wave directions further south than 210° and further north than 280°.

The estimates of wave dampening near the coasts of the northern part of Djursland (north of Fornæs) are based on the above considerations a reduction of 1 % for

waves from 90°, 1-2 % for waves from 67.5°, and of 1 % for waves from 45°. The reductions in wave heights are expected to be insignificant for wave directions further south than 100° and further north and west than 10°.
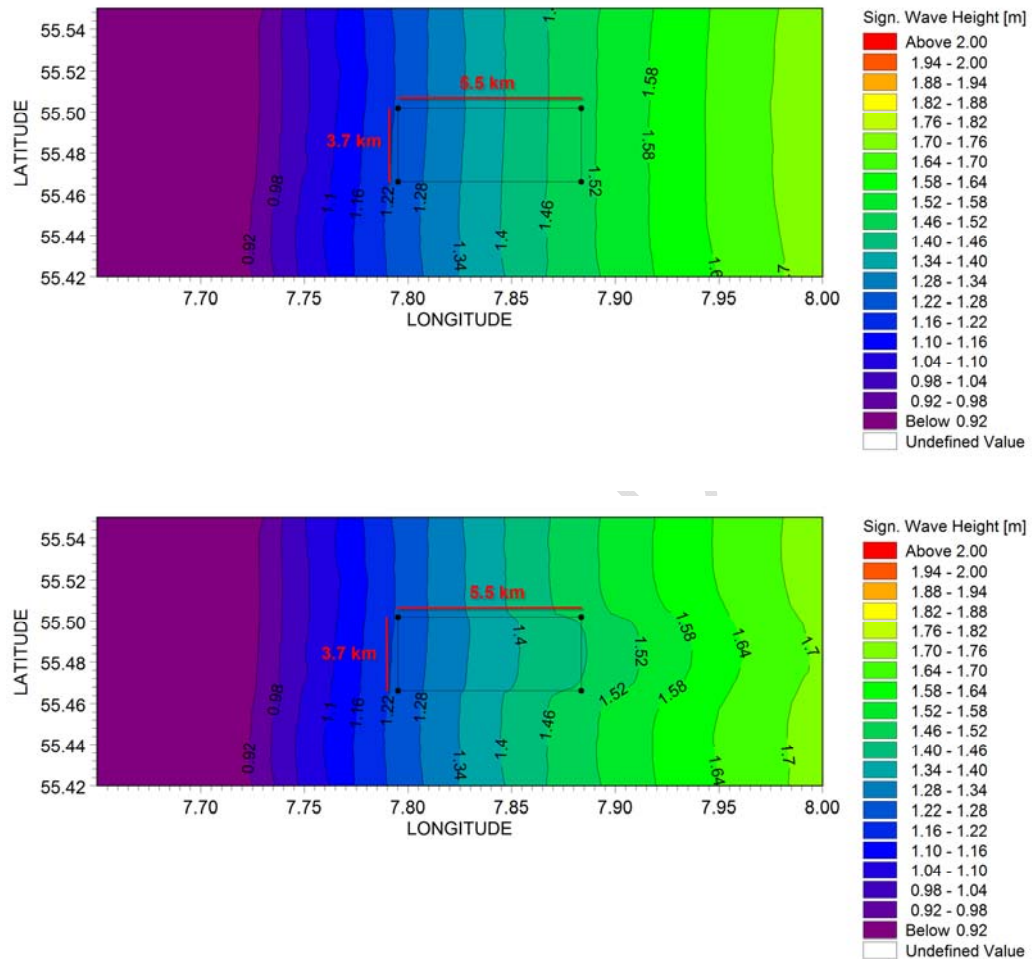
Figure 3-121   Wind speed 20 m/s, free fetch is 10 km. Upper panel without the wind farm, lower panel with the wind farm as marked.
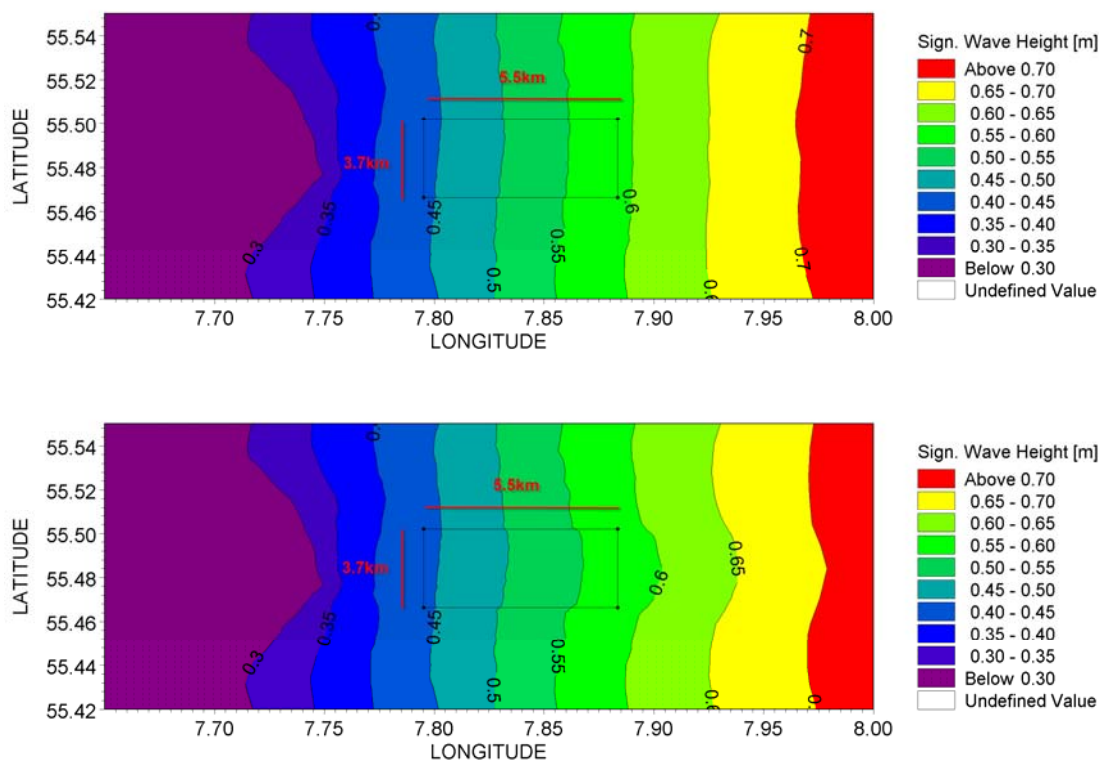
Figure 3-122   Wind speed 10 m/s, free fetch is 10 km. Upper panel without the wind farm.
Lower panel with the wind farm as marked.

3.3.4.3   Conclusions regarding wave dampening during the operational phase

In summary the following conclusions have been reached in the above assessment of the impacts of the wind mill park on the wave field:

The impacts due to reflection/diffraction effects:

- The wave dampening due to reflection/diffraction is estimated to have a small impact on the wave field. The reductions in the wave heights are no larger than 3% within the wind farm area and no larger than 1% in a radius of 10 km from the wind farm.

- The wave height reductions (in % of the incoming wave height) are larger for smaller waves (H_s=<2m) than for more severe waves (H_s=>2m). The changes in wave heights during storm conditions are hence relatively smaller than changes during the annual mean wave climate.

- Near the coasts of Djursland and Anholt, no impacts on the wave field are expected due to reflection/diffraction.

- The differences between Scenario 1 and 2 with respect to wave dampening are insignificant.

The impacts due to wind effects:

- The impacts of wave dampening due to the reduced wind speeds caused by the friction from the wind mills are in the case of Anholt Wind Park estimated to be larger than the impacts caused by reflection/diffraction.

- Near the coasts of Anholt small impacts on the wave heights are expected. Wave heights from a directional sector between 210° and 280° are reduced by up to 1-2 %.

- Near the coasts of Djursland small impacts on the wave heights are expected. Wave heights from a directional sector between 10° and 100° are reduced by up to 1-2 %.

- The applied methodology does not allow to measure differences in the impact between Scenario 1 and 2, but for the two scenarios the same order of magnitude of the impacts are expected.

Table 3-43   Summary of impacts on wave dampening during the operational phase

Impact	Intensity of effect	Scale/geograp-hical extent of effect	Duration of effect	Overall signifi-cance of im-pact
Reflec-tion/diffraction	Minor	Local-Regional	Long term	Minor impact
Wind effect	Minor	Regional	Long term	Minor impact

3.3.5 Influence on water quality

The most conspicuous change in the wind farm area is the introduction of hard sub-strate in terms of foundations and pillars extending from seabed to water surface. Based on observations from other offshore wind farm areas and bridge pillars such hard substrate invariably will become covered by sessile organisms and in particular by blue mussels (/38/). Because the best documented data for marine growth stem from the Great Belt link we have used data from this bridge as a guideline for what can be expected during the operational phase of the wind farm. Other changes include occupation of seabed by foundations, local and regional changes in current regime and waves (see Section 3.3.2.2).

3.3.5.1 Method for impact assessment

In the following effects on water quality during the operational phase have been quantified by model simulations using 1) hydrodynamic forcings resulting from the numerical modelling of the two worst case scenarios (see Section 3.3.2.1) and 2) imposing an additional filtration capacity in grid cells where a wind mill is located.

The additional filtration capacity due to expected population of mussels on the wind mills was calculated from abundance and length distribution determined at Great Belt bridge pillars:

Abu*0.185*(L;cm)^2*24/1000,

where Abu is abundance (ind/m^2), L is the shell length in cm, and 0.185 is a scaling factor. The total filtration capacity in a model depth interval is calculated by summing filtration capacity for all mussel size classes and multiplying with the area of hard substrate in the depth interval. Referring to the study from the Great Belt bridge mussel abundance and size distribution are assumed to be uniform from 2 m below surface to 13 m depth. Outside this interval mussels are not expected to populate the wind mills.
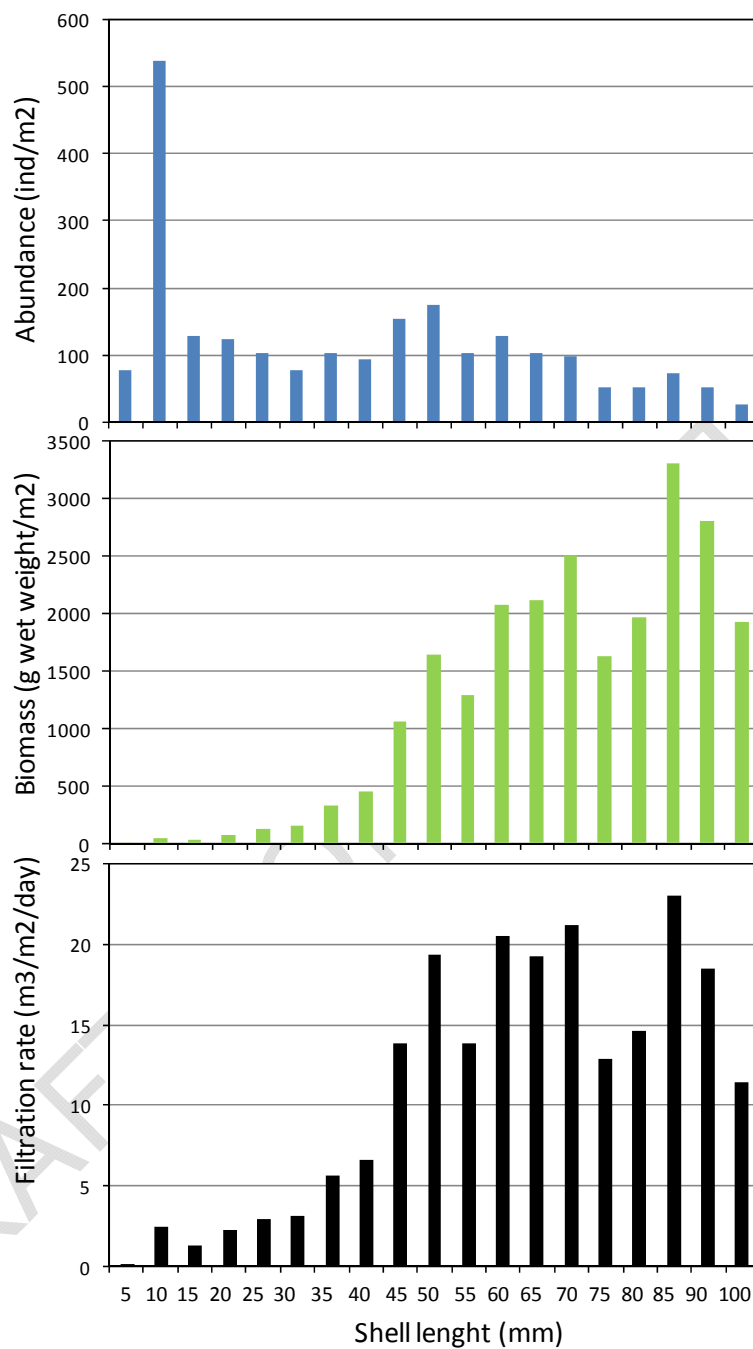
Figure 3-123   Abundance, wet weight and theoretical filtration rate of different sized *Mytilus edulis* at Great Belt Piers. From /38/.

The theoretical filtration capacity is calculated to 3009 m^3 per grid cell volume (617m * 617m*1m) or equivalent to 0.8% of the grid cell volume per day. Because mussels

occur in an approx. 5 cm dense mat the realized filtration is lowered by 30% to account for "refiltration" (/39/).

Table 3-44: Project activities and sources of impact and potential impacts on water quality

Project Activity	Sources of potential impact	Potential environmental impact
Operational phase		Environmental impact parameter affected /target of impact
Structures (foundations and piles)	Hydraulic resistance and blocking of nutrient and plankton flow Changes in vertical mixing of nutrients, plankton and oxygen Increased grazing pressure and nutrient mineralisation from mussels populating foundations and piles	Reduced transport of nutrients, plankton and bottom water oxygen through wind farm park Changes in primary production, sedimentation and mineralisation at seabed

3.3.5.2 **Impacts on water quality conditions during the operational phase**
In the following modelled impacts on water quality resulting from the two wind farm scenarios are depicted as the change (in relation to the baseline condition, see Section 3.2.6) in the various state variables and selected derived variables.

Predicted changes in pelagic primary production are very small in the local model area varying between reductions from 1 gC m^2 y^{-1} to increases up to 1 gC m^{-2} y^{-1}. Changes occur in restricted areas and in about 80% of the model area changes range below -0.2 to +0.2 gC m^{-2} y^{-1} (see Figure 3-123). Compared to a typical baseline primary production of 100-140 gC m^2 y^{-1} (see Figure 3-124 and Figure 3-125) changes are indeed very modest.
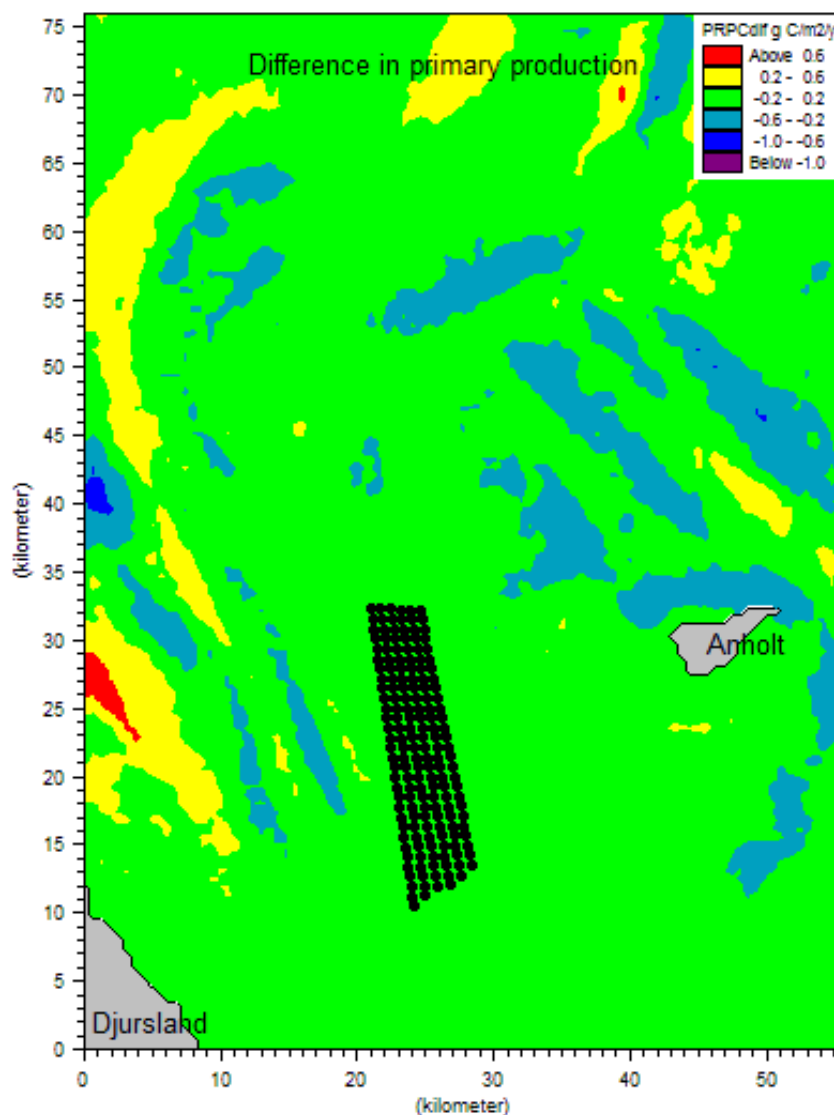
Figure 3-124   Difference in modelled yearly net primary production between reference condi-
tion and scenario 1 of operating wind mill farms.
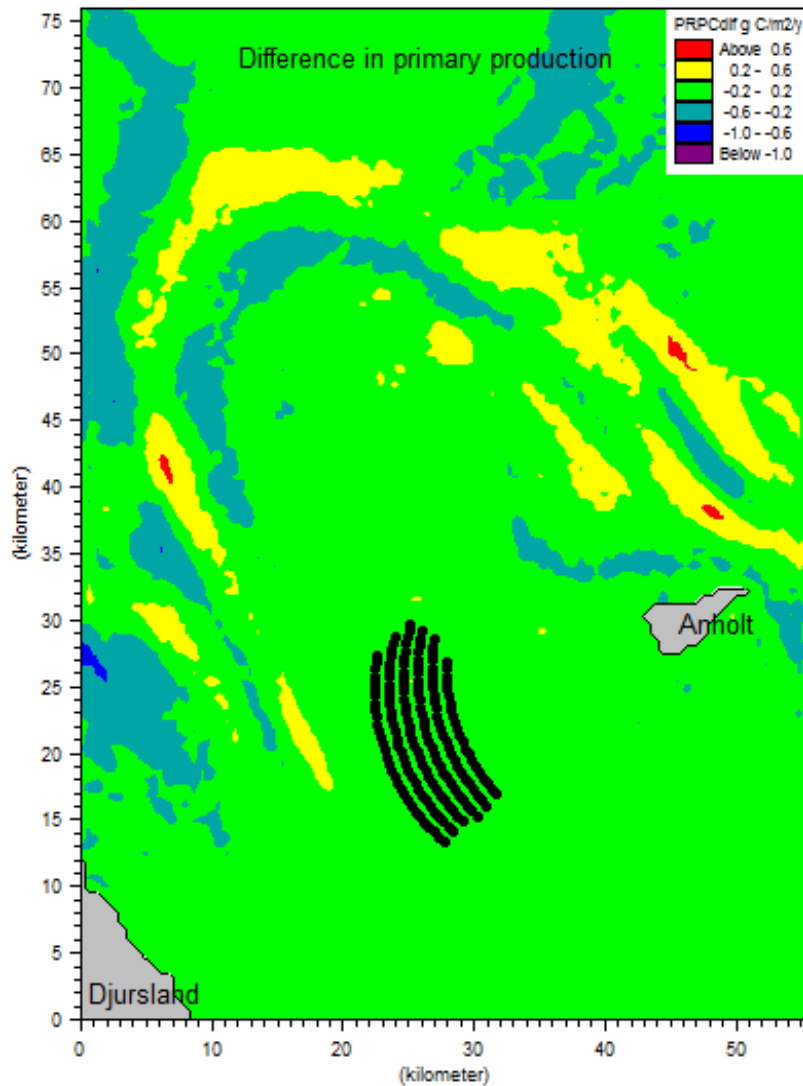
Figure 3-125   Difference in modelled yearly net primary production between reference condition and scenario 2 of operating wind mill farms.

Sedimentation of organic carbon (i.e. detritus and planktonic algae) resulting from primary production is an important process that sustains a significant part of the benthic invertebrate communities, and in particular detritus feeders. In addition to invertebrates microbial food chains account for a large part of the sequestering of organic matter and the mineralisation of nutrients in the settled material. The predicted changes in sedimentation of organic carbon varied between reductions at -0.1 to increases up to 0.06 gC m^2 y^{-1} (Figure 3-126 and Figure 3-127). In both farm scenarios reductions in organic carbon sedimentation occurred in a 200 km^2 area in the northern part of the project area and immediately north of the project area. Further north in the square formation of wind mills increased carbon sedimentation (0.02-0.06 gC m^2 y^{-1}) occurred over an area of about 200 km^2. The spatial distribution of

sedimentation changes show no relation to changes in pelagic primary production but are likely to be an effect of additional filtration pressure from mussels populating the wind mill foundations and eventually also caused by changes in current and wave patterns. Compared to a yearly sedimentation rate of 20-40 gC m^2 y^{-1} the predicted changes must be considered as insignificant.
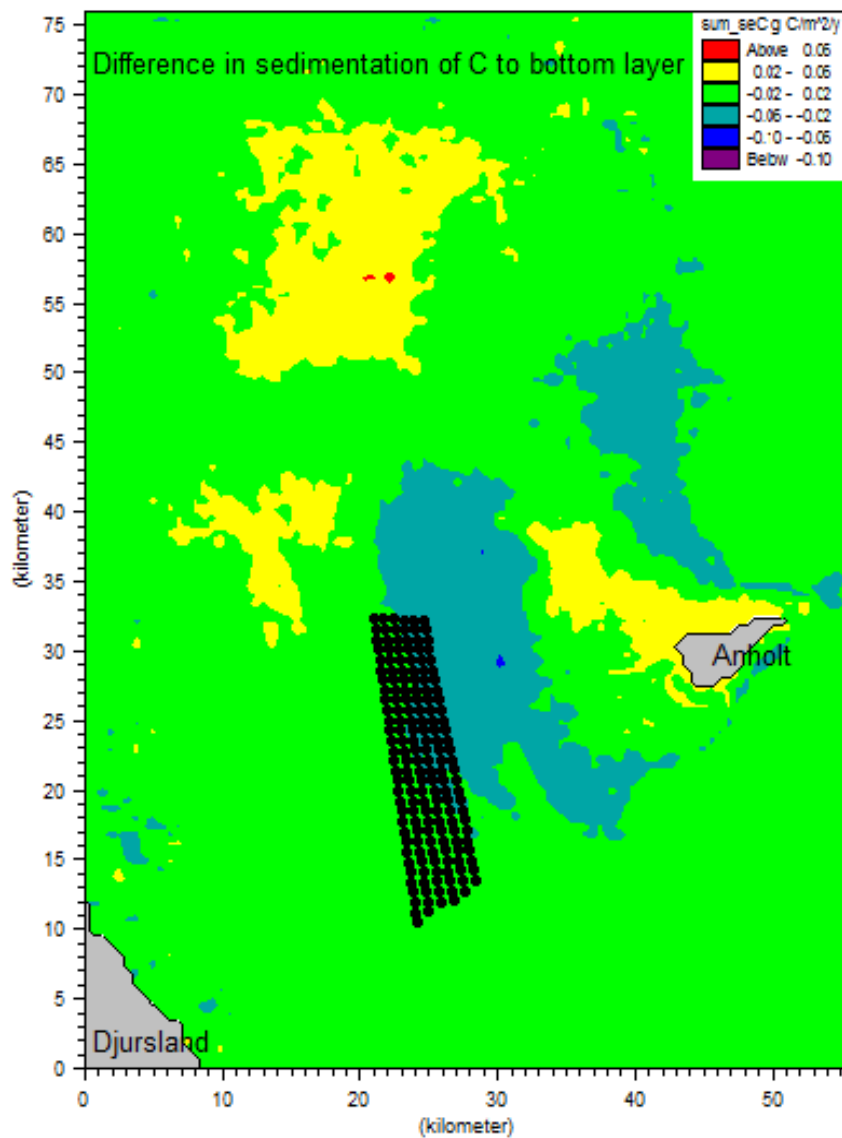

Figure 3-126   Difference in modelled yearly net C sedimentation between reference condition and scenario 1 of operating wind mill farms.
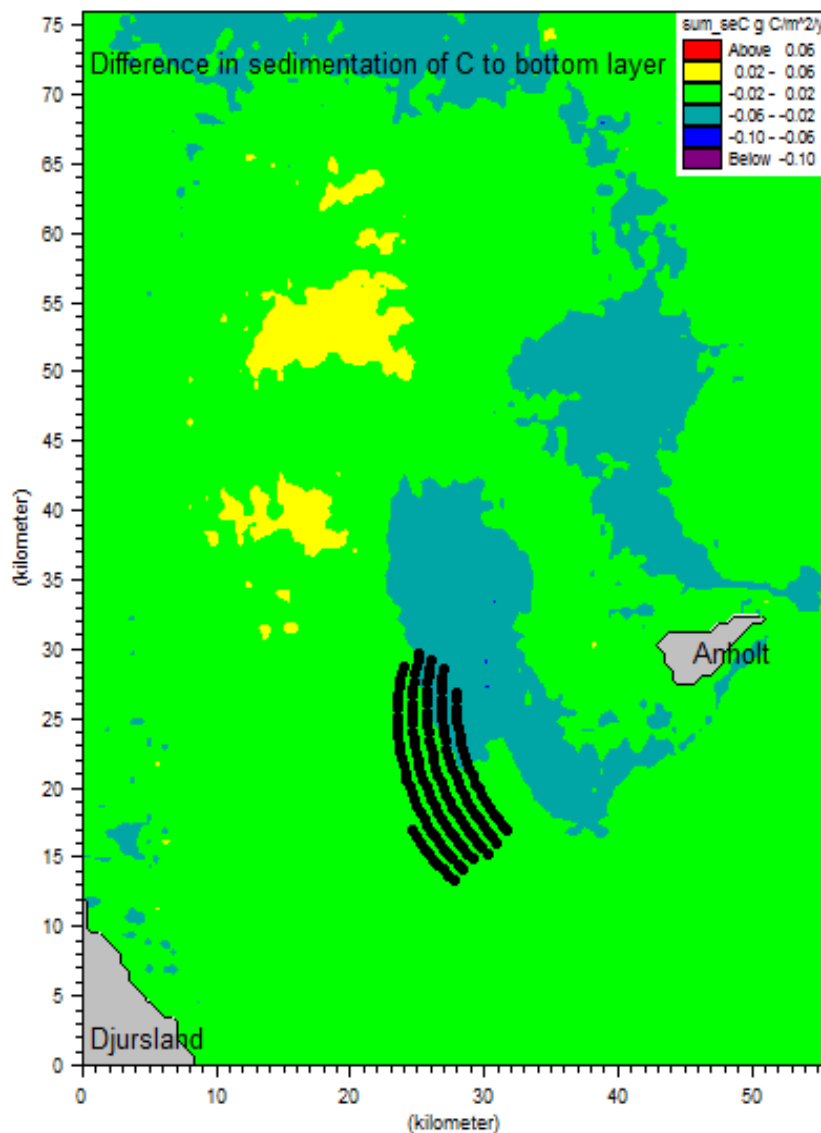
Figure 3-127   Difference in modelled yearly net C sedimentation between reference condition and scenario 2 of operating wind mill farms.

The spatial changes in organic carbon mineralisation closely resemble the changes in sedimentation of organic carbon with decreases in the northern part of the project area (Figure 3-128). The range in changes varied spatially between -0.1 to +0.1 gC m^2 y^{-1} but considering a typical range in carbon mineralisation rate of 20-40 gC m^2 y^{-1} at depths larger than 10 m the changes expected after construction of the wind farm must be regarded as insignificant.
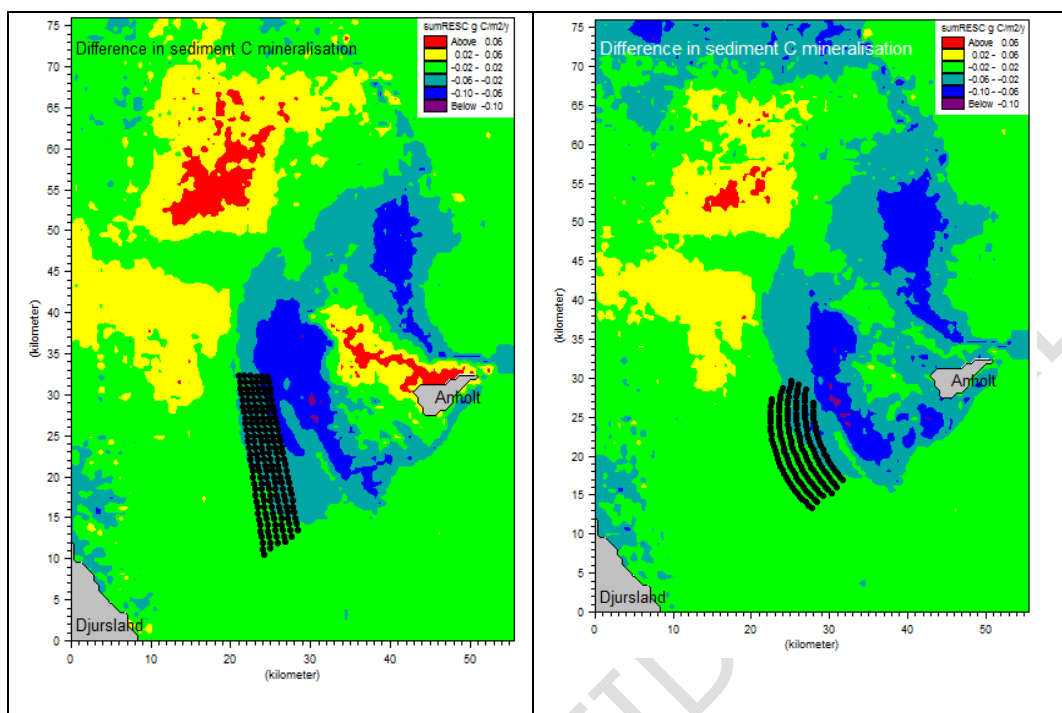
Figure 3-128   Difference in modelled yearly C sediment mineralisation between reference
condition and two scenarios of operating wind mill farms.

Prolonged periods with oxygen concentrations below 4 and 2 mg O_2 l^{-1} in bottom
water can affect both demersal fish and invertebrate communities. During baseline
conditions prolonged periods (> 20 days) with low oxygen concentration occur local-
ized in isolated depressions in seabed and in trenches (Figure 3-128). Predicted
changes in area extension subjected to prolonged oxygen deficiency after establish-
ment of a wind park were very small with localized increases in duration of low oxy-
gen of 1-3 days per year, but also few spots where duration of low oxygen was re-
duced by 1-2 days (Figure 3-129 and Figure 3-130). There was no obvious match
between areas where oxygen conditions were changed and areas with changes in
carbon sedimentation and mineralisation. Hence, changes in oxygen conditions were
probably driven by minor changes in hydrographic conditions.
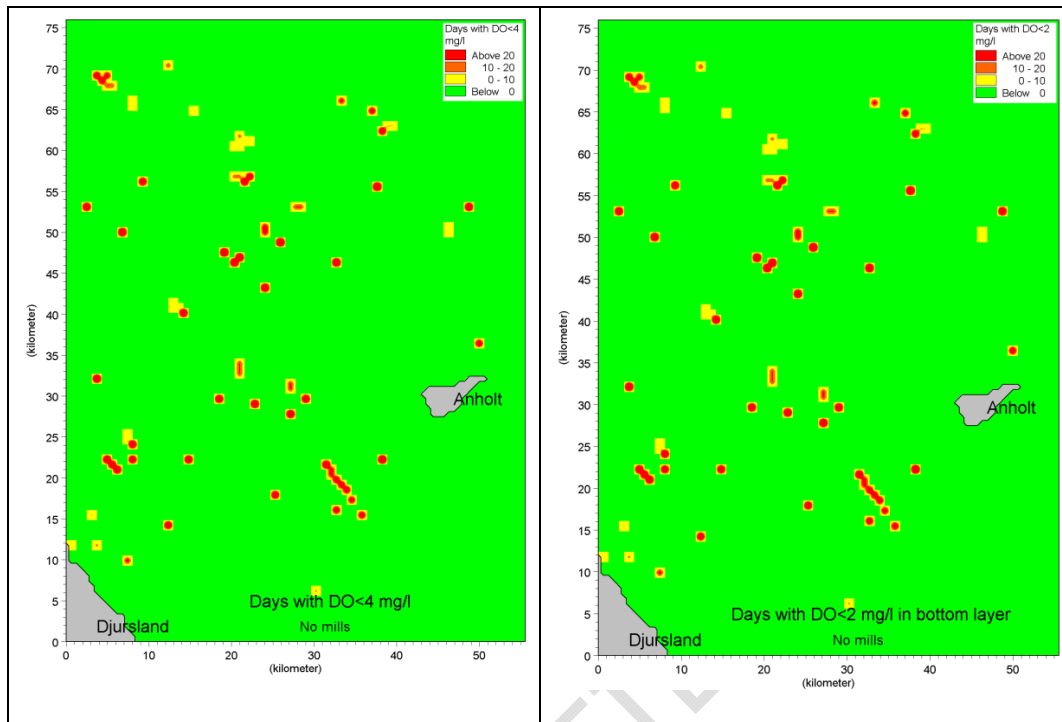
Figure 3-129   Right: Accumulated time with DO<4 mg/l and DO<2 mg/l in reference condition (year 2005). Model results.
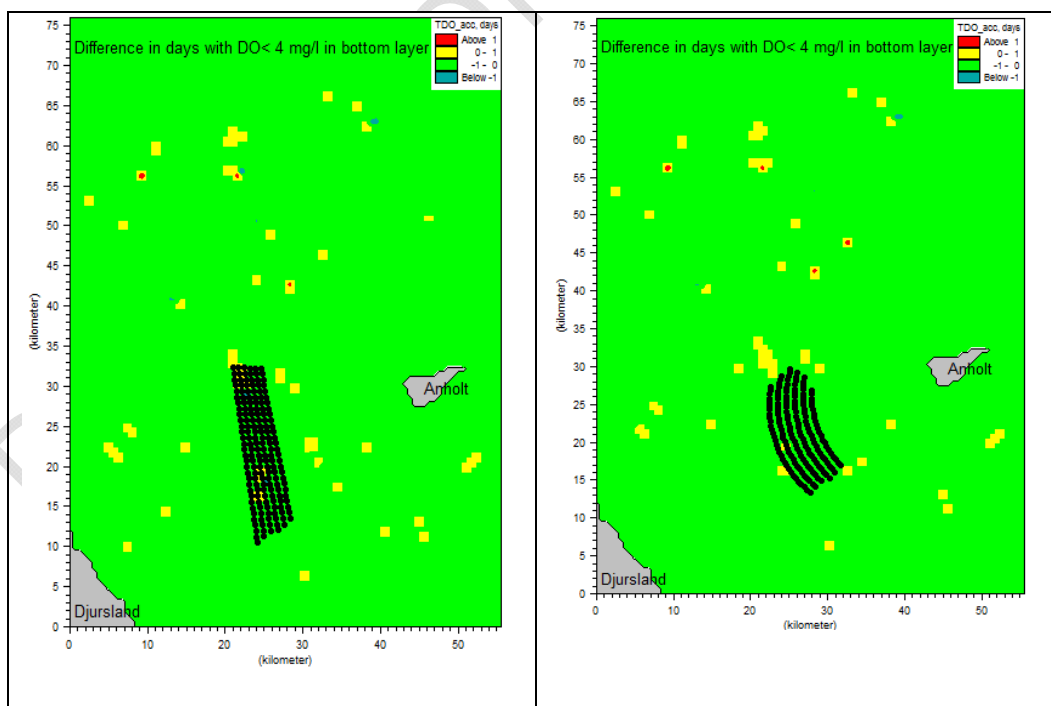
Figure 3-130   Difference in accumulated time with DO<4 mg/l between reference condition and two scenarios of operating wind mill farms. Model results.
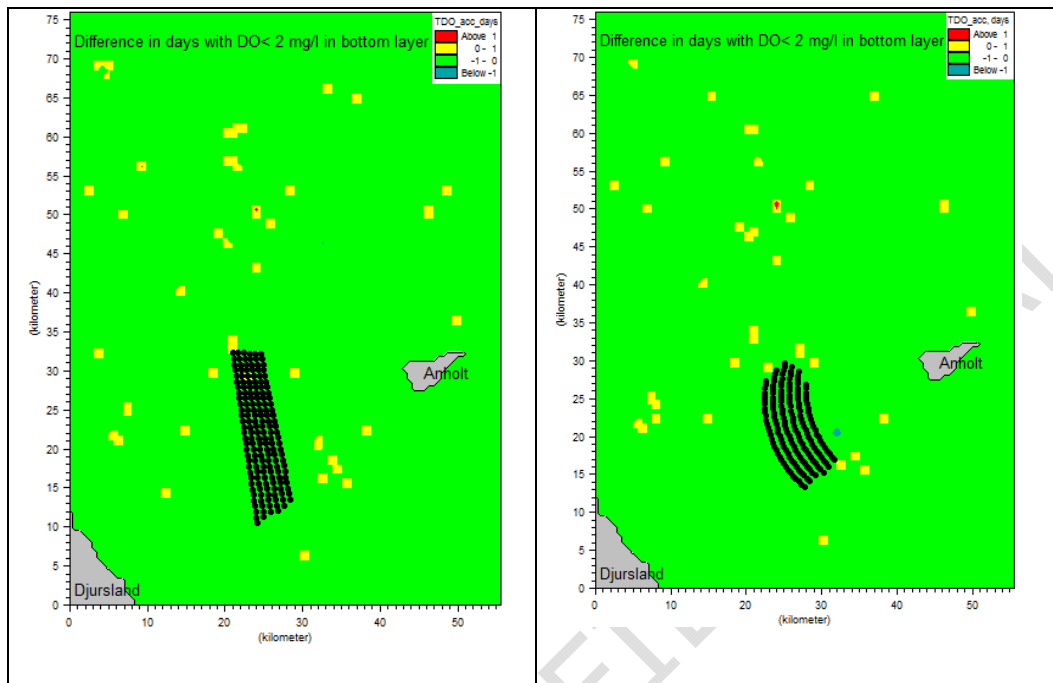
Figure 3-131   Difference in accumulated time with DO<2 mg/l between reference condition
and two scenarios of operating wind mill farms. Model results.

3.3.5.3   Conclusions regarding influence on water quality during the operational phase

The permanent influence on water quality of two different wind farm designs established between Anholt and Djursland was evaluated using a coupled hydrodynamic-water quality model. The main conclusions were:

- Changes in yearly plankton primary production occurred over a rather large area north, east and west of the wind farm but at the maximum the changes did not exceed 0.5% compared to baseline conditions. Averaged over the entire modelled area increases and decreases outbalanced each other, and the overall change was less than 0.03% compared to baseline conditions.

- Changes in yearly sedimentation of organic carbon originating from primary production and the subsequent mineralisation in sediment were most prominent north and east of the wind farm area as a result of prevailing northbound currents. Reductions in carbon sedimentation close to the wind farm area probably were a result of plankton filtration and mineralisation by mussels population the wind mill foundations. Changes were very small and not exceeding 0.3% at any location within the modelled area compared to baseline and, the overall reductions in sedimentation and mineralisation were less than 0.06% compared to baseline conditions.

- Duration of oxygen deficiency in bottom water was hardly effected by the wind farms. At most, in areas affected by prolonged oxygen deficiency under baseline conditions the critical periods with low oxygen concentration was extended by up to 3 days, but in other areas periods with oxygen deficiency was shortened.

The two wind farm designs did show spatial differences in water quality changes but averaged over the entire model area the changes very small and hardly significant. Hence, based on water quality predictions one farm design cannot be considered better than the other design.

Table 3-45   Summary of impacts on water quality during the operational phase

Impact	Intensity of effect	Scale/geograp-hical extent of effect	Duration of effect	Overall signifi-cance of im-pact
Pelagic primary production	Minor	Regional	Long-tern	Minor
Organic carbon sedimentation and mineralisation	Minor	Regional	Long-term	Minor
Near bed oxygen conditions	Minor	Local	Long-term	Minor

3.3.5.4 Impacts on water quality conditions during the construction phase

Dredging activities including the sediment spill and resuspension of sediment in-variably will affect the light availability for phytoplankton and benthic vegetation due to shading from particles with potential effects on primary production. Also mobilisa-tion of inorganic nutrients and reduced substances in sediment pore water may lead to reductions in oxygen concentrations in the water column and increased nutrient availability for plankton algae. Unfortunately, detailed information on depth distribu-tion of sediment characteristics is not available but based on the characteristics of surface sediment, i.e. a low organic content, low percentage of fines etc. (see Sec-tion 6.3) the availability of nutrients and reduced substances such as H_2S in sedi-ments probably are low. Therefore, only the shading effect from sediment spill is considered and as benthic vegetation in the area is rather sparse /8/ only phyto-plankton production will be affected and discussed.

Extinction of light in the water column depends on concentration, nature and size distribution of suspended material, chlorophyll (in phytoplankton), dissolved organic matter and water itself. Extinction is primarily related to two processes, absorption of light (in chlorophyll and organic matter) and light scattering that relates to total surface area of particles. The equation for light extinction coefficient Kd was adapted from Kirk (/40/):

$$Kd=((13.8*Chla+0.015*SS_{20}+0.141)^2+0.265*(13.8*Chla+0.015* SS_{20}$$
$$+0.141)*28.76*Chla^{0.6}+0.03*SS_{20})^{0.5}$$

where 13.8 and 0.015 are specific absorption factors for Chla and suspended solids, respectively, 0.141 is the "background" extinction of water and dissolved organic matter, 0.03 is the specific light-scattering coefficient for 20µm particles and SS_{20} is the concentration of suspended sediment with a equivalent spherical diameter of 20 µm (which was assumed in the spill scenarios, see Section 6.3). The equation is used for calculation of changes in light availability for phytoplankton for the two dredging scenarios defined and reported in Section 6.3, using the predicted additional concentration of light reducing agents in the water column.
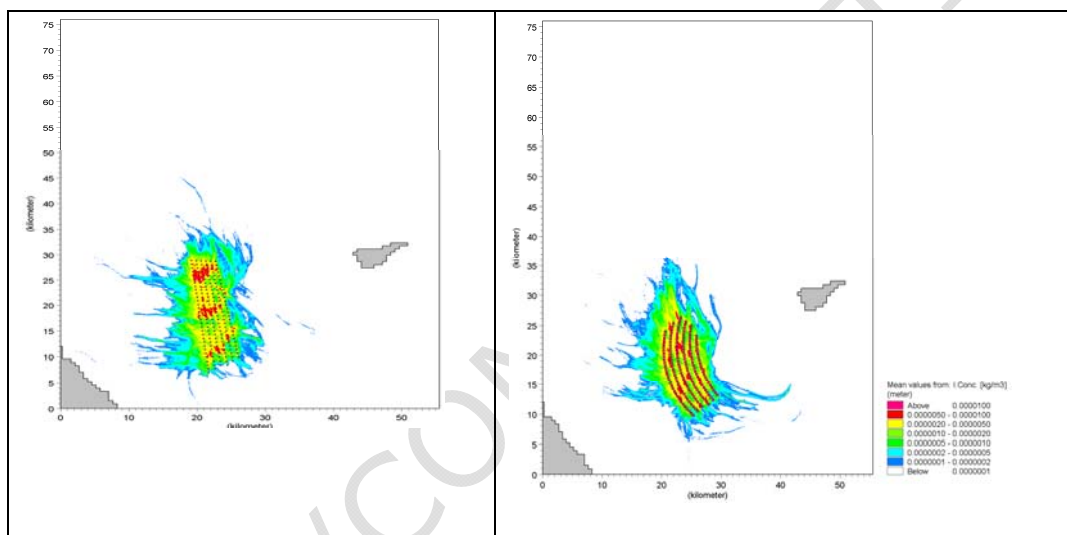
Figure 3-132   Average concentration of suspended solids resulting from dredging operations related to two different wind farm scenarios. Model results.

Concentration of fine sediment (20 µm particle size) averaged over the water column and over the entire dredging period for the two wind farm scenarios was very low attaining a maximum of 0.00001 kg/m^3 in small scattered areas within the wind farm parks (Figure 3-132). Accordingly, the calculated reduction in light availability for phytoplankton in the photic zone (0-12 m water column) compared to baseline was very low ranging 0.6 and 1.2% inside the wind parks.

The predicted reduction in light availability will constitute an upper limit for reductions in primary production because nutrient availability will be more important in limiting the production than light during late spring through summer, when inorganic nutrient concentrations are low (see Figure 3-133). Hence, at the maximum a reduction in primary production much below 1% within the wind park is expected during the dredging operations and no reduction outside the wind park due to shading from spilled sediment.
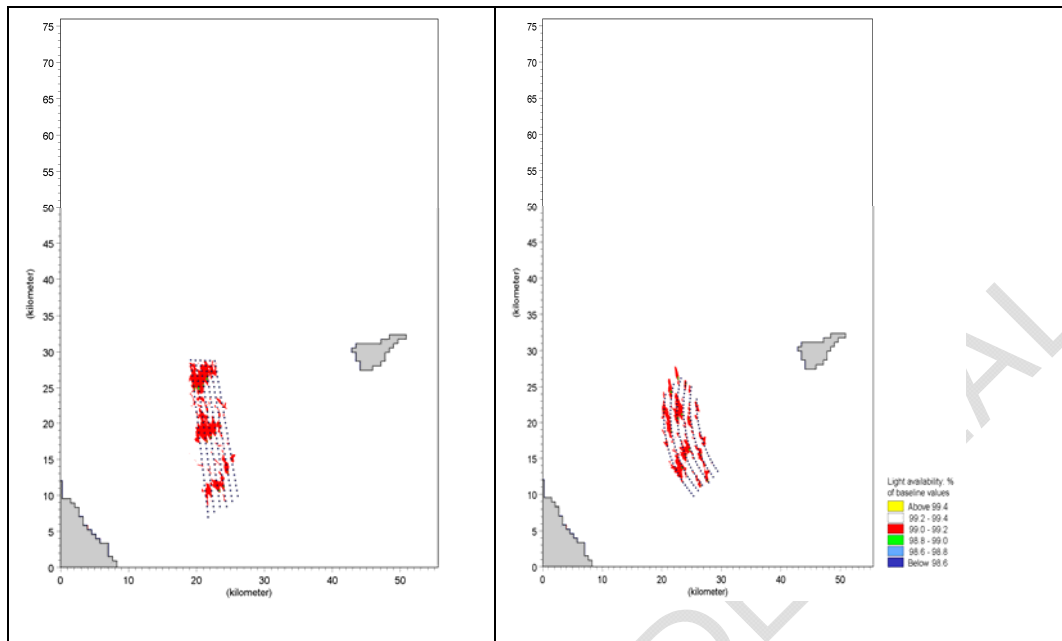
Figure 3-133   Average light availability in surface mixed layer (0-12 m) during dredging operation for two different wind farm scenarios. Calculations based on daily light availability values averaged over the productive period (mid February through November). Percentage of light availability during baseline shown. Model results.

3.3.5.5   Conclusions regarding influence on water quality during the construction phase

The temporal influence on water quality during construction of two different wind farm designs was evaluated based on predicted sediment spread during dredging operations. Influences related to release of nutrients and reduced substances during dredging could not be evaluated in detail because relevant information from the sites to be dredged was not available. The main conclusion was:

- Reduction in light availability caused by shading from sediment spread was very low and confined to the wind park areas. Reduction in phytoplankton production will be very low averaging less than 0.5% inside the wind parks while no reductions are expected outside the wind parks. Benthic vegetation is very sparse in the area and accordingly shading effects are not relevant. Overall, the effect of suspended solids on water quality will be negligible.

Table 3-46   Summary of impacts on water quality during the construction phase

Impact	Intensity of effect	Scale/geographical extent of effect	Duration of effect	Overall significance of impact
Light shading and pelagic primary production	Minor	Local	Short term	Minor

3.3.6 Coastline stability of shorelines at Anholt and Djursland

Impacts on the wind conditions and/or wave conditions at locations in the near-shore areas of Anholt and Djursland can induce changes in the coastline stability.

3.3.6.1 Method for impact assessment

Results from the impact assessment of wave conditions are combined with the information of the shorelines gathered as part of the baseline assessment to form an evaluation of possible changes to the coastal area due to the wind mill farm.

Table 3-47 Sources of impact and potential impacts on the coastlines of Anholt and Djursland

Project Activity	Sources of Potential impact	Potential environmental impact
Operational phase		Environmental impact parameter affected /target of impact
Structures (foundations and piles)	Modifications to the wave field near the shorelines of Anholt and Djursland	Modifications to the natural erosion or accretion along the shorelines of Anholt and Djursland

3.3.6.2 Anholt

The main paths of transport were shown in Figure 3-62. The system is robust in the sense that the transport directions and the areas of erosion and accretion are well defined. Small changes in the near-shore wave conditions are therefore expected to cause correspondingly small changes in the transport intensity. A modest change in the wave conditions will therefore not induce a totally different situation.

In relation to the assessment of impact from the wind turbine park, the coastal sections exposed to waves coming from the park are of most importance. The most directly exposed coast is the west coast (Vesterstrand), from where the path of transport continues from the erosive part of the south coast (Sønderstrand) and further along the gently curved coast (Pakhusbugt) facing towards southeast to end at the spit Totten. The eroding coast to the east of the harbour is less directly exposed to waves from the wind turbine farm, but should also be considered.

The changes in the wave climate at the coasts of Anholt will be small. The most direct effect is expected to be on the south- and southwest-going transport along the eroding southern part of the west coast, which will be reduced slightly. This will cause a very small reduction in the erosional pressure on this coast and a corresponding reduction in the amount of sediment transferred to the coast further east (towards Pakhusbugten).

The effects are expected to be very small in particular because the waves have to pass over a wide (approximately 1 km) shallow area (water depths about 2 m) be-

fore reaching the coast. This shallow area, which possibly is the result of abrasion after thousands of years of coastal erosion, controls to a high degree the height of incoming waves during severe conditions. It may be noted that this may cause the coast to be more sensitive to variations in the water level than to changes in the wave climate.

The erosion of the coast east of the harbour is an ongoing natural process; it has been intensified by the construction of the harbour and possibly also by more recent extraction of aggregates from Nordvestrevet. The slight reduction in the incoming waves from south-westerly and westerly direction may tend to reduce the erosion, but is not expected to have any noticeable effect.

3.3.6.3 Djursland
The impact of the wind mill farm on the coastline of Djursland will be in the form of a change in the incoming wave climate. The wind mill farm will cause a very small reduction in the height of waves coming in from north-east. The coast is at present rather far in the process of reduction (in Danish: udligningskyst) where promontories are slowly eroding and the eroded material contributes to accretion of the coastline in the bays in between.

The wind mill farm is expected to cause a very small reduction in this natural process. In addition the transport at Grenaa, which is supposed to be directed northward can be reduced slightly.

3.3.6.4 Conclusions regarding impacts on the shorelines of Anholt and Djursland during the operational phase
The changes in the wave climate at the coasts of Anholt will be minor.

The slight reduction in the incoming waves from south-westerly and westerly direction may tend to reduce the erosion along Vesterstrand and Sønderstrand, but is not expected to have any noticeable effect. A corresponding weak reduction in the amount of sediment transferred to the coast further east towards Pakhusbugten may be caused by the wind farm.

The erosion of the coast east of the harbour is an ongoing natural process and small changes to the wave field are not expected to have any noticeable effect

The natural processes active on the coastline of Djursland will continue and the change in the wave climate will be so small that no effects will be noticeable even over a long time scale.

Table 3-48   Summary of impacts on the shorelines at Anholt and Djursland during the op-
              erational phase

Impact	Intensity of effect	Scale/geograp-hical extent of effect	Duration of effect	Overall signifi-cance of impact
Modifications to the natural ero-sion/accretion along the shoreline of An-holt	Minor	Local	Long-term	Minor
Modifications to the natural ero-sion/accretion along the shoreline of Djursland	No	Local	Long-term	No

3.3.7   Influence on sea bed morphology

3.3.7.1   Method for impact assessment

The impact from the wind mill farm on the wave- and current conditions in the area
will modify the sediment transport conditions. The effect is assessed on the basis of
the simulated wave- and current conditions and the simple estimates made for the
sediment transport rate in the area.

Table 3-49   Sources of impact and potential impacts on the current and stratification

Project Activity	Sources of Potential im-pact	Potential environmental impact
Operational phase		Environmental impact parameter affected /target of impact
Structures (foundations and piles)	Modifications to the current and wave field in the wind farm area	Modifications to the sea bed

3.3.7.2   Impacts during the operational phase

The wind mill farm will cause slight changes in the wave and current fields in and
around the farm. The sediment transport will change correspondingly. The change in
sediment transport will be associated with bed changes corresponding to the gradi-
ents in the transport.

3.3.7.3   Conclusions regarding impacts on the sea bed morphology during the operational
phase

The annual sediment transport at the sea bed in the area of interest is small – only
up to a few cubic metres per year over a width of one metre. The changes in the

waves and the current are so small and happen gradually over so large areas that no bed level change are foreseen to happen as the result of the wind farm.

It should be noted that this conclusion pertains to the general bed level in the wind farm area. Within a distance of a few diameters from the wind turbine foundations, each wind mill may cause scour associated with considerable bed level change.

Table 3-50   Summary of impacts on the geomorphology during the operational phase

Impact	Intensity of effect	Scale/geograp-hical extent of effect	Duration of effect	Overall signifi-cance of im-pact
Modifications to the annual sediment transport and bed levels	No	-	-	No

3.3.8   Risk of scour

3.3.8.1   Method for impact assessment

The impact from the wind mill farm on the wave- and current conditions in the area will modify the sediment transport conditions. The effect is assessed on the basis of the simulated wave- and current conditions and the simple estimates made for the sediment transport rate in the area. The assessment of scour is carried out given that no measures are taken against scour around the foundations.

3.3.8.2   Impacts during the operational phase

A vertical cylindrical structure will modify the flow and the sediment transport in its vicinity, which can lead to the formation of a scour hole around it. The water motions induced by currents and waves will be affected through a number of mechanisms, which can increase the sediment transport near the cylinder and carry sediment away from the structure, c.f. Figure 3-73 (/37/ and /41/).

- The blocking effect of the structure will increase the flow velocities next to the structure.

- In a current the stagnation at the front of the structure will cause flow sepa-ration and a vortex is formed which curves around the structure near the bed like a horse shoe with a leg at each side of the cylinder and the opening fac-ing downstream. The horse shoe vortex is important for the scour process because it causes a significant increase in the local bed shear stress and a near bed flow away from the cylinder. Depending on the length of the stroke of the near bed orbital motion relative to the cylinder size (quantified through the KC-number: $2\pi a/D$, where a is the amplitude of the near bed or-bital and D is the diameter of the cylinder) a horse shoe vortex can also be formed under waves, but its dimensions are limited by the small thickness of the wave boundary layer.

- The cylinder can cause an increased turbulence level, which increases the local sediment transport capacity.

- For a large cylinder with a diameter of more than 20% of the wave length of the water waves diffraction of the wave around the cylinder may be of significance. For very large cylinders the scour induced by waves alone is often relatively weak, and weak circulation currents (streaming) driven by the non-uniform boundary layer formed along the perimeter of the cylinder can be dominant in the scour process.

The purpose of this discussion is not to predict the actual scour conditions, but to give an indication of the potential problem and its significance. The largest scour holes are found under pure current conditions with rather weak sediment transport at the undisturbed bed away from the cylinder. The depth of the hole will be of the order one times the cylinder diameter. The extension of the hole is determined by the angle of repose at the sides of the cylinder and upstream of it, while the slope of the hole is less on the downstream side. The scour hole thus typically extends 2-4 times the diameter away from the structure.

As outlined, the actual scour may be restricted compared to the conditions outlined above. For small water depths the scour hole will be smaller; for a depth comparable to the diameter of the cylinder it will be reduced to approximately half of the deep water scour. If waves are dominant the scour depth will also be reduced compared to the pure current conditions.

The developing scour may be arrested when encountering a more erosion resistant layer, for example consisting of coarser material or consolidated cohesive sediment. The design of a structure can also reduce the scour hole. For example, if a gravity foundation is buried except for a vertical shaft scour can occur around the shaft, but its development is limited by the hard surface of the buried foundation. However, if the scour around the shaft extends to the edge of the underlying foundation or if it becomes exposed for other reasons the scour will occur around the foundation and will be determined by other length scales than the shaft diameter.

In conclusion the scour hole can be expected to have a depth up to approximately one diameter, but it will probably be reduced due to a number of factors as outlined. The scour process is dynamic. Under the varying forcing conditions the scour hole will always tend to evolve towards equilibrium determined by the actual conditions. The rate of change cannot be assessed on the available knowledge, but apart from the initial formation of a scour hole, the variation in time may not be significant.

In most cases offshore wind mills are protected against scour. A typical scour protection consists of a layer of stones which are coarse enough to remain stable under the waves and current even under the increased forcing in the vicinity of the structure. The stone cover extends approximately two cylinder diameters from the structure. Due to the increased roughness of the stone cover some limited scour may in turn

occur at its edge. This scour will scale by the stone size or the layer thickness and may be countered by increasing the layer of stones near the edge to allow the fall of stones into the scour hole without compromising the safety of the protection (sacrificial protection).

3.3.8.3 **Conclusions related to the risk of scour**
Scour protection is recommended to be considered for the Anholt Offshore Wind Farm. The bed is mobile and without protection the scour process in the vicinity of the foundations – monopile of gravity base - will tend to evolve towards an equilibrium scour hole with a depth up to approximately one diameter of the monopile/gravity base.

Table 3-51   Summary of impacts of scour during the operational phase in case of no scour protection

Impact	Intensity of effect	Scale/geograp-hical extent of effect	Duration of effect	Overall signifi-cance of im-pact
Risk of scour around the founda-tions	Medium /Large	Local	Long-term	Moderate /Significant

3.4   Mitigation measures
In the design phase it is recommended to take the risk of scour around the foundations into account. Mitigating measures such as scour protection should be considered, typical as a layer of stones around the foundations.

3.5   Cumulative effects
There are no expected cumulative effects of Anholt Offshore Wind Farm and other 3rd part projects on the issues covered by this report. The impacts are in general very small and local and do not interact with other known projects.

3.6   Decommissioning
3.6.1   Backfilling of holes left in the sea bed
During the decommissioning phase of a wind farm one option is to completely remove all man-made structures. This may leave holes in the sea-bed left for natural backfilling. Regarding the Anholt Offshore Wind Farm, however, it is intended that the structures and substructures will be removed to the natural seabed level /1/.

This means that independently of the type of foundation of the wind mills (monopile or concrete gravity base), there will not be any holes left in the sea bed due to the removal of the wind farm. Estimation of the natural backfilling rates is therefore not relevant in this study.

3.7   Technical deficiencies or lack of knowledge
The main part of the work described in this report is based on numerical modelling. The modelling was to a large extent drawing on data input and model setup from existing and well calibrated models, which are found trust-worthy for the analyses carried out for this study.

The time schedule for the sediment spreading calculations did not allow awaiting the final analyses of the geotechnical investigations. The sediment spreading calculations were therefore based on:

1. assumptions by Rambøll (personal communication) with regard to the volumes required to be removed at each gravity base to reach a level where undisturbed soil is encountered (/1/) and

2. assumptions with regard to the physical characteristics of the spilled material.

Considering the relatively small volumes being dredged in total and the very small concentration and sedimentation rates obtained, the assumptions regarding 2. are evaluated as being sufficient and not influencing the overall quality of the assessment.

If the assumptions regarding 1. change significantly, it should be considered to revise the assessment.

3.8 Conclusions concerning Anholt Offshore Wind Farm

An Environmental Impact Assessment related to the planned wind farm between Anholt and Djursland has been carried out. The impact assessment comprises issues related to the hydrographic conditions (currents, stratifications, waves), water quality, geomorphology and coastal morphology and assessment of sediment spreading due to dredging activities.

Two worst case scenarios were selected for the analyses within the framework of the project description. Both of these were for 2.3 MW wind turbines on gravity base foundations. Two layouts were tested – one with the wind turbines in linear rows and one with the wind turbines in arcs.

The two layouts showed very small differences in the impacts for all issues covered by the present report. This leads to the conclusion that the park design with regard to the layout of the wind turbines within the designated area for Anholt Offshore Wind Farm, is not critical for the impacts described in the present work.

Only minor modifications to the hydrographic conditions are expected. The additional flow resistance caused by the wind farm implies a reduction in the current speeds in the area of the wind farm of less than 2% and very small increases in the current speed around the wind farm due to flow diversion. A small increase in the turbulence level near the foundations causes the stratification to be slightly weakened locally downstream from the individual wind turbines.

Wave heights will be reduced by up to 3% in the wind farm area. Near the shorelines of Anholt and Djursland the effect has been reduced to about 1-2%. The impacts on the relevant coasts will consequently be very small and not noticeable.

The sea bed was found to consist of non-cohesive sediments, mostly sand. Within the project area sediments in the south are coarser (sand with pebbles and stones) than in the north (sand/silt). Estimations of annual sediment transport rates on the sea bed are in the order of a few cubic metres over a width of one metre of the sea-bed. The sea bed is hence considered quite stable and no changes to the sea bed are expected on a regional scale.

Very locally around each foundation, scour are expected with scour holes reaching a depth in the order of one diameter, if left unprotected. It is recommended to con-sider scour in the design of the wind farm.

From analysis of sedimentation and spreading of sedimentation during dredging ac-tivities it was concluded that depth-averaged concentrations of suspended sediment will exceed 2 mg/l only in short periods (hours or days) and never exceed 10 mg/l. Sedimentation rates less than 1 mm are expected due to the dredging activities.

The impacts and their significance are summarized in Table 3-52.

Table 3-52   Summary of impacts from the Anholt Offshore Wind Farm. Note that conclusions are

Impacts	Overall signifi-cance of impact	Quality of available data
IMPACTS ON THE HYDROGRAPHIC CONDI-TIONS		
Current pattern and velocities	Minor	3
Stratification and mixing of water column	Minor	2
Dampening of wave heights	Minor	2
SEDIMENT SPREADING AND SEDIMENTATION DUE TO EARTHWORKS		
Increased concentrations in water column	Minor	3
Sedimentation	Minor	3
IMPACTS ON WATER QUALITY		
Pelagic primary production	Minor	3
Organic carbon sedimentation and mineralisation	Minor	3
Near bed oxygen conditions	Minor	3
Light shading and pelagic primary production during construction period	Minor	3
IMPACT ON ADJACENT COASTLINES		
Modifications to shorelines and coastal morphology of Anholt	Minor	2
Modifications to shorelines and coastal morphology of Djursland	No	3
IMPACT ON GEOMORPHOLOGY		
Changes to sediment transport rates and sea bed level	No	2
RISK OF SCOUR		

Risk of scour around foundations	moderate/significant	2

Tabel 3-1 Principles for the EIA evaluation of potential impact, the significance rating of the assessed impact and the quality of data/documentation

Quality of availably data

In order to evaluate the quality and significance of data and documentation for the impact assessment a significance rating of data and documentation should be evaluated within the specific technical subject topics using the following categories:

- 1 – Limited (scattered data, some knowledge)

- 2 – Sufficient (scattered data, field studies, documented)

- 3 – Good (time series, field studies, well documented)

For the EIA-document an impact arising from a planned activity will, depending on its magnitude and the environmental sensitivity, be given a significance rating as follows:

: No impact	*No impact*: There will be no impact on structure or function in the affected area;
: Minor impact	*Minor impact*: The structure or functions in the area will be partially affected, but there will be no impacts outside the affected area;
: Moderate Impact	*Moderate Impact*: The structure or function in the area will change, but there will be no significant impacts outside the affected area;
: Significant impact	*Significant impact*: The structure or function in the area will change, and the impact will have effects outside the area as well;

4. Transformer platform and offshore cable

DHI has for Energinet.dk carried out the environmental impact assessment related to the substation and the offshore cable on the issues of water quality conditions, sediment spreading due to dredging activities, coastal morphology at the landfall point and risk of cable exposure. This work is described below.

The work is divided in two main sections. The first part is related to describing the existing conditions at the site, the so called baseline conditions. This part includes establishing also the hydrographic conditions since the water quality conditions depend heavily on this. The hydrographic conditions also form the basis for the analysis of spreading of sediment related to the dredging activities in the construction period, as well as to the evaluation of the risk of cable exposure. The risk of cable exposure is related to the sea bed mobility. Estimates of sea bed mobility in the area of the cable trace are therefore included in the description of the baseline conditions.

DHI has also carried out the environmental impact assessment related to: birds /6/, benthic fauna /7/, benthic habitats /8/ and (in collaboration with Rambøll) marine mammals /9/. DHI furthermore provides metocean data for design and operational conditions /10/.

4.1 Project description

This chapter describes the technical aspects of the Anholt Offshore Wind Farm. For a full project description reference is made to /1/. The following description is based on expected conditions for the technical project; however, the detailed design will not be done until a developer of the Anholt Offshore Wind Farm has been awarded.

An offshore transformer platform will be established to bundle the electricity produced at the wind farm and to convert the voltage from 33 kilovolts to a transmission voltage of 220 kilovolts, so that the electric power generated at the wind farm can be supplied to the Danish national grid.

4.1.1 Transformer platform

Energinet.dk will build and own the transformer platform and the high voltage cable which runs from the transformer platform to the shore and further on to the existing substation Trige, where it is connected to the existing transmission network via 220/440 kV transformer.

The transformer platform will be placed on a location with a sea depth of 12-14 metres. The length of the export cable from the transformer station to the shore of Djursland will be approximately 25 km. On the platform the equipment is placed inside a building. In the building there will be a cable deck, two decks for technical equipment and facilities for emergency residence.

The platform will have a design basis of up to 60 by 60 metres. The top of the platform will be up to 25 metres above sea level. The foundation for the platform will be a floating caisson, concrete gravitation base or a steel jacket.

4.1.2 Subsea Cabling

The wind turbines will be connected by 33 kV submarine cables, so-called inter-array cables. The inter-array cables will connect the wind turbines in groups to the transformer platform. There will be up to 20 cable connections from the platform to the wind turbines. From the transformer platform a 220 kV export cable is laid to the shore at Saltbæk north of Grenå. The cables will be PEX insulated or similar with armouring.

The installation of the cables will be carried out by a specialist cable lay vessel that will manoeuvre either by use of a four or eight point moving system or an either fully or assisted DP (Dynamically Positioned) operation.

All the subsea cables will be buried in order to provide protection from fishing activity, dragging of anchors etc. A burial depth of minimum one meter is expected. The final depth of burial will be determined at a later date and will vary depending on more detailed soil condition surveys and the equipment selected.

The cables will be buried either using an underwater cable plough that executes a simultaneous lay and burial technique that mobilises very little sediment; or a Remotely Operated Vehicle (ROV) that utilises high-pressure water jets to fluidise a narrow trench into which the cable is located. The jetted sediments will settle back into the trench.

4.1.3 Onshore components

At sea the submarine cable is laid from a vessel with a large turn table. Close to the coast, where the depth is inadequate for the vessel, floaters are mounted onto the cable and the cable end is pulled onto the shore. The submarine cable is connected to the land cable close to the coast line via a cable joint. Afterwards the cables and the cable joint are buried into the soil and the surface is re-established.

On shore the land cable connection runs from the coast to compensation substation 2-3 km from the coast and further on to the substation Trige near Århus. At the substation Trige a new 220/400 kV transformer, compensation coils and associated switchgear will be installed. The onshore works are not part of the scope of the Environmental Statement for the Anholt Offshore Wind Farm. The onshore works will be assessed in a separate study and are therefore not further discussed in this document.

4.2 Baseline study

The baseline conditions concerning the hydrographic conditions, the water quality conditions and the coastal and the geomorphological conditions in the vicinity of the offshore cable are described below.

The baseline study providing a thorough description of the present conditions at the site has been carried out. The analysis of the baseline conditions is to a large extent based on numerical modelling of hydrographical parameters (currents, waves, salinity, and temperature) as well as water quality parameters and sediment transport rates. Analyses of available data are included.

4.2.1 Bathymetry

The bathymetries in the models are based on available data from bathymetrical measurements by the Danish Naval Authorities (in Danish: 'Farvandsvæsenet') and from digitized sea maps from C-MAP. The bathymetric data is described in larger details in Section 3.2.1.

The interpolated bathymetry applied in the numerical models is shown in Figure 4-1. The offshore cable location is indicated on the same figure. It can be seen that in most of the area of the offshore cable the sea bed is relatively flat and the water depth varies between 15 and 18 m except for very near the coast.
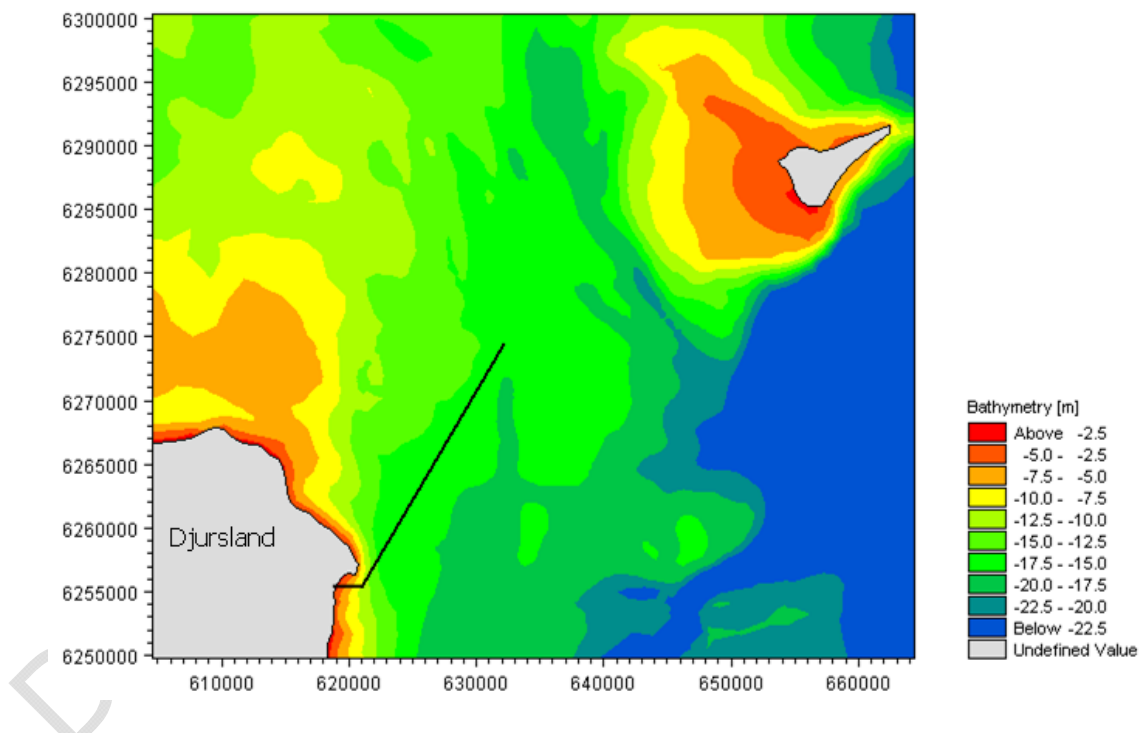
Figure 4-1   Interpolated bathymetry using data as applied in the numerical models for this project. The offshore cable location is indicated by the black curve.

4.2.2 Geology and sea bed sediments

The geology and the sea bed at the surface are described in this section. This provides mainly input to the analysis regarding the sea bed mobility, which is relevant in connection to the risk of cable exposure.

4.2.2.1 **Methods**

The description of the baseline conditions is based on information from the literature and analysis of data collected during the present study on the sea bed sediments.

4.2.2.2 **Data**

A geophysical survey was conducted of the two cable traces by GEUS in April 2009 /11/. The area was surveyed with side scan sonar. From this an image is obtained which can be interpreted to supply information on the geographical distribution of sea bed material which can be found in the area. Diving was used for calibration and verification of the analysis.

4.2.2.3 **Description of geology and sea bed sediments**

The sea bed of Kattegat in the area between Læsø, Djursland and Anholt is very flat with typical water depth between 10 and 20 m. A possible explanation for the very low relief is that melting water deposits discharged into the Yoldia Sea (approximately 15,000 yr b.p.) from the ice sheet lying to the south has covered and smoothed out the contours of the underlying glacial and pre-quaternary deposits. The melting water is supposed to have come through the present mouth of the Randers Fjord and the Great Belt channel.

Figure 4-3 shows the characteristics of the surface sediment along the two cable traces based on side scan surveys. In the selected cable trace (the southernmost), the sea bed nearest the shore is characterized by sandy/silty material until about halfway to the offshore substation and rather mixed with coarser material (sand with pebbles and stones) to be found along the remaining section.
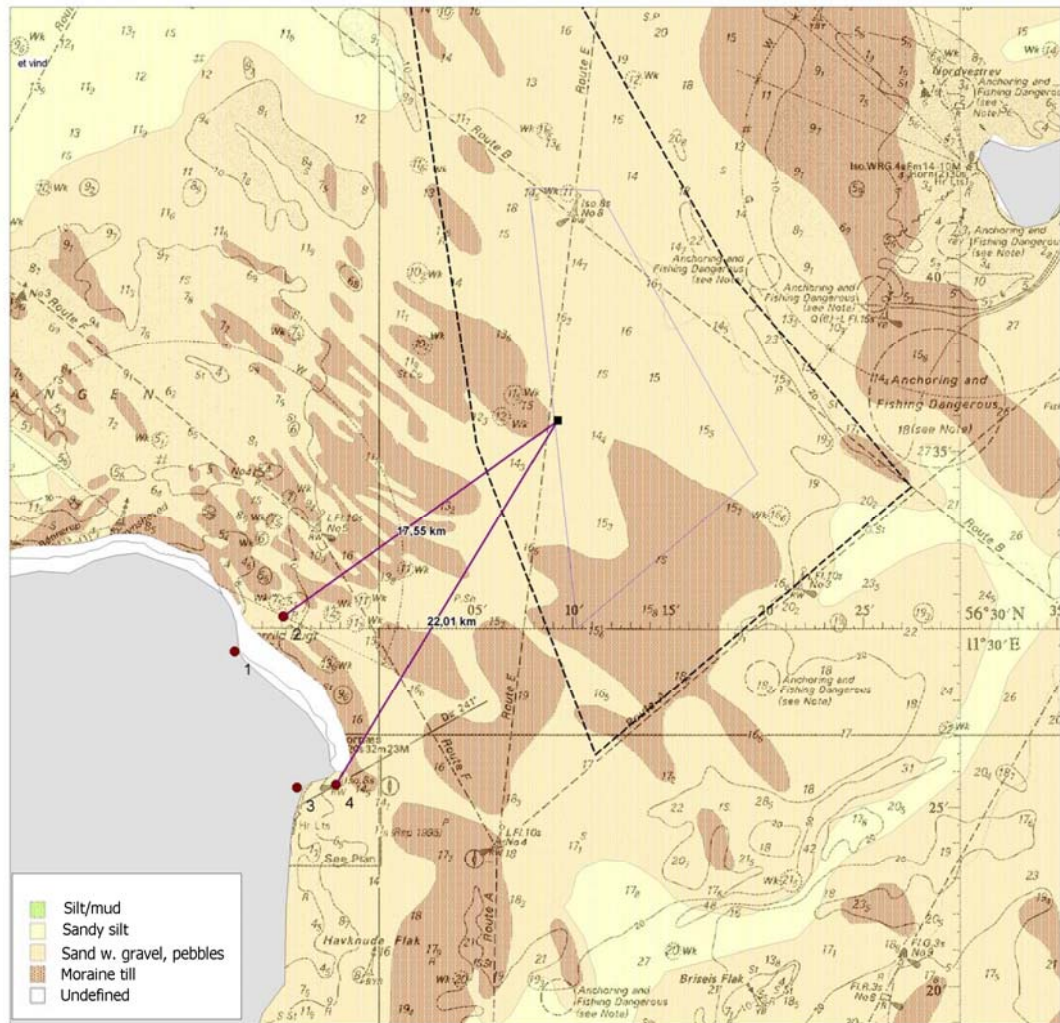
Figure 4-2   Map of sea bed sediment types. Rambøll/GEUS.
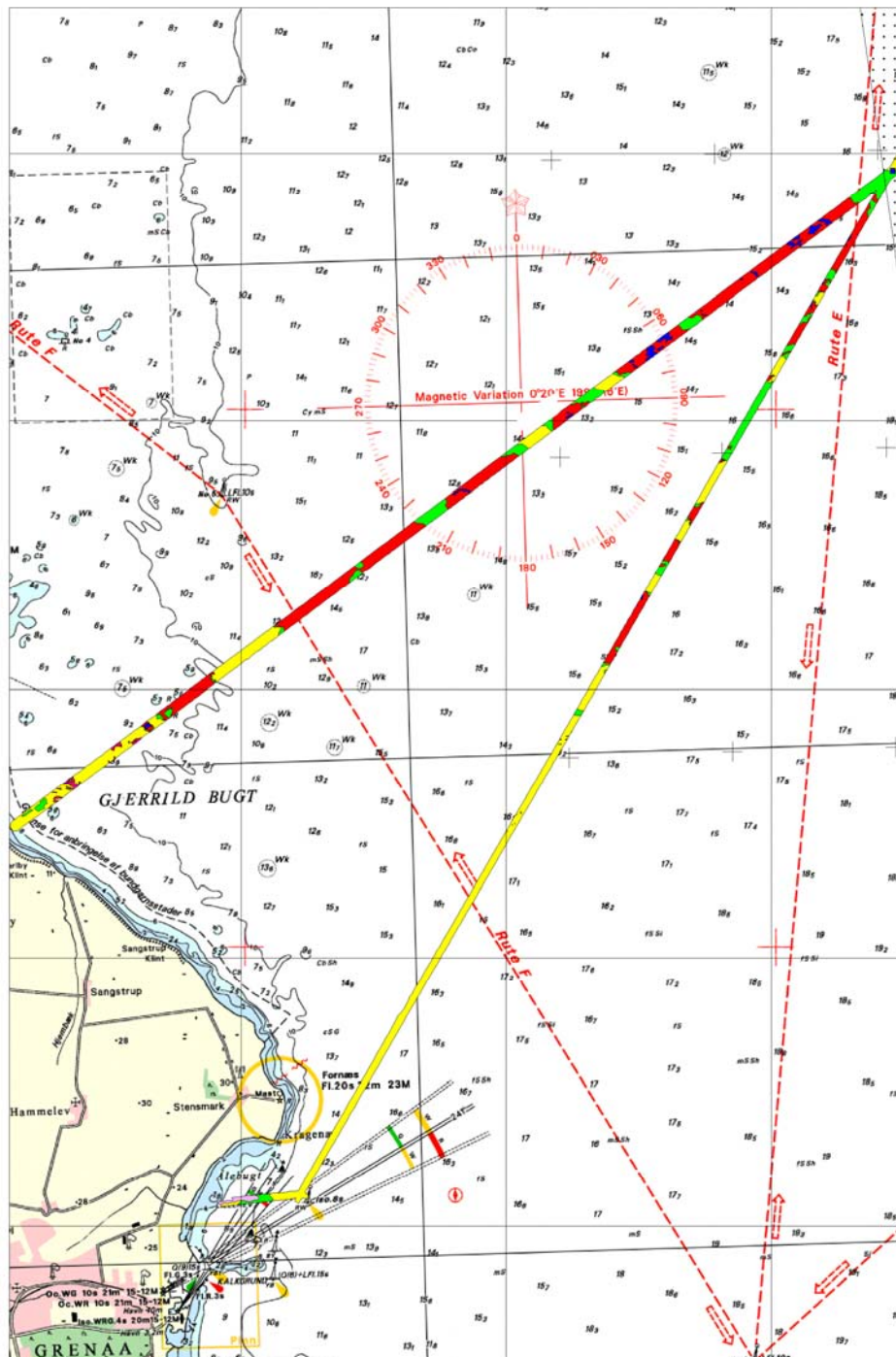
Figure 4-3   Sea bed map along the two cable traces (GEUS). Gravel/pebbles (blue), sand
              and pebbles with boulders with 1-25% boulders (red), mainly sand and pebbles
              with solitary boulders (green), sand and silt (yellow).

The same analysis was carried out in the wind farm area, but here also surface sea bed samples were collected and analysed with respect to grain size and grading coefficient /7/. The fractions finer than sand (d < 63 μm) were found to be insignificant. The coarser materials were having grain sizes of about 0.2-0.7 mm. In some places the sea bed material was relatively homogeneous with a grading coefficient, $\sigma = d_{84}/d_{16,}$ around 1.4, but in some areas especially in the south the sea bed was more inhomogeneous with sea bed material ranging from sand to stones.

Based on this information it is concluded that the bed primarily also along the offshore cable trace is covered by non-cohesive sediments. The mobility and the order of magnitude of the sediment transport rate can be estimated by numerical model calculations.

Due to the small variations in the water depth over the area and the expected small transport rates the seabed is found to be quite stable. Local variations in the bed level in excess of, say 0.1 to 0.2 m, may be associated with the formation and migration of small bed forms like wave or current ripples.

4.2.3 General presentation of existing regional numerical models

The analyses presented in this study are to a large extent based on numerical models. The local models developed for this study of the Anholt Offshore Wind Farm can be considered as 'submodels' of large regional models existing at DHI. The local models are based on input from the large models at the edges of the local models. The qualities of the local models are hence strongly dependent on the regional models. The regional models and the quality of these were described in Section 3.2.3. Details of the model setup are supplied in Appendix A and B along with details of the local models.

4.2.4 Current conditions

The analysis of the current conditions is based on analysis of numerical modelling results for the baseline conditions.

The methodology and models are described in Section 3.2.4. The results for the area of the offshore cable and substation are described below.

4.2.4.1 Annual current conditions for the baseline situation

The area where the offshore cable will be situated is by nature very dynamic with regards to currents. The flow fields show that in periods large eddies are formed in the Kattegat. These eddies may form in all parts of the Kattegat. Especially just south and north of Anholt these eddies are observed. Some of them become almost stationary over longer periods of time. Examples of typical surface flow patterns are seen in Figure 4-4.

Annual depth averaged current roses are shown at 3 points pt1 to pt3 located along the offshore cable on Figure 4-5. It can be seen that the depth averaged current is nearly uniform along the cable and oriented in the NNW-SSE axis mainly towards the NNW. The current magnitude is relatively low, the calculated depth-averaged veloci-

ties reach in 2005 a maximum of 0.5 m/s and exceed in less than 5% of the time 0.3 m/s.
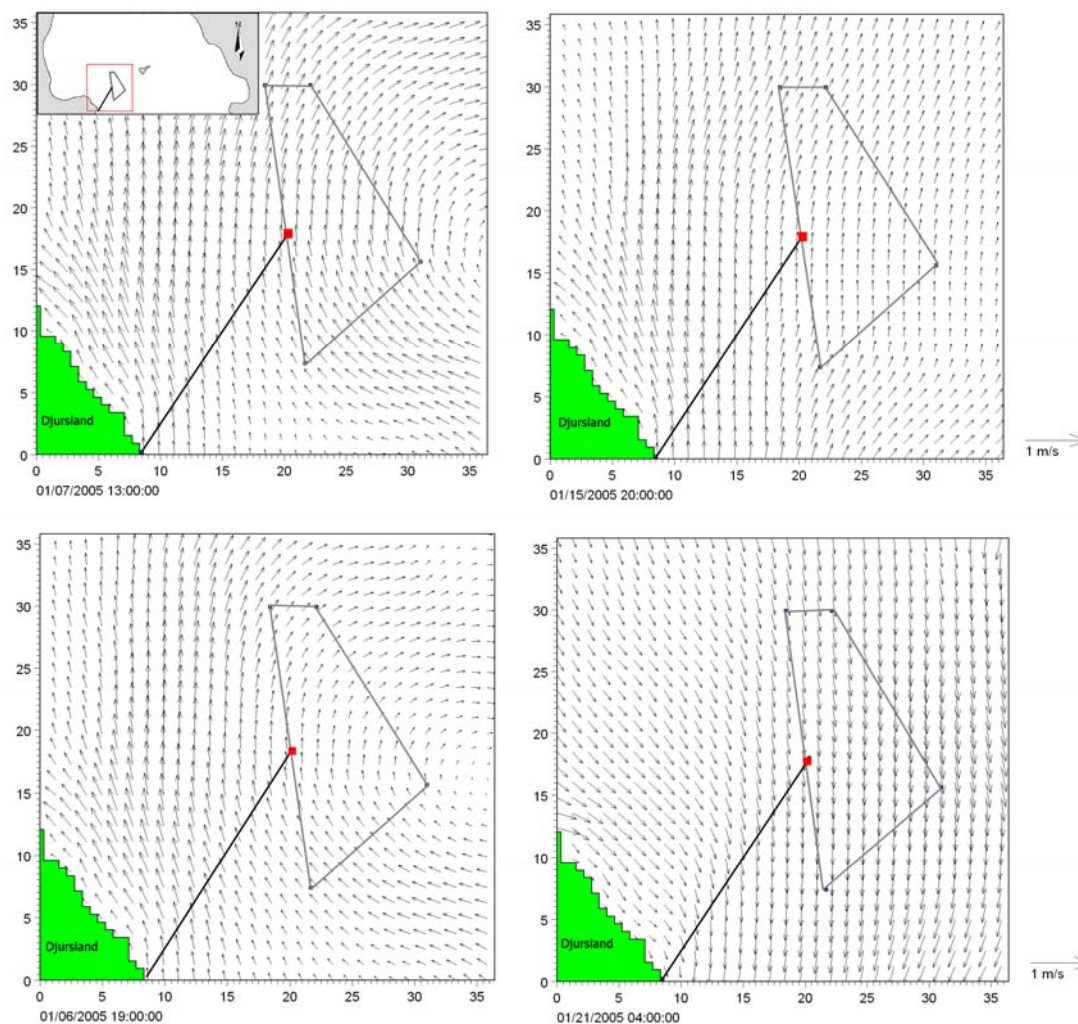
Figure 4-4   A variation of typical surface current patterns from 2005. Results from the local model in the area of interest. The grid spacing is approximately 600 m. The offshore cable is indicated in red.
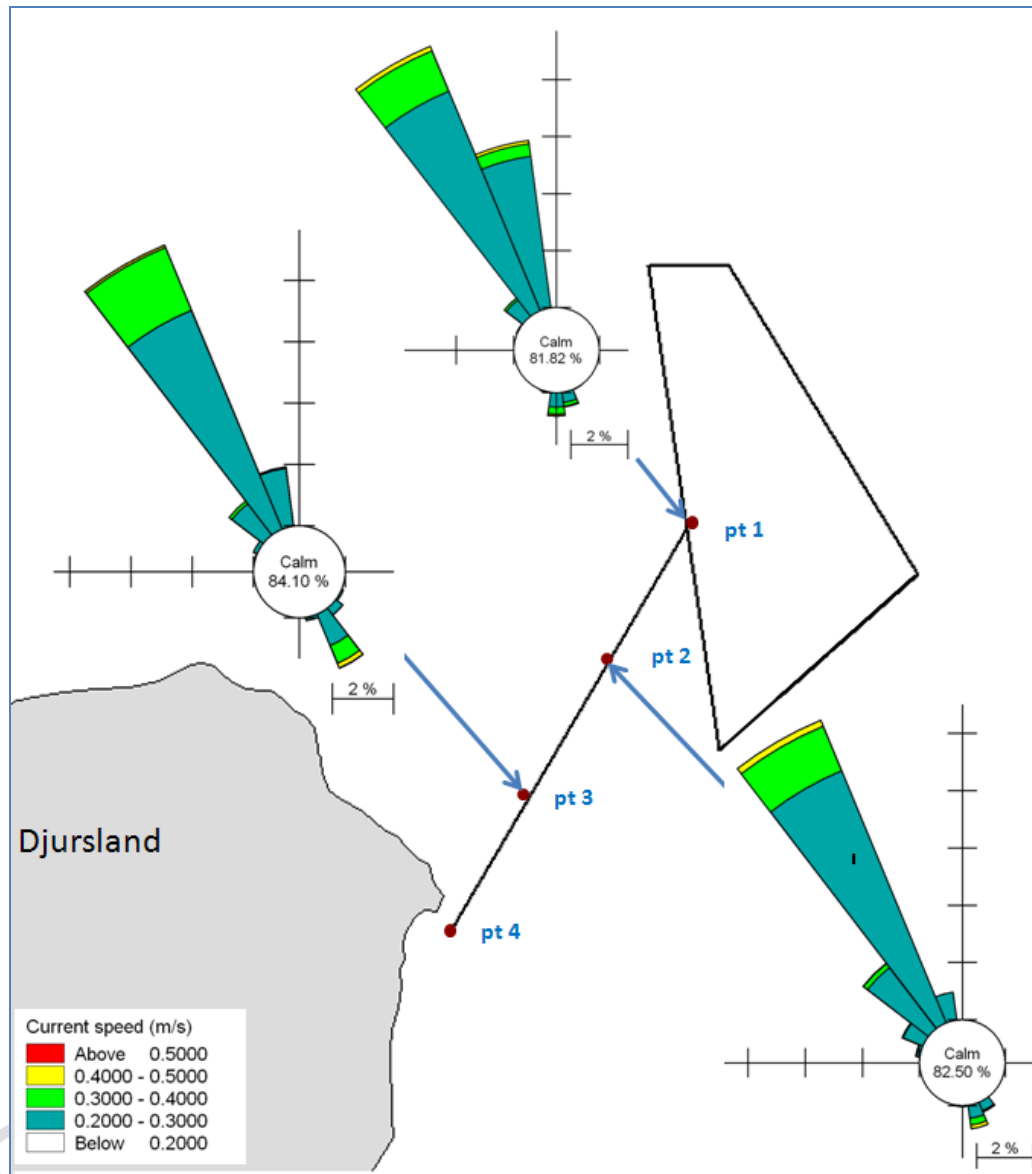
Figure 4-5   Roses representing the annual depth averaged current extracted from the 3D
local current at 3 points along the cable. Directions are defined as 'going to'.

4.2.5   Wave conditions

Annual wave conditions along the offshore cable trace are calculated by numerical models. Results are described below. The applied methodology and setup of numerical models were described in details in Section 3.2.5.

Annual wave conditions
The waves in the project area are wind generated waves. The wind in the period 1998-2007 based on model data from VEJR2 are from directions between south-east and north-west, see wind rose and scatter diagram in Section 3.2.5.

The most common wind directions are from south-west to west. An example of a modelled wave field in the local model from November 2005, where the wind direction in the project area was 236° (south-west) is illustrated in the upper part of Figure 4-6. The figure shows the distribution of wave heights in the local model area. The wave heights are shown as the so-called significant wave height. The significant wave height (trough to crest) is an average of the largest 1/3 of the waves at a given time.

The wind speed at the time shown in the upper part of Figure 4-6 is 13 m/s, which can be characterized as a medium-strong wind speed. From Table 4-1 it can be derived that wind speeds of 13 m/s are exceeded in about 4.5% of the time in an average year, corresponding to about two weeks in total.

The lee effect from Djursland is clearly seen. Along the cable trace, the wave height is limited due to this lee effect as seen when comparing with the wave heights in the area south of Anholt, where the fetch for the waves to grow is larger for this direction.

The strongest wind speeds are from directions between west and north-west (see statistical analysis in Section 3.2.5). Such a situation is shown in the lower part of Figure 4-6. In this situation from December 2005, the wind direction is from WNW in the project area. In this case, Djursland is not restricting the wave heights from this direction at the north-eastern end of the offshore cable. The fetch from the WNW is obviously much longer causing higher waves along the offshore cable.

The influence of the distance to land (fetch) on wave height at different locations along the cable is illustrated in Figure 4-7. The figure shows wave roses at four equidistant locations in the cable alignment. It can be seen that the lee effect from Djursland affect progressively waves from directions between WSW to W along the cable from offshore to onshore. It should be noted that not only the fetch is influencing the wave heights, but also local and regional depth-variations.
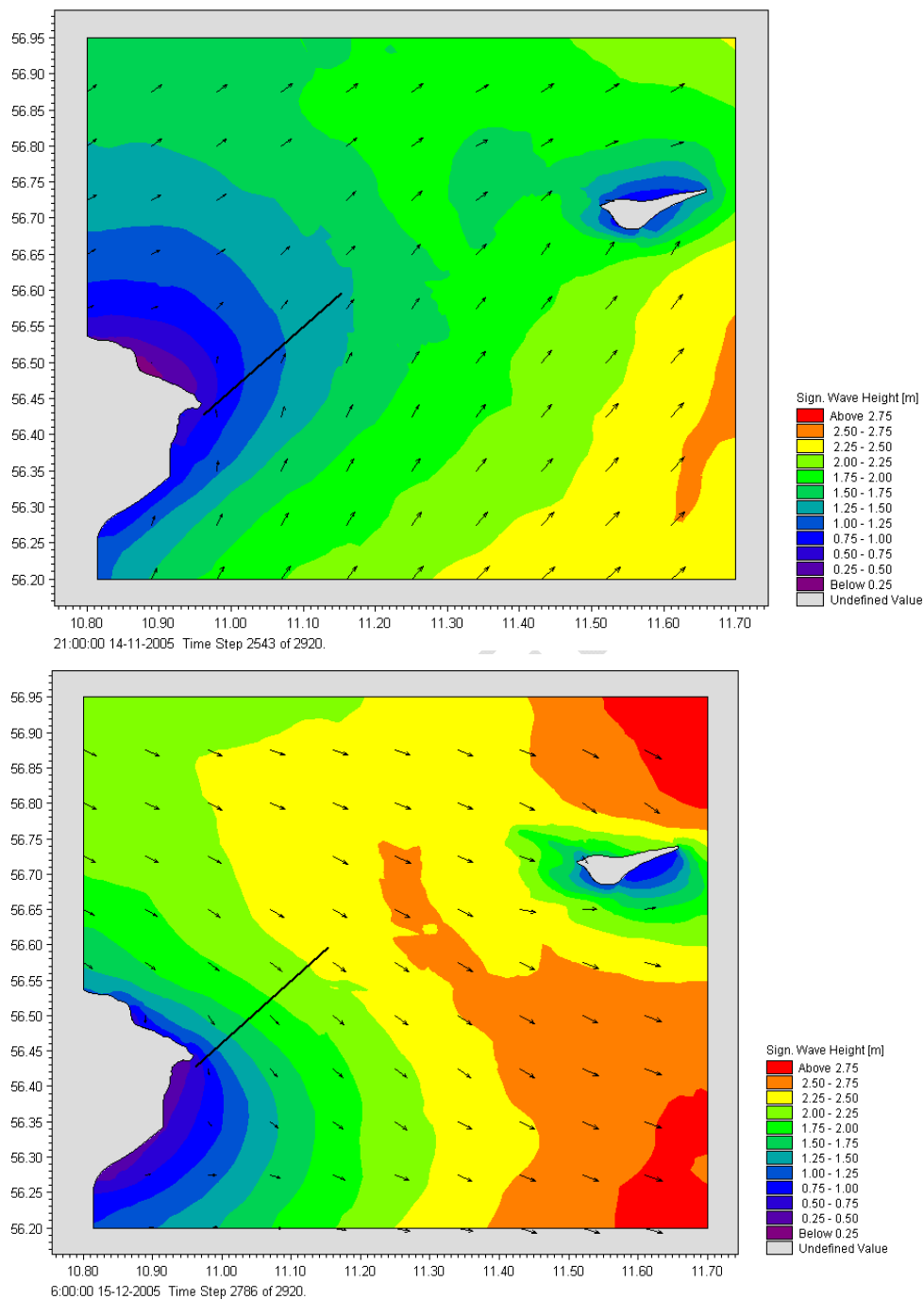
Figure 4-6   Example of wave fields for two characteristic wind directions. Upper figure: example of waves with a wave direction of approx. 202 degr. N at the centre of the cable alignment. Wind speed is 13 m/s and wind direction is 236 degr. Lower figure: example of waves with a wave direction of approx. 336 degr. N at

the centre of the cable alignment. Wind speed is 16m/s and the wind direction is 292 degr. N.
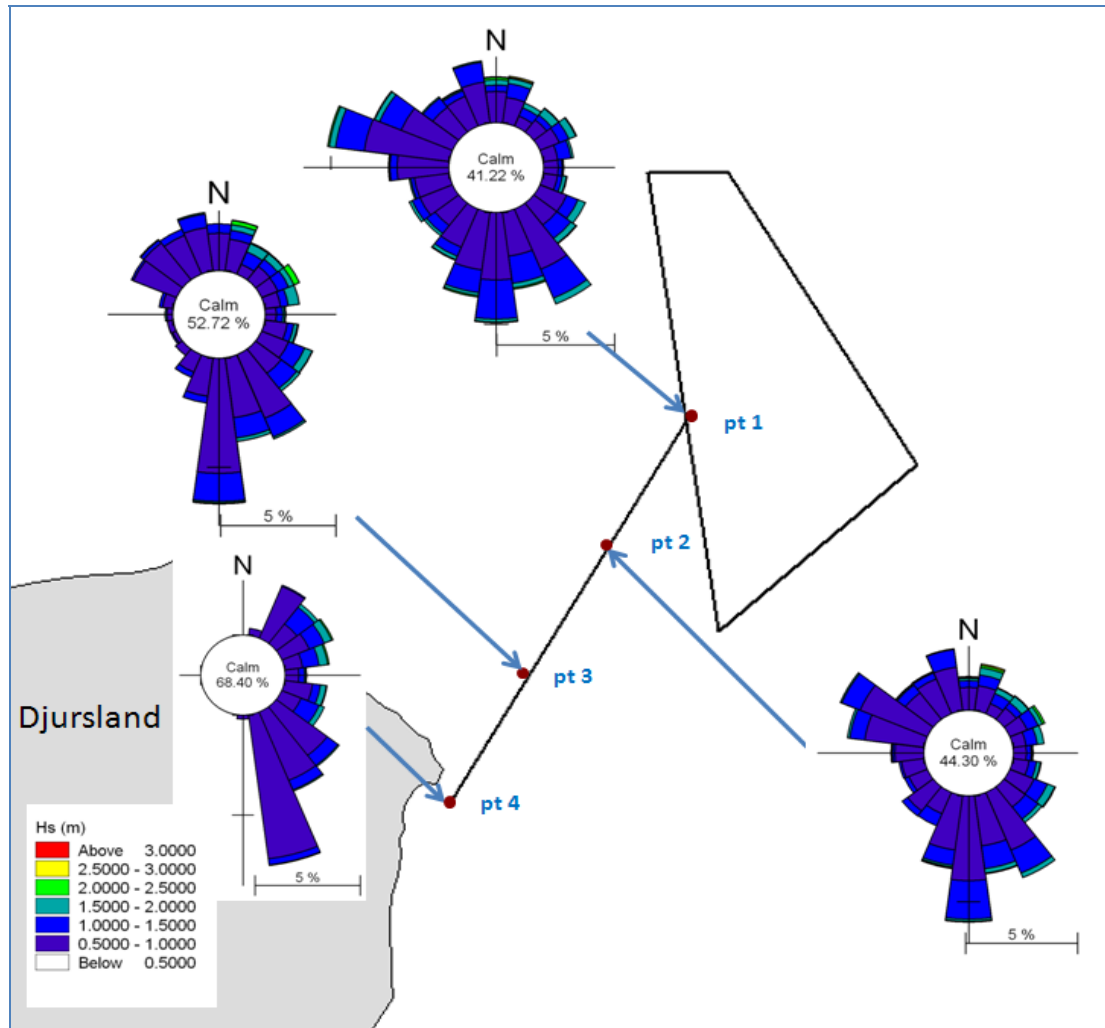
Figure 4-7   Modelled wave conditions from the local wave model at four locations along the offshore cable. Baseline conditions.

4.2.6   Water quality conditions

This section describes the water quality in the area between Djursland and Anholt under baseline conditions (year 2005). Because monitoring data covering water quality do not exist for the project area a calibrated ecological model covering a larger area (e.g. entire Kattegat, see Figure 2-1) was established to resolve the spatial and temporal variability. The baseline conditions are used as a yardstick to evaluate the permanent changes in water quality following the installation of the sea cable and the temporal effects related to earth works.

The results are supplied in the following. The methods and the numerical models applied in the analysis are described in Section 3.2.6.

4.2.6.1 Baseline water quality conditions

The baseline water quality in the area was described in details in Section 3.2.6. The spatial variation in pelagic primary production in the entire Kattegat is shown in Figure 4-8 and a detailed distribution of primary production covering the local model area is shown in Figure 4-9.
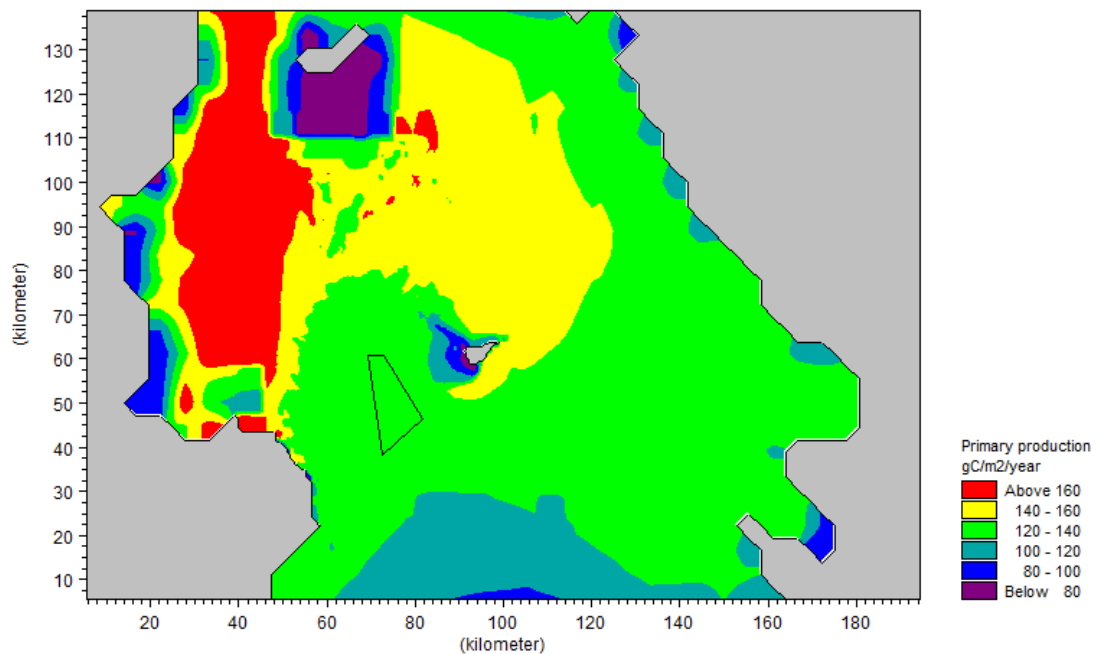
Figure 4-8   Modelled yearly (2005) pelagic primary production (g C/m^2/y) in the Kattegat.

Within the Kattegat the depth integrated primary production peaks along the 10-13 m depth curve in Aalborg Bugt as a result of intense mixing between surface and bottom water bringing nutrients up in the photic zone (Figure 4-8). At shallow waters, e.g. along coasts such as in the area of the cable trace and South of Læsø pelagic primary production is low. Instead, benthic vegetation such as Eelgrass south of Læsø dominates production, but these processes are not modelled as benthic vegetation practically is absent in the wind park area.
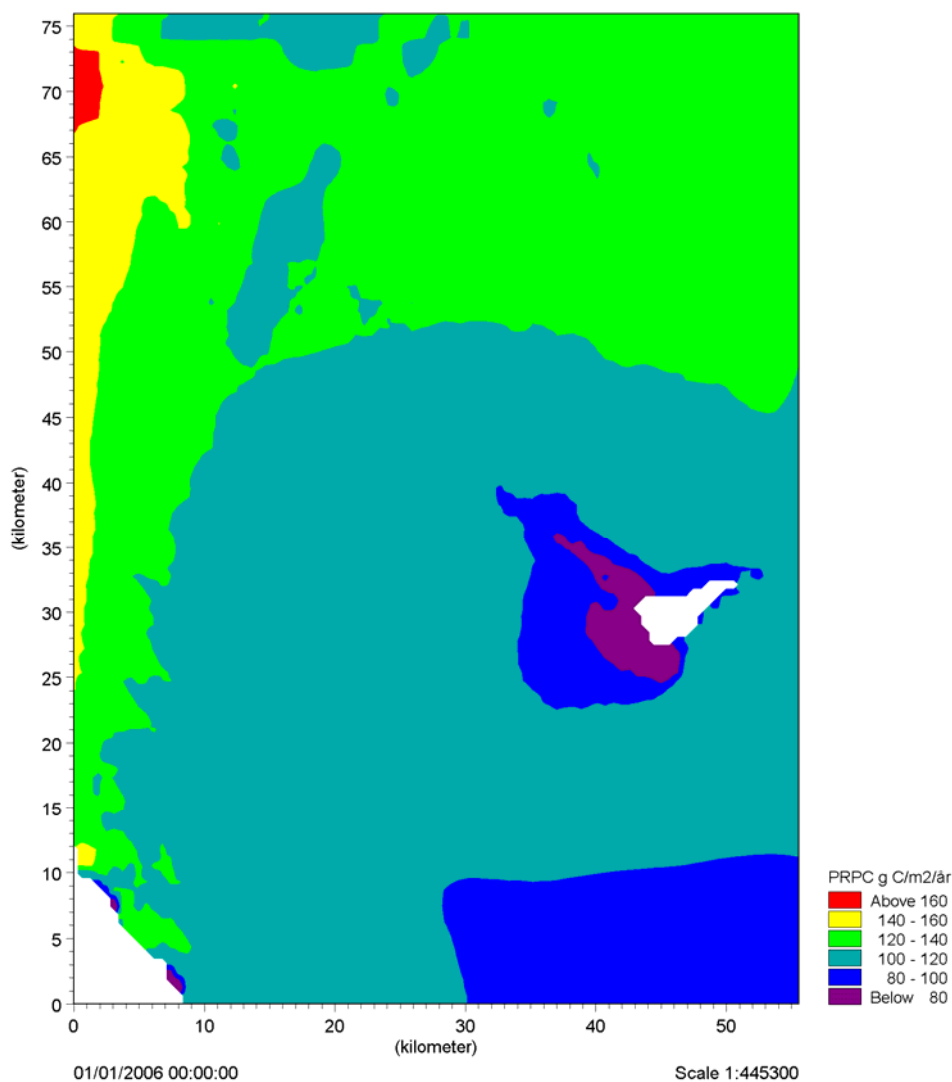
Figure 4-9   Modelled yearly (2005) pelagic primary production (g C/m^2/y) in the local model area.

4.2.7   Coastal morphology

4.2.7.1   Methods

A coastal inspection of relevant sections of the shorelines of the island of Anholt and Djursland was carried out by DHI on May 12-14 2009. The descriptions of the coastal processes are based on the coastal inspection and literature on the issue.

4.2.7.2   Landfall location Grenå Nord

The coast of Northern Djursland is illustrated in Figure 3-63. The coastline is irregular. At some sections it consists of steep or even vertical cliffs of limestone or moraine till. The cliffs are subject to erosion and hardest parts of the eroded material

have been transported to the shingle beaches between the protruding cliffs. At some locations the protruding coastline is protected by shallow submarine ledges of limestone, /19/. The north coast is an open wide sandy beach which is not subject to erosion. To the south the coastal section under consideration ends at the port of Grenaa.
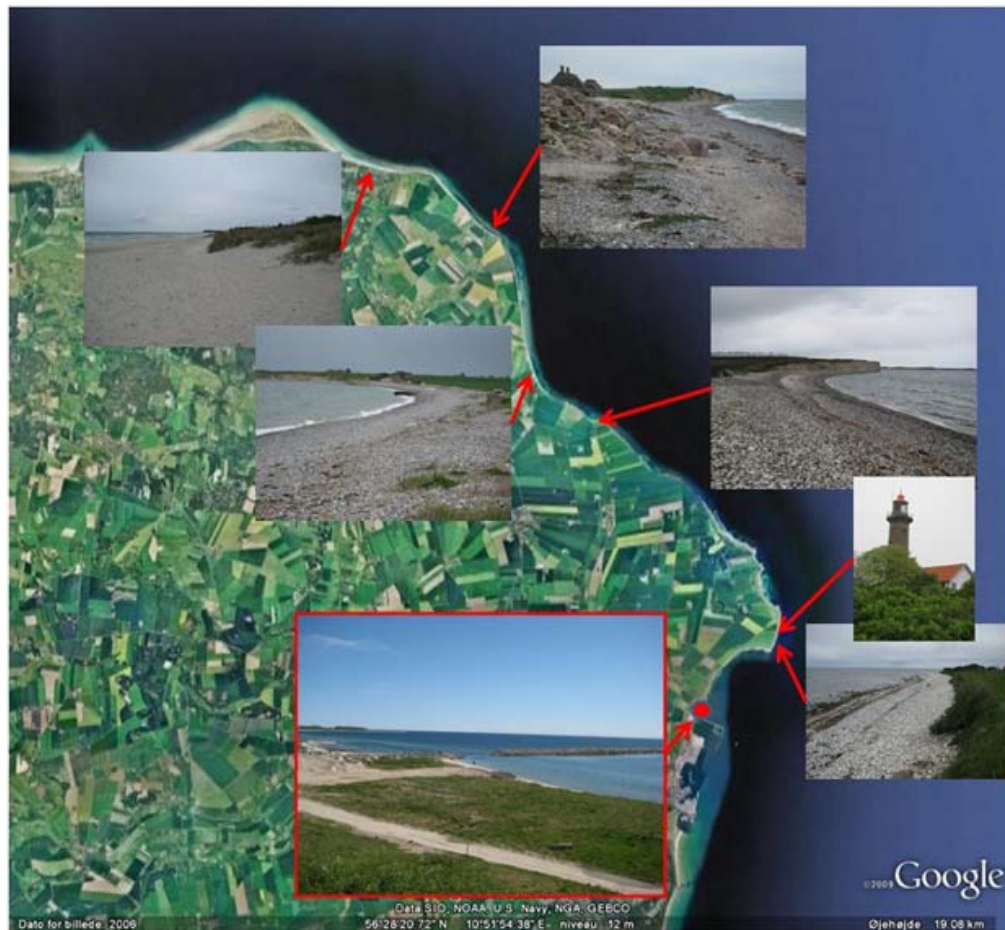
Figure 4-10   The coast of northeast Djursland. Approximate landfall location Grenå Nord

The approximate location of the landfall point for the power cable at Grenå Nord is shown in Figure 4-11. The Saltbækken creek runs through a gentle valley in the landscape. The coast is sandy right at its mouth, but the surrounding coast is stone covered. The coast appears rather stable or slightly erosive.

It should be noted that the potential landfall location is adjacent to a recent extension of the Port of Grenaa in the form of a large rubble mound breakwater. Some adjustments are to be expected to take place for the coast due to this extension. The new breakwater will shelter for southerly waves on the coast immediately to the

north. It is expected that the coast will accrete in the corner just at the breakwater where the landfall is anticipated and that it will tend to erode further away. Because of the stones already at the coast the erosion may not be very pronounced.

In conclusion the coast at the potential landfall location is not expected to erode in the future and from a coastal engineering point of view the location is suitable for a landfall of the power cable.

Figure 4-11   Approximate location of landfall at Grenå Nord.

4.2.8   Geomorphology and sediment transport

In the following the mobility of the sea bed along the cable trace is investigated in connection with analysing the risk of exposure of the offshore cable. Due to the combinations of the water depth being in the order of 15-20 m and the relative small current speeds and waves in the project area the mobility of the sea bed is expected to be small.

The sea bed mobility depends on the combination between local sediment character-istics, and the wave and current conditions in the area of interest.

Waves mainly increase the turbulence near the bed and influence the pick-up rate at the bed. The waves also keep the sediment in suspension in the water column. The current is the main transport mechanism.

The sea bed mobility is quantified by estimations of annual sediment transport rates.

4.2.8.1 **Methods**
Annual sediment transport rates have been estimated at 2 locations pt1 and pt3 along the offshore cable shown in Figure 4-12. These 2 points cover the variation in the non-uniformity of the sediment characteristics (see Section 4.2.2.3) and in the wave and current conditions along the cable.

The transport rates have been calculated using the module LITSTP of DHI's model system LITPACK. A model description and the setup of LITSTP were described in general terms in Section 3.2.8.
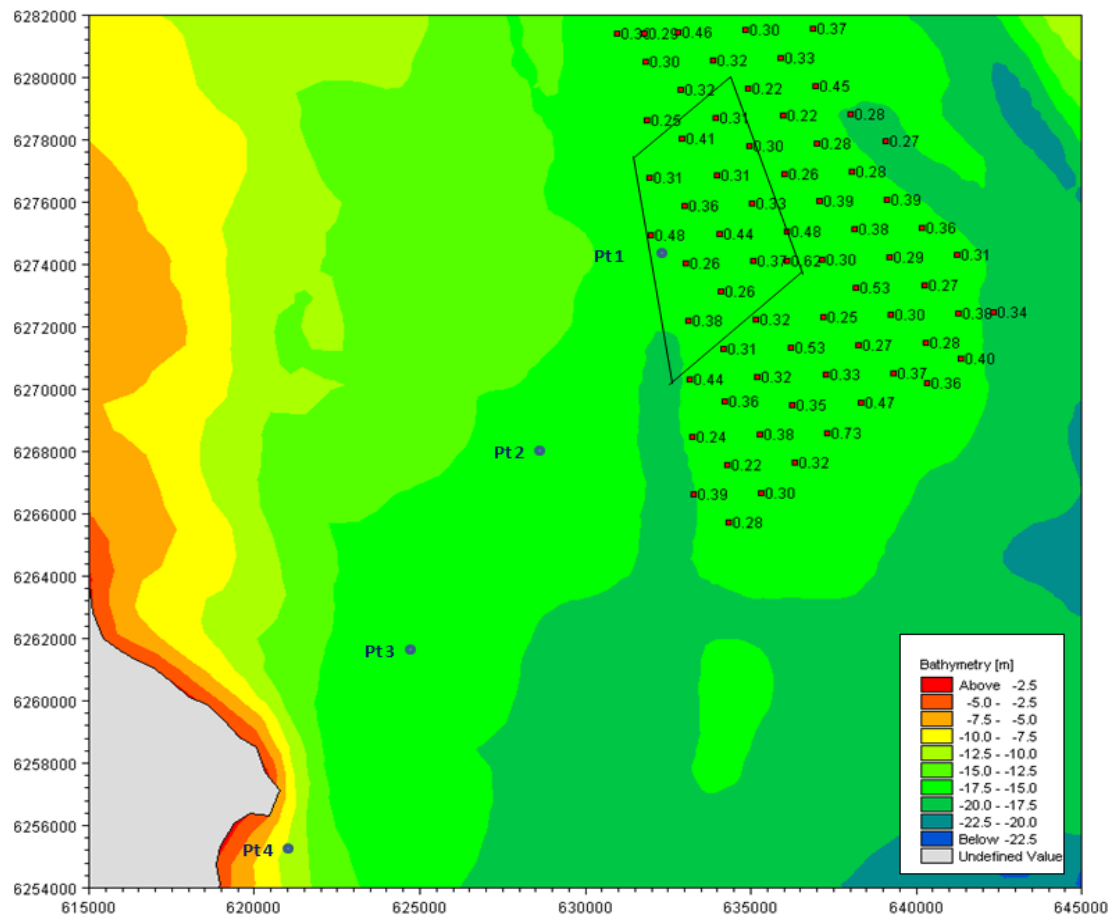
Figure 4-12   Annual sediment transport rates have been calculated in Pt. 1 and 3. The characteristics of the surface sediment samples (collected by DHI /7/) within the box representative of pt1 defined in the figure are applied in the calculations of annual sediment transport rates. At pt3 assessed sediment characteristics are used in the calculations of annual sediment transport rates. Wave and current conditions in pt1 and pt3 are applied. The depth contours are shown by the colour coding on the right.

In the transport calculations, the sediment characteristics at pt1 have been defined by combinations of the minimum and maximum d_{50} and σ collected in the sediment samples within the area located in the vicinity of pt1 (see Figure 4-12). These are given in Table 4-1 together with the sediment characteristics of each of the sea bed samples in the area chosen to represent pt1.

Regarding the sediment characteristics at pt3, the geophysical survey from GEUS (see Figure 4-3) indicates that along the cable trace from the landfall to approximately halfway to the wind farm area, the sea bed is characterised by sand and silt. Based on this, d_{50} has been assessed to 0.22mm which corresponds to the minimum d_{50} of the collected sea bed samples within the wind farm project area. σ has been

set to 1.5. This value represents the mean σ of seabed samples for sediment characterised by a d_{50} between 0.2 and 0.3 mm.

Sediment transport rates have then been calculated at pt1 for four combinations of d_{50} and σ, combining the minimum and maximum values of d_{50} with respectively the minimum and maximum of σ. At pt3, only one sediment transport rate has been determined for the estimated d_{50} and σ defined previously. It should be stressed that the transport rates are calculated assuming that the bed in the area is entirely covered by sediment characterized by the given σ and d_{50}. Potential erosion resistant layers below the sand layer are thus not taken into account.

Table 4-1   Sea bed sample characteristics (d_{50} and σ) within the box representative of pt1. Extreme and mean values of d_{50} and σ are indicated as well. Samples were collected carried out by DHI in the spring 2009 /7/.

Sample nb	d50 (mm)	σ
B6	0.31	1.47
B7	0.48	2.29
C5	0.41	3.18
C6	0.36	1.52
C7	0.26	1.54
C8	0.38	1.58
D5	0.31	1.75
D6	0.31	2.44
D7	0.44	N/A
D8	0.26	N/A
E5	0.30	1.50
E6	0.33	1.64
E7	0.37	1.45
FX6	0.62	1.80
average	0.37	1.85
min	0.26	1.45
max	0.62	3.18

4.2.9   Sea bed mobility – estimations of annual sediment transport rates

The calculated sediment transport rates at pt1 and pt3 are shown in

Table 4-2 (net transport) and Table 4-3 (gross transport, i.e. the absolute mobility rate). At pt1 sediment transport rates are given for four different sediment combinations of the grain size and grading whereas at pt3 only one sediment transport rate has been calculated.

The initiation of movement of sediment depends on the combined waves/currents motion. If the sediment is coarse, the combined forcing from waves and currents has to be strong whereas finer particles are more mobile. The friction on the sea bed, however, also increases with grain size. The transport rates are consequently strongly related to combination of wave and current climates as well as sediment characteristics (d_{50} and σ). No significant variations in the wave climate or currents are found across the area.

Along the north-eastern part of the offshore cable, pt1, the calculated sediment transport rates are very small, less than 0.1 m³/m/yr and 0.5 m³/m/yr for the net and gross transport respectively for the minimum grading coefficient, σ_{min}. The transport rates for the maximum grading coefficient, σ_{max}, are most likely exaggerated, in particular for the small minimum d_{50}. Under such combinations, sand fractions smaller than 0.063 mm, which is the limit for non cohesive sediment, are included in the sediment transport calculation. A small grain size is combined with a small grading coefficient in the present data set; however, the results are included here to cover the variation in the sediment characteristics. Similarly for the combination of the maximum d_{50} and maximum grading at pt1, the transport rates seem exaggerated. The simplified parameterization of the sediment grain sizes in the samples causes the inclusion of very fine sediments in calculations of transport rates in the areas with a large high grading coefficient. These fine sediments are not found in the sediment samples to such a degree. These numbers are hence included in parenthesis.

Along the south-western part of the offshore cable, pt3, the calculated sediment transport rates are in the same order of magnitude in the north-eastern part of the offshore cable. The net transport rate is smaller than 0.1 m³/m/year and the gross rate is smaller than 0.3 m³/m/s.

Estimations of the upper values of the annual and net and gross sediment transport rates in the project area are summarized in Figure 4-13 and Figure 4-14, respectively.

To conclude, sediment transport rates in the project are expected to be low, in the order of a couple of m³/yr/m which is a good indication that the seabed mobility is relatively low under the existing situation. Due to the small variations in the water depth over the area and the expected small transport rates, the seabed is found to be quite stable. Local variations in the bed level up to, say 0.1 to 0.2 m, may be associated with the formation and migration of small bed forms like wave or current ripples.

Table 4-2   Net sediment transport rates (m^3/m/year) calculated at pt1 for four combina-
             tions of σ and d_{50} and at pt3 using one combination of σ and d_{50}. Rates in pa-
             renthesis are not realistic, please refer to text.

Location	min d50		max d50	
	min σ	max σ	min σ	max σ
pt1	0.1	(20.68)	0.07	(11.95)
Pt3	0.09			

Table 4-3   Gross sediment transport rates (m^3/m/year) calculated at pt1 for four combina-
             tions of σ and d_{50} and at pt3 using one combination of σ and d_{50}. Rates in paren-
             thesis are not realistic, please refer to text.

| Location	min d50		max d50	
	min σ	max σ	min σ	max σ
pt1	0.48	(27.9)	0.13	(19.85)
Pt3	0.25			
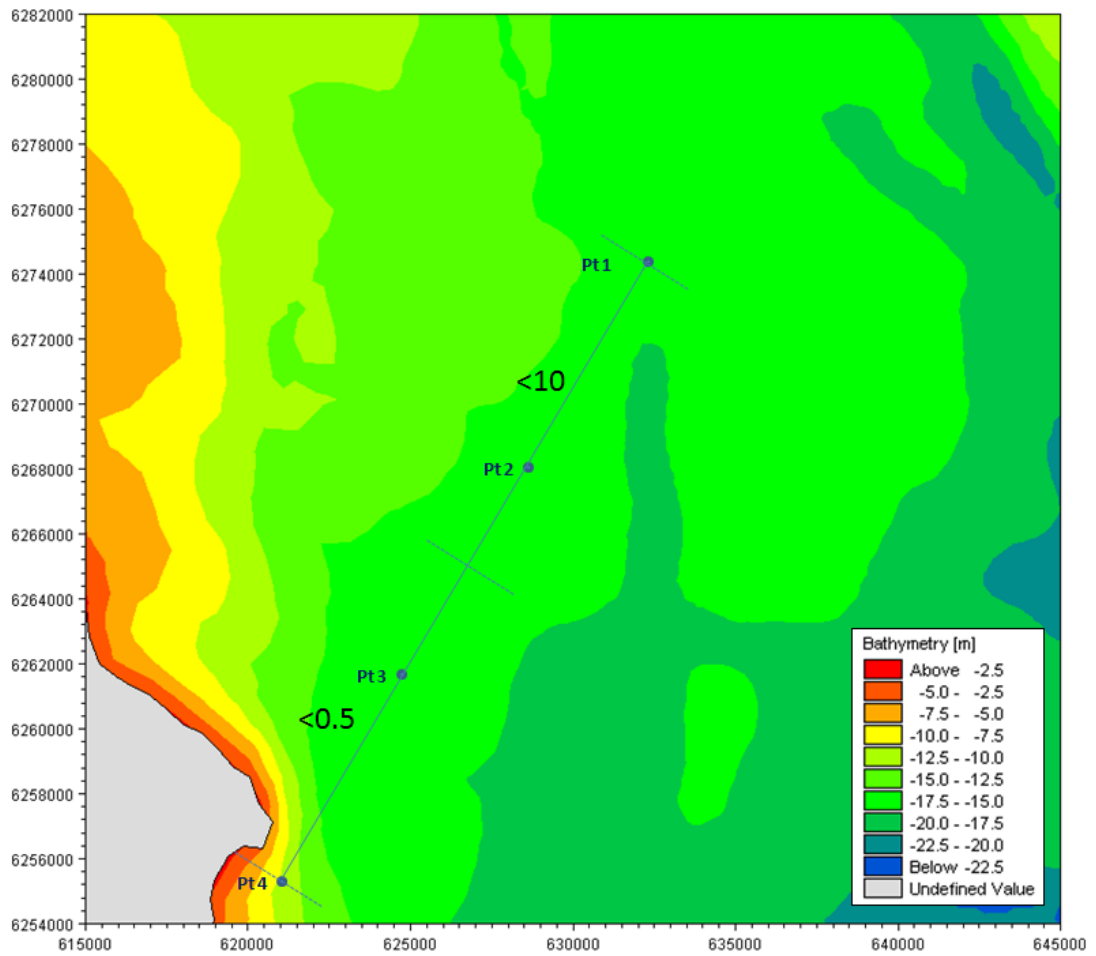
Figure 4-13   Estimations of net transport in m³/m/year along the offshore cable based on calculations.
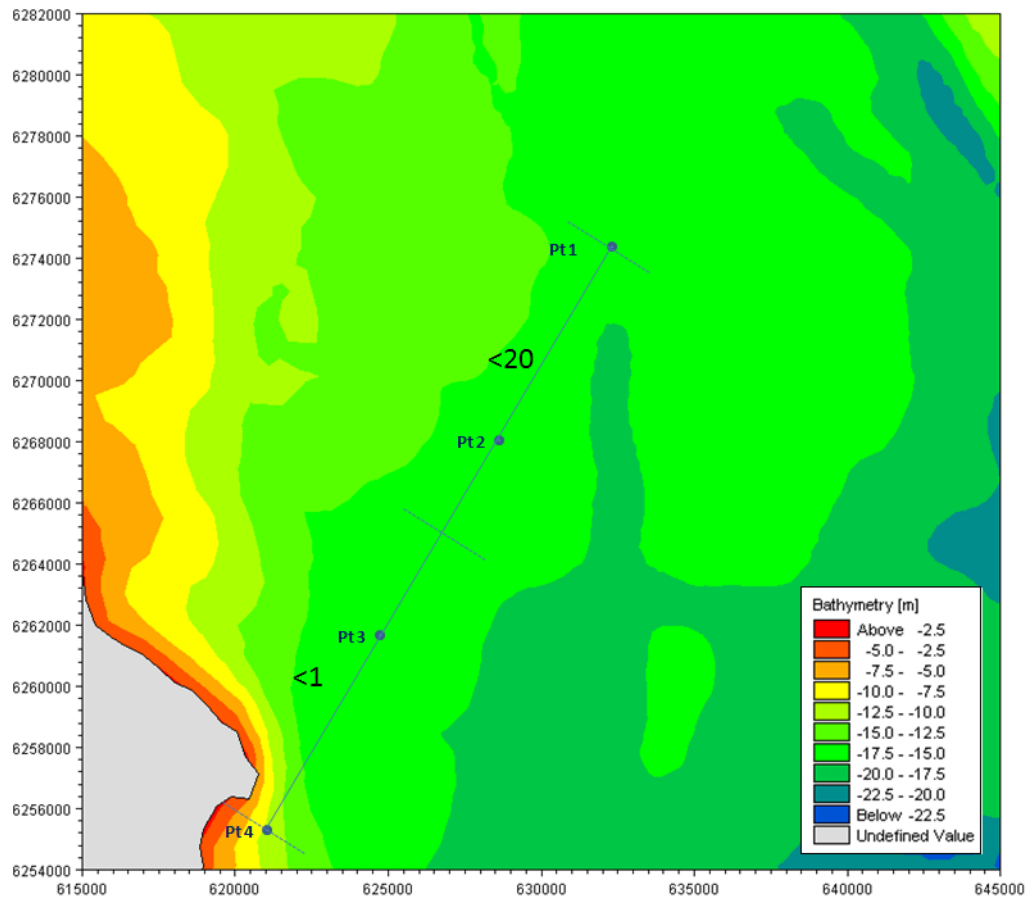
Figure 4-14   Estimations of gross transport in m³/m/year along the offshore cable based on
calculations.

4.3   Environmental Impacts

The environmental impacts on water quality and coastal morphology associated with
the planned substation and offshore cable from the planned wind farm to the landfall
point are described in this chapter section. Sediment spreading due to dredging ac-
tivities during the construction period and the risk of exposure of the cable is also
investigated. The issues are treated in separate subchapters below for the construc-
tion phase and the operational phase, respectively.

4.3.1   Method for impact assessment

The methodology used to assess the environmental impacts is described within each
of the subchapters. Every subchapter will be accompanied by a conclusion at the
end of the section that includes a table with an assessment of the different variables
and an evaluation of the overall significance of the impacts, see Table 3-21. The cri-
teria and methodology of the assessment are described in further details in /34 /.

The environmental impact assessment is based on evaluation of a worst case scenario with respect to the specific choice of foundations, number and size of wind turbines etc. given the limitations in the project description /1/. The worst case scenario could in theory be different for each of the issues studied; however, the combination of 174 2.3 MW wind turbines on gravity foundations turns out as the worst situation for each of the issues. Further details and discussion are included in the subchapters.

Table 4-4   Criteria used in the environmental impact assessment for the off-shore wind park.

Intensity of effect	Scale of effect	Duration of effect	Overall significance of impact[1]
No	Local	Short-term	No impact
Minor	Regional	Medium-term	Minor impact
Medium	National	Long-term	Moderate impact
Large	Transboundary		Significant impact
[1]: Evaluation of overall significance of impact includes an evaluation of the variables shown and an evaluation of the sensitivity of the resource/receptor that is assessed.			

4.3.2   Impacts during the construction period

Sediment spill is to be expected when the sea cable between the wind mill park and the landfall is laid and trenched. During this operation a part of the fine material in the bed will be spilled into the environment. The fate of this material during the laying of the land cable is the topic of this section.

4.3.2.1   Sediment spill during installation of the sea cable
4.3.2.1.1   Method for impact assessment

Sediment spill due to the construction of the land cable for the Anholt Offshore Wind Farm is assessed by studying the sedimentation and spreading of sediment. Simulations are carried out by assuming a realistic schedule, where the jetting rig moves along the route as the cable is being laid out.

The potential environmental impacts of the activities are summarized in Table 4-5.

The material spilled into the water is tracked until two days after the dredging operation is finished to allow for the sediment to settle. As long as the sediment is in the water column, the concentration of sediment is increased in the areas where the sediment drifts to. The spreading is governed by the current speed and direction, the turbulence and the settling velocity of the sediment. When the particles fall to the bed, they may later be eroded if the hydrodynamic conditions are strong enough to erode them from the sea bed.

Table 4-5 Potential impacts from sediment spill during the laying of the land cable.

Project Activity	Sources of potential impact	Potential environmental impact
Construction phase		Environmental impact parameter affected /target of impact
Dredging for cable between the wind mill park and the landfall	Sediment spreading and sedimentation	Water Quality Benthic fauna Benthic habitat Fish

<u>Dredging volumes and soil properties</u>

Geologically the sea bed in the wind mill area consists of layers of mud and sand. The main part of the upper layer of the sea bed is sand. However, below this sandy upper layer, the geotechnical investigations /26/ reveal that in some areas a layer of soft grey mud or clay extending to between 6 m and 10 m is found. The cable is being laid at a depth of 1.2m and is not expected to penetrate through the upper sand layer. The land cable will be laid using a water jet. The affected volumes are given in Table 4-6.

Table 4-6 Volumes affected when burying the cable.

Cables	Volume of sand dredged when the cables are laid down. [m^3/m]
Sea cables	1.5

Available information of the composition of the upper sand layer at the time of writing the report was described in Section 3.3.3.

4.3.2.1.2 **Assumption regarding equipment, dredging patterns, and dredging rates**
Dredging for cables will be done differently from the conventional dredging methods. This operation will be done by jetting. For this process the water from the jet will fluidize and wash the soil in a triangular shape above the cable. For this process it is assumed that the water jetting of the cable takes place with a speed of 1000 m cable per hour.

In the process of jetting the cables into the sea bed, the spill is assumed to be 20% of the affected volume, since the sand is never lifted away from the bottom. Physically what happens is that the water used for the jetting process will create an excess pressure at the jet. Due to this excess pressure the water will try to exit and this can only happen through the soil above. The soil above is therefore lifted slightly while streaming water passes. And thus fine materials can be washed out and released at the soil surface. The sand particles are too big and too heavy to be part of this process. They might be lifted slightly off the bed but they will settle immediately after the jet has passed. Sand is therefore not considered in this process. A sketch of the entire process can be seen in Figure 4-15.
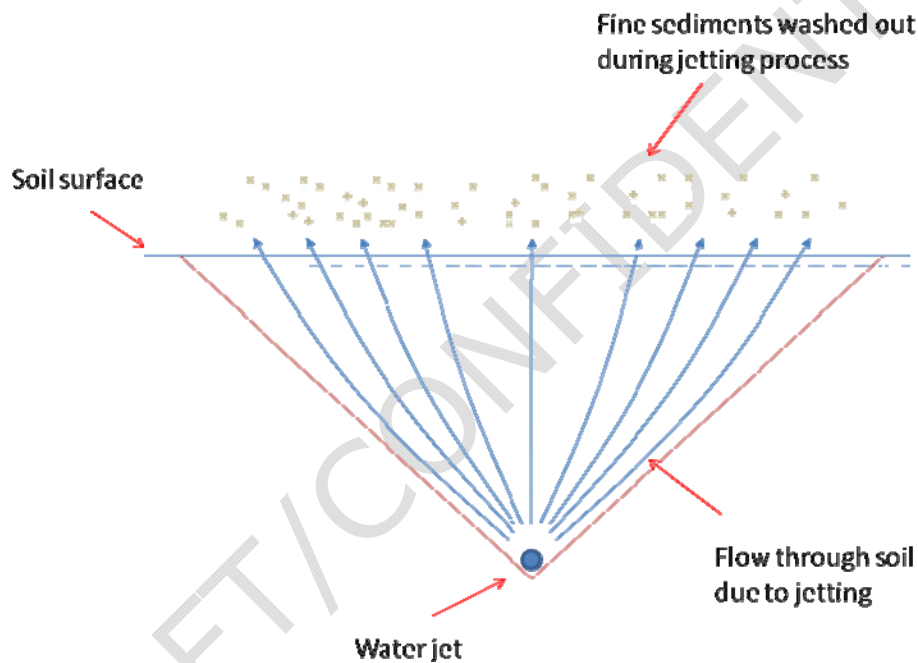

Figure 4-15   Sketch of the water jetting effect

The spill is hence only assumed to consist of 20% of the fines in the sand, which means that in total 2% of the total mass is spilled.

Table 4-7 Spill percentages for water jetting the cables into the seabed.

Jetting of the cables	Spill rates in percentage of the volume affected by jetting
Spill at bottom	2 %

An overview of the total spill rates is given in Table 4-8.

Table 4-8 Assumptions of totally spilled masses.

	Spill percentage	Spill, tonnes/hour (Dredging in sand)
Spill during water jetting (sand)	2%	43

The total amount spilled is given in Table 4-9.

Table 4-9 Total spill of fines.

	Total spill per km cable (tonnes)	Total cable length (km)	Total spill (tonnes)
Cables	43	24	1040

The water jetting will start at the transformer station at the wind mill farm and moves towards land. This is shown in Figure 4-16.
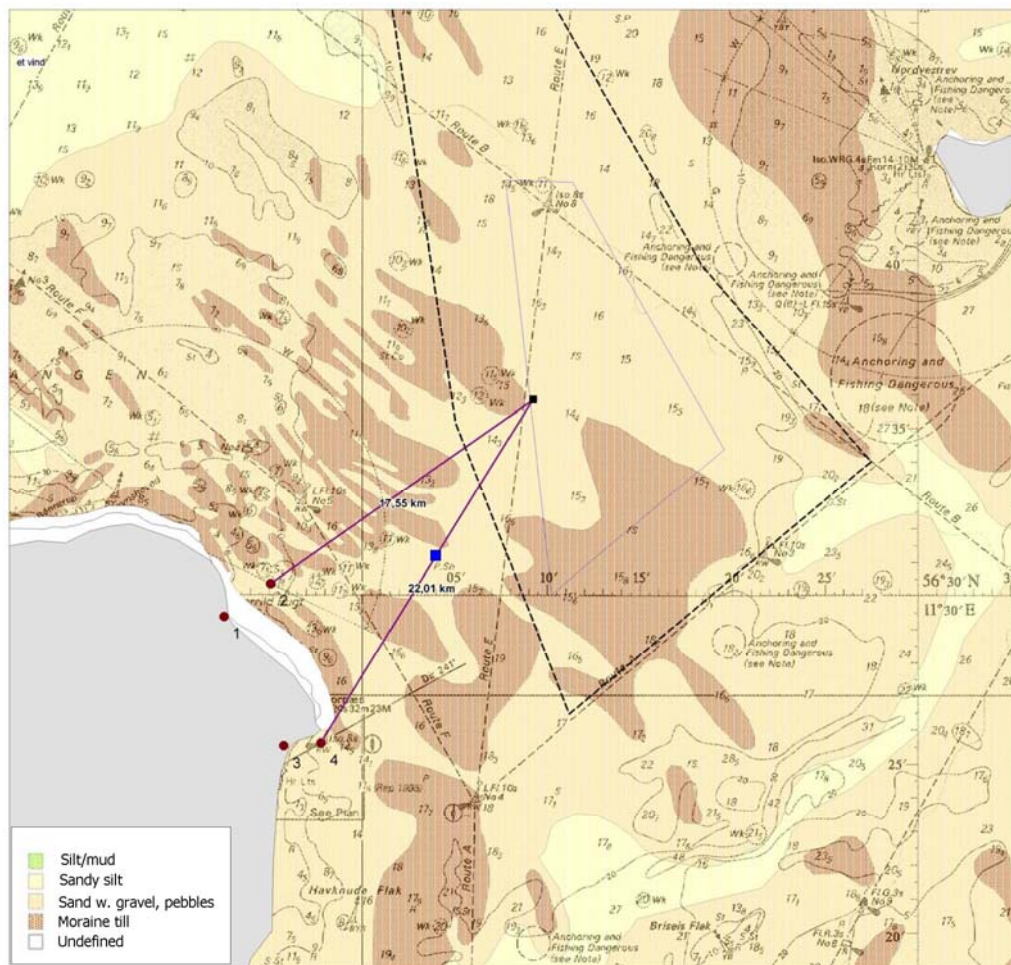
Figure 4-16   Dredging location. Dredging is assumed to start at the wind mill park and move towards the landfall location, Grenå Nord. The pathway will follow the southern route as marked in the figure. Location, where flow conditions are supplied below indicated with a blue marker.

4.3.2.1.3   **Model setup**
The applied model is a so-called particle model (PA). This model follows the path of a number of particles released at the source point under the influence of currents, settling velocities' dispersion and other parameters. The model was briefly described in Section 3.3.3.

With the given dredging rate of 1000 m/hour for the cable it will take approximately one day to place the sea cable. The model is setup for a sufficiently long period of time to cover the dredging operation allowing also for additional two days for the sand to settle out of the water column.

Since the total sea cable can be placed in approximately 1 day, the spreading of sediments will be very dependent of the current conditions on the day of the operation. The area of impact and the concentrations in the water column will depend on the strength and direction of the current.

To account for this in the impact assessment, the operation is simulated with six different current situations covering the variation in the flow conditions at a central location along the cable. The spreading of the sediment will primarily depend on the near bed velocities since water jetting of cables creates a sediment spill near the sea bed. Figure 4-17 shows a current rose representing modelled current speeds and directions near the bed at the indicated location for the year 2005. The simulations are carried out with three levels of near bed current speeds and two different current directions (N-going and S-going)), which describe the variation in the current speed and direction. The maximum current speeds, the main current direction and the start and end times of the simulations are given in Table 4-10.
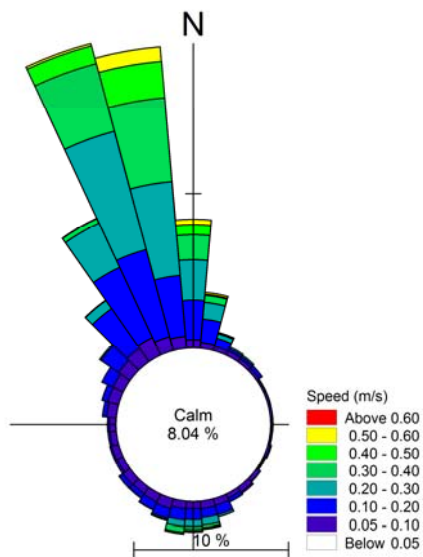

Figure 4-17   Near bed flow conditions for 2005 (4 m above sea bed, water depth 16 m) at location indicated in Figure 4-16. Current data from model results – grid spacing approximately 600 m.

Table 4-10   Simulation periods.

Simulation period	Start time	Maximum near bed current speed* (m/s)	Main near bed current direction* (North/South)
1	16 Jan 2005 00:00	0.4	N
2	28. Mar 2005 12:00	0.1	N
3	14. May 2005 12:00	0.07	N
4	13. Feb. 2005 00:00	0.4	S
5	11. Mar. 2005 12:00	0.2	S
6	6. May 2005 12:00	0.1	S

*Current speed and direction approximately 4 m above sea bed at location shown in Figure 4-16. Model results – grid spacing approximately 600 m.

The spill from the laying and trenching of the cable is represented by a near-bed source. The spill rates and dredging procedures are given in 4.3.2.1.2. The source files will follow the route shown in Figure 4-16 and use the spill rates given in Table 4-8. The operation is assumed to be continuous without breaks or stops. The most important settings regarding sediment properties are given in Table 4-11.

Table 4-11   Model settings.

Model settings	Value
Time step	300 s
Type of particle	Mud
Settling velocity	0.0005 m/s
Critical shields parameter	0.1

Grain size	2e-5m

The most important settings are the settling velocity and the critical shields parameter. No measurements are available for either of these parameters. In reality the fine sediments will flocculate and different floc sizes will be available in the water column at the same time. Since no data are available the settling velocity is chosen as a normal mean value for fine sediment settings based on DHI experience. When evaluating the results one should consider the possibility that some of the finest fractions may travel slightly further than the results show due to lower settling velocities. The critical shields value is chosen slightly bigger than the one usually applied for sand (0.045) because mixtures of mud and sand tend to increase erosion resistance significantly.

4.3.2.1.4 **Impact of sediment spill during the construction phase**
In the following, the results for the simulations of the dredging operation are presented. In general, the operation leaves a plume that is advected around with the currents. The jetting rig moves continuously and the accumulated result is thus the sum of a moving point source creating a plume. An example of an instantaneous plume moving along the cable trace as simulated in Simulation period 1 (see Table 4-10) is shown in Figure 4-18.
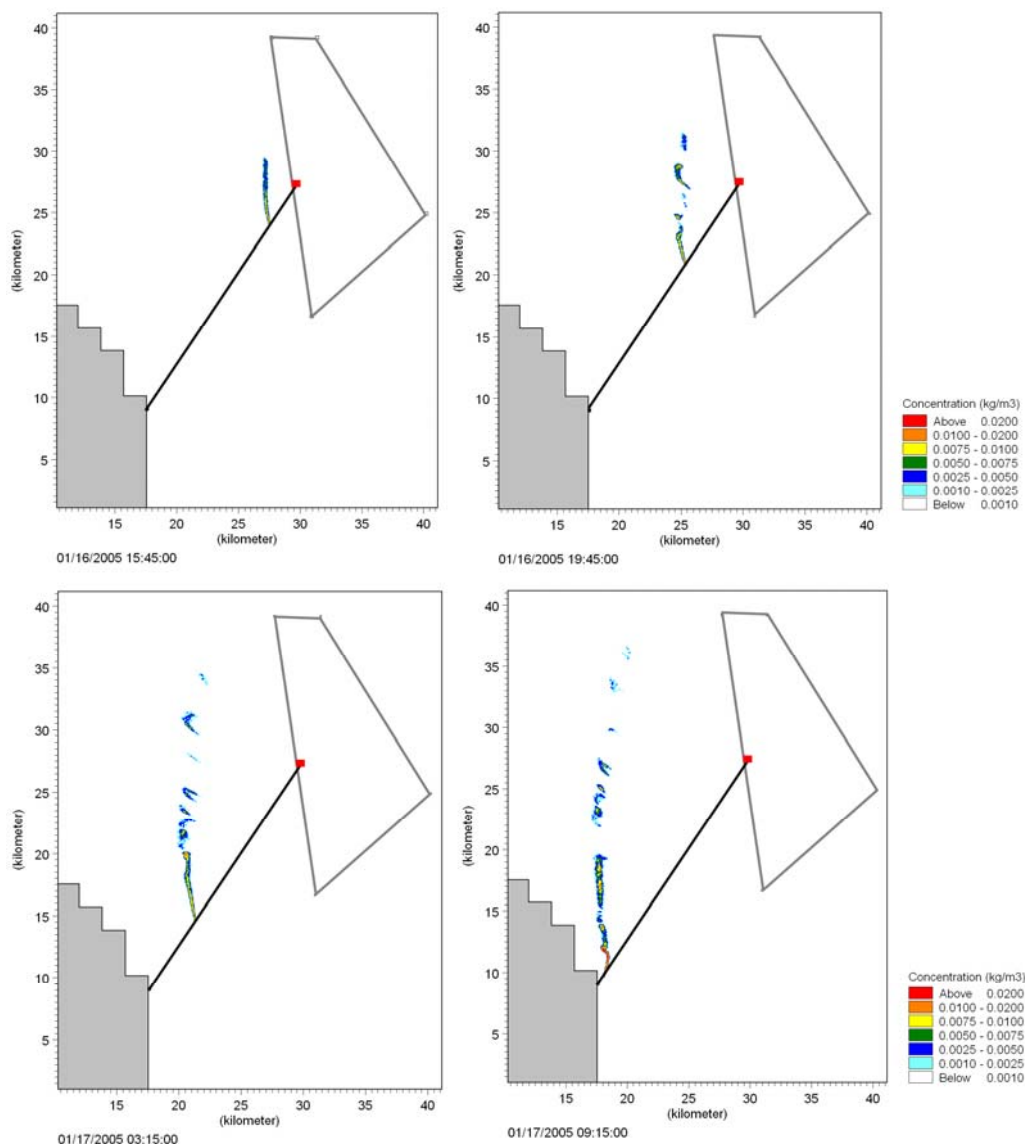
Figure 4-18   Instantaneous concentrations in the water phase showing the plume at four different times during Simulation period 1 (see Table 4-10)

As mentioned above, the short period of operating the jetting rig and hence of disturbing the sea bed implies that the impacts due to sediment spreading will depend highly on the specific flow conditions on the given day.

On days with a very low current speed, the sediment will not be transported very far away from the cable trace but deposit close to the cable. On the other hand higher current velocities will spread the sediment to a larger area but with smaller deposition per square meter. The geographical location of the area of impact will depend on the dominant current directions.

At a given geographical location in the vicinity of the cable trace, the impact is therefore evaluated against the worst case situation in the six representative simulations. The geographical area is divided into cells of approximately 100 m x 100 m, and in Figure 4-19 the maximum sedimentation in each of these cells within one of the six simulations of the dredging operation is shown.

The results show very low patchy sedimentation rates over a large area. The patches are due to sedimentation from individual plumes and this illustrates the random nature of the spreading and shows how far the dredged material travels during the dredging periods simulated. The location of the plumes is determined by the current fields during the simulation times. The main results from this figure and the following figures are therefore the travelling distance and the sedimentation rates/concentrations rather than the exact location of the plumes. The location of the sedimentation areas is seen to be spread over an area between Djursland and the wind mill park consistent with the spill locations. Please note that the shoreline is only coarsely described in the model. For the same reason the near-shore results may be less accurate. The largest sedimentation values are in the order of 100-400 g/m^2. This corresponds to less than 0.5 mm in thickness.

Note that Figure 4-19 does not supply information on the impact area, but merely on the areas that may potentially be affected. The total impact areas where sedimentation rates exceed 100 g/m^2 in the six simulated cases respectively are given in Table 4-12. The impact areas are 4 km^2 or less in all simulated cases. The smaller flow velocities tend to cause a larger area with sedimentation values exceeding 100 g/m^2, while it was found that the sedimentation is spread over a larger area but with smaller sedimentation values in situations with larger current speeds.
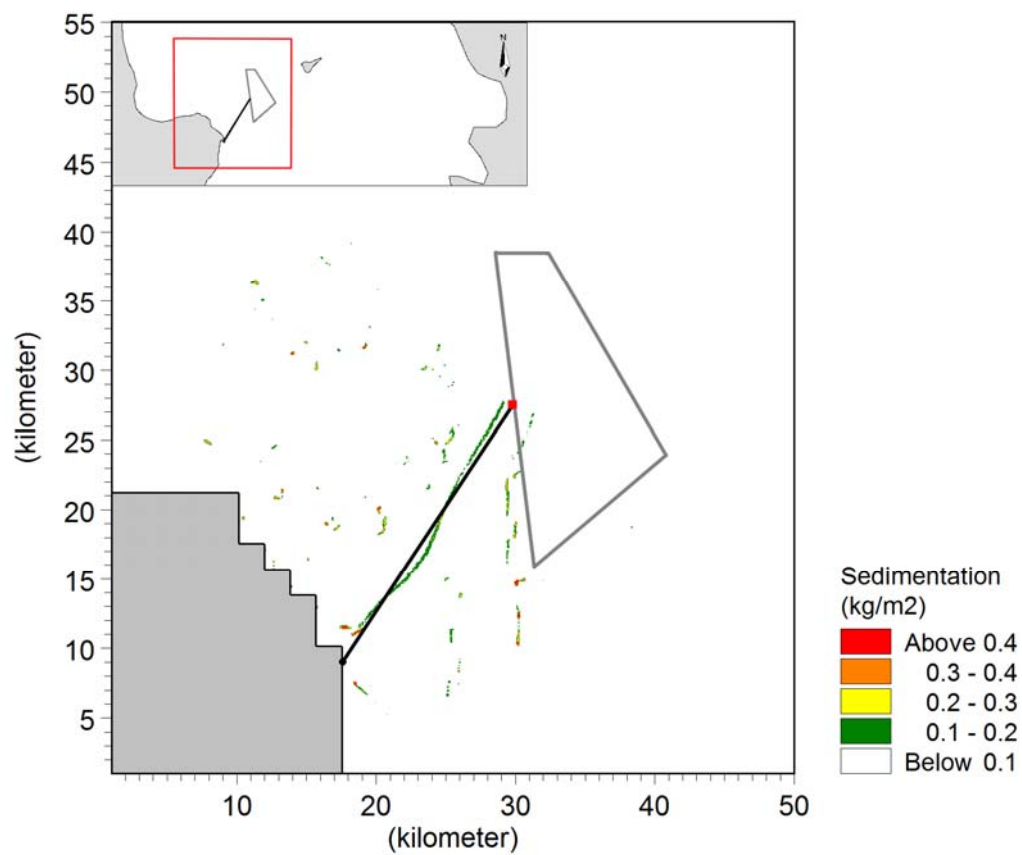
Figure 4-19   Potential areas of deposition and maximum deposition rates due to dredging operation for the land cable.

Table 4-12   Total impact area by deposition larger than 100 mg/m^2 (less than 0.1 mm) immediately (two days) after the finalization of the dredging operation.

Simulation period	Maximum near bed current speed* (m/s)	Main near bed current direction* (North/South)	Total impact area by deposition rates larger than 100 g/m^2 (km^2)
1	0.4	N	2.6
2	0.1	N	4.1
3	0.07	N	3.9
4	0.4	S	2.7
5	0.2	S	3.6
6	0.1	S	4.2

When evaluating the deposition patterns it is important to emphasize that temporarily the deposition rates may be higher at some positions. However, this is a temporary effect that (if present) will be removed by the currents over time. Monitoring after the construction of Nysted Offshore Wind farm showed no changes of the overall sediment composition after the dredging operations; however, at some measuring points close to the construction area, the content of silt/clay was increased after the earthworks /35/.

Based on the above it can be concluded that the deposition of fines from the jetting work will not be a problem. The deposition rates are in general very low since material is spread over a large area, and higher deposition rates are found only within small areas.

With regards to the concentration levels in the water column the general environmental criterion is the visibility of the water. This is evaluated with respect to three effect criteria, see discussion in Section 3.3.3:

Plume visibility (2 mg/l)

Effect on fish (10 mg/l)

Effect on diving birds (15 mg/l)

The first criteria (2 mg/l) is the limit where the plume is visible in the water. How-ever, only higher concentration rates have any critical impacts. Concentrations above 10 mg/l in the water column have been found to have the impact of reducing the sight and hence the ability of hunting for fish and above 15 mg/l for diving birds.

The maximum depth averaged concentrations occurring at each computational area of approximately 100 m x 100 in any of the six simulations in Table 4-10 are shown in Figure 4-20. Note that these concentrations are not reached at <u>all</u> locations in any of the six operation periods, but dependent on the flow conditions the concentration level reaches these levels in the specific computational areas in at least one of the simulation periods.
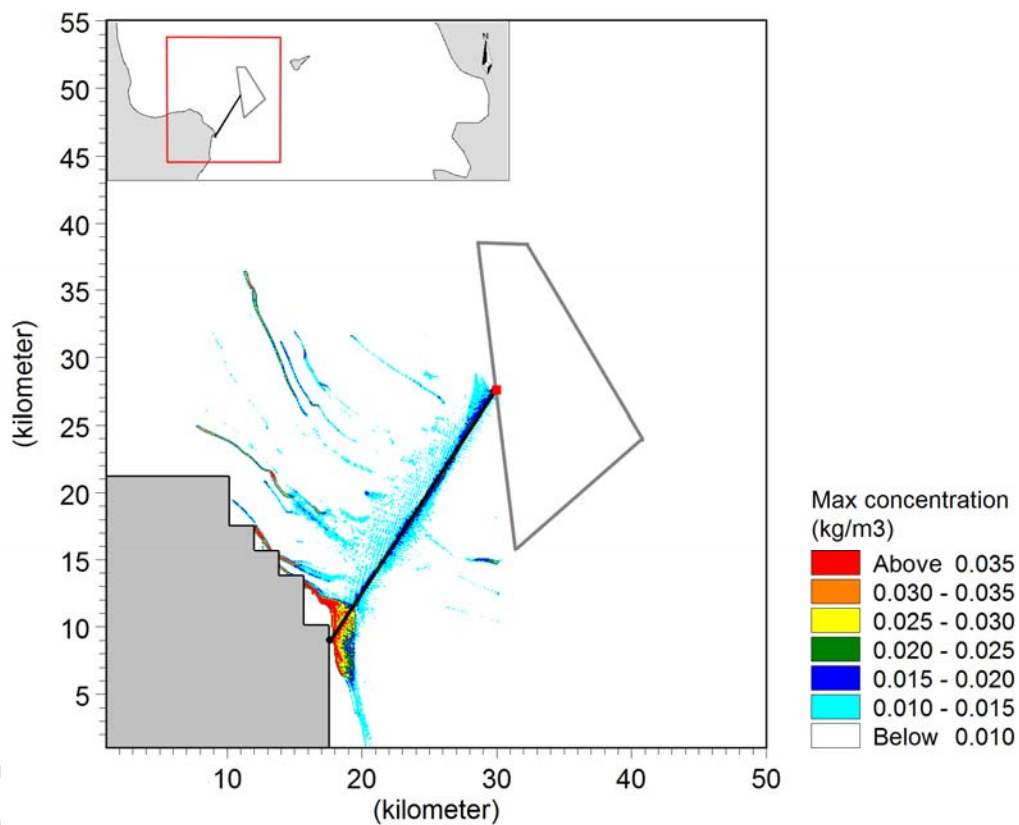
Figure 4-20   Potential maximum concentration during the dredging operation for the land cable.

Results hence show that depth averaged concentrations potentially exceed 10 mg/l and 15 mg/l and therefore the fish and bird criteria may be exceeded during the dredging operation at locations near the cable path. Due to the very short installa-tion period for the sea cable, however, the time period where concentrations poten-

tially exceed respectively 10 and 15 g/l are low. Figure 4-21 shows the number of hours a depth averaged concentration of 10 mg/l is potentially exceeded in the areas near the cable path. 10 mg/l is exceeded in only about 1-4 hours and in limited areas. Figure 4-22 shows similarly how 15 mg/l is also exceeded up to about 3-4 hours, primarily near the coast.

The overall conclusion is that near the cable trace there will be a short-term effect of jetting the sea cable into the sea bed; however, on the long term there will be little or no effect. The plume from the operations will be visible but in a restricted area and for a short time (a few days). The impact of sedimentation will be insignificant. The depth-averaged concentrations from the plumes will exceed levels that may impact fish and birds but for such a short time (less than 4 hours), that no impacts are expected.
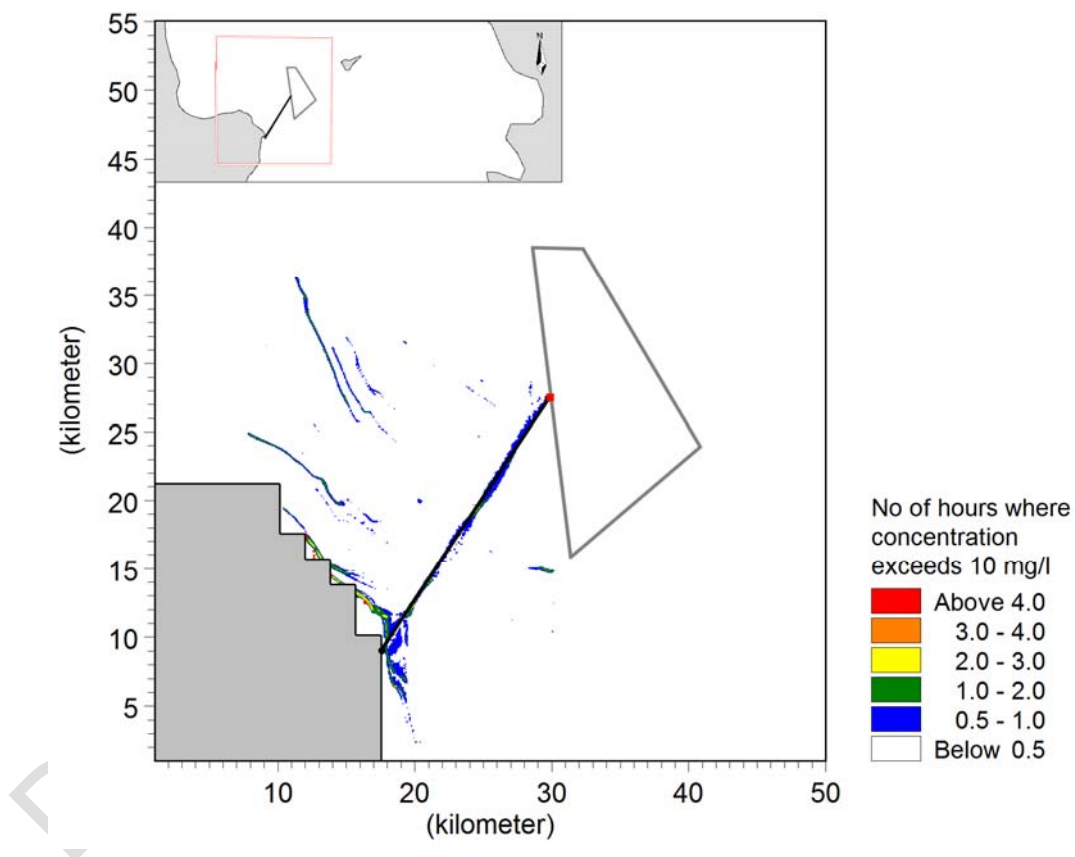

Figure 4-21   Exceedance statistics from sediment spreading calculations for the dredging operation for the land cable. Colour scale indicates percentage of time where concentrations exceed 10 g/m³.
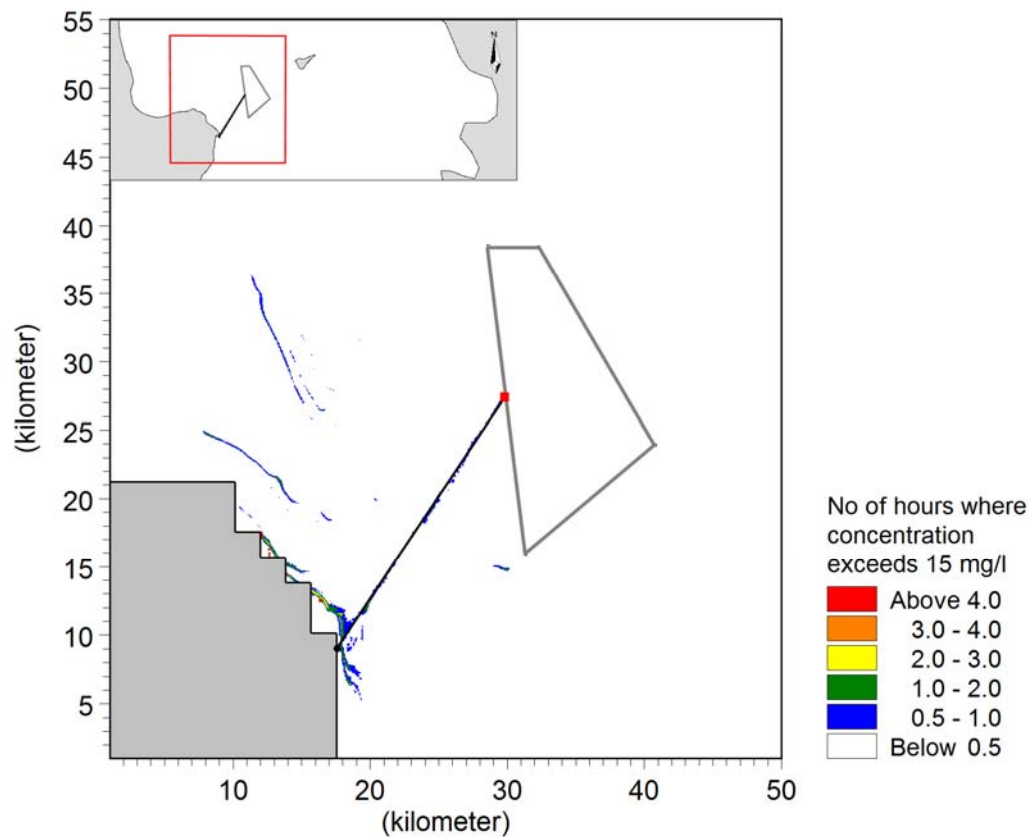
Figure 4-22   Exceedance statistics from sediment spreading calculations during the dredging operation for the land cable. Colour scale indicates percentage of time where concentrations exceed 15 g/m^3.

4.3.2.1.5 **Summary regarding impacts due to spill during the construction phase**
A probable dredging scheme has been simulated under six different flow conditions. The simulations were carried out using a particle model in 3D.

Results showed very small impacts. Depth-averaged concentrations exceeded defined effect criteria for fish and diving birds respectively, but for such short times (< 4 hours) that the impacts are insignificant.

The area where sedimentation spreads over depends on the flow conditions at the time of the jetting. For small flow velocities near the sea bed (<0.2 m/s), a deposition above 100 g/m^2 may take place, primarily near the cable path. For larger flow velocities, the sedimentation was spread over a large area but with very small amounts. The deposition was calculated to be less than 1 mm everywhere in these flow situations and at most locations much smaller. Largest sedimentations were seen near the cable alignment.

Table 4-13   Summary of impacts from sediment spill during the construction phase.

Impact	Intensity of effect	Scale/geographical extent of effect	Duration of effect	Overall significance of impact
Increased concentrations of sediments in the water column	Medium	Local	Short term	Minor impact
Sedimentation on the sea bed	Minor	Local	Short term	Minor impact

4.3.2.2   **Impacts on water quality during the construction phase**
Dredging activities including the sediment spill and resuspension of sediment invariably will affect the light availability for phytoplankton and benthic vegetation due to shading from particles with potential effects on primary production. Also mobilisation of inorganic nutrients and reduced substances in sediment pore water may lead to reductions in oxygen concentrations in the water column and increased nutrient availability for plankton algae. Unfortunately, detailed information on depth distribution of sediment characteristics is not available but based on the characteristics of surface sediment, i.e. a low organic content, low percentage of fines etc. (see section 12.3.2.1) the availability of nutrients and reduced substances such as H_2S in sediments probably is low. Therefore, only the shading effect from sediment spill is considered potentially affecting phytoplankton and benthic vegetation.

Table 4-14   Project activities and sources of impact and potential impacts on water quality.

Project Activity	Sources of potential impact	Potential environmental impact
Construction phase		Environmental impact parameter affected /target of impact
Dredging	Sediment spill and spreading Release of nutrients and reduced substances from sediments	Reduced pelagic primary production due to shading from suspended sediment Reduced benthic primary production due to shading Increased pelagic primary production due to increased nutrient availability Transient reduction of water column oxygen concentration caused by oxidation of reduced substances.

Extinction of light in the water column depends on concentration, nature and size distribution of suspended material, chlorophyll (in phytoplankton), dissolved organic matter and water itself. Extinction is primarily related to two processes, absorption of light (in chlorophyll and organic matter) and light scattering that relates to total surface area of particles. The equation for light extinction coefficient Kd was adapted from Kirk /40/:

$$Kd=((13.8*Chla+0.015*SS_{20}+0.141)^2+0.265*(13.8*Chla+0.015* SS_{20}+0.141)*28.76*Chla^{0.6}+0.03*SS_{20})^{0.5}$$

where 13.8 and 0.015 are specific absorption factors for Chla and suspended solids, respectively, 0.141 is the "background" extinction of water and dissolved organic matter and, 0.03 is the specific light-scattering coefficient for 20 μm particles (which was assumed in the spill scenarios, see Section 4.3.2). The equation is used for calculation of changes in light availability for phytoplankton for the two dredging sce-

narios defined and reported in Section 12.3, using the predicted additional concentration of light reducing agents in the water column.

Average concentration of suspended solids resulting from sediment spills was very low varying between 0.2 and 0.5 mg/l over an area of approx. 200 km^2 during the 24 h dredging period. Consequently the calculated average light availability for phytoplankton was only reduced by 5-10 % on average compared to the baseline, and the light for benthic vegetation was only reduced by 0.5 to 2% (Figure 4-23 and Figure 4-24). Considering the very limited period of light reductions and the numerical small reductions in pelagic and benthic light the dredging of cable trace is very unlikely to cause any harm to either pelagic or benthic vegetation.

Table 4-15   Summary of impacts on water quality during the construction phase

Impact	Intensity of effect	Scale/geographical extent of effect	Duration of effect	Overall significance of impact
Light shading and pelagic primary production	Minor	Local	Short term	Minor
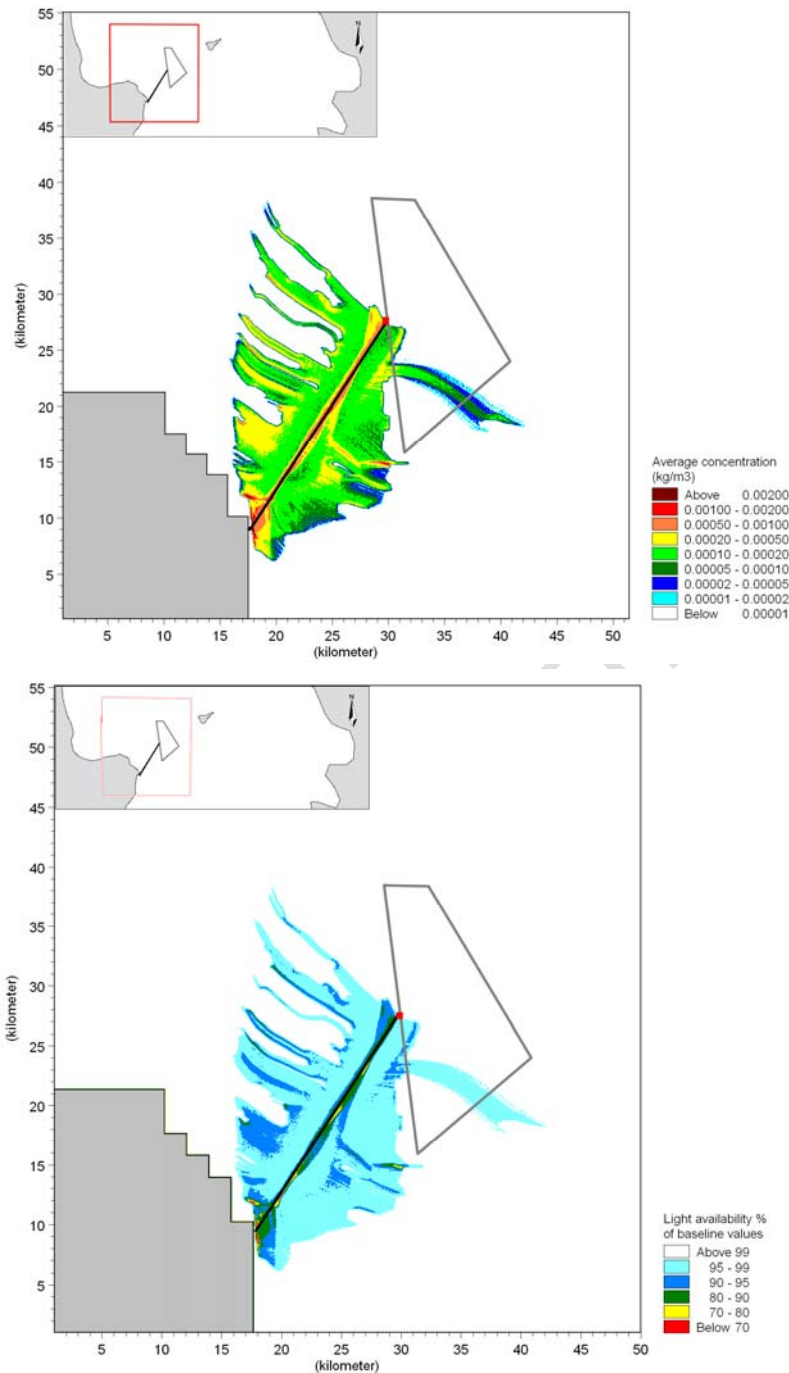
Figure 4-23   Average concentration of suspended solids resulting from dredging operations for cable trace (upper) and average light availability for phytoplankton during dredging as percentage of baseline conditions (lower). Available light for phytoplankton is calculated from average concentration of spilled sediment (over entire dredging period, ca. 24h) and assuming a surface mixed layer of 12 m or in case of lower depth a fully mixed water column.
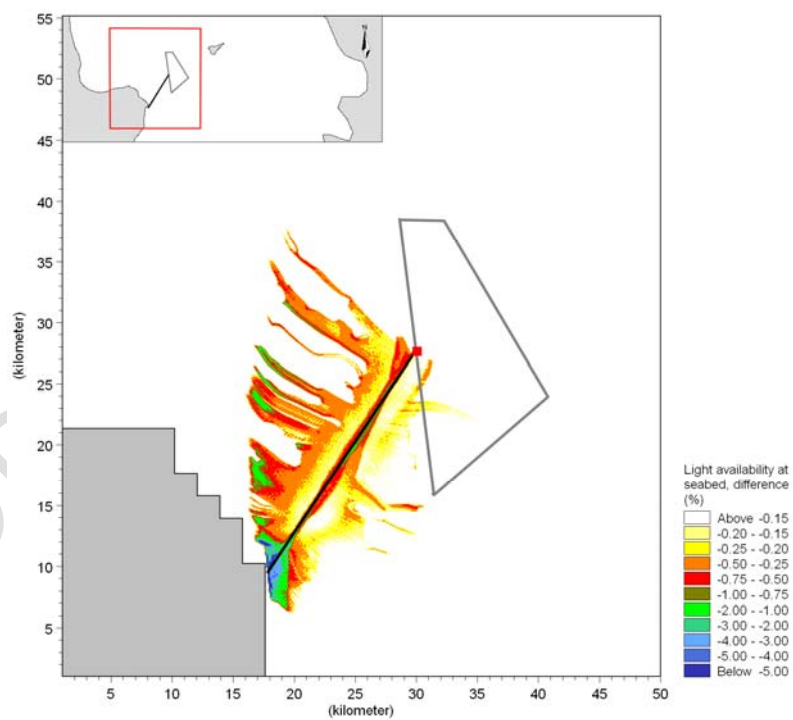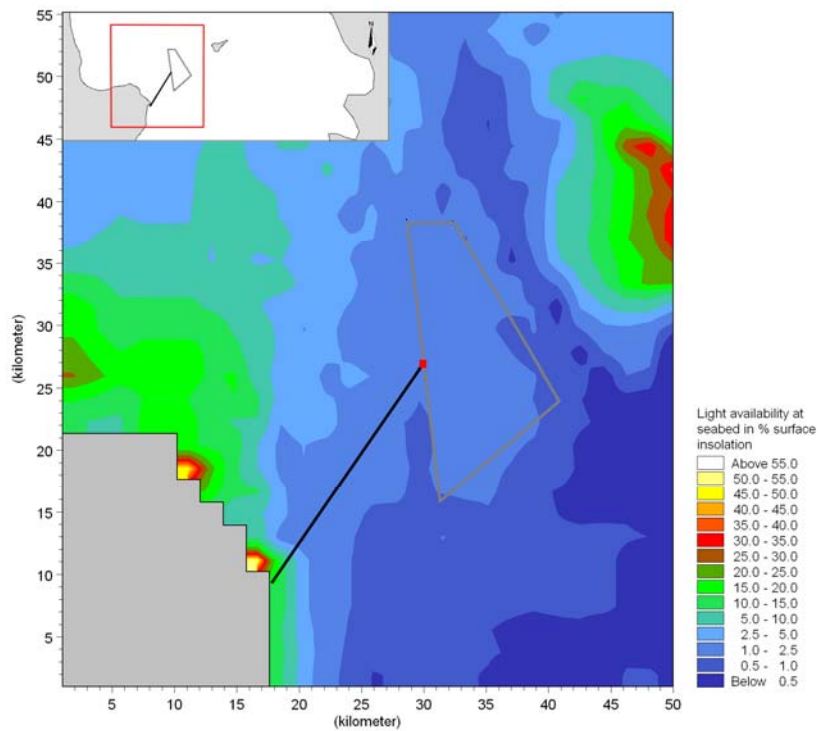
Figure 4-24   Calculated light availability at seabed as percentage of surface intensity (upper) and percentage reduction in light intensity at seabed due to dredging activity (bottom).

4.3.3 Impacts during the operational phase

4.3.3.1 Impacts on coastal morphology at landfall location (Grenå Nord) and risk of cable exposure near the coast

The cable is embedded into the sea bed at a depth of more than 1 m /1/. The planned landfall location is in the corner between the coastline and the northern breakwater of the Port of Grenå. This corner is expected to naturally accrete as described in Section 4.2.7.

The shoreline is hence not expected to retreat in this area and the risk of cable exposure at the point of the landfall site is not existent or minor.

The subsea cable is not expected to cause any impacts on the shoreline at the landfall point at Grenå Nord.

Table 4-16   Summary of impacts on coastal morphology and risk of cable exposure at the landfall position during the operational phase

Impact	Intensity of effect	Scale/geograp-hical extent of effect	Duration of effect	Overall signifi-cance of im-pact
Risk of cable expo-sure at the landfall position	No/Minor	Local	-	No/Minor
Impact of shoreline near the landfall position	No/Minor	Local	-	No/Minor

4.3.3.2 Risk of cable exposure

The cable is expected to be embedded into the sea bed at a depth of more than 1 m /1/. The very small sediment transport rates found in Section 4.2.9 lead to conclude that the sea bed is quite stable. Small undulations in the form of small bed forms of a height of 10-20 cm do not impose any risk of cable exposure along the planned trace.

Table 4-17   Summary of the risk of cable exposure along the cable trace from the offshore substation to the landfall position during the operational phase.

Impact	Intensity of effect	Scale/geograp-hical extent of effect	Duration of effect	Overall signifi-cance of im-pact
Risk of cable expo-sure along the cable trace	No/Minor	Local	-	No/Minor

4.4 Mitigation measures

The impacts from the cable are very small and no mitigation measures are recommended.

4.5   Cumulative effects
There are no expected cumulative effects of Anholt Offshore Wind Farm and other 3rd part projects on the issues covered by this report. The impacts are in general very small and local and do not interact with other known projects.

4.6   Decommissioning
During the decommissioning phase it is intended that the cables will be left in place, see Section 5. No impacts are hence expected in this phase on issues covered by this report.

4.7   Technical deficiencies or lack of knowledge
The main part of the work described in this report is based on numerical modelling. The modelling was to a large extent drawing on data input and model setup from existing and well calibrated models, which are found trust-worthy for the analyses carried out for this study.

The time schedule for the sediment spreading calculations did not allow to await the final analyses of the geotechnical investigations. The sediment spreading calculations were therefore based on:

1. assumptions by Rambøll (personal communication) with regard to the volumes required to be removed at each gravity base to reach a level where undisturbed soil is encountered (/1/) and

2. assumptions with regard to the physical characteristics of the spilled material.

Considering the relatively small volumes being dredged in total and the very small concentrations and sedimentations rates obtained, the assumptions regarding 2. are evaluated as being sufficient and not influencing the overall quality of the assessment.

If the assumptions regarding 1. change significantly, it should be considered to revise the assessment.

4.8   Conclusions regarding substation and offshore cable
An Environmental Impact Assessment related to the substation and the offshore cable connecting a planned wind farm between Anholt and Djursland with land has been carried out. The impact assessment comprises issues related to assessment of sediment spreading due to dredging activities, water quality and coastal morphology at the landfall. The cable is expected to be embedded in the seabed.

The sea bed was found to consist of non-cohesive sediments, mostly sand. Near the wind farm area the sediment is coarser (sand with pebbles and stones) and further towards the coast the sea bed consists of sand/silt.

Estimations of annual sediment transport rates on the sea bed are in the order of a few cubic metres over a width of one metre of the seabed. No changes to the sea bed are expected on a regional scale. Small bed level changes of 10-20 cm related to migrating bed forms such as wave- or current ripples are expected. The sea bed is considered stable and the risk of cable exposure is minor.

From analysis of sedimentation and spreading of sedimentation during dredging activities it was concluded that depth-averaged concentrations of suspended sediment will exceed 10 mg/l and 15 mg/l, but only in short periods (hours). Sedimentation rates less than 1 mm are expected due to the dredging activities.

Based on yearly averaged shading from spilled sediment it was concluded that effects on pelagic and benthic primary production were very unlikely along the offshore cable

The impacts and their significance are summarized in Table 4-18.

Table 4-18   Summary of impacts from the offshore cable

Impacts	Overall signifi-cance of impact	Quality of available data
SEDIMENT SPREADING AND SEDIMENTATION DUE TO EARTHWORKS		
Increased concentrations in water column	Minor	2
Sedimentation	Minor	2
IMPACTS ON WATER QUALITY		
Pelagic primary production	Minor	3
Organic carbon sedimentation and mineralisation	Minor	3
Near bed oxygen conditions	Minor	3
Light shading, pelagic and benthic primary produc-tion during construction period	Minor	3
IMPACT ON COASTAL MORPHOLOGY AT LAND-FALL		
Modifications to shorelines and coastal morphology at landfall location (Grenå Nord)	No	2
RISK OF EXPOSURE OF CABLE		
Risk of exposure of cable	No/Minor	2

5. Decommissioning

The objectives of the decommissioning process are to minimize both the short and long term effects on the environment whilst making the sea safe for others to navigate. These obligations are stipulated in the United Nations Convention of the Law of the Sea (UNCLOS).

There are no specific international regulations or guidelines on the decommissioning of offshore installations. Decommissioning will have to consider individual circumstances, such as comparative decommissioning options, removal or partial removal in a way that causes no significant adverse effects on the environment, the likely deterioration of the material involved, possibilities for re-use or recycling as well as its present and future effect on the marine environment.

Based on current available technology, today's practice for decommissioning would imply to remove the wind turbines completely and to remove all other structures and substructures to the natural seabed level. Infield and export cables would be removed, left safely in-situ, buried to below the natural seabed level or protected by rock placement depending on the hydrodynamic conditions. Scour protection would be left in-situ.

The wind turbines, structures and cables would be dismantled using similar craft and methods as deployed during the construction phase. However the operations would be carried out in reverse order. The recovered materials would be transported to shore for later material reuse, recycle or disposal.

The decommissioning programme will be developed during the operations phase, as regulatory controls and industry practices most likely will have changed in 25 years' time, when the wind farm will be decommissioned. Regardless of decommissioning method, decommissioning will comply with all applicable legal requirements regarding decommissioning at that time.

6. References

/1/ Rambøll, September 2009, VVM Anholt Project Description

/2/ E.On, Rødsand 2 Havmøllepark, Vurdering af Virkninger på Miljøet, VVM-redegørelse, Juni 2007.

/3/ Dong Energy, Horns Rev 2, Vurdering af Virkninger på Miljøet, VVM-redegørelse, oktober 2006.

/4/ Energistyrelsen, Betingelser for offentligt udbud om Anholt Havmøllepark 30. april 2009.

/5/ DHI and Rambøll 2009, Anholt Offshore Wind Farm. Fish.

/6/ DHI and Rambøll 2009, Anholt Offshore Wind Farm. Birds.

/7/ DHI 2009, Anholt Offshore Wind Farm. Benthic Fauna. Baseline Survey and Impact Assessment.

/8/ DHI 2009, Anholt Offshore Wind Farm. Benthic Habitats. Baseline Survey and Impact Assessment.

/9/ DHI and Rambøll 2009, Anholt Offshore Wind Farm. Marine Mammals.

/10/ DHI 2009, Anholt Offshore Wind Farm. Metocean Data for Design and Operational Conditions.

/11/ Rambøll, 2009. Anholt Offshore Wind Farm. Mapping of Substrates and Benthic Community Types.

/12/ DHI, 2006. Baltic Sea – North Sea Transition Area. Environmental status year 2004. Bansai Project. Technical note for the Nordic Council of ministers.

/13/ DHI, 2007. Blue Reef. Hydrographic Design Data. Report for The Danish Forest and nature Agency.

/14/ Pedersen, Fl. Bo. Lecture notes on Environmental Hydraulics. Stratified flows. Technical University of Denmark 1984.

/15/ Rasmussen EK, Svenstrup Petersen O, Thompson JR, Flower RJ & MH Ahmed., 2009. Hydrodynamic-ecological model analyses of the water quality of Lake Manzala (Nile Delta, Northern Egypt) Hydrobiologia 622: 195-220.

/16/ DHI, 2007. Short Scientific Description, DHI Water Environment Health.

/17/ Schou A.,1945. Det marine forland. Folia Geographica Danica. Tom. IV.

/18/ Schou, A.,1960. The Coastline of Djursland. Geografisk tidsskrift, Vol. 59, pp. 10-27.

/19/ Olsen, S. (Ed.), 1998. Danmarks Kyster. Gyldendal, 296 pp.

/20/ Bird, E.C.F. and Christiansen, C.,1982. Coastal progradation as a by-product of human activity: an example from Hoed, Denmark. Geografisk Tidsskrift, Vol. 82, pp. 1-4.

/21/ Christiansen, S.,1960. Wave power and the Djursland coast. Geografisk Tidsskrift, Vol. 59, pp. 28-32.

/22/ Ambient water quality guidelines (criteria) for turbidity, suspended and benthic sediments. British Columbia. Technical Appendix. Update 2001. ISBN 0-7726-3797-0

/23/ Berry W, Rubenstein N, Melzian B & B Hill 2001. The biological effects of suspended solids and bedded sediment (SABS) in aquatic systems: A review. Internal US EPA Report. Available from DHI.

/24/ Bilotta GS & RE Brazier 2008. Understanding the influence of suspended solids on water quality and aquatic biota: A Review. Water Research 42: 2849 – 2861

/25/ Miljø og Energiministeriet. Trafikministeret.Kontroll- och Styrgruppen för Öresundsforbindelsen, 1996. 3. halvårsrapport om miljøet og Øresundsforbindelsens kyst-kyst anlæg.

/26/ GEO. Anholt Offshore Wind Farm. Geotechnical investigations. Wind Farm area.

/27/ Fredsøe, J. and Deigaard, R., 1992. Mechanics of coastal sediment transport. World scientific 1992.

/28/ DHI & LICengineering, 1994. Beskrivelse af graveoperationer. Øresundsforbindelsen. Memorandum 9313-70.

/29/ DHI, 2009. Manual and user guide for PA modelling. "MIKE21 & MIKE3 PA/SA. Particle analysis and oil spill analysis Module User Guide.

/30/ DHI, 1999. Horns Rev Wind Power Plant. Environmental impact assessment of hydrography.

/31/ DHI, 2007. Rødsand 2. Waves and sediment transport. The Effect of Wind Turbines on Nearshore Waves.

/32/ Fredsøe, J., 1990. Hydrodynamik. Den private ingeniør fond. Danmarks Tekniske Højskole (in Danish).

/33/ Sumer, B.M., K. Bundgaard and J. Fredsøe, 2005. Global and local scour at pile groups". International Journal of Offshore and Polar Engineering, vol. 15, No. 3, pp. 204-209

/34/ Rambøll, 400 MW Off-shore wind park in Kattegat, Method for Impact Assessment.

/35/ Dong Energy. 2005. Review Report 2005. The Danish Offshore Wind Farm Demonstration Project: Horns Rev and Nysted Offshore Wind Farm. Environmental impact assessment and monitoring.

/36/ Christiansen, M.B., Hasager, C.B., 2006. Using airborne and satellite SAR for wake mapping offshore. Wind Energy 9 , 437-455.

/37/ Sumer, B.M. and J. Fredsøe. 2002. The mechanics of scour in the marine environment. World Scientific, Singapore, 536 pp.

/38/ COWI/DHI 2008. Mussels and Vegetation in Central Storebelt, 2007: Final March 2008.

/39/ Møhlenberg, 1998. Møhlenberg, F. & Petersen, J.K. Physical forcing and bio-geochemical fluxes in shallow coastal ecosystems (project phase, ELOISE) 3rd European Marine Science and Technology Conference Huelva, p. 835-850.

/40/ Kirk JTO. 1983. Light and Photosynthesis in Aquatic Ecosystems. Cambridge Univ. Press, 401 pp.

/41/ Nielsen A.W., Hansen, E.A. 2007. Time-varying Wave and Current-induced Scour around Offshore Wind Turbines. 2007. Proceedings of the 26th International Conference on Offshore Mechanics and Arctic Engineering (OMAE 2007), San Diego, USA.

/42/ Hansen, E.A., Christensen, E.D. 2007. Scour Holes or Scour Protection around Offshore Wind Turbine Foundations: effect on Loads. Proceedings of the European Wind Energy Conference.